

**Paleolimnological characterization of metal(loid) sources and
transport processes in Canadian subarctic lakes**

By

Nicolas Pelletier

A thesis submitted to the
Faculty of Graduate and Postdoctoral Affairs
in partial fulfillment of the requirements for the degree of

Doctor of Philosophy in Geography

Carleton University
Ottawa, Ontario

© 2021

Nicolas Pelletier

i. ABSTRACT

Human-released metals are present to some extent in soil and sediment from even the remotest areas, including the Canadian Arctic. The cumulative impact of legacy pollution, ongoing release of contaminants and climate change could lead to important modifications to metal transport and transformation processes in the environment that can affect the exposure of biota and humans to metals. Large uncertainties remain regarding the future transport of metals on the subarctic landscape, including those that can be toxic in low dose like lead and mercury. Paleoecology is a powerful tool to evaluate changes in metal pollution and recovery in lakes by providing long-term records of environmental conditions at a relatively low cost and with rapid analysis. Paleoecological records can help fill important research gaps that current monitoring approaches can't address because of the lack of temporal perspective.

In this thesis, the records of multiple environmental archives were analysed and compared to understand the changes in metal accumulation and transport that occurred over the last centuries to millennia in subarctic Canada, from the Yellowknife (Northwest Territories) and the Whitehorse Regions (Yukon). Multiple approaches to times series analysis were developed to evaluate the individual and cumulative impacts of specific sources and processes commonly affecting subarctic boreal lakes. These processes include local point-source emissions, catchment retention and transport of contaminants, and contaminants released by wildfires. This thesis provides quantification for processes that are seldom addressed in the literature so far, especially for subarctic environments. Subarctic lakes will continue receiving anthropogenic metal for years regardless of future emissions because of the impact of catchment retention. Terrestrial heavy metals retained in catchments are susceptible to remobilisation toward aquatic environments by natural processes such as land erosion, permafrost thaw and wildfires; and these processes may be enhanced by climate change. Recovery of any specific site from heavy metal pollution is also dependent on local parameters, explaining the

necessity to characterise ecosystem recovery from heavy metal pollution in different types of ecosystems, including subarctic environments.

ii. ACKNOWLEDGEMENTS

The realisation of this thesis would not have been possible without the continuous intellectual and moral support from my supervisors, Dr. John Chételat and Dr. Jesse C. Vermaire. I am very grateful of the many learning opportunities that were offered by them throughout the last five years, their constructive criticism, exceptional availability and openness. Dr. John Chételat is an example of patience and I hope to always remain inspired by his dedication to producing work of the best quality. More than assisting with the technical and theoretical aspects of my research, he unconditionally encourages me, challenges me and provides opportunities that fosters my career growth. Jesse has been a mentor as much as a friend during my time at Carleton, and I hope this relationship will endure. I was always looking forward to my meetings in Jesse's office and these are memories to forever hold. I wish to sincerely thank my spouse Lyna Lapointe Elmrabti, who moved to Ottawa to join me when with a whim I launched into the PhD program at Carleton. Looking back at the last years, I am not sure I would have had the strength to finish the program, had I been alone. Thanks, Lyna for remaining interested and supportive, and for giving me many, many things to enjoy outside of the PhD.

I want to express my gratitude to the Fonds de Recherche Québécois Nature et Technologies (FRQNT) who provided me with excellent funding during most of my PhD. The FRQNT even renewed my funding for the last year of the program and has avoided us a massive amount of financial stress. The FRQNT has also been extremely easy to work with and empathic. I also acknowledge the following sources of funding without whom my dedication to this research would not have been possible: The Ontario Graduate Scholarship (OGS) and the Cumulative Impact Monitoring Program of the Northwest Territories (CIMP NWT), the Natural Science and Engineering Research Council

(NSERC) and the Northern Scientific Training Program of Polar Knowledge of Canada (formerly from Aboriginal Affairs and Northern Development Canada) (NSTP). A lot of my professional and personal development experiences were rendered possible by the support of this funding. More details on the sources of funding are included in individual projects acknowledgment sections at the end of chapters three to six.

An enormous thank you to the Department of Geography and Environmental Studies (DGES) at Carleton who not only funded my tuition, but also allowed me to be surrounded by exceptionally intelligent and talented people. The DGES holds some of the brightest researchers studying northern Canada and I am very proud to be part of the 2021 vintage of the DGES.

Thanks to the many lab assistants who helped collect data for this thesis. The number of names in this paragraph is a demonstration that I am a cog in a much larger machine. The people I thank are (in no specific order): Michael Murphy, Mike Palmer, Brittany Astles, Christine McClelland, Sarah Sinon, Eric Guitard, Abineaga Muralitharan, Carrington Pomeroy, Emily Cormier, Evaline Harmsen, Sabrina Reaume, Hardeep Gill, Michelle Zanuttig, Fan Yang, Evelyn Tennant, Ashley Abraham and He Kang. For assistance with fieldwork, thanks to Michael Palmer, Fred Sangris, Lukas Mundy, Michael Black, Mary Black, Angus Charlo, William Lines, Katy Alambo, Mary Kelly, Maikel Rosabal, Murray Richardson, Fred Sangris, Narcisse Chocolate and Michael J. Murphy. I also want to thank the project collaborators Michael Palmer, Colin Robertson, Johanne Black, Jody Pellisey, Boyan Tracz, Sean Richardson, and Sjoerd van der Wielen.

A special thank to the Wek'èezhì Renewable Resources Board, Tłı̨ch̓ Government, the Yellowknives Dene First Nation, the Ta'an Kwäch'än Council, Tourism and Culture Yukon and the Aurora Research Institute. These organizations supported this research from day one, even before I got involved in this work.

iii. PREFACE

a. INTEGRATED MANUSCRIPTS

The material constituting chapters three to six of this thesis is adapted from manuscripts that were published in journals or are in preparation for publication at the time of the thesis submission. The original citation for these chapters are as follow:

Chapter 3: Pelletier, N., Chételat, J., Cousens, B., Zhang, S., Stepner, D., Muir, D. C. G., and Vermaire, J. C. (2020). Lead contamination from gold mining in Yellowknife Bay (Northwest Territories), reconstructed using stable lead isotopes. *Environmental Pollution*, 259. <https://doi.org/10.1016/j.envpol.2019.113888>

Chapter 4: Pelletier, N., Chételat, J., Blarquez, O., and Vermaire, J. C. (2020). Paleolimnological assessment of wildfire-derived atmospheric deposition of trace metal (loid)s and major ions to subarctic lakes (Northwest Territories, Canada). *Journal of Geophysical Research: Biogeosciences*. <https://doi.org/10.1029/2020jg005720>

Chapter 5: Pelletier, N., Chételat, J., Palmer, M.J. and Vermaire, J. C. (2021). Bog and lake sediment archives reveal a lagged response of subarctic lakes to diminishing atmospheric Hg and Pb deposition, *Science of the Total Environment*, <https://doi.org/10.1016/j.scitotenv.2021.145521>

and

Chapter 6: Pelletier, N., Chételat and Vermaire, J. C. (in preparation) Wildfires trigger multi-decadal increases in sedimentation rate and metal(loid) loading to subarctic montane lakes.

b. STATEMENTS OF CO-AUTHORSHIP

The authors of each article have read and signed the following four statements outlining the role of Nicolas Pelletier as principal investigator and main author on each publication:

- (1) I, John Chételat, as a co-author of “Lead contamination from gold mining in Yellowknife Bay (Northwest Territories), reconstructed using stable lead isotopes.”, “Paleolimnological assessment of wildfire-derived atmospheric deposition of trace metal (loid)s and major ions to subarctic lakes (Northwest Territories, Canada).”, “Bog and lake sediment archives reveal a lagged response of subarctic lakes to diminishing atmospheric Hg and Pb deposition” and “Metal remobilisation from 1958 and 1998 wildfires in lakes along the southern Klondike Highway, Whitehorse, Yukon, Canada” acknowledge Nicolas Pelletier as the principal investigator and lead contributing author to these manuscripts. Nicolas participated in the study design and the fieldwork and he was responsible for the data analysis, the writing and the revisions of the manuscripts. I, John Chételat, contributed to the published articles in Nicolas’ thesis as his supervisor during his doctoral studies in geography. My contribution comprised advice, assistance and editorial remarks related to the experimental design, fieldwork, analysis and writing of this manuscript. My activities were entirely consistent with the role of thesis supervisor.
- (2) I, Jesse C. Vermaire, as a co-author of “Lead contamination from gold mining in Yellowknife Bay (Northwest Territories), reconstructed using stable lead isotopes.”, “Paleolimnological assessment of wildfire-derived atmospheric deposition of trace metal (loid)s and major ions to subarctic lakes (Northwest Territories, Canada).”, “Bog and lake sediment archives reveal a lagged response of subarctic lakes to diminishing atmospheric Hg and Pb deposition” and “Metal remobilisation from 1958 and 1998 wildfires in lakes along the southern Klondike Highway, Whitehorse, Yukon, Canada” acknowledge Nicolas Pelletier as the principal investigator and lead contributing author

to these manuscripts. Nicolas participated in the study design and the fieldwork and he was responsible for the data analysis, the writing and the revisions of the manuscripts. I, Jesse C. Vermaire, contributed to the published articles in Nicolas' thesis as his supervisor during his doctoral studies in geography. My contribution comprised advice, assistance and editorial remarks related to the experimental design, fieldwork, analysis and writing of this manuscript. My activities were entirely consistent with the role of thesis supervisor.

(3) I, Olivier Blarquez, as a co-author of “Paleolimnological assessment of wildfire-derived atmospheric deposition of trace metal (loid)s and major ions to subarctic lakes (Northwest Territories, Canada).”, acknowledge Nicolas Pelletier as the principal investigator and lead contributing author to this manuscript. Nicolas designed and performed the study, obtained and analyzed all data, and wrote and revised the manuscript. I, Olivier Blarquez, helped designing and implementing the statistical analysis for the published article as a research partner and investigator. This involvement has also included assistance in the editorial revisions of the manuscript. These activities have been entirely consistent with the roles of research partner and investigator.

(4) I, Michael J. Palmer, as a co-author of “Peat bog and lake sediment archives reveal a lagged response of subarctic lakes to diminishing atmospheric Hg and Pb deposition” acknowledge Nicolas Pelletier as the principal investigator and lead contributing author to this manuscript. Nicolas participated in the study design and the fieldwork and he was responsible for the data analysis, the writing and the revisions of the manuscripts. I, Michael J. Palmer, was involved in this research as a research partner and investigator. This involvement has included help with the study design, field and laboratory work and editorial revision of the manuscript. These activities have been entirely consistent with the roles of research partner and investigator.

- (5) I, Brian Cousens, as a co-author of “Lead contamination from gold mining in Yellowknife Bay (Northwest Territories), reconstructed using stable lead isotopes.” acknowledge Nicolas Pelletier as the principal investigator and lead contributing author to this manuscript. Nicolas was responsible for the data analysis, the writing and the revisions of the manuscripts. I, Brian Cousens, was involved in this research as a research partner and investigator. This involvement has included help with the study design, field and laboratory work and editorial revision of the manuscript. These activities have been entirely consistent with the roles of research partner and investigator.
- (6) I, Derek Muir, as a co-author of “Lead contamination from gold mining in Yellowknife Bay (Northwest Territories), reconstructed using stable lead isotopes.” acknowledge Nicolas Pelletier as the principal investigator and lead contributing author to this manuscript. Nicolas was responsible for the data analysis, the writing and the revisions of the manuscripts. I, Derek Muir, was involved in this research as a research partner and investigator. This involvement has included help with the study design, field and laboratory work and editorial revision of the manuscript. These activities have been entirely consistent with the roles of research partner and investigator.
- (7) I, Shuangquan Zhang, as a co-author of “Lead contamination from gold mining in Yellowknife Bay (Northwest Territories), reconstructed using stable lead isotopes.” acknowledge Nicolas Pelletier as the principal investigator and lead contributing author to this manuscript. Nicolas was responsible for the data analysis, the writing and the revisions of the manuscripts. I, Shuangquan Zhang, was involved in this research as a research partner and investigator. This involvement has included help with the study design, field and laboratory work and editorial revision of the manuscript. These activities have been entirely consistent with the roles of research partner and investigator.

(8) I, Dan Stepner, as a co-author of “Lead contamination from gold mining in Yellowknife Bay (Northwest Territories), reconstructed using stable lead isotopes.” acknowledge Nicolas Pelletier as the principal investigator and lead contributing author to this manuscript. Nicolas was responsible for the data analysis, the writing and the revisions of the manuscripts. I, Dan Stepner, was involved in this research as a research partner and investigator. This involvement has included help with the study design, field and laboratory work and editorial revision of the manuscript. These activities have been entirely consistent with the roles of research partner and investigator.

Signed statements are included in Appendix A

c. COPYRIGHTED MATERIAL

The copyright for all figures from Chapter three and chapter five is held jointly by the authors and Elsevier. Inc. The copyright for all figures from Chapter four is held jointly by the authors, the American Geophysical Union (AGU) and John Wiley & Sons, Inc. Elsevier, the AGU and Wiley allow authors to use their works for teaching and scholarly purposes without having to seek special permission. Authors rights comprise the allowance to include the published material in an academic thesis or dissertation, provided that citations and DOI links back to the formal publications on ScienceDirect or Wiley Online Library are included.

d. CITING MATERIAL IN THIS THESIS

Any citation to this material should use the original published article as source. Material appearing exclusively in this thesis can be cited as follow:

Pelletier, N. (2021), Paleolimnological characterization of metal(loid) sources and transport processes in Canadian subarctic lakes, Ph.D. Thesis, Carleton University, Ottawa, ON.

iv. TABLE OF CONTENTS

i.	Abstract	iii
ii.	Acknowledgements	iv
iii.	Preface	vi
a.	Integrated manuscripts.....	vi
b.	Statements of co-authorship.....	vii
c.	Copyrighted material.....	x
d.	Citing material in this thesis	x
iv.	Table of contents	xi
v.	List of Tables.....	xvi
vi.	List of Figures.....	xvii
vii.	Acronyms	xx
1	Overview	1
1.1	Introduction.....	1
1.2	Thesis objectives.....	3
1.3	Thesis structure.....	4
2	literature review and overview of methods	5
2.1	Foreword.....	5
2.2	Sources and geochemical cycling processes for metals in subarctic environments	7
2.2.1	Sources of metals in subarctic environments.....	8
2.2.2	Transport processes to subarctic lakes.....	11
2.2.3	Anthropogenic Metals in the Arctic	21
2.2.4	Impact of climate change on subarctic metal biogeochemical cycling	24
2.2.5	Impact of land-use changes on subarctic metal biogeochemical cycling.....	27
2.3	Remobilisation of legacy pollutants	28
2.3.1	Wildfires as a remobilising agent for anthropogenic metal pollutants.....	29
2.4	Determining sources and trends of pollution from natural archives	33
2.4.1	Types of environmental archives, associated timescale and resolution	33
2.4.2	Metal concentration profile and mass accumulation rate (flux) reconstruction.....	35
2.4.3	Diagenetic modelling	39
2.4.4	Attribution science – a new frontier in paleoenvironment science.....	41
2.5	Study areas	48
2.5.1	Geophysiography of the Taiga Shield and Taiga Plains ecoregions.....	48
2.5.2	Yellowknife: Mining pollution legacy and current challenges	50
2.5.3	Whitehorse Region, Yukon, Canada	52

2.6	objectives of the individual chapters of this thesis.....	54
3	Point-source lead pollution from Gold mines in Yellowknife Bay	55
3.1	Preface.....	55
3.2	Introduction.....	55
3.3	Study area.....	57
3.4	Methods	60
3.4.1	Sample Collection.....	60
3.4.2	Chronology.....	62
3.4.3	Metals concentrations	63
3.4.4	Isotope analysis	63
3.4.5	Isotope mixing model.....	65
3.4.6	Flux calculation.....	68
3.4.7	Spatial distribution of Pb contamination and recovery models.....	68
3.5	Results	69
3.5.1	Chronologies	69
3.5.2	Isotope ratios of Pb sources	69
3.5.3	Sediment metal concentrations	71
3.5.4	Pb stable isotopes in sediment and source partitioning.....	75
3.5.5	Sedimentary Pb fluxes	77
3.5.6	Gold mining Pb contamination footprint over time	79
3.5.7	Estimation of Pb pollution from enrichment factors vs. isotope ratios.....	83
3.6	Discussion.....	85
3.6.1	Sources of Pb to Yellowknife Bay.....	85
3.6.2	Pb stable isotopes as a tool for the identification of mining pollution in sediment.....	86
3.6.3	Evidence for different metal transport processes with distance from the mines	87
3.6.4	Mining-derived Pb contamination footprint.....	87
3.6.5	Lake ecosystem recovery from Pb contamination.....	88
3.7	Conclusions	89
4	Atmospheric transport of metals and Major Ions from subarctic wildfires.....	91
4.1	Preface.....	91
4.2	Introduction.....	91
4.3	Methods	93
4.3.1	Study sites	93
4.3.2	Core collection and subsampling.....	95
4.3.3	Chronology.....	98

4.3.4	Fire reconstruction by macroscopic charcoal analysis.....	99
4.3.5	Metal and Organic Matter Concentration and Flux.....	100
4.3.6	Significance, duration and quantification of impact from wildfire atmospheric deposition. ..	102
4.3.7	Details on the Superposed Epoch Analysis	103
4.4	Results and discussion	104
4.4.1	Fire history.....	104
4.4.2	Impact of Wildfires on Metal Fluxes and Concentrations in Lake Sediment.....	108
4.4.3	Comparison with other assessments of wildfire impact on metal transport	118
4.4.4	Wildfire Impact on Mercury Deposition.....	120
4.4.5	Wildfire deposition compared to anthropogenic sources.....	122
4.5	Conclusion.....	122
5	Atmospheric deposition and catchment transport of Pb and Hg in subarctic taiga lakes determined from lake sediment and bogs archives.....	124
5.1	Preface.....	124
5.2	Introduction.....	124
5.3	Methods	127
5.3.1	Study area.....	127
5.3.2	Core collection and sample preparation	130
5.3.3	Geochemical analyses	133
5.3.4	Chronology.....	135
5.3.5	Flux calculation.....	139
5.3.6	Charcoal accumulation rate.....	143
5.3.7	Smoothing of trends from different regions and types of archive.....	143
5.4	Results	144
5.4.1	Age-depth models	144
5.4.2	Concentrations of Pb and Hg in peat and lake sediments.....	146
5.4.3	Assessment of peatland ombrotrophy.....	154
5.4.4	Lead fluxes.....	155
5.4.5	Mercury fluxes.....	161
5.4.6	Charcoal flux	166
5.4.7	Anthropogenic Pb pollution accumulation rates in lakes sediment and peat bogs	166
5.4.8	Anthropogenic Hg pollution accumulation rate in lakes sediment and peat bogs	168
5.5	Discussion.....	168
5.5.1	Pre-industrial levels of Pb and Hg accumulation near Yellowknife (NT, Canada)	169
5.5.2	Long-term cumulative impact of pollution on Pb and Hg fluxes	170

5.5.3	Long-range atmospheric Hg pollution decreased in step with declining North American emissions	171
5.5.4	The atmospheric deposition rate of Pb	172
5.5.5	Trends in Pb and Hg accumulation	172
5.5.6	Legacy metals retained in Taiga Shield catchments continue to be delivered to subarctic lakes	173
5.5.7	Impact of hydro-climatic changes	175
5.5.8	Mines, roads and wildfires	176
5.5.9	Combining peat cores and lake sediment	181
5.6	Conclusions	181
6	wildfire impact on the catchment transport of metals to subarctic montane lakes	183
6.1	Preface	183
6.2	Introduction	183
6.2.1	Historical wildfire activity in the study area	185
6.3	Methods	189
6.3.1	Sampling procedures	189
6.3.2	Charcoal analysis	189
6.3.3	Core chronology	190
6.3.4	Geochemical analysis	190
6.3.5	Ordination for elements concentration	191
6.3.6	Modelling of excess Pb, Hg and Cd	192
6.3.7	Geochemical fluxes calculation	194
6.4	Results	195
6.4.1	Fire exposure in each lake	195
6.4.2	Variation in sedimentation rate	198
6.4.3	Principal component analysis for sediment geochemistry	200
6.4.4	Concentration of Hg, Pb and Cd in lake sediment	205
6.4.5	Changes in geochemical fluxes after wildfires	208
6.4.6	Modelling of excess Hg, Pb and Cd in the sediments	210
6.5	Discussion	212
6.5.1	Geochemical impact of wildfires in lakes with minor exposure	212
6.5.2	Geochemical impact of wildfires in lakes with major exposure	215
6.5.3	Impact of the timber harvest in the burned catchment	217
6.5.4	Deposition and remobilisation of long-range and regional contaminants in subarctic Canadian lakes	217
6.5.5	Distribution of metals released by wildfires in lakes with a complex bathymetry	221

6.5.6	A proposed conceptual chart of wildfire impacts on lakes metal loading.....	223
6.6	Conclusion.....	225
7	Conclusion.....	228
7.1	Concluding statement.....	228
7.2	Suggestions for future research.....	229
8	Bibliography.....	232
9	Appendix A – Other publications and presentations related to this research.....	312

v. LIST OF TABLES

Table 2.1 Mean and standard deviation of Pb isotope values for the two sources included in the mixing model (baseline sediment and Giant and Con mine ore) as well as isotope values for other potential Pb sources.	46
Table 3.1 Name, location and description of collected sediment cores.....	61
Table 4.1: Location, core sampling depth, lake area and catchment area for each study lake sampled in 2016.	96
Table 4.2: Characteristics of each core including total length, focusing factor as determined from modelled sediment-water interface ²¹⁰ Pb flux, maximum datable depth using the CRS model, modelled age and uncertainty of oldest datable layer, range of organic matter concentration and range of charcoal particles concentration.	97
Table 4.3: Identified fire events in each core with corresponding year according to the sediment dating.	105
Table 4.4: Descriptive statistics on the absolute and relative change in fluxes of trace metals and major ions following identified fire events outside lake catchments in five lake sediment cores.....	111
Table 4.5 Descriptive statistics on the relative change in fluxes of trace metals and major ions following identified fire events outside lake catchments in five lake sediment cores.....	112
Table 4.6: Descriptive statistics on the absolute increase in concentration of trace metals and major ions following identified fire events outside lakes catchment in five lake sediment cores.....	113
Table 4.7: Descriptive statistics on the absolute and relative increase in concentration of trace metals and major ions following identified fire events outside lakes catchment in five lake sediment cores.	114
Table 5.1: Lake sediment core localisation, site description, focusing factor and core length.....	131
Table 5.2: Peat core localisation and site description.....	131
Table 5.3: Cores length, ²¹⁰ Pb inventories, surface ²¹⁰ Pb flux and focusing factor.....	132
Table 5.4: Material used for radiocarbon dating with results for each sample.	137
Table 6.1: Intercepts ± standard error, coefficients ± standard error, R and p-values for linear regressions predicting the concentration of Hg (in ng g ⁻¹) in the pre-industrial sediment of each lake.	193
Table 6.2: Intercepts ± standard error, coefficients ± standard error, R and p-values for linear regressions predicting the concentration of Pb (in µg g ⁻¹) in the pre-industrial sediment of each lake.....	193
Table 6.3: Intercepts ± standard error, coefficients ± standard error, R and p-values for linear regressions predicting the concentration of Cd (in µg g ⁻¹) in the pre-industrial sediment of each lake.	194
Table 6.4: Lake surface area with lake catchment area and surface burned during the 1957-1958 and 1998 fires.	196
Table 6.5: Components loading for PCA.....	201
Table 6.4: Mean ± standard deviation of concentration of selected metals in each core compared to reported values for rock samples from a few nearby boreholes.....	207

vi. LIST OF FIGURES

Figure 2.1: Biogeochemical cycling of metals and metalloids in the environment, adapted from Simon (2014).	8
Figure 2.2: General map of Northwestern Canada showing boundaries of Canada’s territories and major ecozones around the study sites.	49
Figure 3.1 Location of the study area within Canada (A) and on the north shore of Great Slave Lake in the Northwest Territories (B).	58
Figure 3.2 Biplot of stable Pb isotope ratios ($^{208}\text{Pb}/^{204}\text{Pb}$ and $^{206}\text{Pb}/^{207}\text{Pb}$) for sediment layers (baseline pre- 1938, and since the start of mining in Yellowknife in 1938), lichen, bedrock and ore from two gold mines. ...	66
Figure 3.3 Isotope ratios ($^{206}\text{Pb}/^{207}\text{Pb}$) in lichen samples against distance to the Giant mine roaster.	70
Figure 3.4 Lead (a) and antimony (Sb) concentrations in sediment (b), Pb stable isotope ratios ($^{206}\text{Pb}/^{207}\text{Pb}$) (c), and modelled mining-derived Pb contribution (two-source model) for each sediment core (d).	72
Figure 3.5 Concentrations of elements potentially released from mining activities, against depth in sediment cores.	74
Figure 3.6: Ratio of ^{206}Pb : ^{207}Pb vs. inverse Pb concentration for each sediment sample with a linear trend for each core.	76
Figure 3.7: Sedimentation rate estimates from CRS modelling (a), modelled Pb flux (b), modelled mining- derived Pb flux (two-source model) (c), and modelled background Pb flux (d) against sediment age for five dated sediment cores.	78
Figure 3.8: Footprint estimation for maximum mining-derived Pb contribution (a) and recent mining-derived Pb contribution (b).	81
Figure 3.9: Three-dimensional Gaussian model of mining-derived Pb contribution in the sediment layers in relation to distance from the Giant Mine roaster and age of the sediment.	82
Figure 3.10: Relative mining-derived Pb contribution against Pb concentration enrichment factor of sediment samples.	84
Figure 4.1: Map showing the locations of study lakes and documented fire scars from 1965-2016.	94
Figure 4.2: ^{210}Pb and ^{226}Ra activity per depth in lakes. Point colors indicate the laboratory that analysed the sample.	98
Figure 4.3: [left panels] Modelled charcoal accumulation rate (CHAR) at a two-year resolution against year for each site. [right panels] C_{peaks} ($\text{CHAR} - C_{\text{background}}$) against time for each site.	107
Figure 4.4: Composite response of sedimentation rates, organic matter input and element fluxes around fire events in five lakes.	109
Figure 4.5: Composite response of element concentrations around fire events occurring outside the lake catchment in five lakes.	115
Figure 4.6: Probability density distribution of flux EF in the two years following fire events compared to the previous six-years average ($n=20$).	117
Figure 5.1 Map showing the location of lakes and peat bogs sampled for this study.	129
Figure 5.2: ^{210}Pb and ^{226}Ra activity per depth in lakes.	138
Figure 5.3: ^{210}Pb and ^{226}Ra activity per depth in peat.	138
Figure 5.4: Bacon age-depth model for lakes.	145
Figure 5.5: Bacon age-depth model for peatlands.	145
Figure 5.6: Pb concentration per depth in peat cores.	147
Figure 5.7: Lead (Pb) to scandium (Sc) ratio measured by ICP-MS against peat depth with age of certain peat layers in years.	148
Figure 5.8: Pb concentration in lake sediment cores.	150
Figure 5.9: THg concentration per depth in peat cores.	151

Figure 5.10: Mercury concentration per depth in lake sediment.....	153
Figure 5.11: Ca/Mg molar ratio from ICP-MS measurement in peat samples (dark blue dots, left axis) and ash content in peat samples from loss-on-ignition at 550°C (full black line, right axis) plotted against peat depth.	155
Figure 5.12: Average long-term Pb and Hg flux in peat bogs during four key periods (pre-1800; 1800-1938; 1938-2000; 2000-2016).....	157
Figure 5.13: (a) Lead (Pb) flux in peatlands north of Great Slave Lake, NT, Canada since 0 CE.	158
Figure 5.14: FF-corrected lead (Pb) flux in lake sediment of the Canadin Shield and Taïga Plains for the period 0 -2016 CE.	158
Figure 5.15: Lead (Pb) flux in peatlands north of Great Slave Lake, NT, Canada after the post-industrial era (>1800).....	159
Figure 5.16: (a) FF-corrected lead (Pb) flux in lake sediment of the Taïga Shield and Taïga Plains for the period 1800 -2016 CE.....	160
Figure 5.17: Average long-term Pb and Hg flux in lake sediment during four key periods (pre-1800; 1800-1938; 1938-2000; 2000-2016).....	162
Figure 5.18: (a) Mercury (Hg) flux in peatlands north of Great Slave Lake, NT, Canada since 0 CE.....	163
Figure 5.19: (a) FF-corrected mercury (Hg) flux in lake sediment of the Canadin Shield and Taïga Plains for the period 0 -2016 CE.....	163
Figure 5.20: Total mercury (THg) flux in peatlands north of Great Slave Lake, NT, Canada after the post-industrial era (>1800).	164
Figure 5.21: FF-corrected mercury (Hg) flux in lake sediment of the Canadin Shield and Taïga Plains for the period 1800 -2016 CE.	165
Figure 5.22: (A) Modelled fluxes of anthropogenic Pb in peat bogs , in Taïga Plains lakes (blue triangles) and in Taïga Shield lakes; (B) Generalised additive model (GAM) of anthropogenic Pb flux using data points from peat bogs, Taïga Plains lakes and in Taïga Shield lakes.....	167
Figure 5.23: (A) Modelled fluxes of anthropogenic Hg in peat bogs, in Taïga Plains lakes and in Taïga Shield lakes; (B) Generalised additive model (GAM) of anthropogenic Hg flux using data points from peat bogs, Taïga Plains lakes and in Taïga Shield lakes.	167
Figure 5.24: Mining-derived Pb flux in peatlands including the Giant Mine peatland (a) and excluding the Giant Mine peatland (b) and mining-derived Pb flux in lakes (c)	179
Figure 5.25: Aluminum flux enrichment in lakes (a) and peatlands (b)..	180
Figure 6.1: (a) Location of lake sediment core sampled in 2018. (b), Little Fox Lake and GL (small wetland pond barely visible on this map), (c) and Fox Lake with surface shadowing to indicate topography with dashed line indicating the orientation of the profiles presented in (e). (e) Topographic cross-section of the valley crossing the sampling locations for each lake sediment cores.....	187
Figure 6.2: Fieldwork pictures of selected soil profiles in the Little Fox Lake and Little Braeburn Lake catchments.	188
Figure 6.3: Focusing-factor-corrected charcoal accumulation rates in lake sediment cores.....	197
Figure 6.4: Modelled sedimentation rate (CRS model) and uncertainties against time in each core.....	199
Figure 6.5: Principal components scores for sediment samples plotted as (a) PC1 vs. PC2 and (b) PC3 vs. PC4.	202
Figure 6.6: Principal components scores for sediment metal concentration and organic matter, by site and by sediment depth.	203
Figure 6.7: Principal components scores for sediment metal concentration and organic matter, by site and by sediment age.....	204
Figure 6.8: Element concentration profile by depth in each Yukon lake sediment core with charcoal concentration normalised (z-scored) by core.	206
Figure 6.9 Modelled fluxes corrected for sediment focusing and uncertainties for six metals.	209

Figure 6.10: Deconstructed fluxes of Hg in each lake sediment following equation 6.1 and 6.3.....	211
Figure 6.11: Deconstructed fluxes of Pb in each lake sediment following equation 6.1 and 6.2.....	211
Figure 6.12: Deconstructed fluxes of Cd in each lake sediment following equation 6.1 and 6.2.	212
Figure 6.13: Generalised additive model of excess Pb flux from 1800 to 2018 in sites from chapter five and chapter six.	218
Figure 6.14: (a) Generalised additive model of excess Hg flux from 1800 to 2018 in sites from chapter five and chapter six.;(b) Tree-rings THg concentration from North-western Yukon (Clackett et al., 2021).....	220
Figure 6.15: From Sarah Sinon Honor thesis (Carleton, 2020). Location of sample cores in Little Fox Lake overplotted on lake bathymetry.....	223

vii. ACRONYMS

^{14}C	Radiocarbon
^{210}Pb	Radigenic lead
AAS	Atomic absorption spectrometry
A_C	Catchment area
A_L	Lake area
AMAP	Arctic Monitoring and Assessment Programme
AMDE	Atmospheric mercury depletion event
ca.	circa (approximately)
$C_{\text{background}}$	background charcoal accumulation rate
CCME	Canadian Council of Ministers of the Environment
CEAA	Canadian Environmental Assessment Act
CHAR	Charcoal accumulation rate
CI	confidence interval
$C_{\text{interpolated}}$	Interpolated charcoal accumulation rate
C_{noise}	noise component in charcoal accumulation rate
C_{peak}	peak component in charcoal accumulation rate
CRM	Common reference material
CRS	Constant rate of supply
DFO	Department of Fisheries and Oceans
DMA	Direct mercury analyser
DOC	Dissolved organic carbon
ECCC	Environment and Climate Change Canada

EPA	Environmental Protection Agency
et al.	Et alia (and colleagues)
FF	Focussing factors
FRQNT	Fond Québécois de Recherche Nature et Technologies
GAM	Generalised additive model
GD-MS	Glow Discharge Mass Spectrometry
GEM	Gaseous elemental mercury
GEOS-chem	Goddard Earth Observing System atmospheric chemistry model
Gg	Gigagram (10^9 g)
GPS	Global positioning system
Hg ⁰	Gaseous elemental mercury
HgBr	Brominated mercury
HgII	Inorganic mercury
ICP-MS	Inductively coupled plasma mass spectrometry
I _{geo}	Geoaccumulation index
INAC	Indigenous and Northern Affairs Canada
ISQG	Interim sediment quality guideline
LIDAR	Light Detection and Ranging
Me ₂ Hg	Dimethyl mercury
MeHg	methylmercury
NCP	Northern Contaminant Program
NIST	National Institute of Standards and Technology
NSTP	Northern Scientific Training Program
NT	Northwest Territories

NWT	Northwest Territories
NWT CIMP	Northwest Territories Cumulative Impact Monitoring Program
OGS	Ontario Graduate Scholarship
PCA	Principal Component Analysis
PM ₁₀	Particles with a diameter between 2.5 and 10 µm
PM _{2.5}	Particles with a diameter smaller than 2.5 µm
PWGSC	Public Works and Government Services Canada
QA/QC	Quality assurance / quality control
RSD	Relative standard deviation
SEA	Superposed Epoch Analysis
SI	Supplementary information
SRM	Standard Reference Material
t _{1/2}	Half-life
THg	Total mercury
TIMS	Thermal Ionization Mass Spectrometry
UNEP	United Nations Environment Programme
USA	United States of America
USDA	United States Department of Agriculture
USEPA	United States Environmental Protection Agency
XRF	X-Ray Fluorescence

1 OVERVIEW

1.1 INTRODUCTION

Most metal(loid)s are essential micronutrients for life in trace amounts but toxic at higher doses. The anthropogenic release of metals from mines, smelters, refineries, fossil fuel burning and other industrial activities has disturbed the natural cycling of metal(loid)s at the earth's surface during the last few centuries (Brännvall et al., 1999; 2001; Cooke et al., 2009; Hillman et al., 2017; Uglietti et al., 2015; Weiss et al., 1997). Thirteen metal(loid) elements commonly released by modern anthropogenic sources are listed by the USEPA (2014) as priority pollutants to survey, including antimony (Sb), arsenic (As), beryllium (Be), cadmium (Cd), chromium (Cr), copper (Cu), lead (Pb), mercury (Hg), nickel (Ni), selenium (Se), silver (Ag), tellurium (Tl), and zinc (Zn). For most of the 20th century, anthropogenic activities were the main source of Pb, Cd and Hg, to the atmosphere and freshwater, with releases from Eurasia and America exceeding the release from all natural processes combined (E Callender, 2003; Gallon et al., 2006; Pirrone et al., 2010; Streets et al., 2017). Climate and land-use changes are also impacting the cycling of metal(loid)s in the environment, which could lead to harmful consequences for the health of biota and humans (Biswas et al., 2018; Jarsjö et al., 2020; Macdonald et al., 2005; Visser et al., 2012). For metals that can bioaccumulate in animals (e.g., Cd and Hg), even small changes in the environmental concentration or the speciation of metals can lead to significant harm to biota, and this is especially true for Hg that can also biomagnify in food chains (Ali & Khan, 2019).

In Arctic Canada, at the end of the 20th century, virtually all reported values for the concentration of Pb in freshwater exceeded the most stringent water quality guideline of 0.1 µg/L (AMAP, 1998). That is not to say that the levels of Pb are high in the Arctic (0.1 µg/L is a very low concentration), but that Pb is present to some extent even in the remotest regions of the Arctic. In some northern Canadian

lakes, Hg levels in wild fish exceeding Health Canada guidelines for domestic and commercial consumption have been reported (AMAP/UNEP, 2013). Since wild fish are important in the diet of many Canadians, especially northerners, understanding how metals impact aquatic environments can prevent potential human health and environmental problems in the future. Despite the international regulations on Pb and Hg emissions and the gradual ban on leaded gasoline in most industrialised countries, in 2009 there were still populations in northern Canada with blood Pb and Hg levels exceeding the Health Canada guidelines (AMAP, 2009). Since then, multiple countries adopted regulations for Hg emissions, including the result of the United Nations Environment Minamata Convention on Mercury (2017), presently adopted by 124 countries to this day. However, the efficiency of these policies have yet to be evaluated and many uncertainties regarding the future exposure of biota and humans to metal pollution in the Arctic remain (Ali and Khan, 2019; AMAP/UNEP, 2013; Muir et al., 2005). Three major areas of concern for contaminants in the North are (1) the ongoing impact of long-range contaminants emitted worldwide, particularly in countries where environmental regulations on metal(loid) emissions are more lenient, (2) the impact of present and future point-sources of metal(loid) near the Arctic and (3) the fate of previously emitted pollutants accumulated over the northern landscape. The recent and future climate change will impact how legacy contaminants are transported and transformed in the environment (Jarsjö et al., 2020; Klaminder et al., 2010; ydberg et al., 2010; Spence et al., 2015). All these pressures on Arctic metal(loid) biogeochemical cycling are occurring simultaneously and have a cumulative impact. The Canadian Environmental Assessment Act (*Canadian Environmental Assessment Act*, 2012) includes a dedication to studying the cumulative effect of long-range pollution, point source pollution, remobilisation of legacy pollution and changes in the physical environment that could affect biota and humans in the near and far future.

Evaluating and quantifying the individual and cumulative impacts of multiple concurrent environmental changes is a scientific challenge that must be addressed to protect vulnerable populations and wildlife. This thesis is a multi-regional assessment of how aquatic metal(loid) accumulation in a subarctic region of Canada was impacted by the successive pressure of long-range pollution, local mining pollution, land-use change and climate change. Adopting a geographic perspective, i.e., one that addresses problem from a space-specific or regional point of view, is valuable to disentangle the multiplicity of environmental changes affecting subarctic Canada. Local-based information provided an integrated view of impact that is relevant to a specific and tangible context, and it can also be integrated for larger-scale meta-analyses.

In this thesis, geochemical time series are generated from environmental archives and analysed to determine the impact of specific anthropogenic and natural disturbances to the transport and deposition of metal(loids) in subarctic Canada. The components of metal(loid) transport and fate evaluated in this thesis are relevant to subarctic Canada, and include mining activities, climate change, land-use and wildfires. This thesis provides ground-based observations and long-term records that provide new insights to understand how subarctic Canada has responded to the anthropogenic emissions of metals and how natural and anthropogenic metals will be transported toward lakes by processes that are becoming increasingly climate changes such as wildfires and changes in catchment hydrology.

1.2 THESIS OBJECTIVES

This thesis uses paleoecology and paleolimnology to improve our understanding of metal cycling in northern environments by quantifying the impact of specific transport processes between the atmosphere, terrestrial catchments and aquatic environments in subarctic Canada. Multiple methods are explored to determine trends of accumulation and deconstruct paleolimnological records to

distinguish the impact of individual processes on metal loading in lakes. The outcomes of this research will provide evidence to better quantify long-range, local, and remobilized metal pollution in aquatic environments and in the atmosphere over the last few centuries. Multiple lines of geochemical evidence and a combination of two types of environmental archives (peat and lake sediments) are incorporated to evaluate the individual and cumulative impacts of different sources and transport processes for metals in the subarctic landscape. The general goals of this thesis are to:

- Assess the long-term (millennial) cumulative impacts of the regional and long-range anthropogenic emissions of Pb and Hg on the atmospheric deposition of these elements and their accumulation in subarctic Canadian lakes.
- Evaluate the recovery of subarctic Canadian lakes after the (inter)national regulation of Pb and Hg emissions and the reduction of the atmospheric emissions of these contaminants.
- Measure the individual and cumulative impact of some key sources and transport processes impacting subarctic Canadian lake sediment metal loading (i.e., mining, wildfires, erosion) using paleoenvironmental records.

Altogether, this work addresses various pathways of terrestrial metal transport relevant to lakes of the subarctic boreal region. Novel approaches were used to (1) deconstruct the influence of multiple contributors to metal accumulation and (2) untangle the effects of remobilised legacy pollution and modern anthropogenic pollution (local and global) in paleolimnological records. The specific objectives of each individual chapter are presented in chapter 2.6 of the thesis.

1.3 THESIS STRUCTURE

This thesis is in article-compilation format. The bulk of the document is four chapters based on published articles or articles in preparation for publication addressing the objective outlined in section 1.2. The research articles are preceded by an introduction chapter (chapter 2) covering topics relevant

to the integrated research articles. Chapter 2 is divided into six sections including (1) foreword, (2) the sources and geochemical cycling processes for metals in subarctic environments, (3) a literature review on the remobilisation of legacy pollutants toward lakes, (4) a review of paleolimnological methods to evaluate past changes in metal biogeochemistry and predict future trends, (5) a geographic description of the two study regions and (6) an overview of the current research gaps and uncertainties addressed in this thesis. The integrated manuscripts constitute chapters three to six and are followed by a conclusion chapter (chapter seven) relating the outcomes of each chapter and the intersectionality of the findings of each section. To avoid repetition, chapters three to six are not verbatim reproduction of the published manuscripts. Specifically, part of the introduction and methods section of published manuscripts were re-written or removed from the thesis version to avoid repetition but the results, discussion and conclusions sections remained unchanged with the exception that figures in tables included as supplementary information in the published journal articles are now integrated to the corresponding chapters.

2 LITERATURE REVIEW AND OVERVIEW OF METHODS

2.1 FOREWORD

Metal(loid)s are naturally occurring elements found in variable concentration in the earth's crust. The term metal(loid) comprises elements classified as metals, the largest class of elements in the periodic table, and the six metalloid elements (B, Si, Ge, As, Sb and Te). Although most themes, processes and research questions addressed in the background section of this thesis could apply to both metal and metalloids elements, the term "metal" is preferred to "metal(loid)" for brevity and readability after this point in this thesis.

The biological uptake of metals occurs when plants and micro-organisms incorporate metals from the atmosphere (Luo et al., 2019; Naharro et al., 2018; Obrist et al., 2017; Wang et al., 2012), from soil or

sediments (Klaminder et al., 2005; Naharro et al., 2018), or from solution (de Paiva Magalhães et al., 2015; Rieuwerts et al., 2015; Violante et al., 2010). Once metals enter living organisms, they bioaccumulate if the rate of intake exceeds the elimination rate in individual organisms. Bioaccumulation potential varies by organism, metal speciation and environmental conditions (pH, redox, presence of organic matter) (Ali et al., 2019; Shtangeeva, 1995), but some metals are invariably eliminated at a slower rate from organisms and therefore have a greater bioaccumulation potential. The metal with the greatest bioaccumulation potential is Hg in its methylated form (MeHg), which is released largely under anoxic conditions by sulphur-reducing bacteria (Matilainen, 1995). MeHg also has the potential to biomagnify in food chains, a phenomenon where species at a higher trophic level are accumulating greater concentrations of toxic elements than organisms lower in the food chain (Lehnherr, 2014). There is now growing scientific evidence that exposure to low levels of contaminants in the environment is contributing to society's cancer burden and health hazard (Saaristo et al., 2018). The most environmentally hazardous metals, i.e. those that are most frequently reported as problematic in environmental studies, include Cr, Ni, Cu, Zn, Cd, Pb, Hg, and As (Ali et al., 2019).

One important pathway for metal contamination in humans is the consumption of animals with high metals concentration as a result of environmental bioaccumulation and biomagnification (Ali et al., 2019; Ali and Khan, 2019). The impact of bioaccumulation and biomagnification are most important for MeHg accumulation in large predatory fish that have a high trophic level (Chen et al., 2008; Watras et al., 1998). Toxic metals can have a wide range of known impacts on human health, including damage to organs and bones, developmental problem in foetus and child, cancer and cognitive dysfunction, to name a few (Tchounwou et al., 2012). Other problems are more insidious and less understood, like the impact of lead on brain function, which could favor impulsivity and violent behavior even at doses that are below accepted toxic thresholds (Barrett, 2017; Mielke and Zahran, 2012; Stretesky and Lynch,

2001). For instance, a study looking at crime rate fluctuations in eight major USA cities found that the 1950–1985 fluctuation of Pb emissions explained 90% of the aggravated assault variation and that each 1% increase in local Pb release led to a 0.46% increase in aggravated assaults with a lag of 22 years (linked to the time for children to become adult) (Mielke and Zahran, 2012).

Metal pollution is primarily a post-WWII environmental science problem that remains pertinent to this day. The complexity of metal geochemical cycling, the inclusion of new anthropogenic sources and the new interrelations with climate science keeps the topic relevant. Developing our understanding of metal transport and transformation processes in the environment will allow us to better control our impacts on these cycles and predict the outcomes from conditions that are proving more difficult to control, such as climate change.

2.2 SOURCES AND GEOCHEMICAL CYCLING PROCESSES FOR METALS IN SUBARCTIC ENVIRONMENTS

Metals circulate between the lithosphere (bedrock), pedosphere (soils), atmosphere, hydrosphere (streams, rivers, lakes and oceans), biosphere (living organisms) and, in northern environments, the cryosphere (snow, ice and permafrost) (Figure 2.1). The internal cycling, transport and transformation processes occurring within any sphere are outlined in sections 2.2.1 to 2.2.5.

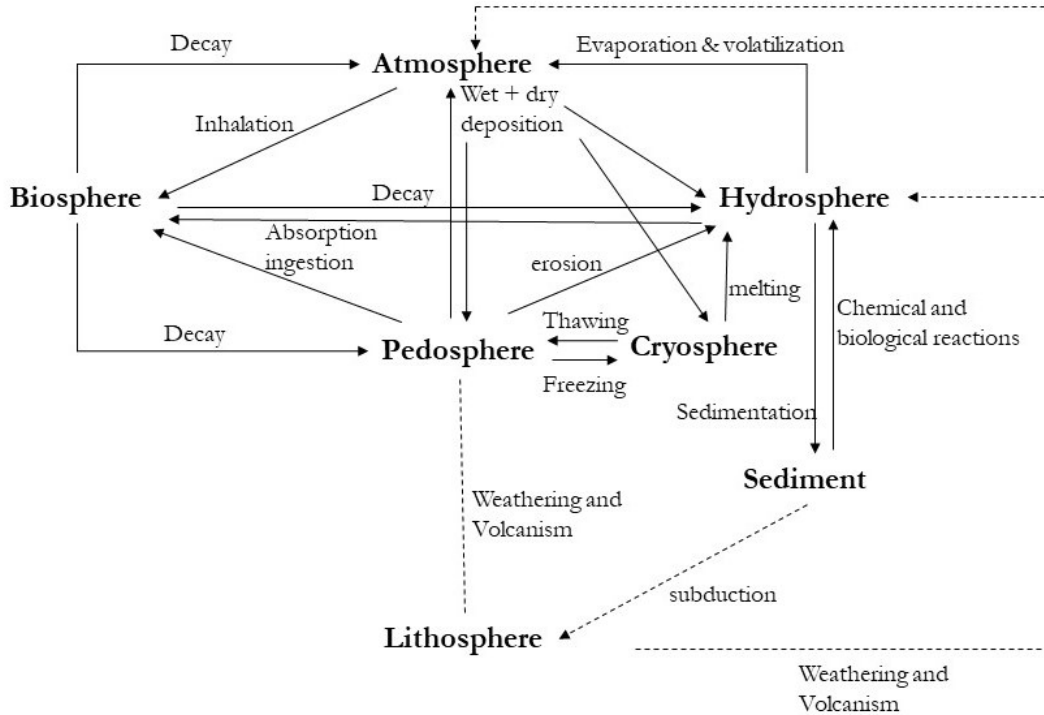


Figure 2.1: Biogeochemical cycling of metals and metalloids in the environment, adapted from Simon (2014). Dashed arrows occur at a geological timescale, whereas full arrows represent more rapid (yearly to centennial timescale) processes.

At a geological timescale, the ultimate fate of any metal released from the lithosphere, which is the largest reservoir, is burial in marine sediments and re-inclusion to the earth's crust in active subduction zones. On a timescale more useful to human environmental management, soils, lacustrine and marine sediments are long-term, stable reservoirs, whereas the atmosphere and the hydrosphere are reservoirs with shorter residence time (Hughes, 1981).

2.2.1 Sources of metals in subarctic environments

All metals in the environment have a common origin in the Earth's mantle and crust. The main natural sources of metals at the earth's surface are volcanic activity and bedrock weathering (Bradl, 2005; Tchounwou et al., 2012). Mining and metallurgical processing of ore since the bronze age (~3000 BC)

is the first historical source of anthropogenic metals to the environment. Over human history, the anthropogenic emissions of metals to the environment increased by orders of magnitude following technological developments in ore smelting (including artisanal mining), industrial processes, fossil fuel extraction, refining and burning, wastewater treatment and waste incineration (Bradl, 2005; Kirk and Gleason, 2015; Tchounwou et al., 2012).

The impact of metal emissions can be characterised at two spatial scales: point-source pollution and global long-range pollution. Point-source pollution is defined by the close-range impact of pollution sources. Most particulates released by industrial processes and in urban centers accumulate in soils, vegetation and water at a close distance from the emission source and the impact decreases with increasing distance from the emissions source (Hocking et al., 1978; Sherman et al., 2015; Wiklund et al., 2017). Elements released by point-sources can be spatially constrained because they are emitted in a constrained medium (e.g., a lake or a watershed) or because their residence time in that medium is short (e.g., most particulate metal in the atmosphere). Heavy metal point-source pollution in northern Canada occurs near mines and metal smelters, coal-burning power stations, incinerators and where hydroelectric reservoirs were created (UNEP, 2013). Mining is a major economic activity in remote Canadian regions, and it comprises the largest portion of sites affected by point-source pollution in the Canadian North (UNEP, 2013). Mining pollution arises from the release from bedrock and ore of dust, sediments, and leachates carrying high levels of metals in the environment. Mining activities also have multiple other effects on freshwater environments that are beyond the scope of this research such as acid-mine drainage, salinization, and eutrophication (Leppanen et al., 2017).

Long-range global pollution describes the part of emissions entering global circulation patterns and affecting metal biogeochemical cycling at a large spatial scale (continental, global). Any atmospheric emission source, natural or anthropogenic, has an impact on long-range pollution to a certain extent

when metals in solid (aerosols) or gaseous phase (for Hg) are transported within atmospheric circulation cells. Near a point-source, the influence of atmospheric deposition from long-range sources may be negligible for many elements compared to the relatively large impact of the point-source (e.g. Roberts et al., 2020; Watmough and Dillon, 2007; Wiklund et al., 2017), but long-range pollution can have a notable impact on otherwise pristine, remote environments (Barrie et al., 1992; Catalan et al., 2013; Kirk et al., 2012; Perez-Rodriguez et al., 2018). In the Arctic, the circumpolar westerlies (Polar Vortex) form an extensive low-pressure system. The high-pressure system over Siberia and the low-pressure system over the Aleutian Islands allows the transport of air masses from Southeast Asia, China, and Japan towards Alaska and Northwestern Canada (Chen et al., 2014; Durnford et al., 2010). Seasonal and climatic variations affect the span of the polar vortex, which can transport air masses from lower latitudes, where metals are emitted in industrial centers (Sturges and Barrie, 1989; Wilkie and La Farge, 2011). In remote areas, long-range atmospheric transport from Asia, Russia, USA and Europe represent most of the anthropogenic metal deposition to the Arctic and subarctic regions of North America (AMAP/UNEP, 2013). Therefore, most Hg in the Arctic comes from distant sources, outside Canadian territory (Dastoor et al., 2015; UNEP, 2013; Simonetti et al., 2003; Zdanowicz et al., 2017).

The situation of Arctic and subarctic regions of the world is particular in that these regions receive a disproportionate amount of long-range pollution emitted at lower latitudes in proportion to the scarcity of sources located within the Arctic circle (Dastoor et al., 2015; Durnford et al., 2010; Pacyna and Keeler, 1995). The convergence of air masses toward the pole and low northern temperatures favorize atmospheric deposition of contaminants in the Arctic and subarctic region (Dastoor et al., 2015; Douglas and Blum, 2019; Outridge et al., 2002). The Arctic Ocean also receives marine metals from ocean currents and continental tributaries entering the Beaufort gyre (Gobeil et al., 2001; Outridge et al., 2008; Soerensen et al., 2016). However, the processes governing the accumulation of

metals in the Arctic environment should not be confused with the “global distillation” or “grasshopper effect” that applies to certain chemicals such as persistent organic pollutants (Gouin et al., 2004).

2.2.2 Transport processes to subarctic lakes

2.2.2.1 Atmospheric deposition

Solid-phase metals have a residence time in the atmosphere that is inversely related to the size of the suspended particles (Mamun et al., 2020). Mercury (Hg) is the only metal with an important gaseous phase (Hg⁰) at the earth’s normal atmospheric temperature and pressure, and this element can therefore reside in the atmosphere for periods varying between several months up to a year and a half (Driscoll et al., 2013; Holmes et al., 2010; Schroeder and Munthe, 1998). The current section (2.2.2.1) will discuss atmospheric deposition of non-gaseous metals, and atmospheric Hg⁰ deposition will be addressed in the section on mercury biogeochemistry (2.2.2.4).

In atmospheric studies, particulates bearing metals in the atmosphere are classified according to their size. An aerosol is a general term that defines small particles that can remain suspended in the atmosphere, but there is no convention on the minimum and maximum diameter that a particle must have in order to be classified as an aerosol. Specific sub-orders of aerosols have been determined for the threshold diameters of 2.5-10 µm (coarse mode, PM₁₀), and <2.5 µm (fine mode, PM_{2.5}). The PM_{2.5}/PM₁₀ designation is a frequently reported measure of size distribution of aerosols in the atmosphere. Metals from natural sources (released from crustal erosion and volcanoes) typically have a lower PM_{2.5}/PM₁₀ ratio (coarser particulates) and therefore have a shorter residence time in the atmosphere compared to anthropogenic metals released by most industrial processes (Mamun et al., 2020). Atmospheric metals precipitate on land by dry deposition, i.e. the deposition of solid-phase particles, or by wet deposition, i.e. the coalescence of metals to rain and snow precipitation (Galloway et al., 1982). The dry deposition rate is typically higher for natural metals than anthropogenically released metals (Mamun et al., 2020). For example, in Greenland, the dry deposition typically

contributes less than 25 % of the total anthropogenic contaminant deposition, with wet deposition covering the majority (>75%) of this flux (Davidson et al., 1981). The dry atmospheric deposition rate of metals depends on parameters such as micrometeorology, geophysical region (soil and bedrock composition) and proximity to natural and anthropogenic sources (Connan et al., 2013; Pryor et al., 2008). Wet deposition rates are influenced by similar parameters to dry deposition with an additional dominant influence of local climate, particularly the frequency of precipitation (rain/snow) and the occurrence of fog (Barrie and Schemenauer, 1989; Rohbock, 1982). Rainfall intensity and particulate matter diameter also influence wet deposition efficiency (Wu et al., 2018). Regions experiencing greater atmospheric concentrations of particulate metals and greater annual precipitation have a larger proportion of metals deposited in wet deposition compared to dry deposition (Rohbock, 1982).

Fine particulates bearing atmospheric metals can be transported within air masses at thousand of km from their emission source before touching ground (Chen et al., 2013; Steinnes and Friedland, 2006). Air masses containing large amounts of aerosol can cross continental and international boundaries (Csavina et al., 2012) and are an important source of metals to remote environments such as the Arctic (Barrie et al., 1992). In Arctic and subarctic regions, there are few long-term records of direct measurements of wet or dry metal deposition (Dastoor et al., 2015) and none that covers more than 20 years. Recent research on Arctic Hg is putting a lot of emphasis on monitoring wet and dry Hg deposition to better constrain global circulation and transformation models (Steffen et al., 2015).

2.2.2.2 Catchment contribution

A varying proportion of material accumulating in lake water and sediment is derived from the lake catchment soils through surface and ground water flows. The lake catchment size, topography, vegetation, and soil composition (texture and organic matter) dictate the extent with which metals can be transported towards the lake (Rosen, 2015). Climate will also impact the transfer of terrestrial metals to downstream environments, including lakes, through the type, magnitude and timing of

precipitation, and the hydrological response of soils (Jarsjö et al., 2020; Spence et al., 2015). The impact of climate in temperate and subarctic regions will partly depend on how the contact between groundwater and the highly water-conducting and geochemically heterogeneous topsoil layers will change in the future (Jarsjö et al., 2020).

Lake catchment size is a determining factor for the transport of contaminants for two reasons. First, larger catchments comprise a greater amount of soil and, therefore, a larger reservoir of leachable metals. Second, a lake's catchment has a funneling effect on atmospheric deposition, acquiring atmospheric deposition over a larger area. In other words, all things otherwise equal, larger catchments naturally contain more metals susceptible to be transported by groundwater flow and have the potential to concentrate greater amounts of atmospheric deposition in the same area. The catchment area is a good predictor of the metal flux that can be transported toward lakes when the regional atmospheric deposition is known (Blais and Kalff, 1993; 1995; Foster and Charlesworth, 1996). Similarly, this calculation can be done backward, i.e. when the catchment size is known along with the catchment retention ratio for an element of interest, one can estimate the regional atmospheric deposition from the accumulation rates per area in lake sediments (e.g. in $\text{g m}^{-2} \text{yr}^{-1}$). Typically, in temperate and subarctic catchments most ($\geq 70\%$) atmospherically deposited metals are retained and delivered to streams and lakes subsequently (Blais and Kalff, 1993; Ukonmaanaho et al., 2001). The retention of atmospheric metal deposition is even more important for some elements like Cu and Pb, of which 94-97% of the deposited mass can be retained in catchment soils following deposition (Ukonmaanaho et al., 2001) with some authors suggesting complete retention of atmospherically deposited anthropogenic Pb (Blais and Kalff, 1993). When multiple lakes with varying catchment size are compared in the same study, one approach to normalise observed flux is to correct them by the ratio of catchment area to lake surface area ($A_C:A_L$ ratio) or the ratio of catchment area to lake volume (Bindler et al., 2008; Blais and Kalff, 1993). Swain et al. (1992) determined that over the same study

region, lake sediment Hg flux is linearly related to the $A_C:A_L$ ratio and flux can be deconstructed following equation 2.1:

Eq. 2.1
$$F = a + b \times \frac{A_C}{A_L}$$

Where F is Hg flux in lake sediments, A_C/A_L is the ratio of terrestrial catchment area (A_C) to lake area (A_L), a is the atmospheric deposition (also the intercept where catchment size is null) and b is a regional constant representing the amount of Hg accumulated in catchment soils in the study region. The metal accumulation in lakes with a lower $A_C:A_L$ ratio (smaller catchments) is inevitably more sensitive to variations in atmospheric deposition, making them better archives of atmospheric deposition than larger catchment lakes (Yang, 2015a).

Topography is important in controlling water residence time in catchments following precipitation (McGuire et al., 2005), and is therefore important in modulating catchment surface flow, soil erosion rates and catchment metal retention (Foster and Charlesworth, 1996; Rose et al., 2012; Wällstedt et al., 2017). Vegetation can alter catchment water flow and limit soil erosion. For example, logging operations and wildfires that deplete vegetation can increase catchment soil erosion and the transport of metals to streams and lakes by orders of magnitude (Garcia and Carignan, 1999; Ice et al., 2004; Nappi et al., 2004), and this impact is amplified in catchments that have a steep topography compared to flatter catchments (Davis et al., 2006; Eckley et al., 2018). The parent material (surficial and bedrock geology) is important because it defines the baseline metal concentration and distribution in soils (Utermann et al., 2019; Wuana and Okieimen, 2011). The presence of organic matter and the drainage potential (i.e. soil texture) are important characteristics that mediate the potential of soils to sequester metals from atmospheric deposition or waste water pollution (Quenea et al., 2009; Rieuwerts et al., 2015; Tomlin et al., 1993).

The parent geology of soils explains the large variability in soil metal concentration in the absence of contamination (Utermann et al., 2019; Wuana and Okieimen, 2011). The soils metal pool is comprised of inert, non-labile and labile metals (Figure 1). The inert metal fraction comprises the metals included within the lattice of clay particles or within the structure of larger mineral particles and the resistant metal compounds that can be inorganic (sulphides, phosphate and carbonates) or organic; natural or anthropogenic (fragments, vitrified particles) but that can only be solubilised over very long periods of time (Young, 2013). The labile metals are those electrostatically held in clay interlayers, those adsorbed onto humus acids or to Fe/Mn/Al hydrous oxides and those at solubility equilibrium with the soil solution (Young, 2013). The labile metals respond immediately to changes in the soil solution equilibrium and can therefore be rapidly transferred to the soil solution or absorbed to a different particle (Guzman-Rangel et al., 2020; Young et al., 2000). Metal ions in aqueous solution are the most biologically available form of metals (Rieuwerts et al., 2015) and these cations are released mostly from the labile fraction of the metal pool, with a slower/smaller contribution from the non-labile metal pool (Figure 1).

A mass balance of metals in forest soil can be expressed following equation 2.2, adapted from an equation for the mass balance of heavy metals in agricultural soils (Wuana and Okieimen, 2011):

Eq. 2.2
$$M_{total} = M_p + M_a + M_d + M_{ip} + M_{lf} - M_{br} - M_l$$

where “*M*” is the metal, “*p*” is the parent material, “*a*” is the atmospheric deposition, “*lf*” is the decaying vegetation in the soil litter and standing biomass, “*ip*” are inorganic pollutants, “*br*” is live biomass removal, and “*l*” is the losses by leaching, volatilization, and so forth.

In subarctic environments, the snowpack is a short-term reservoir for metals deposited from the atmosphere to the catchments over winter (Zdanowicz et al., 2017). At snowmelt, metals remaining in the snowpack are largely transported toward streams and a fraction accumulates in soils (Yuan et

al., 2018). Like other metals Hg can accumulate in snowpack during winter through dry and wet deposition and can be released to streams, lakes, and oceans during spring (Marlon et al., 2012; Zdanowicz et al., 2017), but contrarily to other metals, a portion of Hg accumulating in the snowpack is re-emitted to the atmosphere through volatilisation processes (Durnford and Dastoor, 2011).

Before the turn of the 20th century, Arctic soils and plants had received atmospherically deposited metals emitted by industrial activities, metal production and the burning of fossil fuel (Klaminder et al., 2005; Bindler et al., 2008; Obrist et al., 2017). It is therefore inevitable that the contribution of lake catchments to lake metal loading should have increased over time. Northern boreal forests and peatlands have a high potential to accumulate and sequester Hg over millenia (Grigal, 2003) and Pb has an average residence time of 250 years in the surface organic layer of boreal soils (Bindler et al., 2008). In Sweden it was estimated that the Pb residence time in upper organic soils before migrating through the soil profile is at a centennial to millennial time scale (Klaminder et al., 2006). Soils are the largest Hg pool in the global biogeochemical cycle with a stock of 250–1000 Gg Hg (Horowitz et al., 2014).

2.2.2.3 Internal cycling in lakes

Metals enter freshwater bodies via direct atmospheric deposition (wet and dry) at the surface of streams and lakes and via catchment transport from groundwater flow, overland flow and tributaries when present (Callender and Granina, 1997; Engstrom and Rose, 2013; Rosen, 2015). Metals in water can exist in soluble phase at low concentration, but most are found in solid phase or adsorbed to solid particulates that can be suspended in the water or deposited at the bottom of the lake, after which they become classified as sediments (Figure 2). Metal solubility in water depends on pH and redox conditions (Chuan et al., 1996). Important reactions which may remove soluble elements from the water include adsorption reactions that involve cation or ligand exchange and precipitation reactions

(oxides, hydroxides, carbonates, silicates, phosphates, or sulfides) (Elbaz-Poulichet et al., 1996; McComb, 2014).

The stability of metals in lake sediments depends on sediment disturbance or migration, redox remobilization and chemical interactions between metals in sediments and porewater (Boyle, 2001; Outridge and Wang, 2015a). Most metals of environmental concern have a reactive solid phase that easily and tightly binds with organic matter or Fe- and Mn- oxyhydroxides (Emerson and Hedges, 2003). Arsenic, antimony, and molybdenum preferentially attach to oxyhydroxides, whereas mercury, silver, copper, cadmium, and zinc preferentially bond to organic matter (Feyte et al., 2010). Some strong electrostatic bonds formed with mineral or organic particles can prevent the release of metals to the water column even in the case where sediments are mechanically or biologically resuspended (Fetters et al., 2016). Hg, Cd, Cu, Pb, and Zn are considered very stable once deposited in sediments (Lockhart et al., 2000; Rydberg et al., 2008; Percival and Outridge, 2013). However, evidence suggests that post-remobilization of these elements becomes significant at extremely low sediment mass accumulation rates such as in the high Arctic Ocean (Gobeil et al., 1999; Boyle, 2001).

Zn, Cd, Pb, Ni and Cu are stable in naturally occurring speciation but can be affected by diagenetic processes when released from high-temperature sources such as metal smelters and coal-fired plants (Outridge and Wang 2015). Some metals have more than one oxidation state in lake sediments and can, therefore, undergo diffusive migration in response to redox gradients, such as As, Co, Cr and V (Boyle, 2001; Palmer et al., 2019). Other metals affected by diagenesis include Cd (Alfaro-de la Torre and Tessier 2002), P (Rydin et al., 2000), Tl (Laforte et al., 2005), Re (Chappaz et al., 2008b), Sb (Chen et al., 2003) and Mo (Chappaz et al., 2008a). In subarctic lakes, seasonality can have a strong influence on metal stability in sediment when ice-covered lakes develop an important redox gradient as anoxia builds up in the water column over winter (Palmer et al., 2019).

For metals that are stable in sediments, sedimentation in lakes can be considered a final end-member of metal transport since the residence time of these elements, especially once buried under metres of sediments, approach a geological timescale (Yao and Gao, 2007). Metals in marine sediments have an even longer residence time and can eventually be transported back to the earth's crust and mantle through subduction at active tectonic margins.

2.2.2.4 Mercury biogeochemistry

A separate section on Hg biogeochemistry is necessary because of the importance of Hg in environmental science, the focus on Hg research in this thesis and the unique nature of Hg chemistry compared to other metals and metalloids. There are three main forms of Hg in the environment, each with its own subset of phases and chemical associations. Particulate and gaseous inorganic mercury (HgII and Hg0) are emitted to the atmosphere naturally by volcanic activity. Hg0 is a volatile species that has the potential to travel long distance whereas HgII is found in larger compounds and particulate form (Pirrone et al. 2009). In the atmosphere, HgII can be oxidized to Hg0, and the most plausible pathway is a two-step process where Hg0 reacts with a Br radical to form HgBr. HgBr then reacts with multiple potential oxidants to generate different HgII species (Horowitz et al. 2017). The photoreduction of HgII in the atmosphere is still poorly understood but evidence suggest that in-clouds processes account for most of the atmospheric HgII photoreduction (Horowitz et al. 2017).

The deposition of sea-salt aerosols is the major pathway delivering HgII from the atmosphere to the ocean. (Holmes et al. 2009). A large fraction of Hg deposition occurs as wet deposition in oceans, lands and lakes surface since HgII is relatively soluble in water (Prestbo and Gay 2009). Recent advances in Hg stable isotope analysis (see section 3.2) revealed that dry deposition processes such as foliar uptake by vegetation dominate the deposition in remote terrestrial environments (Enrico et al. 2016; Obrist et al. 2017). The main source of Hg to oceans is the atmospheric deposition of HgII (Driscoll et al. 2013). The erosion of soil and bedrock from the continental shelf also releases

particulate and dissolved inorganic Hg (HgII) that is transported to marine environments and can account for a substantial portion of the mercury loading in nearshore systems and the Arctic Ocean (Amos et al. 2013). Once in the marine environment, HgII can be: (1) reduced to Hg⁰ and evaded to the atmosphere, (2) methylated to either CH₃Hg⁺ (MeHg, methylmercury) or (CH₃)₂Hg (Me₂Hg, dimethylmercury) and scavenged from the water column or (3) deposited in sediments as HgII (Mason et al. 2012). The processes of reduction to Hg⁰ and evasion to the atmosphere is a particularly important mechanism to remove Hg from the ocean, with evasion fluxes removing 50–80% of gross loadings from the atmosphere (Lamborg et al. 2014). Both photochemical degradation and biological reactions are acting rapidly to reduce Hg in the water column (Mason et al. 1995; Qureshi et al. 2010). Biological processes are more important in nearshore environments where productivity is greatest and photochemical degradation is more important than in open oceans, where light penetration is deeper and biological productivity less (Lamborg et al. 2014). The ultimate sink for Hg in the marine or freshwater environment is the burial in sediments, but Hg speciation can vary in the sediments in response to abiotic and biotic processes (Lamborg et al. 2014).

Lakes receive Hg from atmospheric deposition, catchment runoff and the discharge of Hg-containing effluents near anthropogenic activities. In locations not affected by point-source Hg discharge, the relative importance of atmospheric deposition and catchment runoff to total Hg loading depends on the lake area to depth ratio and the catchment area to lake area ratio (Obrist et al. 2018). Comparative studies using Hg stable isotopes (see section 3.2) observed that remote Canadian lakes and Lakes Huron, Superior and Michigan were dominated by atmospheric deposition whereas catchment influence and wastewater efflux were the dominant sources to Lakes Erie and Ontario (Lepak et al. 2015; Chen et al. 2016). Hg enters inland water bodies primarily as HgII and is oxidized to Hg⁰ or methylated to MeHg or Me₂Hg. A large fraction of Hg⁰ is re-emitted to the atmosphere while another fraction can be reduced back to HgII. Over time, HgII and MeHg are deposited with the sediments

where its speciation can change as it is affected by methylation, demethylation or oxidation/reduction. Inorganic Hg can be methylated by micro-organisms in the water column, in the sediments or wet soils. Sulfate-reducing bacteria are responsible for most of the transformation of Hg from inorganic to methylated form (Compeau and Bartha 1985; Gilmour et al. 1992). Demethylation occurs simultaneously in the sites where methylation takes place (Li and Cai 2013). Demethylation of MeHg mainly occurs through biotic processes in the sediments, and through photo-demethylation in the water column. The latter process accounts for the degradation of up to 80% of MeHg entering lakes (Seller et al. 1996). MeHg that is not methylated can be consumed by organisms where it bioaccumulates and transfers to species of increasingly high trophic position (Morel et al. 1998).

In terrestrial environments, the largest available Hg pools (not included in rock formations) are soils (Grigal 2003). The same processes govern the speciation of mercury in soils and in aquatic ecosystems, but methylation is more efficient in wet environments with reducing conditions, and in the presence of dissolved organic matter (Ravichandran 2004; Graham et al. 2012). For these reasons, wetlands are a particular hotspot for terrestrial mercury methylation (St. Louis et al. 1994; Selvendiran et al. 2008). Atmospheric deposition is the main contributor to Hg in most organic-rich upper soils (Obrist et al. 2017; Wang et al. 2017; Enrico et al. 2016), but a fraction of Hg near mineral layers comes from geologic sources (Obrist et al. 2018).

Atmospheric Mercury Depletion Events (AMDE) occur in coastal areas in Arctic and Antarctic regions during polar sunrise. For a brief period, reactive gaseous Hg is rapidly formed through in-situ oxidation of gaseous Hg⁰ by halogens, leading to high Hg deposition fluxes (Carignan and Sonke, 2010). In Canada, AMDEs do not occur in continental (inland) areas (Steffen et al., 2015) and are therefore not impacting the study sites in this thesis. In a study in Alaska, (Johnson et al., 2008) found that early spring AMDE were the main source of Hg to snowpack and that loads of Hg remained

fairly constant from the springtime AMDE season to snowmelt. Contrarily, other modeling studies have shown high levels of volatilization of Hg deposited on the snowpack over the winter period (Durnford et al., 2012).

2.2.3 Anthropogenic Metals in the Arctic

2.2.3.1 Lead (Pb)

Lead has been recognised as a toxic element since antiquity, making it one of the oldest known metals in human history (Riva et al., 2012). For millennia, it has been one of the most widely mined and processed metal for its low melting temperature, resistance to corrosion and abundance in the environment. Arctic Pb pollution is about as old as its usage by Europeans and Pre-colonial American civilisations. The first reported evidence of anthropogenic Pb pollution in remote Arctic environments came from glacier records from the 1960s showing aerosol Pb concentration 300 times greater than 3000 years ago (Murozumi et al., 1969). This finding was corroborated by multiple types of paleoenvironmental records that concluded Pb deposition has increased by hundreds of folds over the last millennia, including glacier (Gabrielli and Vallelonga, 2015), lake sediment (Klaminder et al., 2010; Perez-Rodriguez et al., 2018) and peat cores (Hansson et al., 2017; Talbot et al., 2017).

Most anthropogenic Pb-bearing atmospheric dust reaching the Canadian Arctic has a mass median diameter $<10 \mu\text{m}$ (Prospero, 1999) and fine and ultra-fine dust (<2.5 and $<0.66 \mu\text{m}$ respectively) often dominates the transport profiles (Chen et al., 2013). This fine dust can be transported thousands of kilometers from their source following global atmospheric cells (Sturges and Barrie, 1989; Zhang et al., 2015). Lake sediment reconstructions that included stable isotope measurements show changes in Pb source occurring during the Roman (~ 1 AD) and the Medieval period (~ 1200 AD) in lakes of Sweden (Brännvall et al., 1999; Renberg et al., 1994, 2001) and Greenland (Bindler et al., 2001; Hong et al., 1994). However, the largest changes in human contribution to global Pb deposition occurred

during the industrial revolution after circa 1860 (Brännvall et al., 2001; Marx et al., 2016; Outridge et al., 2002).

In the 20th century, volatile Pb emitted from the combustion of leaded gasoline, coal and other black carbon sources was a major long-range source of Pb to the Arctic (McConnell & Edwards, 2008). The contribution of anthropogenic Pb in lake sediments reached a maximum circa 1970 in North America, preceding the restriction on Pb emission including the gradual ban on leaded gasoline (Gobeil et al., 2013; Kemp et al., 2012; Lima et al., 2005; Marcantonio et al., 2002).

The sources of atmospheric lead in different regions of the Arctic varies with dominant atmospheric circulation patterns (Outridge et al., 2002). Eurasian gasoline emissions were the main anthropogenic contributor in sediments from Northern Sweden (Brännvall et al., 1999) Alaska (Sturges et al., 1993), northwestern Hudson Bay (Outridge et al., 2002) and the high Arctic (Liu et al., 2012a). Canada and the United States were the dominant source of anthropogenic Pb in the southeastern part of the Hudson Bay (Outridge et al., 2002) and Greenland (Bindler et al., 2001; Perez-Rodriguez et al., 2018).

The contribution of anthropogenic Pb to high Arctic lakes remains small (0-19%) compared to normal geologic sources in these lakes (Outridge et al., 2002). However, anthropogenic contributions to subarctic lakes was fivefold more important than for High Arctic lakes because of greater Pb deposition at lower latitudes and lower baseline geological contributions (Chrastny et al., 2018; Klaminder et al., 2010; Outridge et al., 2002).

2.2.3.2 Mercury (Hg)

Mercury is a trace metal of environmental concern because the methylated form of Hg is highly bioavailable and rapidly bioaccumulates in biota and biomagnifies in food chains (AMAP, 2011). Northern environmental Hg cycling was massively affected by anthropogenic emissions from lower latitudes and climate change in the last century (AMAP/UNEP, 2013; AMAP, 2011). The gaseous

phase of mercury (Hg⁰) is transported towards the poles from long-range sources and is deposited on northern landscapes as Hg⁰ and Hg^{II} (Durnford et al., 2010; Fitzgerald et al., 1998). Despite the absence of any major local source, Muir et al., (2009) found that 76% of Arctic and 86% of subarctic lakes sediments (n=50) had recorded distinct increases of Hg loading in the sediments after 1900. This increase in Hg was less pronounced, but still significant, in high-Arctic lakes compared to the subarctic lakes (Muir et al., 2009). Multiple paleolimnological studies have shown that modern Hg loading to remote northern lakes is about three times greater at the beginning of the 21st century relative to 1800 (Fitzgerald et al., 2005; Zhang et al., 2014). In subarctic environments, soils and standing biomass accumulate atmospheric Hg from Hg^{II} deposition and from the uptake of Hg⁰ by plants (Halbach et al., 2017; Obrist et al., 2017). Therefore, the large majority of Hg in northern soils is bound to organic matter (Halbach et al., 2017) and is relatively stable since it accumulates in subarctic forests for millennia in the absence of wildfires (Giesler et al., 2017). Estimating the exact proportion of Hg in soils that is anthropogenic is challenging because of the absence of pristine (control) sites that would allow assessing pre-impact conditions and the lack of data from remote Arctic and subarctic regions (Halbach et al., 2017; Ji et al., 2019; Perryman et al., 2020).

Direct continuous monitoring of atmospheric Hg is still in its infancy in northern Canada. Early results suggest that atmospheric gaseous Hg concentrations have decreased in most parts of the Arctic over the last decade but the rate of decline was less than lower latitudes (Steffen et al., 2015). There are considerable uncertainties regarding the quantification of atmospheric Hg contributions to Arctic ecosystems partly because of the lack of direct measurement of wet and dry Hg deposition (Chételat et al., 2015). Overall, information on the atmosphere-soil-water interactions of Hg remains scarce for some types of northern ecosystems (Obrist et al., 2018).

2.2.3.3 Other metals

There is probably more emphasis on anthropogenic Pb and Hg pollution in northern environments than for all other metal pollutants combined, and probably rightly so given the scale of global Pb and Hg emissions since the industrial revolution coupled with the high toxicity of these elements. However, multiple paleoenvironmental assessments from remote northern regions have revealed that coal burning, metallurgic processing and industrial production have increased the deposition of a range of heavy metals including Tl, Cd, As, Pt, Sb, Zn, Ni, Cu, V, Cr and Co over the last centuries (Barrie et al., 1992; Hermanson, 1993; MacDonald et al., 2016; McConnell and Edwards, 2008; Singh et al., 2013). Recent investigations are showing that over the last century, subarctic Canadian lakes have received an increasing amount of As, Pt, Sb and Zn from global and/or regional sources (Roberts et al., 2020). In the North, mining activities, including ore extraction and metal roasting and smelting processes are important point sources for many metals, including As, Ni, Cu and Zn (Klemm et al., 2020; MacDonald et al., 2016; Makinen et al., 2010; Outridge et al., 2011; Roberts et al., 2020; Thienpont et al., 2016).

2.2.4 Impact of climate change on subarctic metal biogeochemical cycling

Climate change has particularly important impacts on Arctic and subarctic environments (Schindler and Smol, 2006; Vincent et al., 2013). Atmospheric warming in the Arctic implies longer snow- and ice-free periods, growing seasons and induced permafrost thaw (Zhang et al., 2008). With the increasing length of the summer season, the hydrological regime of streams and lakes are also more strongly impacted by climate warming (Bouchard et al., 2013; Callaghan et al., 2010; Rouse et al., 1997; David W Schindler and Smol, 2006). Hydrological processes exert an important control on the rate at which terrestrial metals are transported toward aquatic ecosystems (Foster and Charlesworth, 1996). For example, soil saturation from heavy precipitation and low evaporation (e.g. fall conditions) can increase streamflow and land erosion, which in turn can accelerate the transport of metals toward aquatic environments (Spence et al., 2015; Wijngaard et al., 2017). Temperature of the soil and the

exposure to solar radiation could also accelerate the rate of natural weathering in catchment soils, which can increase the rate of metal leaching from soil and the transport of metals from terrestrial to aquatic environments (Houle et al., 2020; Visser et al., 2012; Wijngaard et al., 2017).

Permafrost thaw has important consequences on metal biogeochemistry in two ways. First, the disappearance of permafrost can rapidly change landscape hydrology when the loss of ground ice leads to the creation of thermokarst (depressions) or allows water to penetrate to deeper soil layers, increasing soil water storage capacity and impacting drainage patterns (Quinton et al., 2011). Secondly, permafrost thaw exposes organic matter, metal hydroxides and organo-complexes that can be mobilised by groundwater flow, mineralised by bacteria and can therefore accumulate in stream and lakes (Macdonald et al., 2005; Perryman et al., 2020; Vonk et al., 2015). Permafrost thaw in subarctic areas can further release metals sequestered in frozen soils (Ci et al., 2020; Rydberg et al., 2010) and often result in an increase in stream concentrations of Hg (Schuster et al., 2011), Pb and other soil-bound metals from natural and anthropogenic sources (Audry et al., 2011; Loiko et al., 2017). The impact is greater in streams where permafrost thaw leads to the creation of large retrogressive thaw slumps (St. Pierre et al., 2018). Permafrost thaw can also release terrestrial nutrients that stimulate stream and lake microbial production, with indirect consequences on metal biological sequestration and metal speciation in aquatic environments (Loiko et al., 2017; Reyes and Loughheed, 2015). The release of nutrients along with the terrestrial Hg environment can favor greater methylation rates in aquatic environments (MacMillan et al., 2015). Similarly, higher temperatures in soils can also prime mercury methylation rates (Yang et al., 2016). The creation of thermokarst and the deepening of the soil water table also creates new submerged anoxic environments favorable to Hg methylation (Gordon et al., 2016). Increasing Hg and MeHg accumulation in subarctic Canadian lakes due to ongoing atmospheric deposition or the release of legacy Hg could explain the increasing concentration of Hg in the tissue of some fish populations in the last decades (Chételat et al., 2015). Another

consequence of climate change on terrestrial metal cycling in the Arctic is the increasing frequency and intensity of wildfires (Coogan et al., 2019). The impact of wildfires on metal biogeochemistry is discussed in more detail in section 2.3.1.

In aquatic environments, warmer water temperature can increase primary production (Häder et al., 2014; Rantala et al., 2016), with potential indirect consequences on underwater solar radiations, dissolved oxygen and redox gradients (Paerl and Huisman, 2009; Sahoo and Schladow, 2008). These impacts can affect metal biogeochemistry by increasing the rate of biological sequestration of dissolved and particulate metals in lakes (Outridge et al., 2007; Outridge et al., 2019; Stern et al., 2009) and favor the mobility of metals in lake sediment (Boyle, 2001). The capacity of sediments to acquire more atmospheric Hg⁰ from the uptake by algae during periods of increased primary production is termed “algal scavenging” (Outridge et al., 2007). While this process is widely recognised as a major factor contributing to marine sediment Hg accumulation, the importance of this process in freshwater is a source of debates (Outridge et al., 2019). Recently, Outridge et al. (2019) demonstrated that algal scavenging explained 76–96% of the variation in THg concentrations over many centuries in Arctic tundra lake sediments but that this relationship was not evident in boreal lakes. The lack of relationship between sediment OM and THg in some boreal lakes could be related to the remineralisation of Hg in the sediments over time (Outridge et al., 2019) or the variations in terrestrial (non-algal) OM in the sediment (Kirk et al., 2011; Korosi et al., 2018)

The thermal regime of lakes can be affected by increasing air temperatures, which can reduce lake mixing by increasing the duration of thermal stratification (Butcher et al., 2015; Schwefel et al., 2016). Increasing air temperatures can lead to a stronger temperature gradient establishing in the water column of lakes and this longer duration of lake stratification decreases the exchanges between the atmosphere and hypolimnetic waters (Butcher et al., 2015) as well as limiting the timing of gaseous

emissions from lakes to early spring and autumnal turnover (Vincent et al., 2013). In some cases, this can lead to anoxia in bottom water (hypolimnetic zone), which favors the mobility of metals bounded to Fe- and Mn- hydroxides (Boyle, 2001) and the release of inorganic phosphorous that can prime lakes primary production (Christophoridis and Fytianos, 2006).

2.2.5 Impact of land-use changes on subarctic metal biogeochemical cycling

Land-use change in urban and industrial areas is limited in northern environments but can nevertheless have an environmental impact. Land-cover change is another way humans can impact terrestrial metal transport to aquatic environments. Anthropogenic activities such as agriculture expansion, deforestation, and reforestation changes affect most biogeochemical cycles at multiple scales (Pouyat et al., 2007). The impact of land-use change on the transport of metals to aquatic ecosystems in natural environments mostly relates to surface erosion that can be severely affected by the loss of vegetation cover (Borrelli et al., 2017). In urban settings, the pavement of surfaces can further accelerate the transport of metals (including those release from urban pollution) to aquatic ecosystems by increasing surface flow during storm events (Makepeace et al., 1995; Murakami et al., 2008). Deforestation and agriculture expansion in forested areas are associated with increased exports of terrestrial metals to aquatic ecosystems (Beliveau et al., 2017; Davis et al., 2006; Ito de Lima et al., 2017; Obrist et al., 2016). On the other hand, the replacement of vegetation cover and changes in plant productivity can also lead to a faster accumulation of atmospheric metals, especially Hg⁰ acquired through stomatal absorption (Zhang et al., 2016). In subarctic areas, agriculture is rare and land-cover changes are limited to urban areas, road networks and deforestation. The construction of a road can affect the loading of terrestrial metals to a lake by accelerating surface flow and facilitating erosion in the affected portion of the catchment (Nosrati and Collins, 2019). Dirt roads transport road dust to the lakes and metal pollutants emitted by cars, including brakes compounds and exhaust emissions (Sb, Pb, Cu, Zn, and others) can accumulate in road dust (Aryal et al., 2017; Hwang et al., 2016; Peikertova and Filip,

2016). For example, stable Cu, Zn and Pb isotopes in road dust samples nears London (UK) showed that Pb from leaded gasoline was present in road dust over 20 years after the ban on leaded gasoline in this country (Dong et al., 2017).

2.3 REMOBILISATION OF LEGACY POLLUTANTS

Remobilization refers to the release of elements, particularly legacy contaminants, accumulated in reservoirs that have a long residence time such as sediment (Boyle, 2001; Saulnier and Mucci, 2000), soils and plant biomass (Isley and Taylor, 2020; Klaminder et al., 2005; Kristensen et al., 2014; Odigie et al., 2015; Odigie and Flegal, 2011). Processes such as permafrost thaw (Rydberg et al., 2010; Schuster et al., 2011), wildfires (Kristensen et al., 2014; Odigie et al., 2015; Odigie and Flegal, 2011, 2014; Turetsky et al., 2006) and hydrological changes (Ciszewski and Grygar, 2016; Foster and Charlesworth, 1996; Jarsjö et al., 2020; Schuster et al., 2011) can remobilise terrestrial metals accumulated in soils and standing plant biomass. The stability of legacy anthropogenic metals in terrestrial environments could have noteworthy consequences on the accumulation of key contaminants such as Hg (Chen et al., 2018; Obrist et al., 2018).

In freshwater ecosystems, terrestrial remobilization of legacy metals can cause important delays between the reduction or elimination of emissions from a source and the ecosystem recovery defined as a return to background conditions (Goodsite et al., 2013). Wiklund et al. (2017) determined that modern Hg deposition fluxes in lakes surrounding a decommissioned metal smelter in Flin-Flon Manitoba were exceeding the modern source emissions, suggesting that remobilization of legacy Hg from catchment soils was likely an important source of Hg for these lakes. Rose et al. (2012) demonstrated in a multi-core, multi-lake, study that the importance of terrestrial remobilization processes after the elimination of a point-source of Pb and Hg was positively correlated to the importance of catchment storage predicted by soils depth. Klaminder et al. (2010) demonstrated that

the levels of contaminant deposited in some subarctic lake sediment was not largely affected by the >90% reduction in global Pb deposition after 1970, likely because of the increased terrestrial erosion caused by climate change. Similarly, the reconstructed metal accumulation in Pyrenean lakes sediments suggest that legacy Pb and As contamination accumulated in catchments is actively transported to the lakes during summers (Bacardit and Camarero, 2010). In three Alaskan lakes within the same region, the trends, behavior, and controls on sediment Hg accumulation in response to climate warming were different from one lake to another because of the specific environmental factors and the changing importance of legacy pollution remobilization at each site (Burke et al., 2018).

The impact of remobilisation processes in the future will partly depend on the impact of climate change (see section 2.2.4). For freshwater ecosystems, the cumulative impacts of the enrichment in legacy metals and the evolution of natural remobilization processes as a result of climate change remains unclear. Understanding the timing, extent and processes that govern the recovery from metal pollution should play an increasingly important role in refining our mitigation strategies for metal pollution and inform efficient policies that can reduce human and animal exposure to legacy pollution.

2.3.1 Wildfires as a remobilising agent for anthropogenic metal pollutants

Wildfires are an essential component of natural succession and regeneration cycle in the boreal forest (Johnson et al., 1998; Nguyen-Xuan et al., 2000). In Canada, over 99% of all wildfires are ignited by lightning (Hanes et al., 2019; Wotton, 2009) and the majority of land is unmanaged to preserve the natural wildfire cycles (Coogan et al., 2019). Wildfire occurrence and intensity in subarctic Canada and the Arctic have increased since the mid-20th century in response to climate change (Balshi et al., 2008; French et al., 2015; Higuera, Chipman, et al., 2011; Hu et al., 2010, 2015) and this trend is predicted to continue in response to future warming (Flannigan et al., 2005; French et al., 2015; Wotton et al., 2017). This change in wildfire dynamics could remobilize legacy Hg and Pb stocks accumulated in the circumpolar boreal forest (Turetsky et al., 2006), with possibly greater consequences in areas heavily

polluted by local point-source pollution (Wu et al., 2017; Zhou et al., 2016). Remobilization of legacy metal contamination comprises a substantial part of total metal emissions in present (and future) wildfire emissions (Isley and Taylor, 2020). For instance, it has been estimated that greater wildfire frequency and intensity due to climate change could result in a 14% increase in global wildfire-related Hg emissions (Kumar et al., 2018).

Wildfires consume organic matter and redistribute metals accumulated therein on the landscape by two pathways, the atmospheric transport of fly ash and volatile compounds and the hydrological transport of ash, leachates and charred material from burned catchment. Multiple studies based on paleolimnology (Dunnington et al., 2017; Kristensen & Taylor, 2012; Kristensen et al., 2017; Odigie et al., 2015; Odigie & Flegal, 2014) or ground-based measurements (Burton et al., 2016; Cerrato et al., 2016; Pompeani et al., 2020; Stein et al., 2012) have shown evidence of excess loading of Hg, Pb, As, Cr, Mn, and Zn in streams and lakes at close distance to recent wildfires.

In 1977, one of the first studies examining metal levels in wildfire ash collected on passive samplers (open beakers) found a high concentration of Cd, Cr, Cu, Fe, Pb, Mn, Ni, Si, and Zn in the fallout from a 1975 Californian wildfire retrieved up to 100 km downwind of the fire (Young & Jan, 1977). Metals released to the atmosphere during wildfires include particulate organic and inorganic aerosols (or gas in the case of Hg) with a variable chemical composition (Bodí et al., 2014; Pereira et al., 2012; Pereira & Úbeda, 2010) depending on the combustible composition (Campos et al., 2015) and the fire severity (Kolka et al., 2017; Webster et al., 2016). Stable isotope analyses demonstrated that legacy anthropogenic metals could account for most of the Pb comprised in wildfire ash (Odigie and Flegal, 2011; Wu et al., 2017). Field based measurements of metal deposition from wildfire plumes are challenging and thus rare (e.g. Isley and Taylor, 2020). The advent of remote sensing methods improved our ability to measure atmospheric transport of metals from fires. Atmospheric chemical

transport models are increasingly accurate (e.g. GEOS-chem), and new remote sensing methods allows one to measure the level of a range of elements in the atmosphere (Finley et al., 2009; Friedli et al., 2003; Popoola et al., 2018). Finally, and nonetheless, paleoenvironmental archives are useful at evaluating long-term changes in ecosystem properties and determining natural baseline conditions (Odigie et al., 2015; Pompeani et al., 2020).

The remobilization of metals by wildfires through terrestrial transport from burned catchments have been more extensively described in the scientific literature than the atmospheric transport pathway. Land erosion increases after a wildfire because (1) infiltration is reduced and surface runoff increases in response to the removal of surface litter and vegetation, (2) water uptake by plants is reduced and (3) hydrophobic layers can be created (Mataix-Solera et al., 2011; Shakesby and Doerr, 2006; Smith et al., 2011). In a Colorado forest where wildfires were suppressed for more than a century and significant amount of legacy metals had accumulated, Ranalli and Stevens (2004) measured 2 to 2500-times more As, Al, Cd, Fe, Pb, and Hg in streams adjacent to a recent wildfire. The importance of catchment erosion processes for the transport of terrestrial metals in burned watersheds can be greater during storm events (Burton et al., 2016; Caldwell et al., 2000), particularly in steep sloped topography (DeLong et al., 2018). As a striking example, the level of copper, lead, and zinc in stormwater from a burned Californian watershed were between 112- and 736-fold higher than before the fire (Burke et al., 2010). In stormwater from a burned watershed, Cu, Pb, and Zn primarily originated from ash, whereas Fe primarily originated from burned soil and As, Mn, and Ni originated from both ash and burned soil (Burton et al., 2016). The cumulative impact of recurrent wildfires can significantly affect metal loading to lakes. For example, Rothenberg et al. (2010) concluded that a lake frequently affected by wildfires within its watershed had ~2.5 times greater Hg concentration and ~3 times greater Hg accumulation rate than a nearby lake where fires were largely suppressed.

Terrestrial Hg transport by wildfires has likely been the most heavily studied because of the large potential for Hg to bioaccumulate and biomagnify in the environment. For example, the impact of wildfires on watershed transport of Hg had demonstrable impacts on some fish populations in small lakes in northern Quebec where an increased concentration of methylmercury in zooplankton was observed in lakes with burned catchments (Garcia et al., 2007; Garcia and Carignan, 1999, 2005). Most Hg released during a wildfire is from biomass, litter, and organic soils but upper mineral soils can also comprise up to 10% of the Hg emitted during wildfires of high intensity (Obrist et al., 2018). The emission of Hg is emitted differently by wildfires compared to other metals of environmental concern because the wildfire heat is sufficient to volatilize Hg into its elemental gaseous phase (Hg⁰). In the boreal forest, wildfires occurring in low-moisture fuels emit terrestrial Hg as gaseous elemental Hg with a small percentage (1-14%) in particulate form, but particulate Hg emissions can comprise >50% of all Hg emissions in high-moisture fuels (Friedli et al., 2003; Obrist et al., 2008). Particulate Hg can be rapidly deposited to soils, streams, and lakes at close distance, or it can adhere to the forest canopy and eventually be redeposited via throughfall (Witt et al., 2009). In its gaseous phase, Hg⁰ has a residence time of several months to a year in the atmosphere, and can therefore travel long distances (>1000 km) following major atmospheric transport cells (Driscoll et al., 2013).

The net effects of wildfire on catchment Hg transport can be complex and environment-specific as highlighted by the mass-balance comparison of a burned and an unburned watershed ~50 years following a wildfire in Maine (Nelson et al., 2007). Nelson et al. (2007) concluded that following the fire there was lower atmospheric Hg deposition due to changes in forest species composition, lower soil Hg pools, but greater ecosystem retention for deposited Hg. The depletion of Hg in forest soils is often recompensated for by a short-term (few months) increase in atmospheric Hg(0) uptake following the fire caused by the chemical alteration of the soil carbon (Burke et al., 2010). While this increase can bring back the Hg content in soils to its initial levels in Californian forest with short return

interval for wildfires, fast vegetation growing rates and elevated annual wet deposition, it does not seem to be the case everywhere. Total Hg stocks in Minnesota forests were still affected by severe wildfires that happened hundreds of years ago (Woodruff and Cannon, 2010). Similarly, Hg content in soils and biomass of Swedish boreal forests were positively correlated to the time since the last wildfire, indicating a potential long-term impact of wildfires in soil Hg stocks (Giesler et al., 2017). In the year(s) following fires, the continuous uptake of Hg⁰ in the dry, hydrophobic, easily erodible burnt soil can increase the delivery of organic- or particulate-bound Hg to surface waters (Burke et al., 2010; Jensen et al., 2017). In a USDA report Kolka (2012) found that evidence exists for the remobilization of legacy Hg by wildfire, but only a few studies have addressed aquatic metal dynamics following a fire. Nine years later, our understanding of wildfire effects on the transport of metals to aquatic environments has only marginally improved. Multiple landscapes and regions should be investigated to allow comparative studies between ecosystem types, yet most studies come from California, Australia or southern boreal forests. The impact of wildfires on metal transport in the northern boreal forest and subarctic environments has yet to be investigated. This research is of capital value in the current context because wildfire frequency and severity have increased in the boreal forest (Kelly et al., 2013) and fire occurs in regions of the Arctic where they did not in the last few millennia (French et al., 2015).

2.4 DETERMINING SOURCES AND TRENDS OF POLLUTION FROM NATURAL ARCHIVES

2.4.1 Types of environmental archives, associated timescale and resolution

Paleoenvironmental studies were essential in demonstrating the extent and the timing of long-term changes in global metal cycling arising from anthropogenic activities and global environmental change during the industrial revolution (Bindler, 2011; Fitzgerald et al., 1998, 2005; Landers et al., 1998; Renberg et al., 1994). Paleoenvironmental studies have the advantage of obtaining long time series of

environmental change in areas that have not been monitored in the past. Such long time series are necessary to evaluate recent dynamics in the context of natural variations and obtain an assessment of background conditions to which current conditions and trends can be compared. Environmental archives have been successfully used to reconstruction point source pollution (e.g., mining, smelters) (Schillereff et al., 2016; Wiklund et al., 2017), in addition to long-range transport (Catalan et al., 2013; Korosi et al., 2018; Muir et al., 2009).

Glacier ice records the atmospheric deposition of metals at a very fine temporal resolution and provide records spanning thousands of years (Schuster et al., 2002). Tree rings can provide information on the historic change in atmospheric metal concentrations with an annual resolution on a decennial scale (Hojdová et al., 2011). Ombrotrophic peatlands receive their input from atmospheric deposition and thus record the atmospheric deposition on terrestrial ecosystems, often at the millennial scale but with a coarse temporal resolution (Biester et al., 2007; Enrico et al., 2017). Lake sediments have the potential to integrate and record changes occurring within the lake and the nearby terrestrial environment at seasonal to millennial timescales (Schindler, 2009). Paleolimnological techniques have been used to acquire essential information on biogeochemical cycles by providing in-situ measurements of past environmental conditions in relation to metals in the sediments. Lake sediments are a useful tool to understand metal transport and their response to human and natural disturbance because they record faithfully sedimentary flux and allow one to extend the reference period into the distant past (Engstrom and Rose, 2013). Therefore, paleolimnology can contextualize contemporary observations within their historical context and provide long time series allowing one to evaluate the relationship between environmental variables, test current biogeochemical models or develop new research hypotheses. Paleolimnological investigations relying on multiple records or meta-analyses drawing from multiple paleolimnological studies are a powerful analytical tool that provides a spatial insight on past environmental trends (e.g. Muir et al., 2009).

2.4.2 Metal concentration profile and mass accumulation rate (flux) reconstruction

Evaluating the impact of pollution using natural archives can be done based on changes in element concentration or changes in element mass accumulation rates in temporally resolved samples (Bárcena et al., 2017; Birch et al., 2001). Methods relying on element concentration can be subdivided into a range of approaches using different mathematical transformations and stoichiometry analysis, including tracer element ratios, enrichment factors, excess measures, and centred log-ratios (Dunnington et al., 2020).

Because each environmental archive has its own environmental context and there is natural variation in metal concentration due to local bedrock and surficial geology, the evaluation of impacts from natural archives is best done as a comparative analysis between pre- and post- disturbance conditions. Most often, pre-disturbance conditions are found within the archive record itself (e.g. bottom of lake sediment or peat cores), but it can also be inferred from other records used as reference sites (e.g. the spatial analysis of point-source impact).

Metal concentrations are determined in various locations within the medium constituting the archive, representing accumulation during different time periods (e.g. depths increment in lake sediment or peat core). Popular methods of measurement for determining the concentrations of metals of environmental concern include mass spectrometry analysis (AAS, ICP-MS, TIMS, GD-MS) and X-ray fluorescence (XRF). Both methods have their strengths and weaknesses. The ICP-MS measurements have an excellent precision and reproducibility but require and acid digestion of the medium prior to the analysis and is therefore destructive. Moreover, the digestion processes may be incomplete and results represent an acid-leachable metal fraction that can vary from one digestion method to another. The XRF core-scanning analysis is non-destructive and rapid, with some instruments now able to provide results on the field (Davies et al., 2015), but measurements are less precise and corrections must be applied to the raw data to account for the irregular shape or relief

effects on the analysed matrix (Gregory et al., 2019; Löwemark et al., 2019). Classical methods (ICP-MS and XRF) have detection limits that are sufficiently low for the determination of environmental concentration for most metals, but the presence of certain elements in the environment (e.g. Hg) can be have ecological consequences at concentration near or below the detection limit. For the determination of Hg concentration in biological or geochemical samples, using a direct mercury analyser (DMA) is now the standard method and is more cost and time effective than any other measurement method. A DMA is an automatic system on which untreated dry samples can be loaded to an autosampler. The Hg in the samples is then purified by catalysing the sample and amalgamating Hg to a gold surface. The Hg can then be detected by absorption spectrometry in the gaseous phase.

Another crucial step in paleoenvironmental reconstructions is obtaining a chronology for the analysed material in order to create time series. This is done in archives accumulating distinct layers of material at a regular time increment (tree rings, varved lake sediment, glacial ice). The dating of environmental archives accumulating at irregular rate or without easily distinguishable time markers relies on radiochronology. A series of radioactive elements accumulating at regular rate and for which the half-life is known can be used to determine the time of deposition (or aggradation) of the material to be dated. The most widely used radioactive elements are radiocarbon (^{14}C) and radiogenic lead (^{210}Pb), because of their ubiquity in the environment, the regularity of their atmospheric concentration and deposition rate, and their half-life ($t_{1/2}$) that allows one to accurately date material accumulated during the Holocene ($t_{1/2}=5700 \pm 30$ yr for ^{14}C , $t_{1/2}=22.6$ years for ^{210}Pb).

From a dated metal concentration profile in peat or sediment, it is possible to observe variations in the concentration of the material deposited, identify disturbances and contextualise the modern concentration in water (for sediment) or the atmosphere (for peat bogs). A good assessment of metal pollution is based on the determination of pre-impact baseline (e.g. pre-industrial) levels for an

individual core or a set of cores and usually includes simple mathematical transformation. The mathematical transformation (commonly using the logarithm of the concentration or flux) allows for reducing the importance of (1) the natural fluctuations in the content of a given substance in the environment and (2) very small anthropogenic influences (Bárcena et al., 2017; S. P. Kumar and Patterson, 2009).

A common approach to report metal contamination is to compare concentration values of individual core slices to the average (or median) value in sediment accumulated before the occurrence of pollution, creating enrichment factors. A more in-depth approach is to use a geochemical index that is log-centered, which reduces the importance of small-scale variations and creates time series that are less noisy. The I_{geo} index (Muller and Muheim, 1969) (Equation 2.3) is one of the first examples in the literature:

Eq. 2.3
$$I_{geo} = \log_2 \frac{C_{HM}}{1.5C_{background}}$$

Where C_{HM} is the heavy metal concentration and $C_{background}$ is the geochemical background concentration of the metal. This geoaccumulation index is defined as local (or in-core) because it relies on information from different sections of the same core. The other possible method is to normalize sediment concentration of a certain element against a global reference material, commonly the average crustal rock estimate by Hans Wedepohl (1995), a method detailed in Boyle et al., (2015), where the $C_{background}$ term in equation 2.3 becomes the global shale concentration of that element. This last method accounts for correction of changes caused by varying particles size but suffers because of crustal heterogeneity in mineral composition (Boyle et al., 2015). Metal fluxes of interest can be corrected using geological tracers and crustal elements (conservative lithogenic elements) commonly attributed to land erosion (commonly Mg, Ti, Al, Rb or Sc) to address changing sedimentation rates (Dunnington et al., 2020). One principal concept governing the use of conservative lithogenic elements ratios is that

during granitic rocks weathering and fractionation, Zr and Ti are enriched in the fine mineral fraction of soils (silt and clay) compared to the parent rock (Taboada et al., 2006). The Zr to Rb, K, and Ti ratios can therefore be used as a coarse proxy for grain size and is useful in interpreting changes caused by catchment weathering, erosion and aeolian inputs in lake sediments and peatlands (Boës et al., 2011; Rydberg et al., 2016; Weiss et al., 1997). elements are in greater concentration in clay-sized particles, and can therefore be indicative of changes in catchment erosion in lake sediment. Ratios to those conservative elements provide a method to identify anthropogenic impact in circumstances where natural inputs of metal (e.g. from mineral weathering) may be changing simultaneously with anthropogenic sources. More methods to account for multiple environmental processes in paleoenvironmental time series are presented in section 2.4.4.

Variations in the concentration of an element can be difficult to interpret in terms of identifying the timing and magnitude of the accumulation of material from a new source in lakes and peat bogs. In well-dated sediment or peat records, the mass accumulation rate of an element, in weight per area per time is often preferred to concentration profiles or geochemical index (Bindler, 2011; Cooke et al., 2020; Dunnington et al., 2020; Engstrom and Rose, 2013). However, each measure has its own limitations and assumptions that must be addressed before choosing an appropriate methodology. In a recent comparative analysis, Dunnington et al. (2020) determined that in lake sediment reconstruction, mass accumulation rates are preferable to methods relying on concentration data alone when there is a low concentration of the target element in the erosional source. If only variations in metal concentration are evaluated (not flux), then tracer element ratios can be used when the erosion rate is constant, whereas excess measures are preferable if erosion is likely to have varied in time (Dunnington et al., 2020).

In lake sediment, the accumulation rate measured in a core can be unrepresentative of the delivery to the whole lake because sediment accumulates preferentially in depressions in the lakebed (Blais and Kalff, 1995). A particle focusing correction method can be applied using a derivate of equation 2.4:

Eq. 2.4
$$FF = \frac{Pb_O}{Pb_P}$$

Where FF is the focusing factor of a single lake core, Pb_O is the observed radiogenic Pb (^{210}Pb) flux at the surface of a core and Pb_P is the predicted ^{210}Pb flux based on several other lake cores of the same area (Kirk et al., 2011; Muir et al., 2009), a latitudinal regression based on several spatially separated cores (Muir et al., 2009) or catchment soils (Blais and Kalff, 1995). This FF correction can then be applied to any element fluxes.

2.4.3 Diagenetic modelling

The reliability of paleolimnological analysis of metal accumulation largely depends on the stability of metals after their deposition in lake sediments and the possibility of inferring the sediment deposition chronology (see section 2.2.2.3 for more information on the stability of metals in lake sediments). The reliability of sedimentary archives of Hg deposition was demonstrated by resampling studies (Rydberg et al., 2008), comparison with well-defined historical deposition (Lockhart et al., 2000) as well as modeling of pore-water metal concentration (Feyte et al., 2012). The stability of Pb in sediments was demonstrated by resampling studies (Percival and Outridge, 2013) and pore-water analysis (Gallon et al., 2004), but Pb mobility was reported in environments with high pH fluctuations (Widerlund et al., 2002). The radiogenic isotope of Pb used for dating lake sediment records (^{210}Pb) is considered immobile in sediments (Crusius and Anderson, 1995). Corrections for diagenetic processes and unstable metal profiles in lacustrine and marine sediment can be applied in some instances by using information on sediment pore water concentrations and estimating diffusion gradients (Couture et al., 2008; Outridge and Wang, 2015; Percival and Outridge, 2013). A review of possible models for

diagenetic corrections and their implementation for metal in freshwater environments can be found in Boudreau (1999). Despite the usefulness of diagenetic correction models in some cases, metal profiles unaffected by diagenesis generally allow for more confidence in interpretations.

The stability of metals in peat bogs, particularly Hg, is often questioned in the literature (Cooke et al., 2020; Goodsite et al., 2013). While some recent advances from Hg stable isotope reconstructions have shown evidence for the stability of Hg in some peat bogs (Enrico et al., 2017), others have also shown that Hg accumulated in peat can be mobilised by fluctuations in water-table depth (Wasik et al., 2015; Demers et al., 2013). Peat decomposition can also increase the concentration of Hg in old peat layers (Haynes et al., 2017a, 2017b; Liu et al., 2003) and ^{210}Pb can be mobilised downcore, leading to underestimation of peat age and overestimation of recent fluxes (Biester et al., 2007). All the aforementioned processes can lead to important errors in the determination of the timing and magnitude of pollution trends. Therefore, metal reconstructions from peat bogs should be critically evaluated on a case-by-case basis and hydrological conditions should ideally be assessed to help reduce the uncertainties related to reconstructions of atmospheric deposition trends. Goodsite et al. (2013) showed that trends in northern Canadian lake sediments and a southern Greenland peat bog did not exhibit good agreement with model predictions of atmospheric deposition since 1990, the Greenland firn gaseous elemental Hg (Hg_0) record, direct atmospheric Hg_0 measurements, or trends in global emissions since 1980. This discrepancy between different archives may be associated with legacy pollution retention and slow release in watersheds, the accuracy of archive chronologies, and/or climate-driven changes in Hg transfer rates from air to catchments.

Using multiple types of archives within the same landscape can provide information on different components of metal transport since each archive has its respective dynamic and is affected by different processes. Yet, the combination of multiple types of environmental archive is seldom applied

when reconstructing metal contamination in the environment. By comparing the Hg and Zn accumulation records in peat and lake sediments around the Flin-Flon metal smelter (MN, Canada) Outridge et al. (2011) noted differences between the records that they could relate to catchment retention processes. The importance of soil retention was also observed by Bindler et al. (2008) that used lake and peat Pb accumulation to calculate the Pb concentration in soils in pre-industrial times and evaluate soil retention time of Pb. Interestingly, there was no discrepancy in pre-1990 Hg, Pb and Cd accumulation rates between peat and lake sediment of the same region in a comparative literature review by Norton et al. (1990). The similar accumulation rates in the two types of archives for pre-1900 records suggests that catchment retention and release processes may have changed over the last 31 years.

2.4.4 Attribution science – a new frontier in paleoenvironment science

Multiple sources and transport processes contribute to the patterns of metal accumulation in environmental archives (Adrian et al., 2009; Smol, 2016). Multiple approaches were developed to quantify the contribution of individual sources or processes from paleoenvironmental time series. These approaches include spatial analysis, flux deconstruction, geotracer elements, data ordination and stable isotope analysis. These methods are all utilized in chapter three to six of this thesis to evaluate the contribution of mining pollution, long-range atmospheric deposition, wildfires and climate to metal accumulation in lake sediment and peatlands.

Developing new methods that allow us to interpret with more confidence the observed changes in paleoenvironmental records will be essential to predict future ecosystems levels of metals. For example, the influence of climate change and its associated disturbances on metal transport processes can only be studied in a context where the impact of most sources and processes (e.g., legacy metal pollution) is considered and quantifiable.

2.4.4.1 Flux deconstruction approach

One avenue of attribution science in the field of paleolimnology is the deconstruction of mass accumulation rates into probable source components using geochemical indices (Hermanns et al., 2013; Sarkar et al., 2015b) or observed changes in environmental processes (e.g. sedimentation rate) (Furl and Meredith, 2011; Perry et al., 2005). A flux deconstruction approach aims to estimate the proportion of metals emitted from different natural and anthropogenic sources or accumulated via certain transport processes. Increased sedimentation rates as a result of higher organic matter transport and mineral erosion in catchments are commonly observed in arctic lakes and can represent the largest part of metal accumulation where atmospheric deposition is low (Fitzgerald et al., 2005; Muir et al., 2009). The equation of Perry et al. (2005) deconstructs total Hg flux (Hg_T) into a background flux, changes in sedimentation rate and anthropogenic excess flux (equation 2.5).

Eq. 2.5
$$Hg_T = Hg_B + Hg_V + Hg_A$$

The background flux (Hg_B) represents the ambient levels of Hg introduced to the sediment as a function of local geology and atmospheric transport from natural sources such as volcanoes, the marine surface, and soil dust. The variations in sedimentation rates caused by a natural or anthropogenic disturbance (Hg_V) is calculated as in equation 2.6:

Eq. 2.6
$$Hg_V = \frac{S_i}{S_b} \times Hg_B - Hg_B$$

Where S_i is the sedimentation rate for any sediment interval and S_b is the pre-industrial sedimentation rate. The residual of equation 3 (Hg_A) represents the atmospheric signal of excess anthropogenic Hg in the lake sediment.

Fluxes have also been deconstructed using geochemical indices allowing one to distinguish the inputs of natural sources of metals to lakes (Boës et al., 2011; Norton, 1986; Tylmann, 2005) and peat bogs

(Roos-Barracough et al., 2002, 2006; Shotyk et al., 2005). For example, bromine (Br) and selenium (Se) can be used to quantify the variations in natural Hg deposition and distinguish them from the excess anthropogenic Hg accumulation in peat bogs (Roos-Barracough et al., 2006; Shotyk et al., 2002). Other geochemical tracers are available to evaluate natural variation in metal accumulation in archives from dust deposition in peat bogs, including Al, Ti, Si and Sc (Shotyk et al., 2002; Weiss et al., 1997; 2002). Similarly, elements such as Al, Si, zirconium (Zr), Ti and rubidium (Rb) are useful to evaluate changes in catchment soil contributions to the metal budget of lake sediments, either by normalizing the metals of interest to these elements (Boës et al., 2011; Norton, 1986) or by quantifying the natural flux from the pre-industrial ratio of conservative lithogenic element to metal of interest (Shotyk et al., 2001).

2.4.4.2 Ordination methods

Ordination methods for peat and lake sediment geochemistry can also provide a view of the relative importance of natural and anthropogenic sources of metals by evaluating the co-variations in conservative lithogenic elements and the elements of interest. Principal component analysis (PCA) is the most widely used ordination technique for geochemical data in peat and sediment. A principal component analysis can reveal how the geochemical composition of sediment or peat changed over time, and assess to what extent these changes were related to variations in the climate (Rydberg and Martinez-Cortizas, 2014), lithogenic dust or terrigenous run-off (Bao et al., 2015; Berg et al., 1995; Ferrat et al., 2012; Muller et al., 2008; Pratte et al., 2018; Shotyk et al., 2016).

2.4.4.3 Metal stable isotopes and mixing models

Stable isotope ratios of metals can provide valuable information to estimate the relative importance of individual sources. Similar mixing models as those used in the context of point-source pollution were applied to northern environments to determine the contribution of anthropogenic Pb pollution and to track potential geographical sources (Bindler et al., 2001). Hg also has stable isotopes, but

multiple and complex fractionation processes render the use of Hg stable isotopes more useful in determining biogeochemical processes than source type or localization. Other metal(oids) such as As do not have multiple naturally occurring stable isotopes.

Variation of the stable isotope ratios of contaminating elements in sediment profiles can be a powerful line of evidence to assess the source of metals, either at the local or global level. Such methods have been useful in determining source attributions for local pollution, the efficiency of recovery processes and the long-range transport of some metals. Metals with multiple naturally occurring stable isotopes can sometimes be traced back to their source when sources are well defined and differ in isotopic composition. Mixing models, originally developed for ecological studies, were applied to heavy metal pollution studies of sediments, dust or dissolved metals to determine their source. The concentration of Pb originating from pollution ($Pb_{pollution\ conc}$) can be modeled using equation 2.7 (Bindler et al., 2008; Brännvall et al., 1999).

$$\text{Eq. 2.7} \quad Pb_{pollution\ conc} = \left(\frac{Pb\ ratio_{sample} - Pb\ ratio_{background}}{Pb\ ratio_{pollution} - Pb\ ratio_{background}} \right) \times Pb_{sample\ conc}$$

The $^{206}\text{Pb}/^{207}\text{Pb}$ ratio is the most commonly used ratio in mixing models because it often exhibits the largest difference in source signatures (Renberg et al., 2002), but ^{204}Pb and ^{208}Pb ratios can be added to the models to refine source attribution (Miller et al., 2007). If the natural background Pb contribution can be properly quantified, including information on its concentration and isotope ratio, the mean isotope composition of the pollution Pb ($^{206}\text{Pb}/^{207}\text{Pb}_{excess}$) can be identified using equation 2.8 (Bindler et al., 2001).

$$\text{Eq. 2.8} \quad {}^{206}\text{Pb}/{}^{207}\text{Pb}_{excess} = \frac{(Pb_{sample} \times {}^{206}\text{Pb}/{}^{207}\text{Pb}_{sample}) - (Pb_{ref} \times {}^{206}\text{Pb}/{}^{207}\text{Pb}_{ref})}{Pb_{sample} - Pb_{ref}}$$

Where $^{206}\text{Pb}/^{207}\text{Pb}_{\text{sample}}$ is the sample isotope ratio, $\text{Pb}_{\text{sample}}$ is the Pb concentration of a given sample, and Pb_{ref} and $^{206}\text{Pb}/^{207}\text{Pb}_{\text{ref}}$ are the mean isotope ratio and concentration, respectively, of pre-impact sediments.

Table 2.1 Mean and standard deviation of Pb isotope values for the two sources included in the mixing model (baseline sediment and Giant and Con mine ore) as well as isotope values for other potential Pb sources.

Source	²⁰⁶Pb/²⁰⁷Pb Average ± Std. dev. (range)	²⁰⁸Pb/²⁰⁴Pb Average ± Std. dev. (range)	Reference
Baseline sediment (pre-1938)	1.2914 ± 0.0142 (1.2635-1.3069)	40.1614 ± 0.1847 (39.8143-40.4462)	This thesis
Bedrock samples	1.1776 ± 0.0970 (1.0554-1.3509)	38.5942 ± 2.3880 (36.1512-42.9022)	This thesis
Lichen samples	1.1657 ± 0.0276 (1.1157 – 1.2076)	37.7583 ± 0.3877 (37.0391 - 38.3735)	This thesis
Con Mine ore	0.9316 ± 0.0017 (0.9303-0.9339)	33.7610 ± 0.1519 (33.5360-33.8700)	Cumming and Tsong (1975)
Giant Mine ore	0.9540 ± 0.0393 (0.9333-1.0334)	34.2783 ± 0.6719 (33.8700-35.6300)	Cousens et al. (2006)
Leaded gasoline (Canada)	1.105 ± 0.086 (0.920–1.190)	-	Sturges and Barrie (1987)
Leaded gasoline (USA)	1.183 ± 0.103 (1.040–1.390)	-	Sturges and Barrie (1987)
Coal (USA)	1.201 ± 0.023 (1.126–1.252)	-	Chow and Earl (1972)
Coal (North America)	1.21 ± 0.01 (1.1907-1.2314)	-	Diaz-Somoano et al. (2009)
Aerosols (Canada)	1.150 ± 0.003	37.43 ± 0.08	Carignan and Gariépy (1995)
Aerosols (Canada)	(1.094 –1.177)	-	Bollhofer and Rosman (2001)

2.4.4.4 Determining the impacts and extent of point-source pollution using spatial analysis

Heavy metal point-source contamination in to the northern boreal region of Canada has occurred near mines and metal smelters, coal-burning power stations, incinerators and reservoir creation (Alaee et al., 2003). Evaluating the geochemical recovery from any pollution source (point-source or long-range) requires the establishment of baseline ecological conditions as a benchmark for recovery. The baseline conditions for an individual site can be inferred from the metal fluxes or concentrations in sediments accumulated before a disturbance (see section 2.4.1).

Studies using multiple sites over a large area can be useful at distinguishing the impacts of a mine point-source from external (long-range) metal contributions. For example, the spatio-temporal pattern of deposition in multiple lakes around a Cu and Zn smelter in northern Manitoba allowed to determine that palladium (Pd), bismuth (Bi), cadmium (Cd), nickel (Ni), strontium (Sr) and copper (Cu) were derived from the smelter whereas As, Hg, Pb, Pt, Sb and Zn were mostly sourced from other global and regional sources (Roberts et al., 2020).

Paleolimnological assessments of point-source metal pollution from mines have most commonly reported on recovery processes of elements such as As, Cd, Pb, Hg, Sb and Zn pollution (Child et al., 2018; Laperriere et al., 2008; Schillereff et al., 2016; Thienpont et al., 2016; Van Den Berghe et al., 2018). Post-mining trajectories can also be described and predicted spatially using spatial regressions from multiple cores. Using the temporal least squares linear model of metal concentration or metal fluxes over time, Schillereff et al. (2016) estimated that the post-mining trajectories for Pb and Zn project a return to pre-mining levels within 54-128 years for Pb and 75-187 years for Zn. However, they highlighted the uncertainties related to changing remobilization regime of legacy contaminants in the watershed.

2.5 STUDY AREAS

2.5.1 Geophysiography of the Taiga Shield and Taiga Plains ecoregions

The study region for chapters three to five of this thesis is a subarctic environment within the northernmost region of the boreal forest, ~100 km below the tree line. The approximate latitude of the study area is 62°30'N. The 1980-2010 climate normals for the nearest meteorological station (at Yellowknife, NT) indicate annual precipitation of 131 mm of rain and 157 mm of rain-equivalent snow per year. The regional temperature is subarctic (mean = -4.3°C) with approximately 115 days per year above 0°C. Air temperatures have increased in the study area in recent decades compared with earlier meteorological records that started in the 1940s at Yellowknife (Evans et al., 2013). The increase in air temperatures has resulted in a shift in the autumn precipitation pattern, with more rainfall and less snowfall (Spence et al., 2011).

The study region spans two ecoregions of the Northwest Territories, the Taiga Shield and Taiga Plains (Figure 2.2). The Taiga Shield ecoregion is part of the Slave Geological Province of the Canadian Shield. The Slave Province is an Archean craton and is primarily composed of felsic to mafic meta-volcanic rocks except east of Yellowknife, where meta-sedimentary rocks are more abundant (Wolfe, Kerr, et al., 2017). The Taiga Shield landscape is dominated by exposed bedrock with thin veneers of glacial till. Thick organic deposits are typically restricted to peatlands that formed in topographic low areas. Taiga Shield vegetation is dominated by stands of black spruce (*Picea mariana*) with lichen understory. Discontinuous permafrost is present on the landscape but localised in thick organic and fine-grained mineral deposits (Wolfe et al., 2017a). The Taiga Plains ecozone is located west of Great Slave Lake. The Taiga Plains is part of the geological province of the Interior Platform. The underlying bedrock is composed of Paleozoic sedimentary rock and the surface geology around the study sites is composed of easily drained coarse-textured calcareous glacial deposits (Wolfe et al., 2017b). Extensive patches of jack pine (*Pinus banksiana* Lamb.) and white spruce (*Picea glauca*) forest are separated by

horizontal fens and calcareous ponds in the Taiga Plains. Permafrost is sporadic in this ecoregion (Wolfe et al., 2017b).

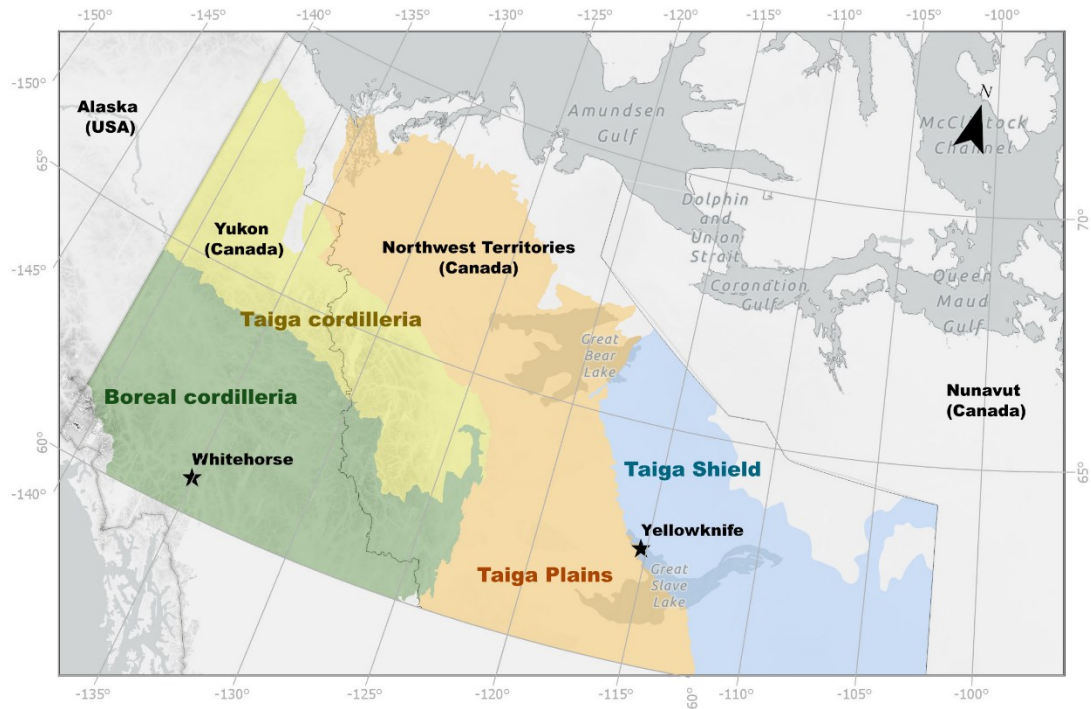


Figure 2.2: General map of Northwestern Canada showing boundaries of Canada's territories and major ecoregions around the study sites. Location of Whitehorse and Yellowknife are indicated with stars.

The Great Slave Lake area of the Northwest Territories and northern Alberta were affected by severe and massive wildfires in 2014 and 2015 which resulted in the burning of millions of hectares of forest (French et al., 2020). Charcoal reconstructions from the area show that fire frequency was higher and fire return intervals were shorter during the early to mid-Holocene for the region (Pisaric et al., 2018), but current long-term trends have yet to be characterized. It is predicted that wildfire frequency and intensity will increase in the area in the near future in response to climate change (Veraverbeke et al., 2017; Wotton et al., 2017). The changes in fire regime will have uncertain consequences on ecosystem and biota exposure to (legacy) metals.

2.5.2 Yellowknife: Mining pollution legacy and current challenges

Located on the shore of Yellowknife Bay in the North Arm of Great Slave Lake, Yellowknife is a mining town with ~20,000 inhabitants and is the capital of the Northwest Territories. The city stands at a junction separating the Taiga Plains and Taiga Shield ecozones (Figure 2.2), which also represents two geological provinces (the Slave Province and the Interior Platform). From 1938 to 2004, two gold mining operations located on the north and northwest shores of Yellowknife Bay were the main activity driving the town's economy. Giant Mine operated from 1948 to 2004 and Con Mine operated from 1938 to 2003. The ore roasting process released metal pollution through a roaster stack, and most stack emissions were deposited within a ~30 km radius around Giant Mine (Cheney et al., 2020; Houben et al., 2016; Palmer et al., 2015; Chapter 3 of this thesis). The bulk of historical atmospheric mining emissions in the region were from Giant Mine in the early years of operations (1949-1958), before the implementation of emission controls (Hocking et al., 1978). Stack emissions from Giant Mine contained several metals including: arsenic, antimony, lead, and mercury (Chetelat et al., 2017; Thienpont et al., 2016). Arsenic trioxide (AsO_3) is by far the most problematic contaminant emitted in the Yellowknife area. The AsO_3 emissions resulted from roasting to separate the gold from arsenopyrite. The impacts of metal contamination on soils and sediments surrounding the mine are

still evident more than twelve years after the complete closure of the mine. Elevated concentration persist in soils within a four kilometers radius of Giant Mine for As (Bromstad et al., 2017), Zn, Pb and Cd (Hutchinson et al., 1982). Persistence of mining-derived metals in soils of the Taiga Shield is explained in part by topographic restriction and the cold climate, limiting post-deposition mobility (Bromstad et al., 2017). Mining-related metal contamination in the Yellowknife area is actively studied to this day because of the risk of human exposure to wildlife (mostly fish) with elevated metal concentration. For example, the levels of As in the tissue of lake whitefish and burbot is greater at closer distance to Giant Mine than in unimpacted lakes in small disconnected lakes (Cott et al., 2016) and in the Yellowknife Bay (Chételat et al., 2019).

Non-atmospheric sources of metals were also released to the Yellowknife Bay by Giant Mine, including the discharge and redistribution of tailings in the Back Bay by Giant Mine between 1948 and 1951 (Indigenous and Northern Affairs Canada INAC, 2013) and effluents of tailing decant from Baker Creek (Andrade et al., 2010). The extent of mining-related metals in the Yellowknife Bay, from the cumulative impacts of atmospheric and non-atmospheric sources were still unclear before the study presented in chapter three of this thesis. Previous paleolimnological investigations of Yellowknife Bay revealed sub-surface peaks in heavy metal concentrations in sediment profiles attributed to local mining activity (Andrade et al., 2010; Fawcett et al., 2015; Galloway et al., 2015), but source tracing had not been investigated for any mining-related metals yet.

Source attribution analysis for Pb in the Yellowknife Bay sediment could provide information on processes impacting the transport and cycling of other mining-derived metals. For example, recent studies have consistently shown that AsO_3 is redox-sensitive and mobile in lake sediments near Yellowknife (Andrade et al., 2010; Palmer et al., 2019; Van Den Berghe et al., 2018), but Hg, Pb, Zn, Cu, and Sb appear to be largely unaffected by remobilization (Andrade et al., 2010; Houben et al.,

2016; Palmer et al., 2019). Because As mobility is affected by redox conditions, it is unclear to what extent elevated As concentrations in surface sediments results from large-scale transport processes from the catchment or small-scale As mobility in the sediments from diagenetic processes. The extent at which Pb is still actively deposited at the sediment surface, years after mine closure can provide information that could help distinguishing the importance of remobilization from diagenetic changes in the sediment affecting the levels of metal in recently accumulated sediments.

2.5.3 Whitehorse Region, Yukon, Canada

The study presented as chapter six of this thesis was conducted in the Yukon Southern Lakes Ecoregion, which is included within the ecozone of the Boreal Cordillera Ecozone (Figure 2.2). The study lakes (Figure 6.1) are located in a broad glacial valley filled with Holocene alluvium and colluvial deposits covered by open coniferous and mixed woodlands. The surrounding topography is moderately rugged, with elevations ranging from 670 to 1280 m. The study area is within the Terrane Geological Province. The underlying bedrock around Fox Lake (FL), Grayling Lake (GL) and Little Fox Lake (LFL) consists of Jurassic sedimentary strata (arkosic sandstone and minor shale, pebble and boulder conglomerate) to the West and Jurassic sedimentary/volcanic strata to the East (khaki-green dacite crystal tuff and volcanoclastic sandstone), with minor-sized igneous intrusions near summits. Bedrock surrounding the Little Breaburn Lake area is Upper Triassic sedimentary strata made of shale, siltstone, calcareous greywacke and argillaceous limestone.

The regional dry subarctic climate (mean annual temperature of -1°C) is influenced by a rain shadow effect of the coast mountains (Smith et al., 2004), resulting in low precipitation (200-325 mm year⁻¹). Dominant tree species at low elevations are Jack Pine (*Pinus banksiana* Lambert), white spruce (*Picea glauca* (Moench) Voss) and trembling aspen (*Populus tremuloides* Michaux). The higher elevation slopes are gradually covered by shrubs of decreasing size with altitude, with mountain summits dominated by a dwarf shrub tundra. The Yukon Southern Lakes Ecoregion is located within the

sporadic discontinuous permafrost zone, and permafrost is rare along the direct study area (i.e., along the Klondike Highway) (Smith et al., 2004; Public Works Commission, 1986). However, some isolated lenses of ice-rich permafrost have previously been identified in thick surface organic deposits located on north-facing slopes and at high elevations (Smith et al., 2004).

The study lakes were located along a 40 km stretch of the Klondike Highway (Yukon Highway 2), running North-South along the study area (Figure 6.1). The region has been accessible since the 1898 Klondike Gold Rush and First Nations travelled through the region long before (Yukon Department of Tourism & Heritage Branch, 2019). The construction of the current road began in the post WWII period and the road was paved between 1979-1982.

The Whitehorse Copper Belt (WCB) and the historic mining town of Whitehorse are located approximately 50-80 km south of the study lakes. The City of Whitehorse has a rich mining history that started with the Klondike Rush of the late 1890s and perdured until the early 1980s. The Little Chief and Middle Chief Mines (1966-1982) had the largest production in the area and at their closure had produced 85% of all the copper from the WCB as well as 150,000 ounces of gold (Indian and Northern Affairs Canada INAC, 1984). Many smaller base metal (Pb, Cu, Zn) and Au/Ag mines operated around Whitehorse, Carmacks (~70-100 km N of study lakes) and Mt. Nasen (100-130 km NW of the study Lakes). Only basic processing of the extracted ore (e.g., milling) was performed on site or near Whitehorse (i.e., no roasting or smelter).

2.6 OBJECTIVES OF THE INDIVIDUAL CHAPTERS OF THIS THESIS

This thesis aimed to improve our understanding of sources of metal contamination and important transport processes for subarctic Canadian lakes. Despite the large (inter)national efforts on reducing emissions of metals such as Hg and Pb in recent decades (EPA, 2014; ECCC, 2020), uncertainties persist regarding the fate of legacy contaminants accumulated on the northern Canadian landscape (NCP, 2017). Specifically, the four data chapters of this thesis will fulfill the following objectives:

Evaluate the spatial footprint and recovery of lake sediment from Pb pollution by gold mines roasters and the dumping of tailings in The Yellowknife Bay, Great Slave Lake (chapter three);

Measure the impact of wildfires on the transport of metals to lakes via the atmospheric and catchment-based transport pathways (chapter four and six respectively);

And,

Partition the contribution of individual sources or processes (catchment erosion, aeolian dust, wildfires, mining pollution) to the metal accumulation in lake sediment and peat bogs of the Taiga Plains Lakes and Taiga Shield Lakes (chapter five).

3 POINT-SOURCE LEAD POLLUTION FROM GOLD MINES IN YELLOWKNIFE BAY

3.1 PREFACE

The first data chapter of this thesis will investigate the spatial extent and recovery of mining pollution in the Yellowknife Bay, NT, Canada using a combination of geochemical fluxes and Pb isotopes from multiple sediment cores. Abandoned mines offer a rare perspective into the recovery processes from metal pollution in lake sediments. The stable Pb isotopes offer a novel perspective into the partitioning of sediment Pb attributable to mining-related contamination vs. changes in natural Pb derived from local catchment weathering. The validity of Pb isotopes to determine the importance of anthropogenic Pb pollution has been demonstrated in multiple studies (Bindler et al., 2008) but is rarely applied to mining-related contamination (e.g., Cuvier et al., 2016) and therefore represents a novel application of this method in paleoenvironmental studies. A precise quantification of Pb accumulation derived from mining in sediments from the Yellowknife Bay will help understand the current and past sources of other mining-related metals that don't have stable isotopes and are not as stable in sediments (such as As).

3.2 INTRODUCTION

The characterization of mining-related contamination of freshwater ecosystems is important to assess hazards from exposure and develop effective and realistic remediation plans. Paleoenvironmental methods have been established to detect and quantify mining-related metal pollution, and novel approaches are being developed to predict future ecosystem recovery (Kirk and Gleason, 2015). Gradients of metal fluxes and concentrations or comparison between control and contaminated sites can give good approximations of environmental baseline conditions (Kurek et al., 2013; Sprague and Vermaire, 2018a, 2018b; Wiklund et al., 2014). However, source attribution, whereby the relative contribution of observed metal fluxes in sediments are partitioned among anthropogenic and natural

sources, remains challenging. Anthropogenic contaminants that are recirculated in the environment from various biological and geochemical processes are hard to distinguish from newly released contaminants or variation in background flux. Since a wide variety of environmental changes have occurred concurrently during the Anthropocene (Waters et al., 2016), the interactive effects of multiple disturbances (e.g. pollution, legacy contamination, land-use change, and climate) may confound interpretation of sediment records (Guilizzoni, 2012; Hawryshyn et al., 2012; Smol, 2010).

Lead isotope ratios are useful tracers of metal pollution sources because there are four stable isotopes (^{204}Pb , ^{206}Pb , ^{207}Pb and ^{208}Pb), and they have been widely used in paleolimnology (Cheng and Hu, 2010; Komárek et al., 2008) due to the stability of Pb in sediments (Outridge and Wang, 2015). One of the most common applications of Pb isotope ratios in sediment is for identification of atmospheric sources of Pb deposition from local, regional and long-range transport, typically measured on one sediment core to reconstruct the lake's contamination history (Babos et al., 2019; Gallon et al., 2006; Liu et al., 2012b; Outridge et al., 2002). Isotope mixing models can resolve the relative contributions of different Pb sources if the source isotope ratios are known and distinct (Bird et al., 2010; Mariet et al., 2018), although precise quantification of source attribution is often not possible in lake sediment studies because isotopic information is not available for all sources (Cheng and Hu, 2010). This study presents a novel application of Pb stable isotopes involving quantitative source apportionment to reconstruct within-lake transport and burial of point-source mining pollution, which had a distinct and well-defined isotopic signature. Lead contamination from gold mining was investigated in Yellowknife Bay (Great Slave Lake, Northwest Territories, Canada) by measurement of Pb concentrations and isotope profiles in multiple sediment cores to characterize the within-lake accumulation rates, dispersion and burial of mining-derived Pb in sediment and to predict the future recovery rate of Pb contamination in the bay. The application of Pb isotopes was particularly useful for resolving Pb of mining origin when Pb concentrations approached background and provided

insights into the persistence of Pb contamination in surface sediment following mine closure. The findings are relevant for assessment of point-source contamination of lakes from metal mining around the world.

3.3 STUDY AREA

Yellowknife Bay is located on the north shore of Great Slave Lake, near the City of Yellowknife, Northwest Territories, Canada (Figure 3.1). The surface area of the bay covers approximately 20 km² out the 27,200 km² surface of Great Slave Lake. Maximum water depth in the bay varies from 15 m at the north end to 30 m at the south end (Canadian Hydrographic Service, 2005).

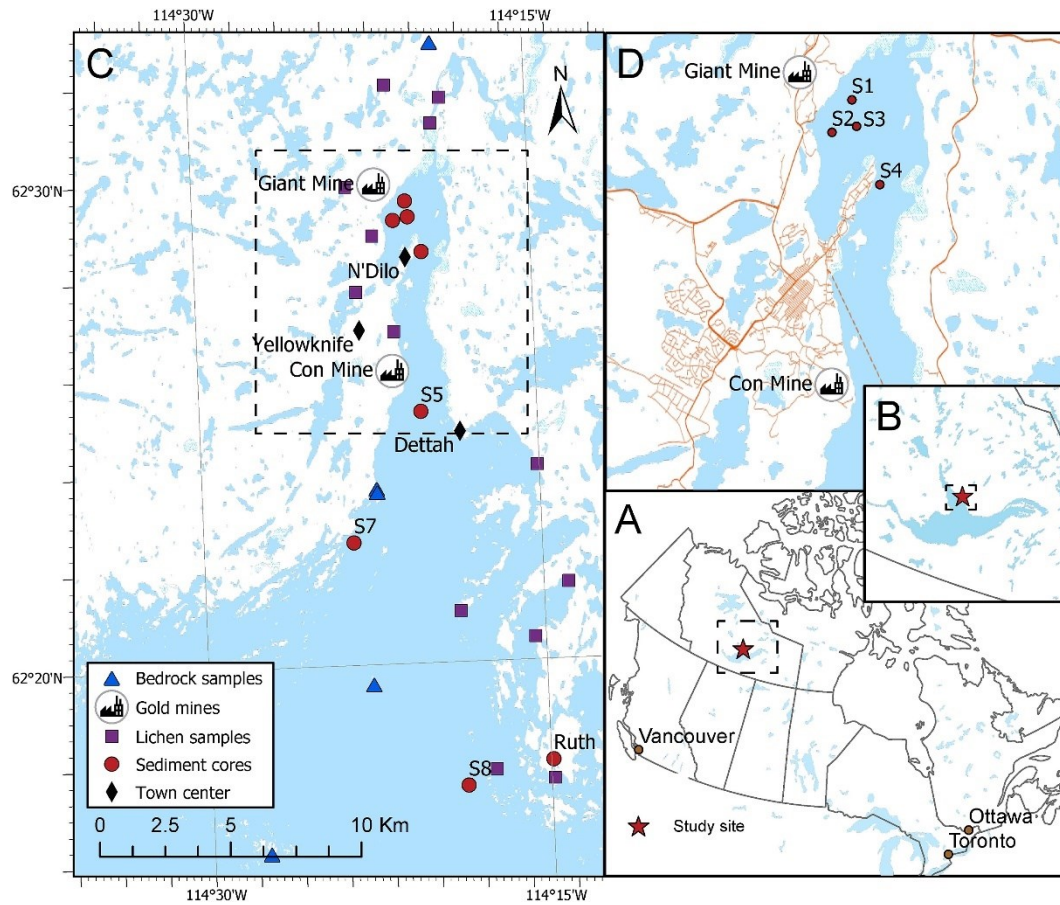


Figure 3.1 Location of the study area within Canada (A) and on the north shore of Great Slave Lake in the Northwest Territories (B). View of Yellowknife Bay and the main body of Great Slave Lake (C) including locations of the two gold mines and sampling sites for sediment cores, bedrock samples, and lichen samples, with a close-up view of the north end of the bay (D).

Gold production in Yellowknife spanned six decades during the 20th century, principally at the Giant and Con Mines, resulting in large releases of arsenic, antimony and metals (including Pb) to Yellowknife Bay via effluent, tailings dumps and atmospheric deposition of ore roasting emissions (Chetelat et al., 2017). Gold production officially ceased in Yellowknife in 2005, but legacy contaminants are still present in the surface layer of lake sediments, which are enriched for some elements by orders of magnitude compared to background conditions (Chetelat et al., 2017; Galloway et al., 2015; Palmer et al., 2015).

The dust emitted during the ore roasting process at Con Mine until 1970 and at Giant mine until 1999 was a major source of metal contamination (mainly arsenic, antimony and to a lesser extent metals such as lead) to lake water, sediment, and catchment soils (Bromstad et al., 2017; Fawcett et al., 2015; Thienpont et al., 2016). The greatest emissions of metals occurred during the earliest years of operation when few pollution control measures were in place and no environmental monitoring was being conducted. An estimated 86% (or 17,800 tonnes) of the total arsenic emissions at the Giant Mine occurred in the first 15 years of production (Jamieson, 2014). Estimates of metal pollution release, based on arsenic trioxide emissions, are 6.6 times greater for Giant Mine than Con Mine (INAC, 2013; Hocking et al., 1978). Arsenic and antimony concentrations in lake water and surficial sediment currently provide the best estimates of the footprint of stack emissions (Houben et al., 2016; Palmer et al., 2015). Non-atmospheric sources of anthropogenic metals released to Yellowknife Bay from Giant Mine included the dumping of metal-rich tailings directly into the bay between 1948 and 1951 (INAC, 2013) and effluent flowing into the bay from Baker Creek (Chetelat et al., 2017).

3.4 METHODS

3.4.1 Sample Collection

A total of nine sediment cores were collected from the study area during the summers of 2013 to 2015 by boat using an 8.6 cm diameter UWITEC gravity corer (Figure 3.1). Eight of the cores were collected in offshore depositional areas along a transect from Yellowknife Bay into the main body of Great Slave Lake with increasing distance from the mine roasters to determine the historical input of Pb to the sediments. The ninth sediment core was collected from a small unnamed lake on Ruth Island (referred to as Ruth Lake). Ruth Lake is disconnected from Great Slave Lake waters and is located outside of Yellowknife Bay. It offered an opportunity to compare sediments affected by the transport of metals within Great Slave Lake to lake sediment only (potentially) affected by atmospheric deposition such as from roaster emissions or aerosol Pb from long-range transport. The cores ranged from 13 to 40 cm in length and were collected between 1 to 24 km from the location of the now decommissioned Giant Mine roaster stack (Figure 3.1 and Table 3.1).

Table 3.1 Name, location and description of collected sediment cores.

Site ID	Dated	Latitude (°N)	Longitude (°W)	Distance from Roaster* (km)	Collection Date	Water Depth (m)	Core Length (cm)
S1	No	62°29.515'	114°20.502'	1.4	Aug 2015	8	19
S2	No	62°29.127'	114°21.067'	1.9	Aug 2015	9	13
S3	Yes	62°29.189'	114°20.409'	1.9	Sept 2014	11	40
S4	Yes	62°28.375'	114°19.956'	3.5	Sept 2014	16	36
S5	Yes	62°25.181'	114°20.156'	9.2	Sept 2013	25	25
S7	No	62°22.532'	114°23.357'	14.2	Aug 2015	25	26
S8	Yes	62°17.461'	114°18.702'	23.7	Sept 2013	29	25
Ruth	Yes	62°17.928'	114°14.907'	23.4	Sept 2014	0.8	36

*Aerial distance to location of the now decommissioned Giant Mine ore roaster.

Sediment cores were sliced every 0.5 cm in the top 10 or 15 cm and every centimeter below that depth. Sediment slices were packed in plastic bags, freeze dried, weighed and homogenized prior to chemical analysis. All measurements are reported on a dry weight basis. Surficial bedrock was sampled from nine locations in the Yellowknife Bay catchment to obtain an estimate of Pb isotope values for potential natural weathering sources of Pb. The samples include lavas and intrusions from the Kam and Banting Groups of the Yellowknife greenstone belt and two granitoid intrusions (Cousens et al., 2002, 2006; Cousens, 2000). All samples were collected using INAC geological maps of the region. Lichen samples were collected on young branches of trees, mainly *Picea Mariana*, to estimate the Pb isotopic composition of local aerosol deposition (Carignan and Gariépy, 1995; Simonetti et al., 2003). Locations of sediment, bedrock and lichen samples were determined using a hand-held GPS unit (Figure 3.1).

3.4.2 Chronology

Five of the sediment cores were dated using radiogenic lead (^{210}Pb) and cesium (^{137}Cs) measurements. Radioisotopes were measured at one of three labs in Canada over the three-year study: the Canada Centre for Inland Waters (Burlington, Ontario), Flett Research Ltd. (Winnipeg, Manitoba) or MyCore Scientific Inc. (Dunrobin, Ontario). Disintegrations per minute of the radioisotopes were counted using gamma or alpha spectrometry. Supported radiogenic lead activity was estimated by measuring the activity of the ^{226}Ra isotope in the sediments (Appleby and Oldfield, 1978). Radiogenic lead dates were calculated using the constant rate of supply (CRS) model (Appleby and Oldfield, 1978), and age uncertainties were estimated by Bayesian statistics using the Sanchez-Cabeza et al. (2014) iterative calculation sheets implemented in Microsoft® Excel. The calculated ages and uncertainties were interpolated using the *Bacon* package (Blaauw and Christen, 2011) implemented in R (R Development Core Team, 2018). The age of sediment slices is reported here as the median of 2000 stored Markov Chain Monte Carlo iterations for that slice. Age-depth models were compared to the ^{137}Cs activity

profile for independent validation. The age-depth models for the cores are provided in Chételat et al. (2017).

3.4.3 Metals concentrations

Sediments from cores S1, S2, S4, S7 and Ruth Lake were analyzed for 30 elements by inductively coupled plasma mass spectrometry (ICP-MS) at RPC Laboratories in Fredericton, New Brunswick, Canada. Sediments from three other cores (S3, S5, S8) were analyzed for 46 elements by ICP-MS at the Canada Centre for Inland Waters (Burlington, Canada). Sediments were digested with *aqua regia* at the Canada Centre for Inland Waters while samples at RPC Laboratories were digested with hydrochloric acid and hydrogen peroxide. Both methods do not completely decompose siliceous materials; therefore, the Pb analytical results represent leachable concentrations. Recoveries of leachable lead represented $65\pm 2\%$ ($n=14$) of the total Pb concentration in the certified reference material San Juan soil (Mackey et al., 2010). Relative standard deviations of duplicate samples from RPC Laboratories were $1\pm 2\%$ for bulk concentrations of Pb ($n=7$). Several sediment samples were analyzed for Pb concentration at both the Canada Centre for Inland Waters and RPC Laboratories for comparison, and relative standard deviations of these results were $4\pm 2\%$ ($n=5$). Measured concentrations of Pb for procedural blanks at both laboratories were below detection limit (<0.01 mg kg^{-1} , $n=14$). All ICP-MS measurements along with QA/QC data are presented in Chételat et al. (2017).

3.4.4 Isotope analysis

Five to 18 sediment layers from each core along with lichen and bedrock samples were analyzed for Pb stable isotopes ratios on a Thermo-Finnigan TRITON mass spectrometer at the Isotope Geochemistry and Geochronology Research Centre at Carleton University (Ottawa, Canada). Approximately 100 milligrams of each sediment sample was weighed into a Teflon screw-cap vial and dissolved in a mix of 75% HF and 25% 15N HNO₃. Samples were left on a hotplate at 145°C for two days, after which caps were removed and the HF/HNO₃ was evaporated to form a moist paste. The

residue was then treated with 7N HNO₃, dried down, then 2ml of 6N HCl was added to each sample, the beaker was capped and left on a hotplate for 24 hours. After drying down the HCl, the residue was then dissolved in 1N HBr for column chemistry. For the bedrock samples, a weighed aliquot of the HBr was removed for Pb concentration determinations by isotope dilution. A weighed amount of ²⁰⁸Pb spike was added to the aliquot and returned to the hotplate for several hours to ensure complete mixing of the dissolved sample and the spike. All reagents were ultrapure, with Pb blanks <1 pg/g.

Lead was isolated in Bio-Rad 10-ml polyethylene columns and Dowex AG1-8X anion resin, using 1N HBR to elute other elements and 6N HCl to elute Pb. The collected Pb solution was dried, dissolved in 1N HBr, and the above procedure was repeated with a small volume resin bed. After final drying, the residue was treated with 7N HNO₃ to eliminate bromides and residual organic matter in the Pb solution.

Total procedural blanks for Pb were <150 pg and were insignificant relative to the Pb content of samples (<<1% of total Pb). The samples were loaded onto single Re filaments with H₃PO₄ and silica gel and were run manually at a filament temperature of 1275°C in a Thermo-Finnigan TRITON mass spectrometer. Lead isotope ratios were corrected for fractionation using the NBS 981 standard values of Cliff et al. (1996). The total ranges measured for NBS 981 in a 2-year period bracketing the analyses are (2σ errors) ±0.017 for ²⁰⁶Pb/²⁰⁴Pb (0.05% RSD), ±0.021 for ²⁰⁷Pb/²⁰⁴Pb (0.07% RSD), ±0.038 for ²⁰⁸Pb/²⁰⁴Pb (0.05% RSD), ±0.0021 for ²⁰⁸Pb/²⁰⁶Pb (0.05% RSD), ±0.00038 for ²⁰⁷Pb/²⁰⁶Pb (0.02% RSD). The precision of the Pb concentration values in the bedrock samples is estimated at less than 1%. Within-run errors on the reference material isotopic ratios (n=7) were below the aforementioned values for each ratio.

3.4.5 Isotope mixing model

Isotopic data expressed as $^{208}\text{Pb}/^{204}\text{Pb}$ vs. $^{206}\text{Pb}/^{207}\text{Pb}$ ratios were well described using a linear regression fit ($R^2=0.98$, $p<0.001$) between the isotopic values of mining ore used at Giant Mine and Con Mine, lichen, bedrock and sediment samples (Figure 3.2).

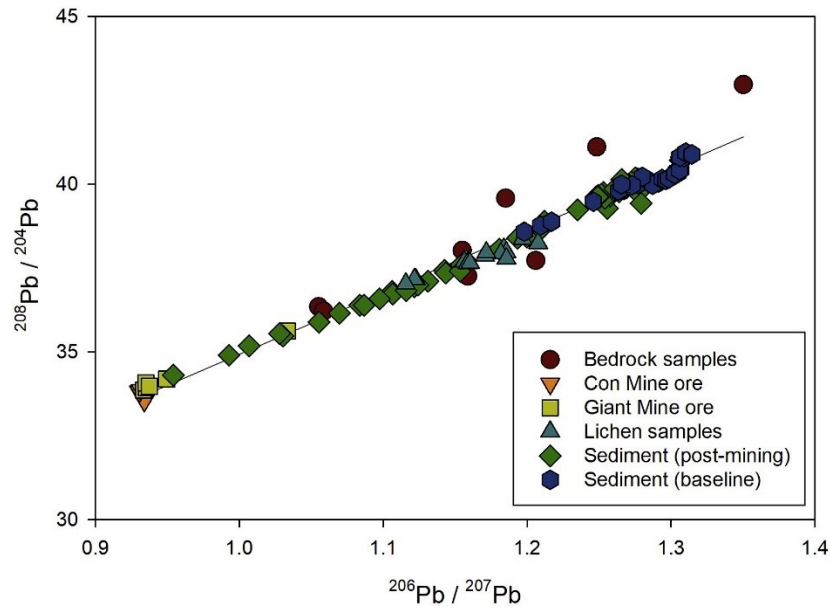


Figure 3.2 Biplot of stable Pb isotope ratios ($^{208}\text{Pb}/^{204}\text{Pb}$ and $^{206}\text{Pb}/^{207}\text{Pb}$) for sediment layers (baseline pre-1938, and since the start of mining in Yellowknife in 1938), lichen, bedrock and ore from two gold mines. The Pb isotope data for ore are from Cousens et al. (2006) and Cumming and Tsong, (1975).

We used a well-established Bayesian mixing model to resolve the source partitioning in our sediment samples. We used the *Simmr* package implemented in R (Parnell and Inger, 2016), which was initially conceived to resolve mixing equations for quantifying the diet of an organism using an isometric log-ratio transformation (Egozcue et al., 2003; Parnell et al., 2013). However, the model can be implemented for geochemical studies by assuming a null trophic enrichment factor for each source. Source partitioning uncertainty is estimated with a classical bootstrapping method (>10,000 iterations). Source attribution is reported as the average contribution from the Bayesian distribution and 2- σ uncertainties are reported.

We modeled the contribution of two sources to the Pb in the sediment using a linear mixing model relying on two isotope ratios ($^{206}\text{Pb}/^{207}\text{Pb}$ and $^{208}\text{Pb}/^{204}\text{Pb}$). The two sources included in this model were (1) background Pb occurring from stream sediment and watershed erosion, (2) mining-derived Pb released by the local gold mining industry. The isotope ratio of background Pb was estimated from the mean and standard deviation of Pb isotope values in the sediment layers dated prior to mining in the area (< A.D. 1938, 95% CI). The ratio of mining-derived Pb corresponded to the mean and standard deviation of isotopic values for pyrite, chalcopyrite and sphalerite processed at Giant Mine as measured by Cousens et al. (2006) and galena processed at Con Mine as measured by Cumming and Tsong, (1975).

As a separate analysis, source partitioning in samples from the sediment-water interface and sediment layers dated 1995 onward (last ~20 years) were modelled using the two previously mentioned sources and an additional source representing aerosol input to the sediment. The isotope value of aerosol input was determined from the isotopic composition of lichen samples. We used this model to assess the sensitivity of sediment Pb source partitioning to the inclusion of aerosols as a source. We evaluated the relevance of the three-source model vs. the two-source model based on a comparison among sampling

sites and geochemical profiles of Sb, Cu and Zn, which were emitted along with Pb during the mining operations (Chételat et al., 2017).

3.4.6 Flux calculation

Total Pb flux was calculated using equation 3.1 and the Pb flux contribution from mining pollution (Pb_m) was estimated from equation 3.2.

$$\text{Eq. 3.1} \quad Pb_f = \frac{\rho Pb_c}{A_r}$$

$$\text{Eq. 3.2} \quad Pb_m = Pb_f \times f_m$$

Where Pb_f is the Pb flux for a sediment slice ($\text{mg cm}^{-2} \text{yr}^{-1}$), ρ is the dry density of the sediment slice (g cm^{-3}), Pb_c is the Pb concentration in the sediment slice (mg g^{-1}), A_r is the average estimated accumulation rate for that depth (yr cm^{-1}) and f_m is the ratio of mining-derived Pb in the sediment according to the isotope mixing model (fraction varying between 0 and 1).

3.4.7 Spatial distribution of Pb contamination and recovery models

The past and current extent of mining-derived contamination in the sediment was estimated by extrapolating the log-linear trend in the relative contribution of mining-derived Pb versus distance from the Giant Mine at maximum impact and in surface sediment. Similarly, a recovery model was generated by extrapolating the log-linear trend in relative contribution of mining-derived Pb over time at each site. The sediment layers dated after 1958 were used for the recovery model since >85% of Giant Mine roaster emissions occurred before that date (Bromstad et al., 2017). The intercept of this log-linear trend provides a timeline for mining-derived Pb to be completely buried in the surface layer at each site. We also generated a three-dimensional gaussian spline based on the sediment core distance from Giant Mine (km), the average age of the sediment layers according to the age-depth models and the estimated contribution of mining Pb (f_m) for that age and location. The gaussian spline was

modeled using *Sigmaplot 14.0* software. This model provides a spatially smoothed estimation of recovery time over the studied area similar to a kernel density estimation.

3.5 RESULTS

3.5.1 Chronologies

Chronologies for the five dated sediment cores showed that the sediment records extended back to pre-mining conditions (pre-1938). In each core, the modeled age of the peak in radiogenic cesium, which occurs in A.D. 1963±2 (Pennington et al., 1973), was consistent with the 95% confidence interval of our age-depth model for that slice. The cores showed a linear decrease in unsupported ^{210}Pb activity with sediment cumulative dry weight down to a depth varying between 6 and 28.5 cm.

There was a clear trend of higher sedimentation rate with increasing distance from the Giant Mine. Dry sedimentation rate in the shallow Ruth Lake was $73 \pm 17 \text{ g m}^{-2} \text{ year}^{-1}$ (average and standard deviation), which was lower than anywhere in Yellowknife Bay, where it varied between 795 ± 351 and $1138 \pm 505 \text{ g m}^{-2} \text{ year}^{-1}$.

3.5.2 Isotope ratios of Pb sources

The Pb isotope values of sediment dated prior to the opening of the mines ($^{208}\text{Pb}/^{204}\text{Pb} = 40.089 \pm 0.208$ and $^{206}\text{Pb}/^{207}\text{Pb} = 1.2914 \pm 0.0142$) were significantly different from mining-derived Pb ($^{208}\text{Pb}/^{204}\text{Pb} = 34.071 \pm 0.574$ and $^{206}\text{Pb}/^{207}\text{Pb} = 0.9450 \pm 0.0299$) (Mann–Whitney U test, $p < 0.001$) (Figure 3.2). Bedrock samples showed a large variability in Pb isotope ratios. Bedrock samples had significantly lower $^{206}\text{Pb}/^{207}\text{Pb}$ ratios (1.2466 ± 0.2259) but no difference in $^{208}\text{Pb}/^{204}\text{Pb}$ ratios (38.098 ± 2.237) compared to baseline sediments (Mann–Whitney U test, $p = 0.018$ and $p = 0.157$ respectively). One outlier, collected at a further distance from Yellowknife Bay than other bedrock samples, was present among our bedrock samples (DL-3, $^{208}\text{Pb}/^{204}\text{Pb} = 58.737$ and $^{206}\text{Pb}/^{207}\text{Pb} = 1.7983$). Lichen samples had Pb isotope values comprised within mining ore and baseline sediments in the biplot space ($^{208}\text{Pb}/^{204}\text{Pb} = 37.758 \pm 0.402$ and $^{206}\text{Pb}/^{207}\text{Pb} = 1.1657 \pm 0.0276$). There was no significant trend

predicting isotope values of lichen samples with respect to the distance from the city or either of the mines (Figure 3.3).

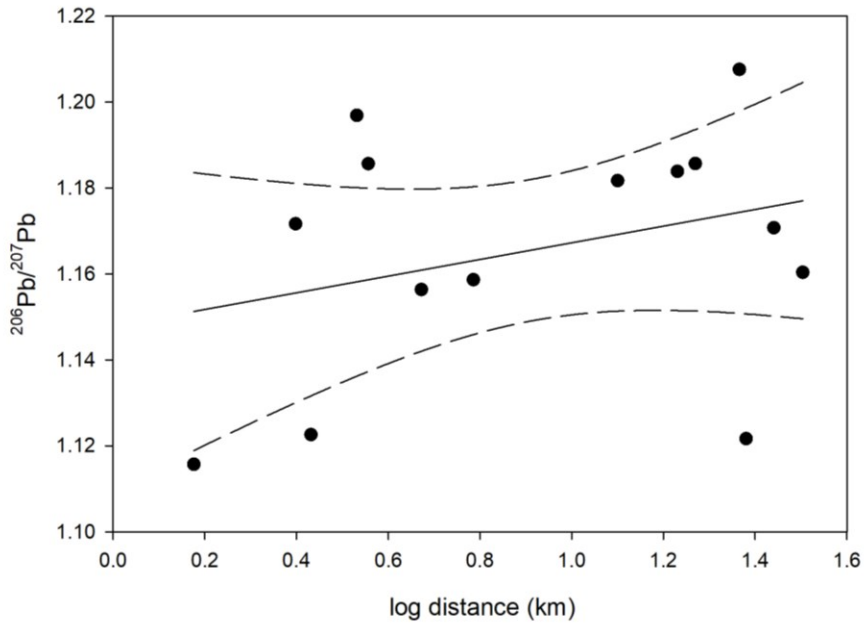


Figure 3.3 Isotope ratios ($^{206}\text{Pb}/^{207}\text{Pb}$) in lichen samples against distance to the Giant mine roaster. The linear regression is not significant ($R^2=0.1$, $p=0.28$)

3.5.3 Sediment metal concentrations

The mean background Pb concentration in sediments (pre-1938) was $14 \pm 3.7 \text{ mg kg}^{-1}$ (mean and standard deviation, $n=15$) in all cores from Great Slave Lake while Ruth Lake sediment had a lower background concentration at $7 \pm 0.2 \text{ mg kg}^{-1}$. Sediment Pb concentrations in cores from the north end of Yellowknife Bay exhibited sharp sub-surface peaks followed by a rapid decrease and a slower attenuation near the sediment-water interface (Figure 3.4a). The maximum recorded Pb concentration in each core decreased with distance from Giant Mine (Figure 3.4a). Core S1, located closest to the mine (1.4 km), had a maximum Pb concentration of $351 \pm 4 \text{ mg kg}^{-1}$, while core S4, located 3.5 km away, reached a maximum Pb concentration of $71 \pm 1 \text{ mg kg}^{-1}$. The sub-surface peaks in sediment concentration exceeded the Canadian sediment quality guideline within 4.5 km of Giant Mine (Interim Sediment Quality Guideline for Pb = 35 mg kg^{-1} , probable effect level = 91 mg kg^{-1}) (CCME, 2002).

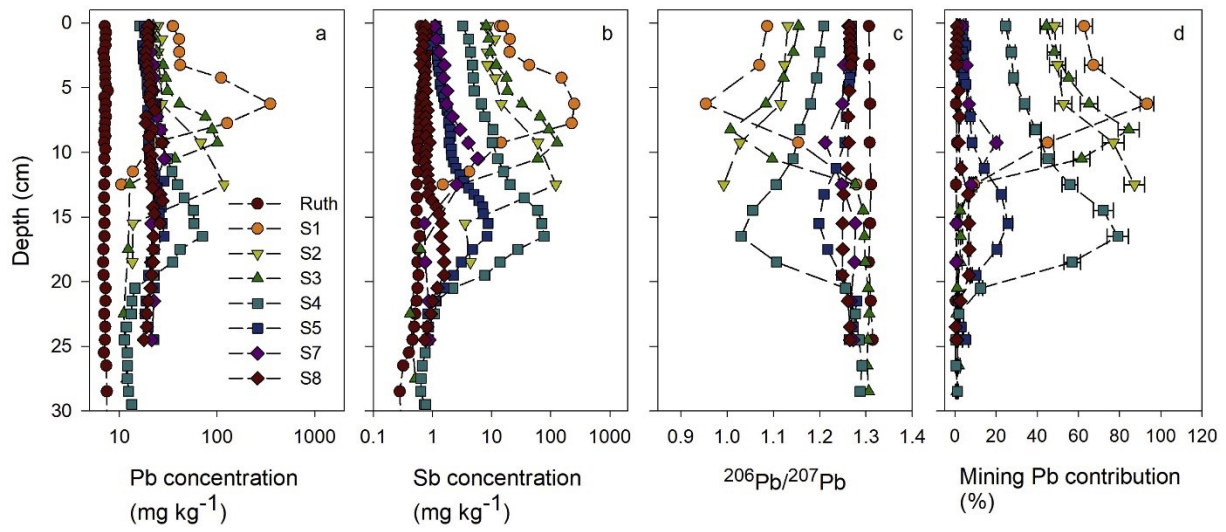


Figure 3.4 Lead (a) and antimony (Sb) concentrations in sediment (b), Pb stable isotope ratios ($^{206}\text{Pb}/^{207}\text{Pb}$) (c), and modelled mining-derived Pb contribution (two-source model) for each sediment core (d). Note the \log_{10} axis for concentrations in (a) and (b).

Although all sites recorded a simultaneous increase in Pb concentration during the 1950s, the timing of the maximum recorded concentration was slightly different among sites. Sites closer to the mines recorded a maximum impact slightly before far-field sites. In cores S3 and S4, Pb concentrations reached a maximum of 101 ± 10 and 71 ± 7 mg kg⁻¹ respectively between 1955 and 1965. Site S5 peaked at 27.5 ± 0.4 mg Pb kg⁻¹ between 1960 and 1975 and site S8 peaked at 26.3 ± 0.4 mg Pb kg⁻¹ between 1973 and 1985.

The Pb concentrations of the sediment surface layers (0-1 cm depth) varied between 16 ± 0.1 and 35 ± 0.4 mg Pb kg⁻¹ in all cores (enrichment factor of 1 to 2.2), following a log-linear relationship with the distance from the mines. Surface sediments had slightly elevated Pb concentrations compared to the background in cores S3 and S4 ($+4 \pm 1$ mg kg⁻¹ and $+10 \pm 0.6$ mg kg⁻¹; enrichment factors of 1.9 and 1.3, respectively) but comparable to the background in cores S5 and S8. The Pb concentrations in the sediment were directly correlated to concentrations of other mining-released elements (Sb, Zn and Cu) in all cores except Ruth Lake (Figure 3.5, Pearson coefficients = 0.67-0.90, $p < 0.001$). The concentration, flux and modelled contribution of Giant Mine ore were all significantly correlated, except in the Ruth Lake sediment (Table 3.2).

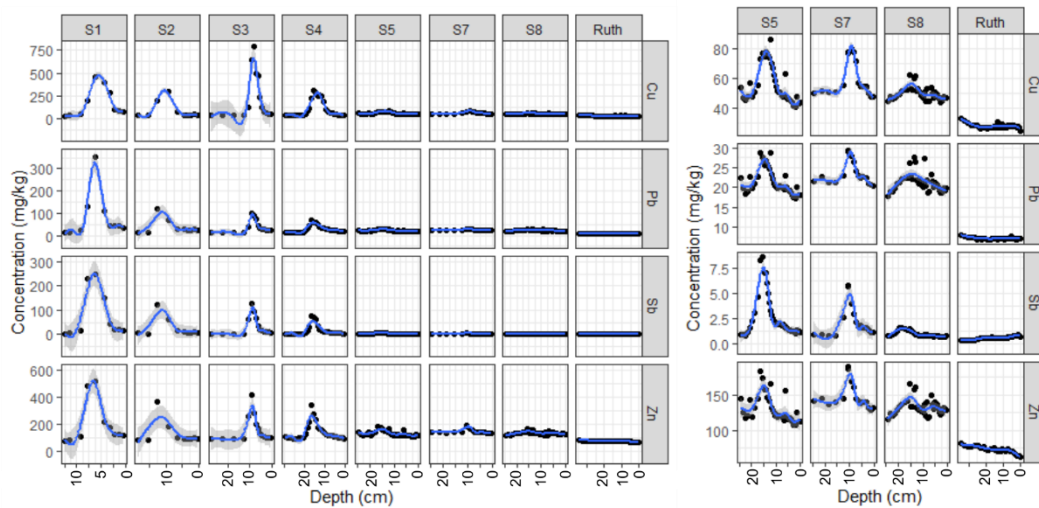


Figure 3.5 Concentrations of elements potentially released from mining activities, against depth in sediment cores. Right side panel is a duplicate of last four panels with a small y axis range. Blue line and grey areas are a generalised additive model and 95% confidence interval respectively.

Table 3.2: Spearman correlation coefficients between Pb concentration (mg kg^{-1}), Pb fluxes ($\text{mg m}^{-2} \text{yr}^{-1}$) and modelled mining-derived pb contribution (%) at each site. Correlations with fluxes were not possible for undated cores. $P < 0.05^*$, $p < 0.01^{**}$, $p < 0.001^{***}$

Core	Concentration vs. flux	Concentration vs. contribution	Flux vs. contribution
S1	-	0.768*	-
S2	-	0.970**	-
S3	0.922***	0.877***	0.819*
S4	0.962***	0.945***	0.957***
S5	0.474**	0.892***	0.457*
S7	-	0.956***	-
S8	0.593***	0.615**	0.408
Ruth	0.062	-0.443	-

3.5.4 Pb stable isotopes in sediment and source partitioning

There were clear changes in the isotopic ratios of Pb that accumulated in sediments over time at sites located closer to the mines (Figure 3.7c). The timing of isotopic changes was consistent with increases in Pb and Sb concentrations at these sites (Figures 3.5 and 3.7) and dated back to the early years of mining operations (1945 to 1955). Sediment from the nearest sites to the mines had the largest changes in Pb isotope ratios throughout the core profiles. The furthest site from the mines (S8) in the main body of Great Slave Lake recorded limited change in Pb isotope ratios (Figure 3.7c). Ruth lake, at the same distance as S8 but disconnected from the main water body, had no change in isotope ratio throughout the core (Figure 3.7c). Isotope values closest to mining ore were found in sediment dating between 1955 and 1978. Partitioning the sediment Pb using a two-source mixing model suggested that at its peak, mining pollution represented $92 \pm 8 \%$ of all Pb deposited at the study site closest to the Giant Mine roaster (core S1, 6 cm depth, undated) and $8 \pm 4 \%$ at the furthest study site (core S8, 17 cm depth, c.a. 1965) (Figure 3.8). The estimated contribution of mining-related Pb for sediment deposited prior to the initiation of mining activity was close to but not zero ($2 \pm 2\%$) due to uncertainties for both sources included in the model (background Pb and mining ore).

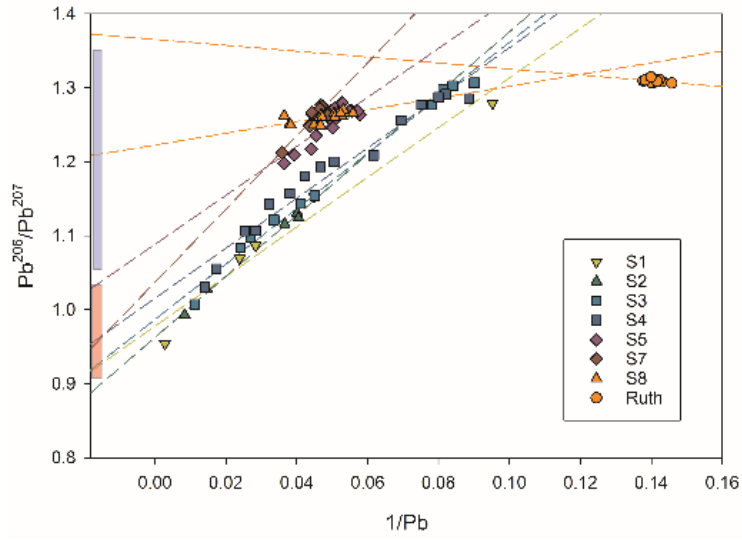


Figure 3.6: Ratio of $^{206}Pb: ^{207}Pb$ vs. inverse Pb concentration for each sediment sample with a linear trend for each core. The red box represents the range of $^{206}Pb: ^{207}Pb$ ratio of Giant Mine and Con Mine ore (Cousens et al., 2006; Cumming and Tsong, 1975).

Including aerosols as a possible Pb source for recent surface sediment resulted in large uncertainties for the source attribution because of multiple possible solutions for the isotopic mixture. The Bayesian estimations from the three-source model diverged by as much as 85% (positive and negative) from the two-source model estimate for certain samples. The latter model suggested that mining-derived Pb at the sediment-water interface was <5% at all sites except S1 (30 ± 16 %) and S4 (11 ± 10 %). However, when using a three-source model, the spatial relationship between mining-derived Pb in surface sediment and distance to the mines was non-linear.

3.5.5 Sedimentary Pb fluxes

Background Pb fluxes (pre-1938) in cores S3, S4, S5 and S8 were $5.6 \text{ mg m}^{-2} \text{ yr}^{-1}$, $12.2 \text{ mg m}^{-2} \text{ yr}^{-1}$, $3.5 \text{ mg m}^{-2} \text{ yr}^{-1}$ and $7.4 \text{ mg m}^{-2} \text{ yr}^{-1}$, respectively. Ruth Lake had a lower background flux at $0.6 \text{ mg m}^{-2} \text{ yr}^{-1}$. A trend of increasing Pb flux started between 1940 and 1952 at all locations in Yellowknife Bay (Figure 3.7), concurrent with the opening of Con and Giant mines. Ruth Lake did not show a trend in Pb accumulation rate over time but only the top 5 cm of this core was datable, corresponding to sediment accumulated since *c.a.* 1944. Annual Pb fluxes in Yellowknife Bay reached their maximum between 1955 and 1978 depending on the location, which is consistent with the rise in Pb concentration and Pb isotope ratios approaching values for mining ore. Sites that were located closer to the mines reached their maximum recorded Pb flux earlier (S3 and S4, 1960 and 1955, respectively) than further sites (S5 and S8, 1970 and 1978, respectively). The maximum recorded Pb flux at each site varied between $0.7 \text{ mg m}^{-2} \text{ yr}^{-1}$ [Ruth] and $63 \text{ mg m}^{-2} \text{ yr}^{-1}$ [S4] (Figure 3.7b).

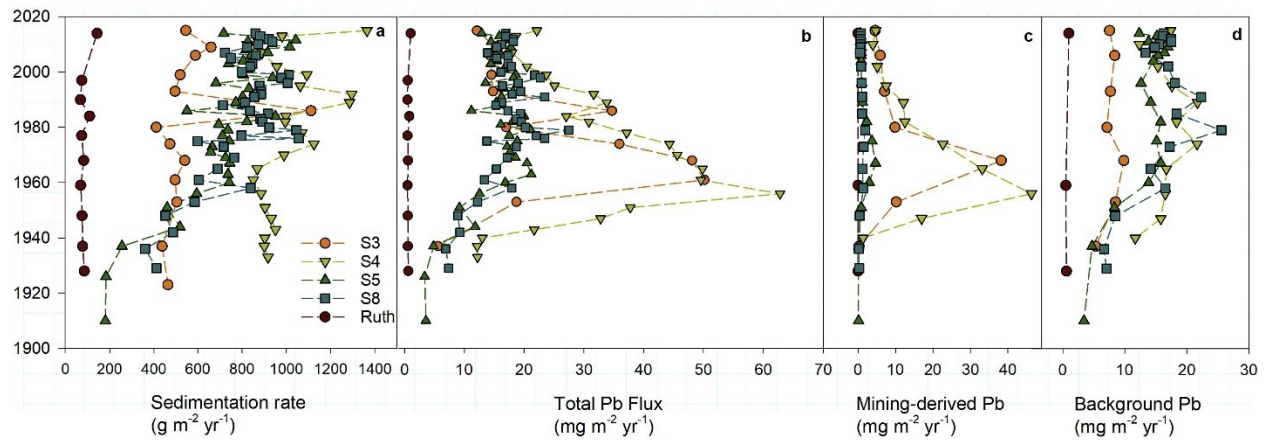


Figure 3.7: Sedimentation rate estimates from CRS modelling (a), modelled Pb flux (b), modelled mining-derived Pb flux (two-source model) (c), and modelled background Pb flux (d) against sediment age for five dated sediment cores.

Over the years of operation, fluxes of Pb attributed to gold mining in the Yellowknife Bay area varied between 0 and 47 mg m⁻² yr⁻¹. At the time cores were collected (nine to eleven years after mines closure), surface Pb fluxes were higher than pre-mining fluxes at each site except at Ruth Lake. Higher fluxes were due to the ongoing accumulation of mining-derived Pb within at least 3.5 km of the mine (sites S1 to S4) and an increase in background Pb accumulation rate (mainly driven by increasing sedimentation rate) at sites within the main body of Great Slave Lake (Figure 3.7b). Lead fluxes attributed to gold mining in the surface sediments were 4.5 and 4.7 mg m⁻² yr⁻¹ at sites S3 and S4, respectively, and approached zero at far-field sites S5 and S8 (0.2 and 0.4 mg m⁻² yr⁻¹, respectively). The two-source isotope mixing model suggested that higher Pb loading to the sediment was attributable to background Pb input (higher sedimentation rates) in cores S4, S5 and S8 (Figure 3.7a), whereas mining-derived Pb input was still present in cores S1, S2, S3 and S4 (Figure 3.7c).

3.5.6 Gold mining Pb contamination footprint over time

Using a linear regression model between the maximum inferred contribution of mining ore Pb and log distance to the Giant mine roaster (Figure 3.8), we estimated that mining pollution extended 27 km south of Giant Mine at the time of maximum loading to the bay (18-45 km, 95% confidence interval, R²=0.96, p<0.001). A linear regression of mining ore contribution of Pb in surface sediment against log-distance had an intercept at nine km (5-23 km, 95% confidence interval, R²=0.92, p<0.001), indicating the presence of mining ore in surface sediment within 9 km of the mine more than forty years after the initiation of pollution reduction measures at the mine and ten years after complete mine closure. Mining-derived Pb was below 1.5% throughout the Ruth Lake core, which was not different from pre-mining sediment in the main body of Great Slave Lake.

It took one to six years after the closure of Giant Mine before mining-derived Pb was absent from surface sediment >9 km away from the source (linear regression, 95% CI, Figure 3.8).

Extrapolating the recovery rates since the maximum recorded impact suggested that mining-derived Pb will be absent of surface sediment 23-56 years after mine closure at 3.5 km and 46-97 years after mine closure at 1.9 km (95% CI). The distribution of mining ore contribution of Pb against space and time was well described by a Gaussian regression centered around the source and the period of maximum contribution from the mine (ca. 1970) (adj $R^2=0.85$; all parameters $p<0.0001$, Figure 3.9).

However, this model underestimated the most recent contribution of mining-derived Pb in cores within 3.5 km from the source and predicted a more rapid recovery than the linear regression approach. The Gaussian spline intercept for the absence of mining-derived Pb was 11 years beyond 10 km of the source and 34 years within 3 km of the mine.

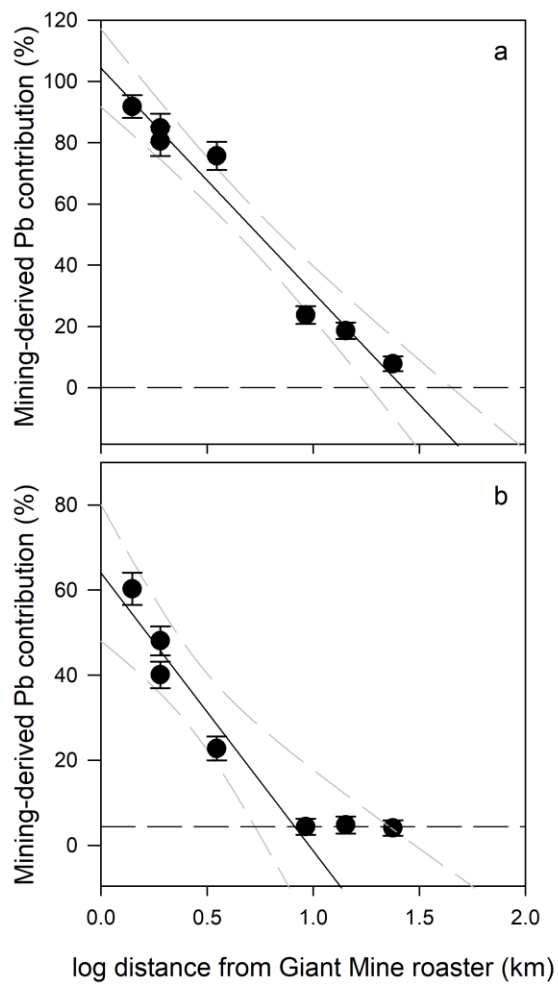


Figure 3.8: Footprint estimation for maximum mining-derived Pb contribution (a) and recent mining-derived Pb contribution (b).

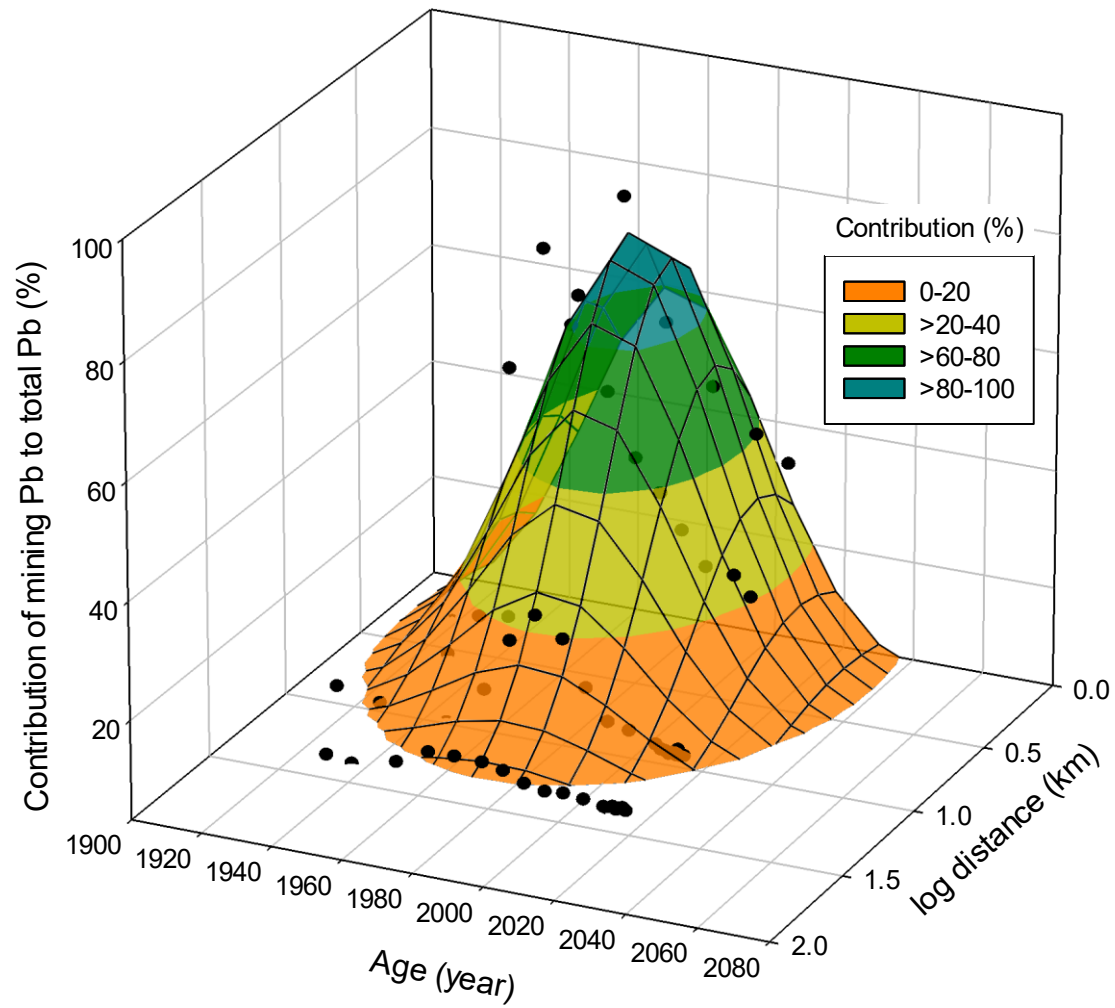


Figure 3.9: Three-dimensional Gaussian model of mining-derived Pb contribution in the sediment layers in relation to distance from the Giant Mine roaster and age of the sediment.

3.5.7 Estimation of Pb pollution from enrichment factors vs. isotope ratios

The relative contribution of mining derived Pb in sediment followed a rational function ($R^2=0.96$, $p<0.001$) with the Pb concentration enrichment factor as expected from a situation where enrichment factors are controlled by the addition mining-derived Pb alone as described by equation 3.3.

$$\text{Eq.3.3} \quad \text{Contribution (\%)} = \frac{EF-1}{EF} \times 100\%$$

Where EF is the enrichment factor defined by the ratio of observed Pb concentration to background concentration for that core. Slight deviations between the idealized curve produced by equation 3.3 and our data (Figure 3.10) suggest that a portion of Pb enrichment is caused by the changes in natural Pb flux over the sediment accumulation period (Figure 3.10). Based on this simple analysis, we can determine that using concentration enrichment factors alone could overestimate by up to 26% the contribution of mining ore to changes in Pb concentration.

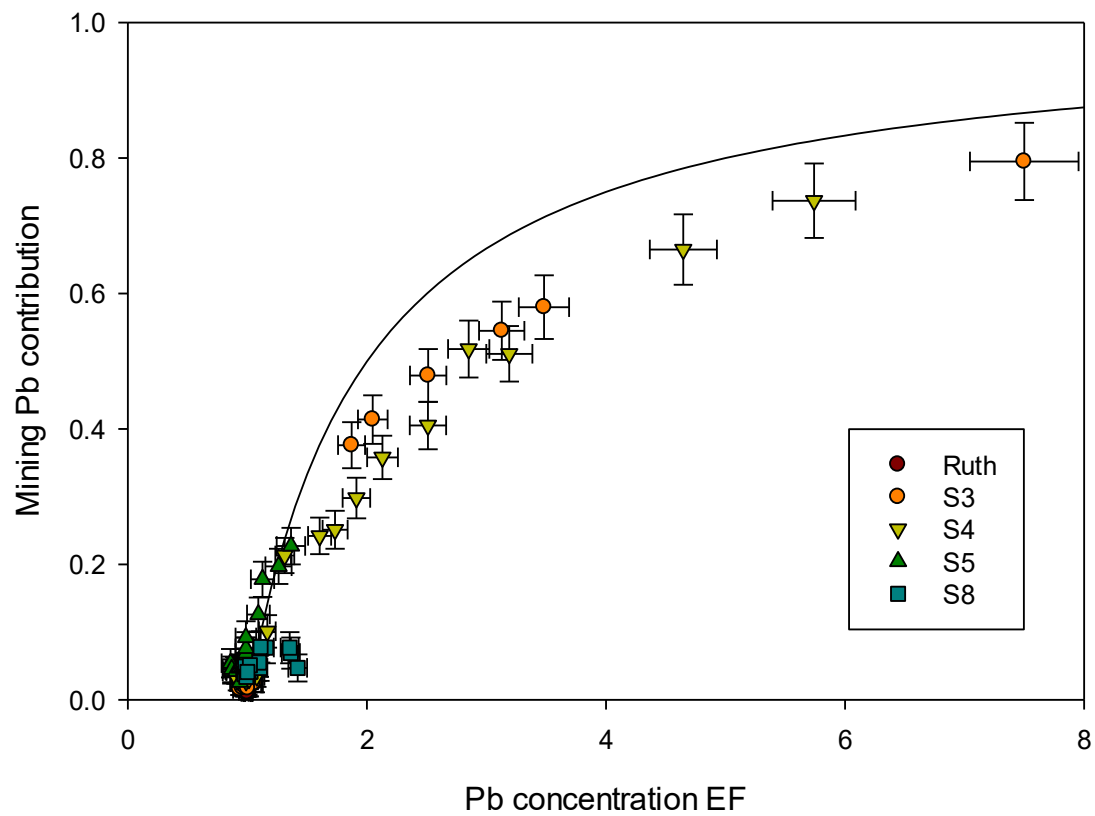


Figure 3.10: Relative mining-derived Pb contribution against Pb concentration enrichment factor of sediment samples. The black line represents the idealised relationship between enrichment factor and mining-derived Pb pollution if all changes in concentration were due to mining contamination (eq. 3).

3.6 DISCUSSION

3.6.1 Sources of Pb to Yellowknife Bay

Background weathering of Pb from bedrock and mining-derived Pb were found to be the dominant sources of Pb to Yellowknife Bay sediments. Several lines of evidence indicated that aerosol inputs were a minor source of Pb to the lake sediment in the study area. First, the lack of change in the Pb isotope composition of sediment from Ruth Lake (a “control” site) and the return of Pb isotope ratios of surface sediment to pre-disturbance values at the far-field sites (cores S5, S7 and S8) indicated that regional aerosol deposition from anthropogenic sources during the mid-to-late twentieth century were not likely significant (Figure 3.7c). Second, the enrichment of Sb and metals in addition to Pb at affected sites provided a geochemical signature of mining pollution that is unrelated to inputs from leaded gasoline, aviation fuel (*avgas*) or Pb contained in long-range aerosols (Figure 3.5). Third, estimates of regional Pb aerosol deposition in northwestern Canada, based on peat and ice cores, are very low at $<1.5 \text{ mg m}^{-2} \text{ yr}^{-1}$ (Gross et al., 2012; Shotyky et al., 2017). That magnitude of aerosol deposition represents $<5\%$ of the total sediment Pb flux in the cores post-1960. Negligible anthropogenic Pb enrichment from long-range atmospheric transport was observed in lakes of the high Canadian Arctic, which was attributed to low precipitation with increasing latitude (Outridge et al., 2002). Yellowknife has a dry continental climate which could also result in low aerosol deposition. Nevertheless, our three-source mixing model could not adequately resolve the contribution of Pb aerosols, and it is possible that inputs from other anthropogenic sources of Pb (regional or local) may have also had a minor contribution to excess Pb in the surface layers of sediments, which could have influenced our assessment of recovery from mining-derived Pb. However, even the model that included Pb aerosols as a third source estimated that mining-derived Pb was present in surface sediment at nearfield sites S1 and S4.

3.6.2 Pb stable isotopes as a tool for the identification of mining pollution in sediment

The source attribution modelling using Pb isotopes highlights the persistence of Pb pollution within lakes. The presence of mining-derived Pb in surface sediments within 9 km of the source, ten years after the closure of the gold mines, suggests an ongoing input of legacy pollution in the lake. Sources of legacy metal pollution specific to Yellowknife Bay may include a combination of effluent release from Baker Creek, sediment focusing from tailings dumped in the early years of mining, and/or catchment erosion of mining-derived Pb from the surrounding terrestrial environment. However, our model estimates indicated that higher background Pb fluxes in recent years also contributed to Pb enrichment in surface sediment. Using a Pb concentration gradient alone would have overestimated the pollution contribution by up to 26% (Figure 3.10).

This information is relevant for assessing the fate of other metal pollutants emitted from the mines such as arsenic, which does not have multiple stable isotopes and is subject to remobilization upon change in redox conditions. It should be noted that in this study, metal concentrations from the sediments were determined following an acid-labile digestion method, whereas a total dissolution technique was used to liberate the Pb from sediment for isotopic analysis. The total dissolution method included inert Pb bound within silicate minerals, which would not have been included in the acid-labile measurements of Pb concentrations. Therefore, our measurements of Pb concentration and Pb flux are conservative estimates of mining impact (due to partial digestion). However, we assume that the largest part of Pb in the Giant Mine ore was in sulfide minerals such as galena and various sulfosalts which would have been digested in the partial dissolution method (Jamieson, 2014; Walker et al., 2015). We nevertheless recommend that future investigation of sediment Pb isotopes use a consistent digestion method for both the measurement of Pb isotope ratios and concentrations.

3.6.3 Evidence for different metal transport processes with distance from the mines

The timing between mining activities and sediment flux records suggest different pathways for the transport of Pb at various locations in Yellowknife Bay. In lakes near a copper smelter in Eastern Canada where Pb pollution was atmospherically deposited, there was a 1-4 year delay between peak emissions and the peak flux in nearby lake sediment (Couillard et al., 2008). A similar short delay between the opening of Giant Mine and increases in sediment metal concentrations was evident in a smaller lake close to the mine (Thienpont et al., 2016). An onset of Pb accumulation in sediment coeval with the time of Giant Mine opening was only visible at coring sites closer than 3.5 km from the mine, suggesting that the deposition of roaster emissions may have had limited impact on far-field sites. Peak metal emissions from the Giant Mine roaster occurred around 1950 (Hocking et al., 1978) whereas peak flux in our sediment occurred only in 1970 at 9 km (1968-1971, 95% CI) and in 1979 at 24 km (1978-1981, 95% CI). This large delay is likely due to particle focusing rather than direct atmospheric deposition. The mining-derived Pb did not reach the isolated Ruth Lake but a small amount reached an equal distance on the main water body, suggesting that sediment migration transported mining-derived Pb over a longer distance than atmospheric deposition along this southward transect. Mining-derived Pb was deposited at the north end of the bay from atmospheric deposition, solid tailings or effluent flowing down Baker Creek, and a small fraction of this pollution then likely moved slowly southward over time by sediment migration.

3.6.4 Mining-derived Pb contamination footprint

We measured sediment Pb concentration gradients comparable to those reported for lakes near Canadian gold mines but well below the reported values for sediment in tailing ponds for the same mines (Azcue et al., 1995; Mudroch et al., 1989; Wong et al., 1999). The maximum mining-derived Pb flux reported in this study ($63 \text{ mg m}^{-2} \text{ yr}^{-1}$) was comparable to the maximum recorded Pb fluxes from lakes located between 6 and 36 km from copper smelter of the Rouyn-Noranda mining area ($27 - 58 \text{ mg m}^{-2} \text{ yr}^{-1}$) (Couillard et al., 2008; Gallon et al., 2006).

Our estimation of the mining pollution footprint at its peak (~27 km) is consistent with previous investigation of the Giant Mine footprint relying on arsenic concentrations in sediment and soils (Galloway et al., 2018; Hocking et al., 1978; Hutchinson et al., 1982; Kerr, 2006; Palmer et al., 2015). This footprint is site-specific since factors such as stack height and wind speed influence the distance that contaminants are dispersed. As a comparison, the footprint of copper smelters in Rouyn-Noranda, Québec, is 30-40 km (Zdanowicz et al., 2006), but their stacks are taller at 82 m and 116 m compared to now decommissioned roaster stack at Giant Mine (46 m).

3.6.5 Lake ecosystem recovery from Pb contamination

The recovery trends for mining-derived Pb in sediment differed with distance from the Giant Mine. A decrease in mining-derived Pb flux following the implementation of pollution mitigation measures in the first two decades of operations (e.g., reductions in roaster emissions and tailings management) is evident in the sediment records near Giant Mine. Sites further from the mines had lower recovery rates from Pb pollution, but also a lower impact magnitude. Similarly, closer to the source, the recovery rate gradually decreased, suggesting rates more typical of catchment retention and effluents (e.g. Ek and Renberg, 2001; Wong et al., 1999) than atmospheric deposition (e.g., Renberg et al., 2002).

Abandoned mine sites such as at Yellowknife provide useful data to predict recovery from point-source metal pollution. Our estimation of recovery time for Pb contamination of Yellowknife Bay was 1-97 years after mine closure, depending on the distance from the source, which is slightly lower than the 54–128 years estimated for the recovery from Pb pollution of a lake near a gold mine in Brotherswater, northeast England (Schillereff et al., 2016). Mining activity went on for 250 years in Brotherswater compared to the ~65 years gold mining and ore processing history at Yellowknife. The surface sediment from Yellowknife Bay could have received recent anthropogenic contributions from additional modern point-sources of Pb pollution from the City of Yellowknife, such as from the local aviation industry (which still uses leaded aviation fuel in piston engines) or household wastes. Such

new sources of Pb would dampen the recovery rates of Pb in sediment. Comparing paleolimnological data from a greater number of decommissioned mining sites would improve our understanding of the factors involved in Pb pollution recovery (e.g., catchment retention, sediment burial, lateral transport, sediment mixing).

3.7 CONCLUSIONS

This study demonstrated that mining-derived Pb and background Pb were the two main sources of Pb in Yellowknife Bay sediments. Aerosol inputs were a negligible source of Pb to the lake sediment, probably due to low precipitation. Mining-derived Pb was still accumulating at the sediment-water interface in Yellowknife Bay more than ten years after the mine closure and that pollution is predicted be an on-going source of Pb to the sediment for up to a century after mine closure. Remobilisation processes may include a combination of effluent loading from tailings ponds, sediment focusing from tailings dumped directly into the bay in the early years of mining, and erosion of mining-derived Pb retained in catchment soils.

The use of Pb stable isotopes provided insights into the impact of mining pollution that concentration gradient methods could not provide, namely, (1) the distinction between changes in background Pb, mining pollution and aerosol inputs affecting Pb deposition, and (2) a more precise estimation of the distance reached by mining pollution from a point-source at different times during of mining operations. Further, Pb stable isotopes were used to quantitatively estimate a timeline for return to baseline condition. At low concentrations, it can be challenging to distinguish changes in pollution Pb flux from natural variability. Concentration factors are a more common and less expensive way of determining metal pollution impact in paleolimnological studies, but our results indicate that using concentration enrichment factors alone would have resulted in an overestimation of the impact of mining pollution at the highest concentrations by not accounting for changes in background Pb

contribution over time. This study demonstrates the potential for Pb isotopes to inform the remediation of metal mining pollution. Assessments of sediment recovery from metal mining pollution in a large water body are rare, and natural isotopic tracers have the potential to improve the accuracy of dispersion modeling and recovery prediction through further process research.

4 ATMOSPHERIC TRANSPORT OF METALS AND MAJOR IONS FROM SUBARCTIC WILDFIRES

4.1 PREFACE

Most paleolimnological studies looking at metal fluxes caused by wildfires have focused on catchment transport processes (e.g. Garcia and Carignan, 1999; Jensen et al., 2017; Rothenberg et al., 2010). However, the impact of wildfire on the short-distance atmospheric transport of metals (within km) is seldom addressed in the current literature, and paleolimnology seems well suited to provide answers to this question. No study has directly addressed potential input of metal in lakes from the atmospheric transport of particulate metal and direct deposition on lake surface or deposition onto watershed and subsequent erosion to the lake. Quantitative estimates of atmospheric fallout are important for modelling and evaluating element transport and climate change impacts on a broader scale. The close-range atmospheric transport is often assumed to be negligible, justifying the use of lakes within a few km of known fire scar as control site in wildfire-metals studies (e.g., Rothenberg et al., 2010), but actual accumulation rates caused by wildfire have yet to be measured. In this chapter, the evidence for the significance of atmospheric transport of metals by wildfires was investigated in five northern boreal lakes. The research has provided a quantified metal flux response in lake sediment attributable to individual wildfires in the last ~200 years for multiple elements.

4.2 INTRODUCTION

The subarctic boreal forest is facing major changes in fire regimes in response to climate change, land-use change, insect outbreaks, and historical fire management (Balshi et al., 2008; Coogan et al., 2019; Hu et al., 2015; Veraverbeke et al., 2017). As a result of these environmental changes, it is predicted that wildfires will become increasingly frequent and severe in the near future, including in the Arctic (Hu et al., 2015; Teufel and Sushama, 2019; Wang et al., 2015; Wotton et al., 2017). These new fire regimes may alter freshwater ecosystems by rapidly liberating metals slowly accumulated in soils and

biomass over centuries or millennia (Abraham et al., 2017; Giesler et al., 2017). Burned catchments result in elevated loading of sediment, organic matter, nutrients, major ions and metals to connected streams and lakes for decades following wildfires because catchment erosion is facilitated by fire (Dunnette et al., 2014; Ice et al., 2004; Jensen et al., 2017; Nelson et al., 2007; Rothenberg et al., 2010; Stein et al., 2012). While the impact of wildfires on catchment geochemistry and export to aquatic environments has been examined, less is known about the material transported through the atmosphere in wildfire plumes. Yet, the atmospheric transport of wildfire ash could add an additional pressure to the water quality of lakes in wildfire areas. Since wildfire plumes are not constrained to drainage patterns, the atmospheric load of each fire event affects larger areas and more lakes than catchment processes, potentially representing a frequent disturbance to lake metal inventories. Elevated concentrations of labile toxic and non-toxic metals have been observed in ash samples (Bodi et al., 2014; Kristensen et al., 2014; Odigie and Flegal, 2011; Young and Jan, 1977), satellite imagery of wildfire plumes (Finley et al., 2009; Friedli et al., 2001) and precipitation following wildfires (Witt et al., 2009). Wildfire emissions of particulate and gaseous mercury are 3-7 times greater than anthropogenic emissions in Canada (Fraser et al., 2018). However, the impact of ash fallout from local fires on lake chemistry and metal loading has been rarely addressed (e.g. Abraham et al., 2017; Odigie et al., 2016) and is therefore not well quantified.

We used a paleolimnological approach to assess the importance of wildfire fallout on loading of metals and major ions in subarctic boreal lakes by measuring changes in element fluxes in lake sediment archives in a study region with recent (and documented) wildfires. Short cores from five small lakes with a limited catchment contribution were dated and analyzed for metals, major ions and macroscopic charcoal particle concentration. We hypothesized that atmospheric fallout from wildfires is a significant source of elements to these lakes, even for fires occurring outside of the lake catchment. We identified fire events in the sediment from peak charcoal accumulation rates and analyzed the

changes in element fluxes in relation to these fires. We also validated the sediment records of fire events using historical fire maps. This research provides rarely addressed quantitative estimates of changes in trace element flux and concentration in lake sediment due to wildfire fallout. Contrary to punctual measurement or short-term monitoring, paleolimnological records provide a temporally integrated view of these impacts. These estimates will be useful for predicting the impact of future changes in the wildfire regime to lake water quality in subarctic regions and for the interpretation of paleolimnological records affected by input of wildfire ash.

4.3 METHODS

4.3.1 Study sites

We examined sediment cores from five lakes located along the two highways leading out of Yellowknife, NT, Canada, a region at the transition between the boreal forest and the Taïga Plains ecoregion (Northwest Territories, Canada). Three lakes separated by 12-14 km intervals were sampled along the Ingraham Trail highway (IGT, HL1, and PL2) running east of Yellowknife through the Taïga shield ecoregion (Figure 4.1).

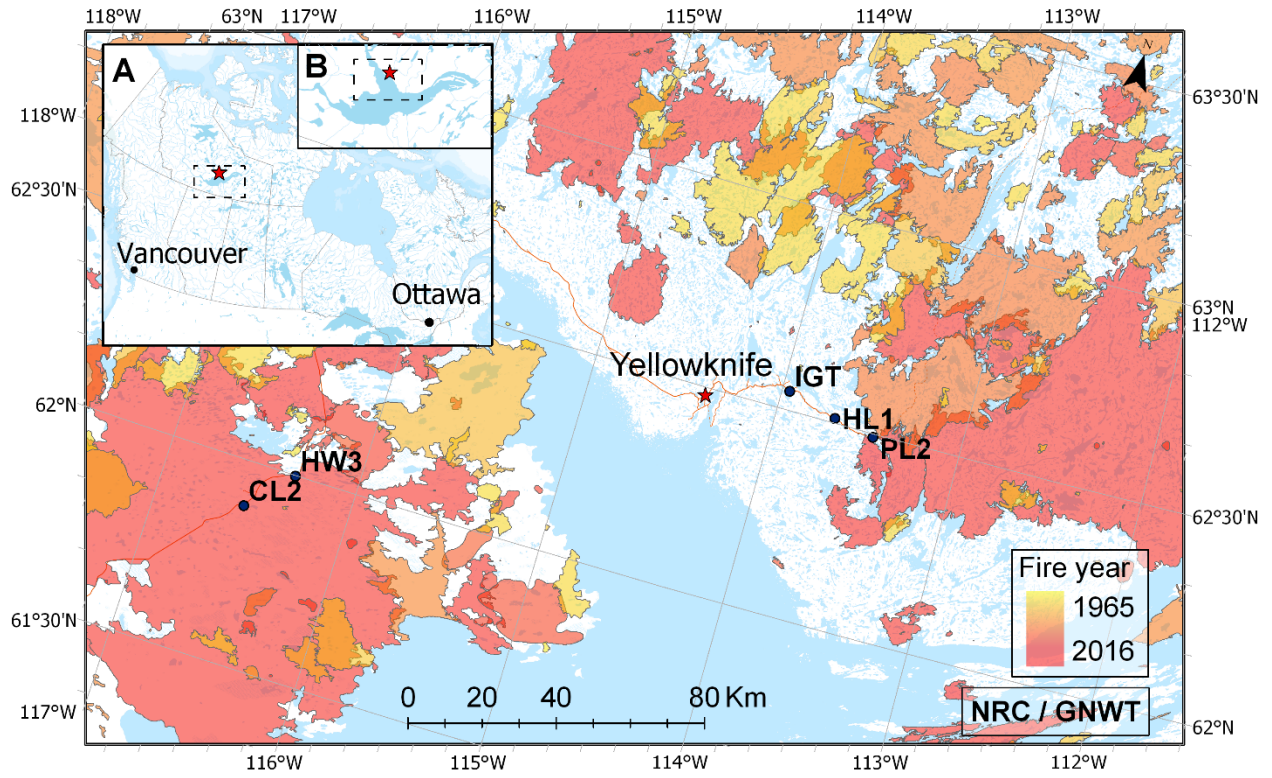


Figure 4.1: Map showing the locations of study lakes and documented fire scars from 1965-2016. (Government of NWT with permission from Environment and Natural Resources, 2018)

Two lakes separated by 22 km were sampled along Highway 3 (HW3-1 and CL2) west of Yellowknife in the Taiga Plains ecoregion. Yellowknife is a historical gold mining town with a legacy of metal pollution (mainly arsenic and antimony) accumulated in regional soils and lake sediment. Four out of five selected lakes were more than 30 km away from the gold mines, which is the approximate zone where roaster-derived deposition has been detected (Galloway et al., 2018; Houben et al., 2016; Palmer et al., 2015; Chapter three of this thesis). Only the IGT site was located near the limit of the estimated pollution footprint of the roaster (~20 km from Giant Mine).

4.3.2 Core collection and subsampling

Sediment cores were collected from a canoe in July 2016 using an 8.6 cm diameter UWITEC gravity corer and extruded on the same day using the UWITEC extruding system. The core length varied between 28 and 50 cm, with an average of 38 cm (Table 4.1). The top 1 cm of each core was collected as a single layer due to high water content, and the rest of the layers from each core were sectioned in 0.5 cm increments. A one cm³ subsample of wet sediment was taken from each slice for charcoal analysis. The remaining sediment from each layer was freeze-dried to obtain dry sediment density and to perform geochemical and radio-chronology analyses.

Table 4.1: Location, core sampling depth, lake area and catchment area for each study lake sampled in 2016.

Lake	Core ID	Latitude	Longitude	Region	Max lake depth (m)	Sampling depth (m)	Lake area (km ²)	Watershed area (km ²)	L:W ratio
Pickerel	PL	62°29'32.8"N	113°28'07.4"W	Ingraham Trail	9.2	9.2	1.7	7.1	0.24
Little	IGT3	62°32'47.2"N	113°57'29.4"W	Ingraham Trail	1.5	1.3	0.14	0.87	0.16
Hidden Park (AKA Davidson lake)	HL	62°30'41.6"N	113°41'13.9"W	Ingraham Trail	8	1.8	0.20	0.69	0.29
Buffalo	HW3	61°59'59.6"N	116°20'06.0"W	West of Behchoko	Unknown	0.7	0.68	3.06	0.22
Chan	CL	61°53'35.9"N	116°32'14.4"W	West of Behchoko	Unknown	1.5	0.84	1.29	0.65

Table 4.2: Characteristics of each core including total length, focusing factor as determined from modelled sediment-water interface ^{210}Pb flux, maximum datable depth using the CRS model, modelled age and uncertainty of oldest datable layer, range of organic matter concentration and range of charcoal particles concentration.

Lake	Label	Core length (cm)	Focusing factor	Organic matter content (%)	Charcoal content (# cm^{-3})
Pickerel	PL	28	16.113	10 - 15	17 - 157
Little	IGT3	50	1.476	50 - 65	0 - 90
Hidden Park	HL	37	1.442	55 - 65	1 - 34
Buffalo	HW3	35	1.571	50 - 60	7 - 107
Chan	CL	41	3.327	45 - 65	21 - 705

4.3.3 Chronology

Sediment cores were dated by radiogenic lead (^{210}Pb) measurement at Flett Research Ltd (Manitoba, Canada). In each core, 10-15 measurements of the daughter isotope ^{210}Po activity were counted using alpha spectrometry (Flynn, 1968). The supported radiogenic lead activity was estimated with two or three ^{226}Ra activity measurements per core (Appleby and Oldfield, 1978), also counted by alpha spectrometry. Radiogenic lead dates and uncertainties were calculated using the constant rate of supply (CRS) model (Appleby and Oldfield, 1978). The complete ^{210}Pb and ^{226}Ra profiles are provided in Figure 4.2.

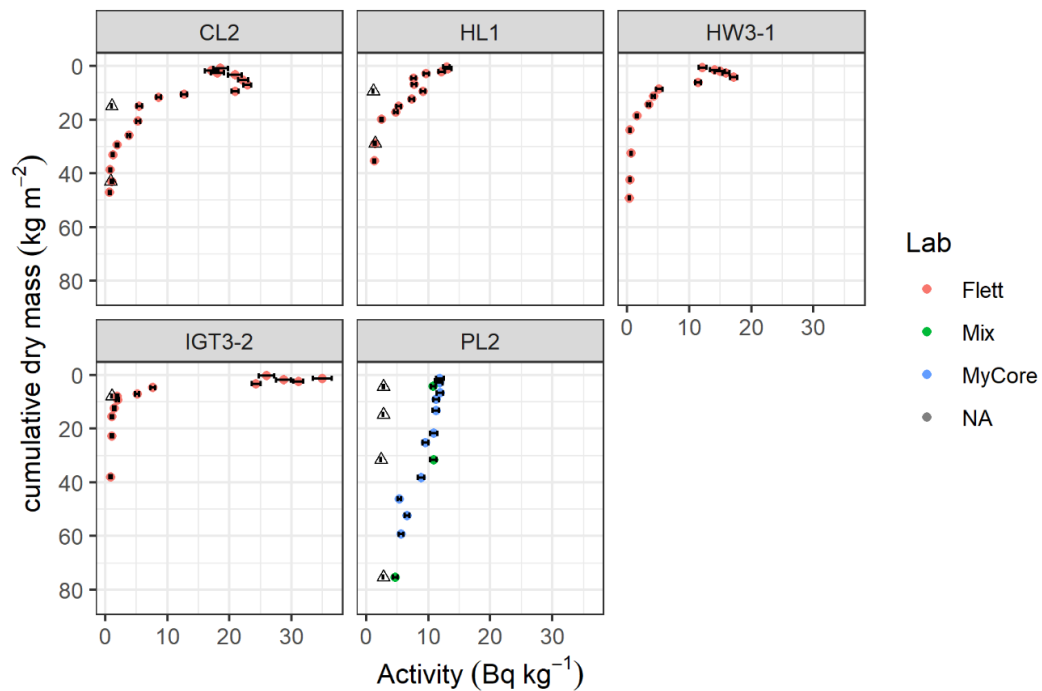


Figure 4.2: ^{210}Pb and ^{226}Ra activity per depth in lakes. Point colors indicate the laboratory that analysed the sample.

4.3.4 Fire reconstruction by macroscopic charcoal analysis

A one cm³ sub-sample of wet sediment from each slice was submerged in a 1:1 mixture of 5% sodium hexametaphosphate (*CALGON*®) and 11% sodium hypochlorite (household bleach) for 24h to deflocculate the sediment and discolor uncharred organic matter (Carcaillet et al., 2001). The bleached sediment was then gently sieved through a 100 µm sieve and the retained material was washed into a Petri dish. Charcoal particles > 100 µm were manually counted under a dissection microscope at 40× magnification.

The charcoal concentration data were statistically analyzed to identify fire events using a method based on the *Charanalysis* protocol (Higuera et al., 2009). The charcoal particle fluxes derived from particle concentration and sediment accumulation rate time series were resampled and interpolated at equal time increments corresponding to the median temporal resolution of all cores (2 years in our case). We used the *pretreatment* function in the *paleofire* package (Blarquez et al., 2014), implemented in R (R Core Development Team, 2020) for this pre-treatment. The resampled and interpolated data ($C_{\text{interpolated}}$) were smoothed using a loess function spanning 50% of the datable core accumulation period ($C_{\text{background}}$), and the residuals from the long-term trend represented peak components (C_{peak}). The positive C_{peak} population was decomposed into noise and signal using a two-source Gaussian mixture model in which we included a high-frequency, low-magnitude peak population corresponding to noise (C_{noise}) and a low-frequency, high magnitude peak population corresponding to local wildfires. We used the 99th percentile of the C_{noise} distribution as a threshold to identify the C_{peaks} corresponding to fire events (Higuera et al., 2011). When adjacent sediment layers exhibited charcoal fluxes over the threshold value, we only included the bottom layer (i.e. oldest layer) of these series of peaks as a fire event. To determine if a wildfire burned any of the lake's watershed we compared the historical fire maps covering the 1965-present period (Government of NWT with permission from Environment and Natural Resources, 2018) with watershed delineation for each lake from LIDAR data (Porter et

al., 2019). Fire events are defined in this context as sediment layer affected by charcoal deposition from (1) a single fire, (2) multiple fires in the same year, or (3) multiple fires in two to six consecutive years.

Based on available fire mapping from 1965 to the present, two out of the 23 fire events identified in the sediment records occurred within the catchments of the study lakes and nine identified fire events occurred before the period covered by fire mapping. We excluded from the atmospheric deposition analysis the most recent events in HW3-1 and CL2 (2014-2016) because they were catchment fires (i.e. fires affecting the study lake's catchment), and a fire in 1966 (1964-1968) in CL2 because the high C_{peak} suggested that the fire could have occurred in the catchment (Table 4.3). Other fires that occurred before fire mapping had relatively low C_{peak} values consistent with more recent fire events outside the catchment, and we therefore assumed they occurred outside of the lake catchment.

Lake sediments, charcoal traps and modelling studies have revealed that macroscopic ($>150 \mu\text{m}$) charcoal deposition is biased toward local influences, but signals are often identifiable from fires up to tens of kilometers away from the source (Oris et al., 2014; Peters and Higuera, 2007; Pisaric, 2002; Tinner et al., 2006). In this study, some fires identified in the sediment record did not have a corresponding fire scar that was closer than ~ 30 km of the lake. However, not all historical fires within a ~ 30 km radius of the lakes were identifiable in the charcoal record. Despite possible errors in the presented sediment chronology, using the same chronology for fire identification and element flux reconstruction ensures correspondence between fire events and metal response.

4.3.5 Metal and Organic Matter Concentration and Flux

For each 0.5 cm interval, a 1-3 cm^{-3} subsample of fresh sediment was dried overnight at 105°C and then analysed for organic matter content by loss on ignition at 550°C for four hours (Dean, 1974; Heiri et al., 2001). Sediment was initially analyzed every cm for total element concentrations.

Additional measurements were performed on sediments from all layers within 1.5 cm above or below of fire events identified by charcoal analysis. Sediments were analyzed for 30 elements by inductively coupled plasma mass spectrometry (ICP-MS) at RPC Laboratories in Fredericton (New Brunswick, Canada; 123 samples) or Bureau Veritas in Vancouver (British Columbia, Canada; 38 samples) in accordance with method EPA 3050B and the digests were analysed following EPA 200.8 and EPA 200.7. The concentrations of 20 different elements were determined with a Finnigan ELEMENT2 high-resolution inductively coupled plasma mass spectrometer (HR ICP-MS). Duplicates for 22 samples, 20 procedural blanks, 18 replicates of National Institute of Standards and Technology (NIST) Standard Reference Material (SRM) NIST2709a (San Joaquin soils), and six replicates each of National Research Council of Canada (NRC) SRM MESS-3 and PACS-2 were also digested and analysed following the same methods as the sediment samples.

Each 0.5 cm interval was analysed for total mercury (THg) concentration using a Direct Mercury Analyser (Milestone DMA-80). Samples were combusted at 750°C and gaseous Hg was trapped on a gold collector for analysis by cold vapor atomic absorption spectrometry. Each run of analyses (20-80 readings) was initiated with five analytical blanks and a measurement of the sediment SRM MESS-3 and PACS-2. Every 10 samples, a sample duplicate, the SRM MESS-3 and an analytical blank were measured. The complete QA/QC data for the ICP-MS and DMA analyses, including detection limits, digestion recovery (duplicates and SRM), blanks, and analytical precision for each element, are available in the SI. Inter-lab comparison for ICP-MS metal concentrations was assessed from measurements of the SRMs MESS-3 and PACS-2 analyzed at both labs.

Elemental fluxes to the sediment were calculated following equation 4.1:

Eq. 4.1
$$M_F = ([M] \times s)/FF$$

Where M_F is the metal (M) flux for a layer ($\text{mg m}^{-2} \text{yr}^{-1}$), $[M]$ is the metal M concentration (mg g^{-1} or $\mu\text{g g}^{-1}$) and s is the sedimentation rate ($\text{g m}^{-2} \text{yr}^{-1}$) from the CRS age-depth model, and FF is a focusing factor (unitless) correcting for sediment migration on the lakebed (Perry et al., 2005) and possibly the funneling effect of the catchment. The focusing factor for each core was estimated using the method presented by Wiklund et al. (2017) by comparing the surface ^{210}Pb flux at the sediment-water interface of each core to the predicted regional ^{210}Pb flux for the lake latitude according to an equation from (Muir et al., 2009).

4.3.6 Significance, duration and quantification of impact from wildfire atmospheric deposition.

The impact of wildfires on metal fluxes and concentration were evaluated using superposed epoch analyses (SEA). Statistical treatment for the SEAs was conducted following procedures based on Adams et al. (2003) and Dunnette et al. (2014). The difference between our analysis and the Dunnette et al. (2014) procedure is the inclusion of five time series (sediment core profiles) in the same SEA to obtain a larger sample size of events (fires) despite the short length of the cores. The 95% and 99% confidence intervals around composite metal fluxes were assessed using a block bootstrap procedure with an independently calculated block length (Adams et al., 2003).

The impacts from wildfire fallouts on element fluxes were quantified from the residuals of the modelled time series used for SEA calculations. The impacts were estimated as the difference between the average flux in the two years following fire events and the six years preceding that period. We report descriptive statistics on the responses obtained from this analysis in terms of absolute change ($\pm \text{mg m}^{-2} \text{yr}^{-1}$) and relative change (% increase in flux). We followed the same protocol for the interpolated element concentration data.

4.3.7 Details on the Superposed Epoch Analysis

A SEA is a non-parametric statistical compositing method that attempts to distinguish the impact of discrete events in a time series by calculating the average response of a time series at different periods (lags) around key events. In this case, key events used in the SEA corresponded to wildfire events inferred from macroscopic charcoal records. Most previous applications of SEA for paleolimnological data used a single continuous record for the analysis (e.g. Dunette et al., 2014), but we combined five time series (sediment core profiles) in the same SEA to obtain a larger sample size of events (fires) despite the short length of the cores. We re-sampled each element accumulation rate to a common resolution corresponding to the overall median resolution (2 years) using the *paleofire* package implemented in R (R Core Development Team, 2020) on the mass of each metal and major ions accumulated in sediment layers (dry density \times concentration). The two-year resolution also corresponded to the re-sampling resolution of the charcoal data analysis. The re-sampled time series were then smoothed using a loess function spanning 50% of the core length to limit the impact of long-term trends and the smoothing residuals were then analyzed by SEA. Windows of ten data points before and after fire events (-20 years to +20 years) were extracted and normalized (z-scored) using the mean and standard deviations of values within each window. The arithmetic mean of all z-scores for a given lag interval constituted the SEA response for that lag. The confidence intervals for the SEA response were computed by 10 000 iterations of block bootstrapping using the procedure of Adam et al. (2003) to automatically calculate the length of independent blocks from the lag-one autocorrelation coefficient. The 0.5th, 2.5th, 97.5th, and 99.5th percentiles from the 10 000 random composites were used to construct 95% and 99% confidence intervals. Changes in sedimentation rate were estimated the same way from the re-sampled total dry sediment mass accumulated in the layers. The R codes for re-sampling, smoothing, SEA and confidence intervals estimation are available in the supplementary information.

We also used a SEA to estimate the impact of wildfires on element concentrations in the sediments. In this case, we used a linear interpolation between measured element concentrations and depth instead of re-sampling the time series. We then used the same procedure on these time series to perform the SEA as described for the flux data.

4.4 RESULTS AND DISCUSSION

4.4.1 Fire history

Two to six fires were identified within the ^{210}Pb dated portion of each core, which represented accumulation from the late 1800s to present (Table 4.3). A total of 23 recorded fire events were identified in the cores, 20 of which were used in the SEA and the quantification of fire impact due to exclusion of three catchment fires. Because of low catchment contribution to the charcoal input in the studied lakes, the background influx of charcoal was low (Figure 4.3). Therefore, the charcoal accumulation rates in our analysis were sensitive to fires that are smaller, less intense, and further away from the catchment. For this reason, the time intervals between identified fires events in this study were relatively short (35-80 years) and not representative of the local fire return interval, normally defined as fire frequency at a specific geographic point. The observed long-term average fire cycle is ~100 years in the boreal forest (Johnson, 1992).

Table 4.3: Identified fire events in each core with corresponding year according to the sediment dating. Age range in brackets is the minimum and maximum of two-sigma uncertainties from the CRS model. $C_{\text{peak max}}$ is the maximum recorded charcoal flux (background corrected) corresponding to the fire event or the fire period. Indication whether the fire occurred inside or outside of a lake watershed is based on fire maps (Government of NWT with permission from Environment and Natural Resources, 2019) and drainage basin delineation with LIDAR (Porter et al., 2019). An asterisk (*) indicates fire events occurring before the fire mapping period (<1965) for which wildfire location is assumed, based on C_{peak} magnitude.

Core	Year (CE) [$\pm 2 \sigma$]	$C_{\text{peak max}}$ (pieces $\text{cm}^{-2} \text{yr}^{-1}$)	Length of fire period (years)	Location (inside or outside watershed)
IGT	2016	2.2	1-2	Out
	1986 [1985-1987]	2	5-6	Out
	1962 [1960-1964]	5.3	7-8	Out*
	1950 [1947-1953]	3.6	7-8	Out*
	1898 [1889-1908]	9.9	5-6	Out*
CL2	2016	52	1+	In
	2010 [2009-2011]	55	1-2	Out
	1966 [1964-1967]	108	9-10	In*
	1950 [1948-1952]	28	3-4	Out*
	1944 [1942-1946]	22	3-4	Out*
	1924 [1908-1940]	64	3-4	Out*
HW3-1	2014	43	2+	In
	1982 [1981-1983]	4	1-2	Out
HL1	2014	1.9	3-4	Out
	2006 [2005-2007]	2.6	5-6	Out
	1996 [1995-1997]	1.9	7-8	Out
	1992 [1991-1993]	2.9	3-4	Out
	1904 [1876-1912]	0.8	7-8	Out*
	1882 [1871-1893]	1.5	15-16	Out*
PL2	2012 [2011-2013]	62	5-6	Out
	1992 [1991-1993]	9	1-2	Out
	1972 [1970-1974]	13	3-4	Out
	1964 [1962-1966]	9	1-2	Out*

Charcoal accumulation rates were an order of magnitude lower in the three smallest lakes (HL1, IGT, and HW3-1) compared to the two biggest lakes (PL2 and CL2), leading to substantial differences in threshold values to identify fires among cores (Table 4.3, Figure 4.3). Factors influencing charcoal accumulation rate between sites other than proximity/severity of the fires may be related to differences in lake morphometry and catchment characteristics (Whitlock and Millsaugh, 1996), including those influencing sediment focusing (Blais and Kalff, 1995; Mustaphi et al., 2015), that is, the transport of sediment from shallower to deeper sections of the lake. The sites CL2 and PL2 had higher focusing factors (3.3 and 16.1, respectively) than the smaller lakes (1.4–1.6 in IGT, HW3-1, and HL1).

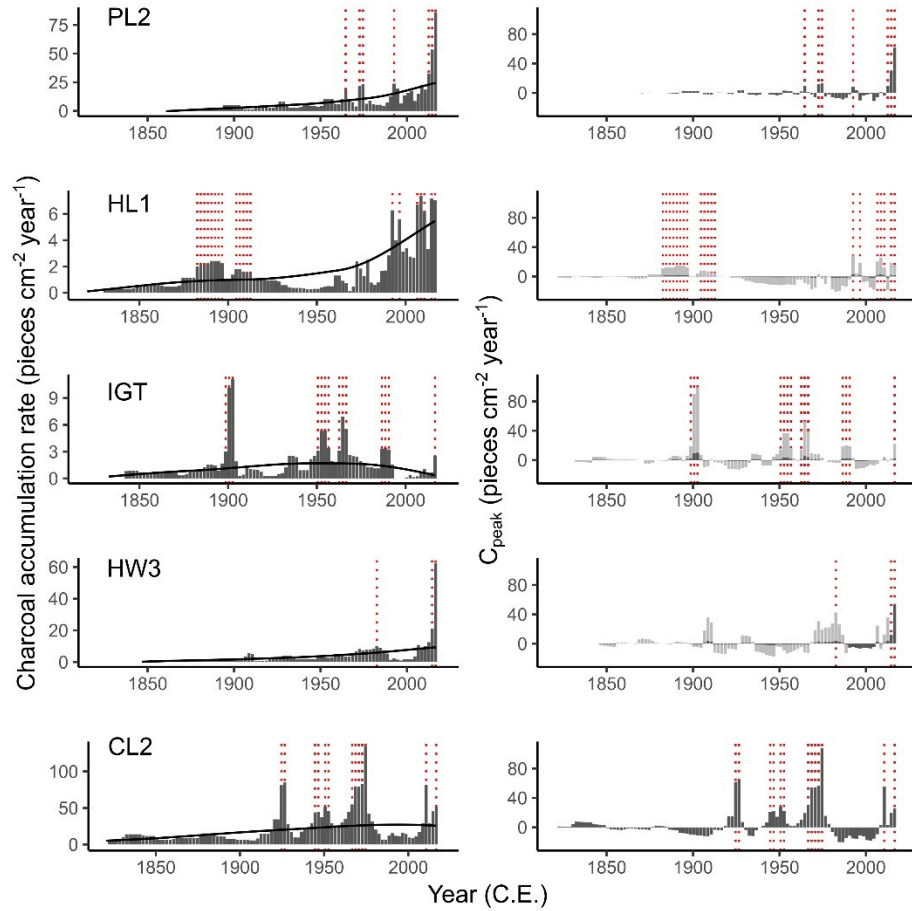


Figure 4.3: [left panels] Modelled charcoal accumulation rate (CHAR) at a two-year resolution against year for each site. The black line represents the loess smoothing applied to the time series ($C_{\text{background}}$). [right panels] C_{peaks} ($\text{CHAR} - C_{\text{background}}$) against time for each site. The vertical red dotted line identifies C_{peak} values that exceeded the threshold for a fire event (99th percentile of C_{noise} distribution). Dark bars represent real values, and grey bars represent 10 \times exaggeration.

Varying baseline charcoal influx suggests that there are differences in wildfire signal sensitivity, with lakes having a higher background or noise component being less sensitive to small charcoal influxes from distant fires. Therefore, we could not use C_{peak} as a proxy for fire distance or fire impacts related to fire intensity and severity.

4.4.2 Impact of Wildfires on Metal Fluxes and Concentrations in Lake Sediment

The atmospheric transport of material from wildfires resulted in small increases in the fluxes of trace metals and major ions of the five study lakes (Table 4.4). The SEA indicated that the fluxes of all major ions (Ca, K, Mg, Na, Sr), most metals (Ba, Cr, Cu, Fe, Mn, Mo, Ni, Pb, U, V, and Zn) and metalloids (As and Sb) were significantly elevated up to two years after a fire event (Figure 4.4). Of all the analyzed variables, only Cd, Pb, and organic matter flux did not reach the significance level in the SEA at lag=0 ($p=0.06-0.11$), but there was still a clear positive response around fires for this element and Pb flux was significantly higher at a lag of two years.

Sedimentation rates increased 3-5 fold over the last 100 years in the five lakes. Most of this long-term trend was corrected in the statistical pre-treatment but sedimentation rates were still significantly greater at lag=0 (Figure 4.4), indicating a temporary increase in sedimentation rate coeval with wildfire fallouts. From analysing the distribution of responses to wildfire disturbance in fluxes, we estimate that major ions and metal fluxes increased by an average of 5-16% (depending on the element, median = 3-10%) compared to the six-year average preceding fire events, whereas sedimentation rate increased by $6 \pm 14\%$ (average and standard deviation) over the same reference period (Table 4.4).

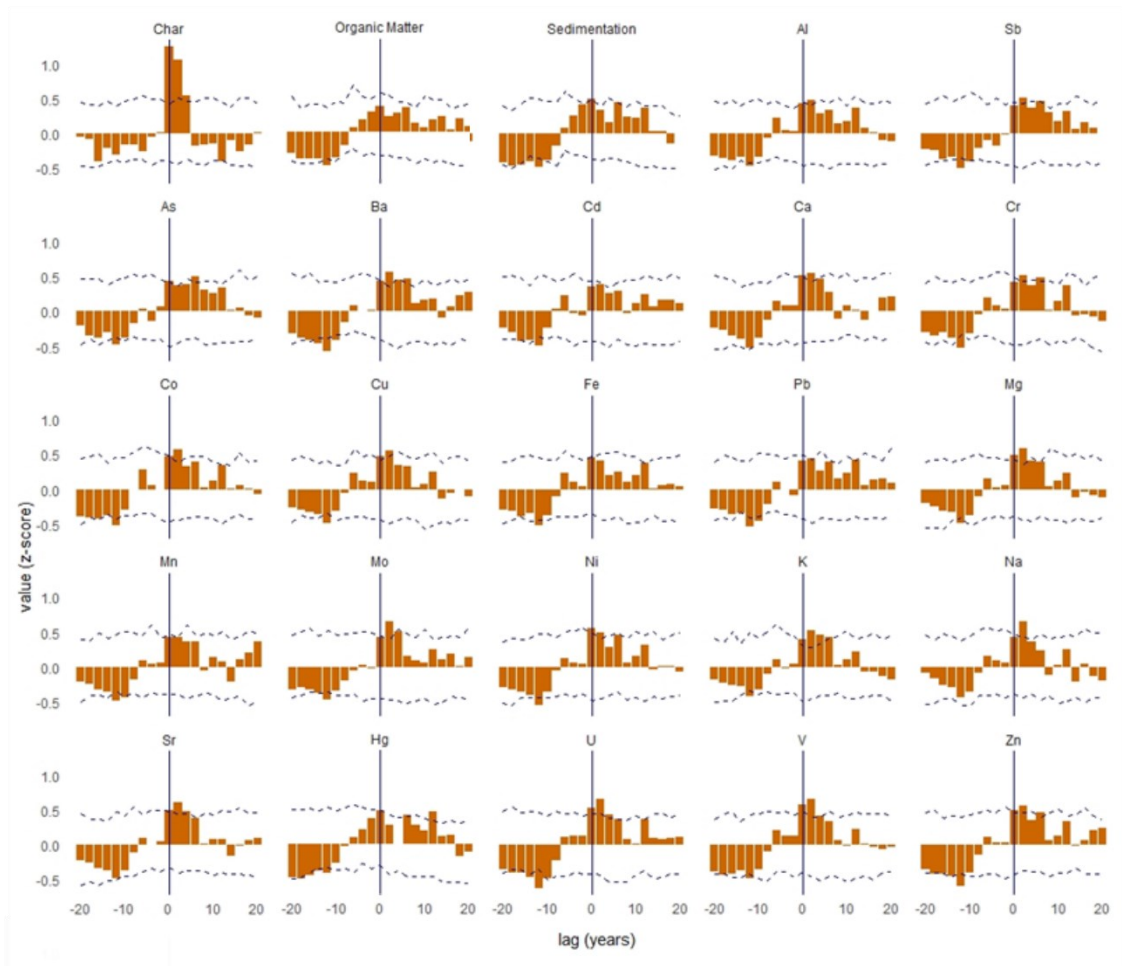


Figure 4.4: Composite response of sedimentation rates, organic matter input and element fluxes around fire events in five lakes. Only fire events confirmed outside of the lake catchment ($n=20$) were analysed in this SEA. Values for lags on the x axis represent the number of years before fire events (negative values) or after fire events (positive values). Vertical lines represent fire events ($\text{lag}=0$). Orange bars represent the composite response of all fire events as z-scores for two-year intervals. Dashed lines represent the significance level ($p < 0.05$).

Changes in concentration in the two years following fire events varied by element between a decrease of 6 ± 16 % in Cd to an increase of 8 ± 29 % in Mn (average \pm sd). However, there was no statistically significant difference in pre- and post-fire concentrations for any element based on a SEA (Figure 4.5). The most recent fire affecting Lake IGT (2016) was associated with large excess concentrations of metals in the surface sediment that was particularly important for Ni ($+47 \text{ mg kg}^{-1}$, $+222\%$), Mn ($+801 \text{ mg kg}^{-1}$, $+163\%$), Cr ($+20 \text{ mg kg}^{-1}$, $+123\%$), Ba ($+119 \text{ mg kg}^{-1}$, $+128\%$), Zn ($+116 \text{ mg kg}^{-1}$, $+114\%$) and Bo ($+28 \text{ mg kg}^{-1}$, $+111\%$). Thus, although there was no overall wildfire effect on element concentrations averaged over all fire events, some concentration increases were observed for individual fires at all sites except HW3-1.

In absolute terms, the most important changes in metal flux attributed to fires were for, in order, Ca, Fe, Al, Mg, K, Mn and Na (Table 4.4). These results are mostly in line with the main constituents of wildfire ash produced at high temperature ($>450^\circ\text{C}$), which are carbonates and oxides formed mainly of Ca, Mg, Na, K, Si with a lower proportion of Al, Fe, Mn and Zn (Bodí et al., 2014; Pereira et al., 2012). Compared to pre-fire conditions, the most important relative changes in flux occurred for Sb, As, Ba, Ni and Mn (Table 4.4). The distribution of changes in sedimentation rate and element flux in fire periods corresponded to a skew-normal or gamma distribution centered around a small increase ($+0-25$ % increase) with a slightly elongated tail in the large positive values (Figure 4.6). The largest increases in flux observed in our dataset were rare events that caused a 33-111% increase in lakes metal fluxes, depending on the element (Table 4.4).

Table 4.4: Descriptive statistics on the absolute and relative change in fluxes of trace metals and major ions following identified fire events (n=20) outside lake catchments in five lake sediment cores. Changes were calculated as the difference between average flux during the six years preceding fire events and average flux two years following fire events. Negative flux indicates a decrease. Fluxes were previously smoothed to account for background long-term trend. Elements are presented in order of decreasing mean flux associated with fire events.

	Absolute change (mass m ⁻² year ⁻¹)					
	Unit	Average	Median	SD	Min	Max
Charcoal	#	2.83	0.87	18.15	4.81	0.26
Dry mass acc.	g	3	2.86	14.22	-31.04	38.29
Organic matter	g	0.29	0.04	3.1	-7.65	8.91
Ca	mg	393.14	30.64	1058.14	-628.91	3328.86
Fe	mg	85	29.2	240.18	-415.56	738.88
Al	mg	80.31	27.48	253.4	-352.69	880.49
Mg	mg	49.42	22.03	122.2	-189.88	393.37
K	mg	17.1	5.93	57.33	-93.58	185.96
Mn	mg	4.39	1.3	8.46	-2.62	33.59
Na	mg	2.41	1.47	12.77	-35.53	31.82
Ba	mg	1.34	0.41	2.27	-0.63	8.22
Sr	mg	1.18	0.18	2.65	-1.42	8.58
Zn	µg	414.47	267.24	1062.54	-2207.44	3060.17
Ni	µg	302.85	89.52	735.52	-1321.58	2224.3
V	µg	200.59	69.01	537.55	-748.34	1862.25
Cr	µg	125.05	63.1	421.68	-1007.24	1129.21
Cu	µg	115.06	75.77	736.85	-1550.74	2176.2
As	µg	78.16	21.83	237.36	-433.18	726.38
Mo	µg	44.5	12.63	128.94	-86.34	562.74
Co	µg	37.23	16.85	148.54	-318.27	425.14
Pb	µg	32.48	17.97	107.48	-207.78	307.37
U	µg	24.42	24.69	98.34	-270.64	237.24
Sb	µg	4.46	1.18	10.44	-7.27	35.46
Cd	µg	0.91	0.86	5.52	-12.63	12.06
Hg	ng	91.66	124.4	994.49	-2933.14	2632.78

Table 4.5 Descriptive statistics on the relative change in fluxes of trace metals and major ions following identified fire events (n=20) outside lake catchments in five lake sediment cores. Changes were calculated as the difference between average flux during the six years preceding fire events and average flux two years following fire events. Negative flux indicates a decrease. Fluxes were previously smoothed to account for background long-term trend. Elements are presented in order of decreasing mean flux associated with fire events.

	Average (%)	Median (%)	SD (%)	Min (%)	Max (%)
Charcoal	118	96	90	21	325
Total Dry Sedimentation	6	5	14	-13	41
Organic matter	3	5	23	-81	30
Ca	10	5	20	-20	51
Fe	9	5	19	-19	52
Al	10	5	22	-34	56
Mg	10	5	19	-19	51
K	10	3	22	-22	55
Mn	14	6	20	-13	50
Na	9	5	19	-25	53
Ba	14	5	21	-7	65
Sr	13	5	20	-13	53
Zn	11	7	18	-20	51
Ni	14	6	25	-18	91
V	12	6	21	-21	56
Cr	9	5	17	-20	51
Cu	9	6	19	-31	49
As	15	6	32	-25	111
Mo	13	10	20	-30	53
Co	9	5	19	-25	52
Pb	9	6	18	-21	53
U	11	8	22	-35	51
Sb	16	6	29	-21	77
Cd	8	5	23	-38	54
Hg	5	5	12	-19	35

Table 4.6: Descriptive statistics on the absolute increase in concentration of trace metals and major ions following identified fire events outside lakes catchment in five lake sediment cores (n=20). Increases were calculated as the difference between average flux during the six years preceding fire events and average flux two years following fire events. Fluxes were previously smoothed to account for background long-term trend.

	Unit	Absolute change (mass per kg)			
		mean	median	sd	max
Charcoal	# cm-3	29	10	54	212
Org. Matter	%	0.3	0	0.9	2.5
Ca	mg	541	28	1997	6256
Mg	mg	1	4	271	526
Mn	mg	27	-1	122	530
Na	mg	11	-3	69	197
K	mg	5	2	100	223
Ni	mg	1	0	6	25
Ba	mg	2	0	9	26
Bo	mg	0.71	0.55	2.6	7.93
Sr	mg	1.6	0.01	6.34	21.48
V	mg	0.1	-0.05	1.09	1.64
As	mg	0.19	0.05	1.89	4.35
Cr	mg	0	0.02	1.05	2.18
Mo	mg	0.08	0.01	0.35	1.41
U	mg	0.03	0.04	0.24	0.55
Hg	µg	0.63	-0.32	7.74	29.19
Sb	µg	-4.23	3.78	70.95	90.94
Cd	mg	-0.02	0	0.1	0.02
Pb	mg	-0.05	-0.02	0.39	0.77
Co	mg	-0.1	-0.1	0.2	0.4
Zn	mg	0	0.1	6.2	11.4
Cu	mg	-0.2	0	2.1	3.3
Fe	mg	-70	-83	473	897
Al	mg	-67	-29	446	563

Table 4.7: Descriptive statistics on the absolute and relative increase in concentration of trace metals and major ions following identified fire events outside lakes catchment in five lake sediment cores (n=20). Increases were calculated as the difference between average flux during the six years preceding fire events and average flux two years following fire events. Fluxes were previously smoothed to account for background long-term trend.

	mean % increase	median % increase	SD % increase	max % increase
Charcoal	62	33	74	233
Ca	6	0	21	91
Mg	6	0	25	107
Mn	9	0	38	163
Na	6	0	28	115
K	6	0	24	103
Ni	10	-1	52	222
Ba	8	0	30	129
Bo	9	2	27	111
Sr	7	0	23	99
V	6	1	26	109
As	6	1	27	90
Cr	5	0	29	123
Mo	8	2	26	109
U	7	1	25	107
Hg	6	0	21	85
Sb	4	0	15	32
Cd	1	0	25	91
Pb	4	0	25	100
Co	5	0	25	106
Zn	6	0	27	115
Cu	5	1	24	101
Fe	4	-1	25	105
Al	4	0	22	91

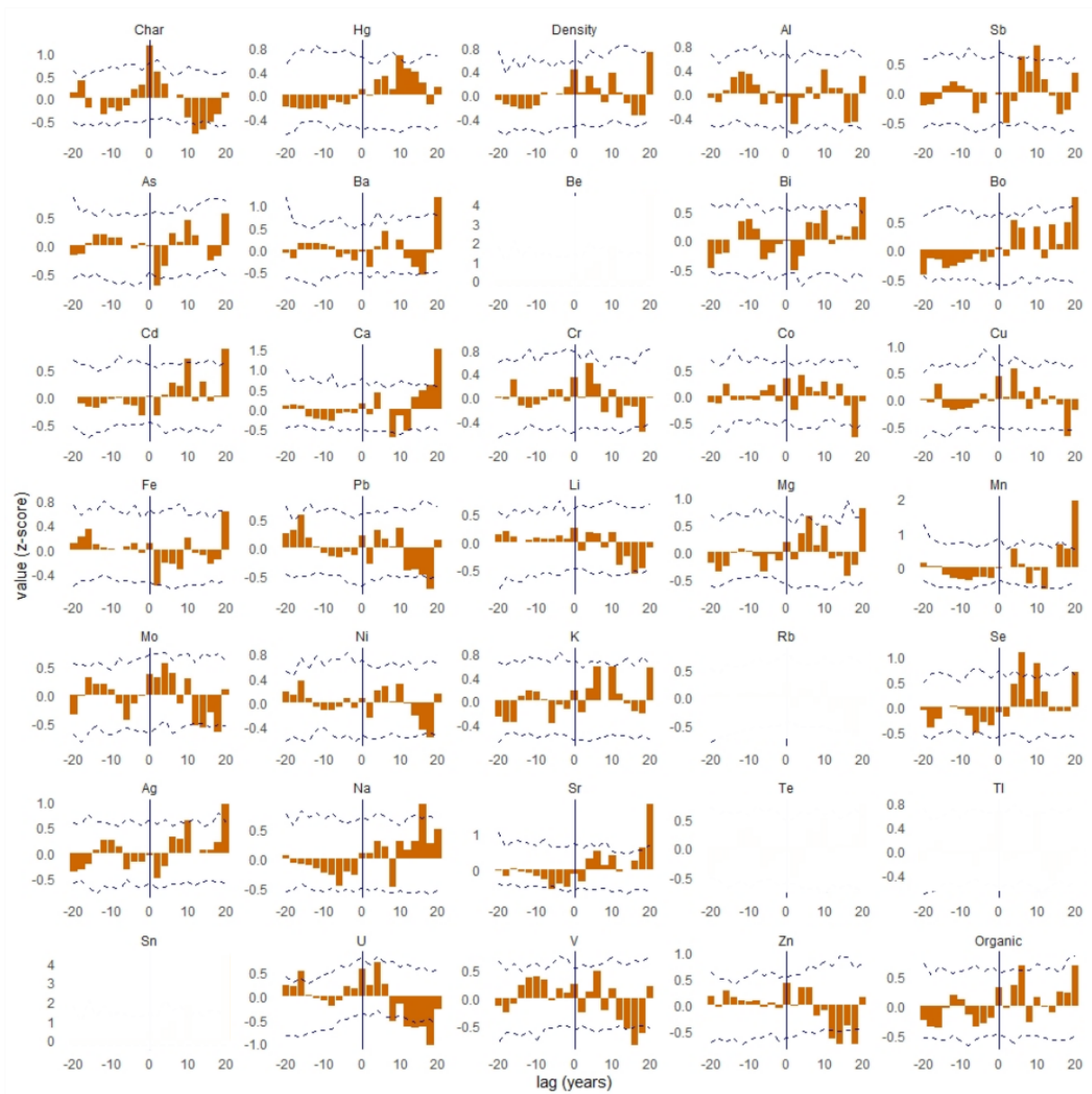


Figure 4.5: Composite response of element concentrations around fire events occurring outside the lake catchment in five lakes. Value for lags on the x axis represent the number of years before fire events (negative values) or after fire events (positive values). Vertical line represents fire events (lag=0). Orange bars represent the composite response in z-score for two-years intervals. Dashed lines represent the significance level $p < 0.05$.

The significant SEA results for flux and sedimentation rate but not for sediment metal concentrations around fire events indicates that most of the impact of wildfire fallout on element fluxes was caused by changes in the sedimentation rate. Therefore, more sediment accumulated in lakes when fire fallout was present, but it did not change the sediment metal composition significantly. It is worth noting that fire identification was driven by variation in both sedimentation rate and charcoal concentration in the sediment. Charcoal concentrations, not just charcoal accumulation rates, were significantly greater in layers corresponding to fire events (Wilcoxon signed-rank test, $p < 0.001$, Figure 4.5). Increased sedimentation driving higher metal fluxes likely represents the direct ash deposition to the lakes. Other factors that may contribute to greater sedimentation during and after wildfires include organic matter deposition (e.g., charcoal), in-lake organic matter production from nutrient priming (Goldman et al., 1990) or aeolian transport of ash from fire scars (Odigie and Flegal, 2014) caused by the loss of surface roughness after wildfires (Sankey et al., 2010). Based on the modest variations in sediment organic matter around fire events and the lack of significant SEA response, changes in organic matter deposition or production were not likely major contributors to the observed variation in metal fluxes. This result contrasts with the impact of wildfires that occur within a lake's watershed, where erosional fluxes following the fire can increase nutrient loading to lakes and stimulate primary production (Millsbaugh and Whitlock, 1995; Pompeani et al., 2020).

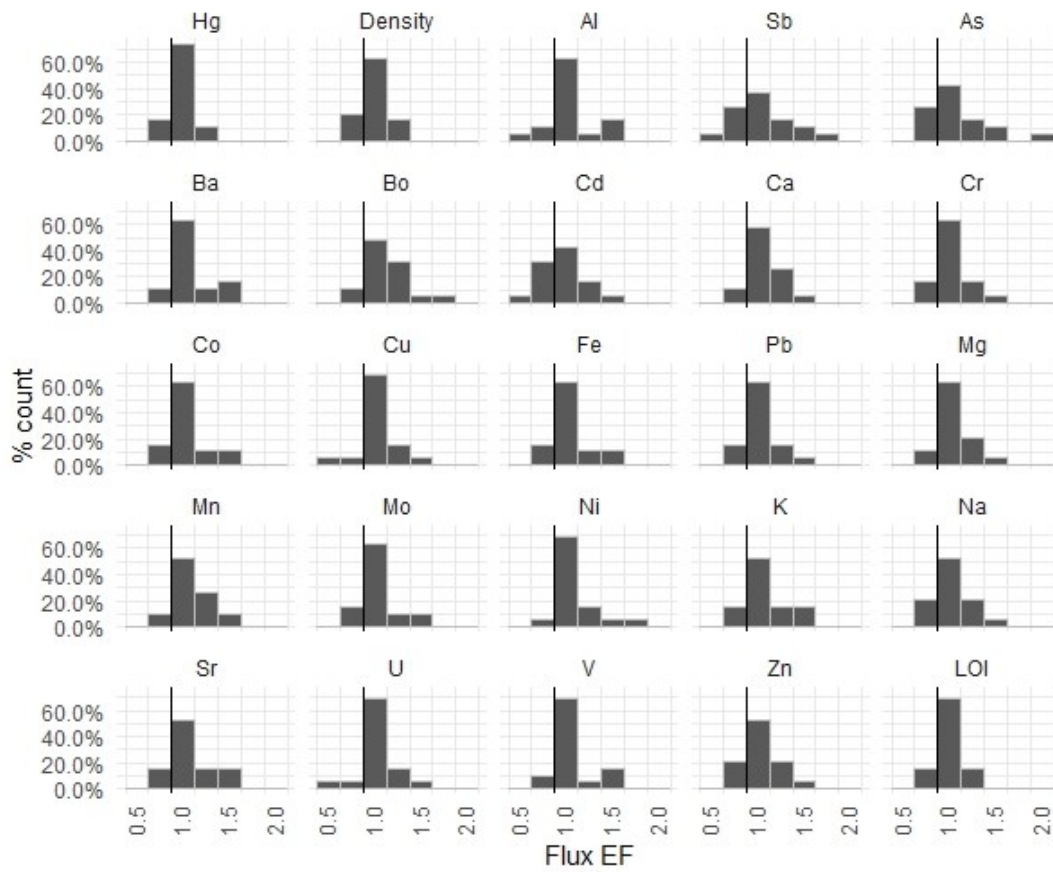


Figure 4.6: Probability density distribution of flux EF in the two years following fire events compared to the previous six-years average (n=20).

4.4.3 Comparison with other assessments of wildfire impact on metal transport

Burned catchments can have high erosion rates leading to greater organic matter and metal accumulation in lakes for 20-50 years following fires (Dunnette et al., 2014; Leys et al., 2016), whereas the impact of atmospheric deposition in this study was last less than two years. Element fluxes associated with wildfire fallouts in this study were two to three orders of magnitude below some estimates of fluxes from burned Californian catchment to lakes and streams (Rothenberg et al., 2010; Stein et al., 2012). Higher flux in these burned watersheds are expected due to the different geographical context (latitude, proximity to pollutant sources), but the difference in transport pathways (atmospheric vs. erosional and atmospheric combined) is also important. For example, in a California watershed where both transport pathways were evaluated for the same fire events, burned catchment streams had a 112–736 fold increases in trace metal concentrations, whereas ash fallout in unburned catchments only caused a three-fold increase of the same elements in stream water (Stein et al., 2012). However, the impact of watershed erosion in a burned catchment is dependant on the burn severity (Dunnette et al., 2014; Rhoades et al., 2019) and the rainfall intensity for multiple years following the fire (Vieira et al., 2018). This might explain why some studies report a decrease in metal concentration in lake sediment following catchment wildfires (Pompeani et al., 2020) while others report the opposite (Leys et al., 2016). Therefore, catchment erosion may have a greater influence than atmospheric deposition for the accumulation of metals in streams and lakes, but terrain slope, burn severity, and rainfall intensity can affect catchment erosion.

In this study, the median change in Cd, Cu, Mn and Zn flux attributed to wildfires were comparable to dry deposition rates measured by passive sampling during a California wildfire in the late 1970s (Young and Jan, 1977). However, our estimation of deposition rate for Fe, Cr and Ni were seven to fourteen fold higher and our estimation of Pb deposition was seven fold smaller than values reported for the same fire (Young and Jan, 1977).

The greatest enrichment factors in element deposition observed in this study are 1–2 orders of magnitude lower than enrichment factors of atmospheric deposition during wildfires using direct measurements (Sabin et al., 2005; Stein et al., 2012; Witt et al., 2009; Young and Jan, 1977). Direct measurement of element deposition caused by wildfires fallout are conducted by measuring deposition in passive sampler during the period of highest ash deposition and comparing them to non-fire periods. The coarse temporal resolution of lake sediments, which integrate multiple months/years of sedimentation in the same sample makes direct comparison with monitoring data challenging and inevitably results in lower enrichment factors.

In Patagonia lake sediments, intense periods of wildfire activity were associated with increased atmospheric loading of As, Mn, Pb, Zn, Co, Cu, and Ni, with the largest effects on As, Mn, Pb, and Zn (Odigie et al., 2015). In comparison, we also measured the greatest relative increases in fluxes for As, Mn, and Ni whereas relative changes in Pb and Zn flux were smaller. However, differences in fluxes related to wildfire ash deposition were small between elements (Table 4.5, Figure 4.3). The reported impact of wildfire Mn fluxes are among the highest in this study, and this is consistent with previous research on wildfire fallout (Abraham et al., 2017; Odigie et al., 2015; Sabin et al., 2005). We found a lower change in Pb flux than most other trace elements whereas other studies reported that wildfire caused an increase in Pb that was equal to or greater than changes in other trace metals (Odigie et al., 2015; Sabin et al., 2005; Stein et al., 2012; Young and Jan, 1977).

Differences in ash chemical composition depend on vegetation, soil type, soil organic matter, pre-fire element concentrations in the soil, and fire characteristics (Abraham et al., 2017; Bodí et al., 2014). In an analysis of trace metals released by a wildfire in California, As, Mn, and Ni originated from both ash and burned soil, Fe originated from burned soil, and Cu, Pb, and Zn primarily originated from ash (Burton et al., 2016). Based on this assessment, the changes in elements flux recorded in the

sediment and attributed to wildfires in this study ($As > Mn > Ni > Zn > Pb = Fe = Cu$) suggests a possible contribution from both ash and burned soil to metal fluxes. Soil, in this context, would have been transported by wind, although further research is needed to examine the influence of wind on the transport of ash and soil from burned areas.

The use of macroscopic charcoal as a proxy for fire events instead of finer particles may limit the signal to elements deposited closer to the fires. Therefore, it is unclear if the fluxes of metals reported in this study are representative of the deposition rate over the whole plume area. Future studies aiming at quantifying the impact of wildfire atmospheric fallout on element fluxes in lakes could also include proxies of fires from various source areas, such as microscopic charcoals, fire biomarkers or polycyclic aromatic hydrocarbons (Dietze et al., 2019; Wakeham et al., 1980).

It is well established that in polluted sites, the ash from vegetation can concentrate pollutants that were already present in the biomass and necromass (Wu et al., 2017). The high impact of wildfires on Sb and As compared to other metals in the Yellowknife area may be due to the remobilisation of industrial pollution from local mining industry, which released large amounts of these element in the environment via ore roaster emissions, mainly from the 1950s to the mid-1970s (Chetelat et al., 2017).

4.4.4 Wildfire Impact on Mercury Deposition

There has likely been more research done on Hg loading from wildfires than any other trace element (Carcaillet et al., 2001; Finley et al., 2009; Fraser et al., 2018; Hans R Friedli et al., 2001; Jensen et al., 2017; Nelson et al., 2007; Obrist et al., 2008; Rothenberg et al., 2010; Witt et al., 2009). In this study, the greatest increase in sediment THg flux observed following a fire corresponded to a 35% increase compared to pre-disturbance condition. The average increase in THg flux around fire events in this study was $0.092 \pm 0.994 \mu\text{g Hg m}^{-2} \text{ yr}^{-1}$ (max $2.633 \mu\text{g Hg m}^{-2} \text{ yr}^{-1}$), representing a $5\% \pm 12\%$ increase in flux. Our estimate of wildfire close-range (~ 30 km) impact is comparable to those from a recent

modelling study by Fraser et al. (2018), which estimated that the average annual deposition from wildfires in our study area (Yellowknife) associated with the intense 2014 wildfire season was $\sim 2.5 \mu\text{g Hg m}^{-2} \text{ yr}^{-1}$. Overall, Hg had the smallest median increase in flux (5%) following wildfires compared to other metals. However, from the SEA there was a significant increase in Hg flux co-occurring with fire events (Figure 4.3).

The low impact of local wildfires on atmospheric deposition on Hg to lakes reflects the large proportion (50-95%) of terrestrial Hg that is converted to gaseous elemental mercury (GEM) during wildfires (Finley et al., 2009; Friedli et al., 2001; Obrist et al., 2008). The ratio of GEM to particulate Hg production in wildfires depends on the burning conditions, with higher temperatures causing more complete combustion and greater GEM release (Obrist et al., 2008). GEM is a gaseous species that can be transported over very long distances as opposed to particulate Hg, which has a more limited source area. We provide evidence that local mercury deposition can increase during wildfires, likely as a result of increased inorganic and particulate mercury deposition. Supporting this point, the THg concentration in precipitation increased 2.5 times following a boreal wildfire in northern Minnesota (Witt et al., 2009). While wildfires are recognized as an important source of atmospheric Hg at the global or continental scale, (Fraser et al., 2018; A. Kumar et al., 2018) their influence at smaller spatial scales (~ 30 km in this study) was detectable, yet limited, in this subarctic study. In comparison, multiple fires over a ~ 100 year period in a California watershed released an estimated $570 \pm 1200 \mu\text{g Hg m}^{-2} \text{ yr}^{-1}$ to a lake, representing a long-term enrichment factor of 2.2-3.3 resulting from catchment transport (Rothenberg et al., 2010). Wildfires can deplete the reservoir of Hg stored in soil, especially if the fire intensity is high (Biswas et al., 2007). Logically, this would reduce the catchment contribution of mercury to a lake in the years following a fire. However, a decrease in catchment release of mercury following wildfires has seldom been reported. The reason may be that 20-73% of the soil Hg is retained after wildfires (Biswas et al., 2007; Campos et al., 2015) and this Hg is more mobile (susceptible to

catchment transport) than in an unburned catchment, especially in period of intense rain (Burton et al., 2016; Campos et al., 2015). The mobility of Hg released by wildfires decreases rapidly, reaching pre-fire conditions after ~4 years (Moreno et al., 2016), but the uptake of mercury in the catchment can be accelerated in the years following a fire if an organic layer subsists in the soil (M. P. Burke et al., 2010). Depending on the geographical context, the history of pollution in the catchment and the fire characteristics, fluxes of Hg from soil erosion, leaching of DOC-bound metals from soils and the transport of ash in surface runoff can be orders of magnitudes greater than direct atmospheric deposition fluxes measured in this study (Rothenberg et al., 2010).

4.4.5 Wildfire deposition compared to anthropogenic sources

In response to global anthropogenic pollution during the 20th century, trace metal loading in Canadian subarctic lakes has increased by a factor of ~2.7 for Hg, 1.2–6.6 for Pb and 1.0–1.5 for Cd (Hermanson, 1993; Muir et al., 2009; Skierszkan et al., 2013). Assessment of point-source impacts in early industrialisation, when emission controls were limited, showed that trace metal fluxes of Pb, Hg, Cd, Bi, Co, Cu and Zn sometimes increased by a factor of 4 to 8 by local mining activity (Skierszkan et al., 2013) and by orders of magnitude near metal smelters (Shotyk et al., 2016; Wiklund et al., 2017), with cumulative effects over decades. In comparison, the enrichment factors from wildfire events for all trace metal fluxes in our study lakes were always below 2 and represented short-term enrichment lasting ≤ 2 years.

4.5 CONCLUSION

This study provides the first quantitative assessment of wildfire-derived atmospheric fluxes of elements to subarctic lakes. The findings indicate that future changes in the wildfire regimes of northern boreal forests could affect the biogeochemical cycling of major ions, many metals and metalloids through increased accumulation in lakes. The atmospheric deposition from wildfires was detectable in lake sediment. However, the enrichment from individual fire events was small relative to

reported long-term enrichment from global anthropogenic pollution or point-sources evaluated in other subarctic lake reconstructions. Future studies should aim to evaluate how fire severity (in terms of burning temperature and fire type) affects the atmospheric transport of metals as well as the long-term implications of exposure to fallout from frequent fire events.

Wildfires contribute to the remobilisation of natural and anthropogenic pollutants at the local scale and on a broad scale (Odigie et al., 2015; Odigie and Flegal, 2011; Wu et al., 2017). In areas affected by point-source metal pollution, wildfires will redistribute contaminants accumulated over decades in soils and vegetation, which could concentrate certain site-specific contaminants in ash fallouts (Kristensen et al., 2017; Odigie and Flegal, 2011; Wu et al., 2017). Wildfires could be viewed as a climate-change process that may dampen environmental recovery expected from reducing anthropogenic emissions of trace elements (Klaminder et al., 2010). Nevertheless, the amount of metal deposited by wildfires in this study was modest in comparison to many anthropogenic sources. The quantitative estimates measured here can be used for modelling larger-scale impacts of wildfires on element cycles in the subarctic boreal forest and predict the influence of a changing fire regimes on surface water and soil geochemistry.

5 ATMOSPHERIC DEPOSITION AND CATCHMENT TRANSPORT OF Pb AND Hg IN SUBARCTIC TAIGA LAKES DETERMINED FROM LAKE SEDIMENT AND BOGS ARCHIVES

5.1 PREFACE

In recent decades, anthropogenic emissions of mercury (Hg) and lead (Pb) to the atmosphere have been reduced in Canada and the United States through domestic and trans-boundary regulatory actions. The response of northern lakes, however, to these decreases in North American emissions is unclear and may be influenced by local environmental processes such as catchment retention, internal cycling and local pollution sources. Here we evaluate individual and cumulative impacts from long-range and local pollution sources and the role of catchment processes and wildfires on Hg and Pb fluxes in subarctic Canadian lakes. We used a flux deconstruction approach on peat and sediment archives of five bogs and five lakes from two subarctic taiga ecoregions of the Northwest Territories (Canada) to distinguish the atmospheric and catchment-based responses to changing metal pollution emissions over the last 2000 years. Bogs tracked the atmospheric signal, whereas lake sediments provided a mixed atmospheric and catchment-based response. The combination of multiple environmental archives in the same analysis provided novel insights on the impact of catchment retention of metals in lakes' catchments. These insights imply an important interaction between climate, catchment soils and hydrology that modulates the accumulation of legacy metals in subarctic lakes.

5.2 INTRODUCTION

Northern Canada is a geographic sink for the long-range transport of global emissions of Pb and Hg pollution (Dastoor et al., 2015; Outridge et al., 2002; Steffen et al., 2015), and this region also contains some local point-sources of these contaminants, such as from mining-related industrial activities

(Thienpont et al., 2016; chapter 3 of this thesis). Environmental archives (lake sediments, bogs, tree rings, ice cores, marine sediments) provide unequivocal evidence that long-range pollution substantially increased the concentrations of Pb and Hg in Arctic and subarctic environments since the beginning of the industrial era (Bindler, 2011; Cooke et al., 2020). The atmospheric deposition of Hg and Pb are of concern to human and ecological health because of their toxic properties, and the biomagnification potential of Hg.

While anthropogenic emissions of Pb and Hg to the atmosphere have decreased in Canada and the United States following regulatory actions in recent decades (USEPA, 2020; ECCC, 2020), one of the primary uncertainties surrounding ecosystem responses to Hg and Pb pollution is centered on understanding the sequestration and remobilization of previously emitted contaminants (Chen et al., 2018). Studies have suggested that the retention of pollutants in lake catchments can delay reductions in metal loading to lakes in response to decreasing atmospheric emissions, particularly for lakes with a large catchment area relative to the lake area (Yang, 2015; Yang et al., 2018). Furthermore, factors such as permafrost degradation, wildfires hydrological changes and organic carbon cycling can further delay ecological recovery by accelerating the remobilization of legacy contaminants from soils (Bacardit and Camarero, 2010; Burke et al., 2018; Macdonald et al., 2005; Whitehead et al., 2009). Environmental drivers of biogeochemical cycling that are independent from anthropogenic Hg and Pb emissions (e.g., those caused by large-scale climate change) need to be understood and quantified to better predict future conditions of exposure of these contaminants to humans and wildlife.

Combining different types of environmental archives into the same paleoenvironmental study can provide information that would not be accessible from either type of record if taken independently (Bindler, 2011; Kokfelt et al., 2009; X. Liu et al., 2012a; Outridge et al., 2011). The accumulation of Hg and Pb in lake sediment is primarily derived from watershed inputs of terrestrial particles in lakes

with a large catchment (Chen et al., 2016), and from direct atmospheric deposition (Drevnick et al., 2016) to lakes with a limited catchment contribution (Blais and Kalff, 1993; Chen et al., 2016; Drevnick et al., 2016). In contrast to lakes, peat bogs acquire Hg mostly from the photosynthetic uptake of atmospheric elemental Hg (Hg⁰) by peatland vegetation (Cooke et al., 2020; Enrico et al., 2016; Obrist et al., 2017) and through atmospheric deposition for Pb (Shotyk et al., 2000; Shotyk, 1996). Because peat bogs and lake sediments accumulate Hg and Pb through different pathways (atmospheric vs. catchment-derived), they provide complementary information on biogeochemical cycling of elements at the landscape scale. Comparing accumulation records from lake sediments to those of peat bogs in the same area can reveal discrepancies attributed to the retention of anthropogenic pollution in lake catchments (Klaminder et al., 2010; Liu et al., 2012b; Norton et al., 1990). Cooke et al. (2020) emphasized the need for data from multiple environmental archives in a recent review and recommended that future studies combine peat and lake sediment cores to help resolve the current trends of Hg accumulation in each type of archive.

The objective of this study was to deconstruct the cumulative impacts of anthropogenic sources (local and long-range) and natural processes (catchment contributions and wildfires) on Pb and Hg loading to aquatic ecosystems in a dynamic subarctic region in the Northwest Territories, Canada. This information is important because increasing bioaccumulation of Hg has been reported for some fish populations in the region (Carrie et al., 2010; Evans et al., 2013), yet there has been little attention paid to understanding continued fluxes of Hg from terrestrial to aquatic environments in the region. There is also limited information related to trends in accumulation and the environmental fate of Pb in subarctic North America. We used geochemical tracers and two complementary types of environmental archives (i.e. peat and lake sediment cores) from subarctic Canada to examine complex ecosystem responses to reductions in anthropogenic emissions of metals.

5.3 METHODS

5.3.1 Study area

The study lakes (surface area between 0.1 and 1.7 km²; max depth between 2 and 9 m; Table 5.1) and bogs were located in subarctic Taiga Ecoregions north of Great Slave Lake, NT, Canada. The approximate latitude of the study area is 62°30'N. The 1980–2010 climate normals from the nearest meteorological station (at Yellowknife, NT) indicate annual precipitation of 131 mm of rain and 157 mm of rain-equivalent snow per year. The regional temperature is subarctic (mean = -4.3 °C) with approximately 115 days per year above 0 °C. Air temperatures have increased in the study area in recent decades compared with earlier meteorological records that started in the 1940s at Yellowknife (Evans et al., 2013). The increase in air temperature as resulted in a shift in the autumn precipitation pattern, with more rainfall and less snowfall (Spence et al., 2011).

Three of the lakes and all six peat bogs were located within the Taiga Shield ecoregion, that is part of the Slave Geological Province of the Canadian Shield (Figure 5.1, Table 5.1 and 5.2). The Slave Province is an Archean craton and is primarily composed of felsic to mafic meta-volcanic rocks except east of Yellowknife, where meta-sedimentary rocks are more abundant (Wolfe et al., 2017). The Taiga Shield landscape is dominated by exposed bedrock with thin veneers of glacial till. Thick organic deposits are typically restricted to peatlands that formed in topographic low areas. Taiga Shield vegetation is dominated by stands of black spruce (*Picea mariana*) with lichen understory. Discontinuous permafrost is present on the landscape but localised in thick organic and fine-grained mineral deposits (Wolfe et al., 2017).

Two of the study lakes (CL2 and HW3-1) were located west of Great Slave Lake, in the Taiga Plains ecozone (Figure 5.1, Table 5.1). The Taiga Plains is part of the geological province of the Interior platform. The underlying bedrock is composed of Paleozoic sedimentary rock and the surface geology

around the study sites is composed of easily drained coarse-textured calcareous glacial deposits (Wolfe, Morse, et al., 2017). Extensive patches of jack pine (*Pinus banksiana* Lamb.) and white spruce (*Picea glauca* (Moench) Voss) forest are separated by horizontal fens and calcareous ponds in the Taiga Plains. Permafrost is sporadic in this ecoregion.

The city of Yellowknife developed as a gold mining town in the late 1930s. Two concurrent mining operations, Con Mine (1938–2003) and Giant Mine (1948–2004), processed gold bearing arsenopyrite ore from the Yellowknife Greenstone Belt. The ore roasting process released metal(loid) pollution through a roaster stack, and most stack emissions were deposited within a ~30 km radius around Giant Mine (Cheney et al., 2020; Houben et al., 2016; Palmer et al., 2015; Chapter 3 of this thesis). The bulk of historical atmospheric mining emissions in the region were from Giant Mine in the early years of operations (1949-1958), before the implementation of effective emission controls (Hocking et al., 1978). Stack emissions from Giant Mine released several metal(loid)s including: arsenic, antimony, lead, and mercury (Chetelat et al., 2017; Thienpont et al., 2016).

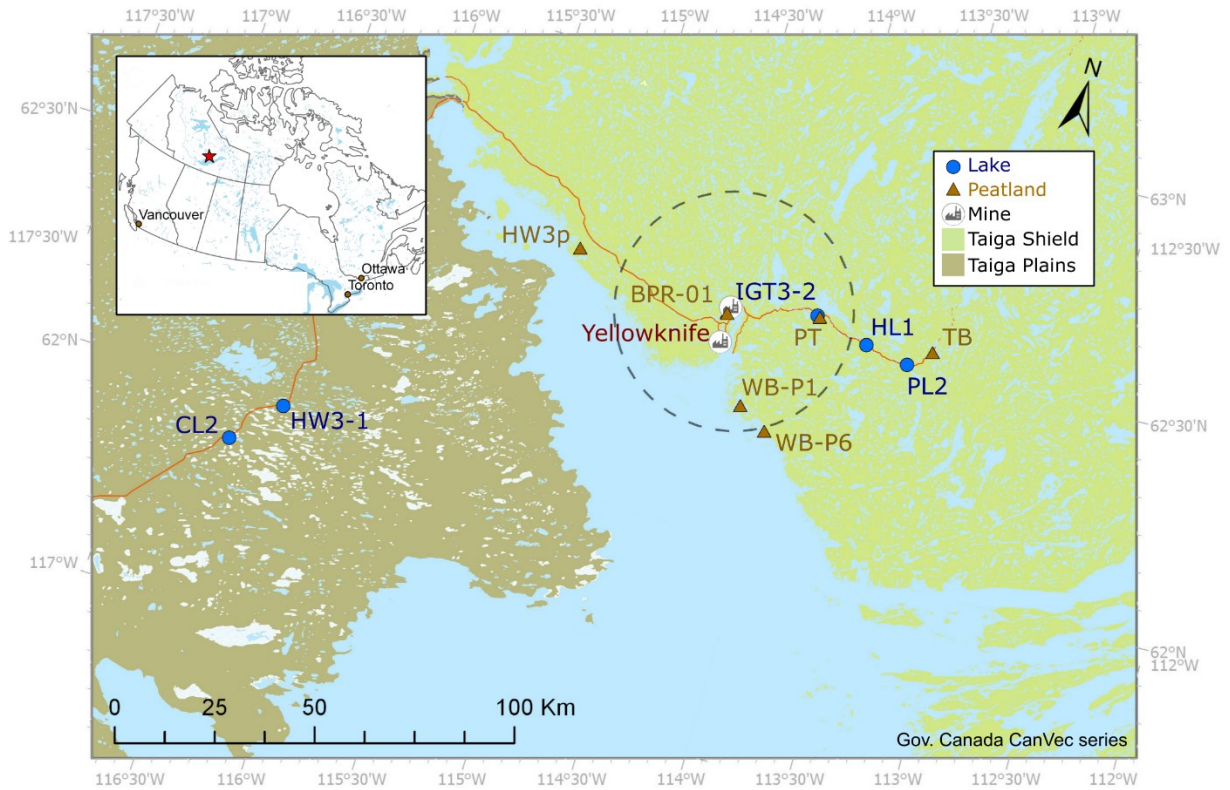


Figure 5.1 Map showing the location of lakes and peat bogs sampled for this study. The location of the nearest city (Yellowknife, NT) is indicated along with the location of the two largest historical mines in the area. The dashed circle represents a 30 km radius around the largest mine, representing an estimate of the soils and lake sediments most impacted by legacy mining emissions in the region (Cheney et al., 2020; Houben et al., 2016; Palmer et al., 2015).

5.3.2 Core collection and sample preparation

Study lakes and lake sediment cores analysed for this study are described in chapter four of the thesis (Section 4.3.1 and 4.3.2, Tables 4.1 and 4.2), along with the processing of sediment to obtain freeze-dried samples (Section 4.3.2). Table 5.1 repeats the information presented earlier in the thesis.

Peat cores were collected in August 2016 using a *Wardenaar* type square peat corer (Hoskin Scientific, Saint-Laurent, QC, Canada). Core length varied between 34 and 75 cm (Table 5.3). Cores were wrapped in a plastic film, protected with a hard vinyl cover and frozen before shipping to the National Wildlife Research Center, in Ottawa, Canada. The frozen cores were sliced at 1 cm intervals using a band saw with a stainless-steel blade following procedures outlined in Givelet et al. (2004). Care was taken to avoid cross-contamination between samples by cleaning the bandsaw blade with distilled water between each layer. The external 1 cm layer was removed from each peat slice with an acid-washed ceramic knife to prevent contamination from the coring or cutting process. Four 3-5 cm³ sections from each slice were sub-sampled. Sub-samples were used for different measurements, namely, peat density, radiogenic isotope activities (²¹⁰Pb, ²²⁶Ra) and metal concentrations (Hg, Pb, aluminum [Al], antimony [Sb]). The fourth sub-sample was archived for future use or to complete minimal weight requirements for other analyses. The volume of the subsamples for estimating peat density were measured with an electronic caliper and dry weights were obtained by freeze-drying the sample.

Table 5.1: Lake sediment core localisation, site description, focusing factor and core length

Core ID	Lake	Latitude	Longitude	Region	Lake area (km ²)	Watershed area (km ²)	W:Lratio
PL2	Pickereel	62°29'32.8"N	113°28'07.4"W	Taiga Shield	1.7	7.1	4.2
IGT3-2	Little	62°32'47.2"N	113°57'29.4"W	Taiga Shield	0.14	0.87	6.3
HL1	Hidden Park (AKA Davidson lake)	62°30'41.6"N	113°41'13.9"W	Taiga Shield	0.20	0.69	3.4
HW3-1	Buffalo	61°59'59.6"N	116°20'06.0"W	Taiga Plains	0.68	3.06	4.5
CL2	Chan	61°53'35.9"N	116°32'14.4"W	Taiga Plains	0.84	1.29	1.5

Table 5.2: Peat core localisation and site description

Core ID	Site Name	Latitude	Longitude	Distance to Giant Mine (km)	Distance to nearest wildfire scar since 1955 (km)
BPR-01	Giant Mine peatland	62°29'10.37"N	114°23'35.05"W	1.75	30
PT	Pontoon Peatland	62°32'46"N	113°56'48"W	22	20
WB-P6	Wool Bay peatland A	62°15'43"N	114°3'32"W	24	25
WB-P1	Wool Bay peatland B	62°18'12"N	114°12'20"W	31	25
HW3p	HW3 peatland	62°35'28.68"N	115°10'34.05"W	42	10
TB	Tibbitt	62°32'12"N	113°21'51"W	52	0

Table 5.3: Cores length, ^{210}Pb inventories, surface ^{210}Pb flux and focusing factor

Core ID	Site	Core length (cm)	Surface ^{210}Pb flux (dpm m ⁻² yr ⁻¹)	± 1 SD	Focusing Factor Using Muir et al. (2009)	Using peat bogs surface flux
BPR-01	Giant Mine peatland	51	850	190	-	-
PT	Pontoon Peatland	36	2717	377	-	-
WB-P6	Wool Bay peatland A	75	unmeasured	unmeasured	-	-
WB-P1	Wool Bay peatland B	42	1521	10	-	-
HW3p	HW3 peatland	84	4384	27	-	-
TB	Tibbitt	33	2898	82	-	-
Peat bog median		NA	2717	1363	-	-
PL2	Pickerel	28	42855	44	12.7	15.8
IGT3-2	Little	39	3926	36	1.2	1.4
HL1	Hidden Park (AKA Davidson lake)	37	4884	18	1.4	1.8
HW3-1	Buffalo	34	4177	27	1.2	1.5
CL2	Chan	39	11272	38	3.3	4.1

5.3.3 Geochemical analyses

Organic matter content in the sediment and peat samples was estimated by loss-on-ignition on a 1-3 cm³ dry sub-sample at 550°C for 4 hours in a muffle furnace (Dean, 1974; Heiri et al., 2001). We used the Ca/Mg ratio in peat samples to determine the ombrotrophic portion of each peat core. Ombrotrophic peat should have a Ca/Mg molar ratio similar or below the average rainwater Ca/Mg molar ratio, whereas this ratio will be greater than atmospheric deposition in fens (groundwater-fed peatlands) (Shotyk, 1996). We obtained the local Ca/Mg ratio from precipitation at the Snare River meteorological station (~140 km from Yellowknife) over the period 2007–2016, averaged all measurements validated by ECCC within a yearly dataset (n = 52 to 106) and compared our peat sample data Ca/Mg ratio obtained by ICP-MS to the 10-year average, minimum yearly average and maximum yearly average. The ash content from the loss on ignition is also reported to further support the classification of the peatlands as ombrotrophic (Shotyk, 1996).

The concentrations of Pb, Al, and Sb in 132 lake sediment samples were measured by inductively coupled plasma mass spectrometry (ICP-MS) at RPC Laboratories (Fredericton, NB, Canada). Peat samples (n = 220) and 32 additional lake sediment samples were analysed for the same elements at Bureau Veritas Commodities Canada Ltd. (Vancouver, BC, Canada). Ground and homogenized sediment or peat samples were digested according to EPA Method 3050B. The resulting solutions were analysed for trace elements by ICP-MS following method EPA 200.8/EPA 200.7. Therefore, measured element concentrations in this study represent the acid-extractable fraction. For quality assurance and quality control (QA/QC), RPC Laboratories digested and analysed 19 procedural blanks, 18 replicates of National Institute of Standards and Technology (NIST) Certified Standard Reference Material (CRM) NIST2709a (San Joaquin soils), three replicates each of National Research Council of Canada (NRC) CRM MESS-3 and PACS-2, and 21 duplicates of lake sediment. The

QA/QC procedure at Bureau Veritas was based on 11 procedural blanks, five replicates of the CRM OREAS 45E-A (OREAS©, Bayswater North, Victoria, Australia), six replicates of the CRM OREAS 262 (OREAS©, Bayswater North, Victoria, Australia), one sample of the in-house reference material DS-10 (ACME Analytical Laboratories, Vancouver, BC, Canada), ten replicates of the in-house reference material DS-11 (ACME Analytical Laboratories, Vancouver, BC, Canada), three replicates of the NRC CRM MESS-3, seven replicates of the NRC CRM PACS-2, and six duplicate samples.

Procedural blanks were near or below detection limit for Pb, Al and Sb at both labs ($n = 30$). The ratio of recovered leachable elements to the total expected mass-fraction in the CRMs was $81 \pm 15\%$ for Pb, $31 \pm 9\%$ for Al and $68 \pm 22\%$ for Sb. These values are greater than the expected recovery from weak acid digestion for Pb, but lower for Al and Sb (see spreadsheet in SI). The relative standard deviation of lake sediment duplicates was $5 \pm 10\%$ for Pb, $2 \pm 2\%$ for Al, and $3 \pm 9\%$ for Sb ($n = 22$). The relative standard deviation measured in peat sample duplicates was $3 \pm 2\%$ for Pb, $3 \pm 6\%$ for Al, and $13 \pm 19\%$ for Sb ($n = 5$). Both laboratories had similar CRM recoveries of the MESS and PACS-2 for Pb, Al and Sb. Detailed results for blanks, CRMs and sample duplicates are included in the supplementary information of the published article related to this chapter.

Dried and homogenized samples from each sediment interval ($n = 358$) and peat interval ($n = 237$) were analysed for total mercury (THg) concentration according to EPA method 7473. Approximately 100 mg of sediment or 30 mg of peat was analysed in nickel (Ni) boats with a Milestone-80 (Milestone, USA) Direct Mercury Analyser (DMA). The replicate precision of THg measurements was $2 \pm 3\%$ for lake sediment ($n = 29$) and $5 \pm 6\%$ for peat samples ($n = 24$). Analytical blanks had 0.01 ± 0.02 ng of THg ($n = 160$) and the SRMs MESS-3 and PACS-2 had a $103 \pm 3\%$ ($n = 58$) and $103 \pm 13\%$ ($n = 15$) recovery for THg, respectively.

5.3.4 Chronology

An age-depth model was developed for each sediment and peat core based on radiogenic lead (^{210}Pb) activity in the upper portion of the core and radiocarbon (^{14}C) dating of material for the section below background level of ^{210}Pb (generally below ~ 30 cm depth). Analysis for ^{210}Pb was completed at *MyCore* (Ottawa, ON, Canada) or Flett Research Ltd (Winnipeg, MB, Canada). The total ^{210}Pb activity in peat and sediment was estimated by counting the activity of the daughter isotope ^{210}Po by alpha spectrometry (Flynn, 1968). Supported ^{210}Pb activity was estimated with one to three measurements per core of the activity of the radioisotope ^{226}Ra , which is at secular equilibrium with ^{210}Pb activity from in-situ U-Th disintegration. The CRS model (Appleby and Oldfield, 1978) was applied to the cumulative sediment mass accumulation and unsupported ^{210}Pb activity profile to obtain a first estimate of the age and uncertainty of each sediment layer. The surface of the WB-P6 peat core was not dated with radiogenic lead and was not included in flux reconstructions except for the background fluxes that could be estimated from radiocarbon data. We used the pre-industrial fluxes of Hg and Pb from this site as background flux for nearby WB-P1 that did not extend to pre-industrial time.

Radiocarbon was measured at A. E. Lalonde AMS Laboratory (University of Ottawa, Ottawa, ON, Canada). Whenever possible, we dated sphagnum leaves and stems or spruce needles to obtain an age representative of deposition time (Table 5.4). When no plant macrofossils were identifiable, we dated bulk peat or bulk sediment (Table 5.4). Radiogenic lead measurements are available in Figure 5.2 for lakes and Figure 5.3 peat bogs.

Dates obtained from ^{210}Pb were included with those obtained from ^{14}C in a Bayesian age-depth model computed with the Bacon software (Blaauw and Christen, 2011), implemented in R version 2.14.0 (R Core Development Team, 2020). Modern post-bomb ^{14}C dates were excluded from the age-depth model.

Based on whole records, average long-term vertical accumulation rate was 41 yr cm⁻¹ in peat cores (range 16-67 yr cm⁻¹) and 34 yr cm⁻¹ in lake sediment cores (range 12-102 yr cm⁻¹). The median temporal resolution was 22 years/sample in peat cores (average=34, sd=44, n=318) and 10 years/sample in the lake sediment cores (mean=10, sd=46, n=360). Due to compaction in the deeper layers, the temporal resolution of the lake sediment layers was coarser with depth, and values exceeded 10 yr cm⁻¹ in the sediment accumulated before 1900 at all sites. Peat compaction also led to coarser resolution in peat with depth at all sites except the Wool Bay peat sites (WB-P1 and WB-P6), where vertical peat accumulation was particularly rapid compared to other sites.

Table 5.4: Material used for radiocarbon dating with results for each sample.

Type	Site	Interval depth (cm)	Material dated	Lab ID	¹⁴ C BP	±	F ¹⁴ C	±
Lake	CL2	39-39.5	Spruce needle	UOC-5037	1104	74	0.8716	0.008
	HL-1	36.5-37	Sedge stems/leaves	UOC-5038	785	23	0.9069	0.0026
	HW3-1	34-34.5	Birch leaves & twigs	UOC-5035	1963	23	0.7832	0.0023
	IGT3-2	44.5-45	Wood fragment	UOC-5034	2948	22	0.6928	0.0019
	PL2	15-15.5	Bulk lake sediment	UOC- 3426	>Modern	35	1.00573	0.00432
	PL2	27.5-28	Bulk lake sediment	UOC- 3425	632	35	0.92435	0.00402
	WB-P6	17.5-18	Sedge stems/leaves	UOC-5036	1461	50	0.8337	0.0052
Peat	BPR-01	19-20	Bulk peat	UOC-11792	149	23	0.9816	0.0028
	BPR-01	48-49	Bulk peat	UOC-11793	796	22	0.9057	0.0025
	HW3	50-51	Sphagnum	UOC-5039	825	21	0.9024	0.0023
	HW3	60-61	Sphagnum	UOC-5040	2042	23	0.7755	0.0022
	HW3	70-71	Spruce needle	UOC-5041	2124	21	0.7677	0.002
	HW3	80-81	Spruce needle	UOC-5042	2634	22	0.7204	0.002
	PT	36-36.5	Spruce needle	UOC-5043	1292	23	0.8515	0.0025
	TB	12-13	Sphagnum	UOC- 3418	300	31	0.96338	0.00375
	TB	17-18	Sphagnum	UOC- 3419	893	31	0.89476	0.00348
	TB	22-23	Sphagnum	UOC- 3420	1499	31	0.82973	0.00323
	TB	27-28	Spruce needle	UOC- 3421	2892	32	0.69767	0.00272
	TB	32-33	Spruce needle	UOC- 3422	3170	35	0.67396	0.00266
	WB-P1	15-16	Sphagnum	UOC- 3413	>Modern	31	1.08837	0.00424
	WB-P1	20-21	Sphagnum	UOC- 3417	>Modern	31	1.18031	0.0046
	WB-P1	25-26	Spruce needle	UOC- 3414	>Modern	31	1.00052	0.0039
	WB-P1	35-36	Bulk peat	UOC- 3415	94	31	0.98839	0.00385
	WB-P1	42-43	Spruce needle	UOC- 3416	68	31	0.99153	0.00386
	WB-P6	30-31	Sphagnum	UOC-6658	902	28	0.8938	0.0031
	WB-P6	40-41	Sphagnum	UOC-6659	1735	26	0.8057	0.0026
	WB-P6	49-50	Spruce needle	UOC-6660	1924	27	0.7853	0.0026
	WB-P6	60-61	Spruce needle	UOC-6661	2081	29	0.7718	0.0028
	WB-P6	70-71	Wood fragment	UOC-6662	2267	30	0.7541	0.0028
	WB-P6	75-76	Bulk peat	UOC-6663	2422	28	0.7397	0.0025

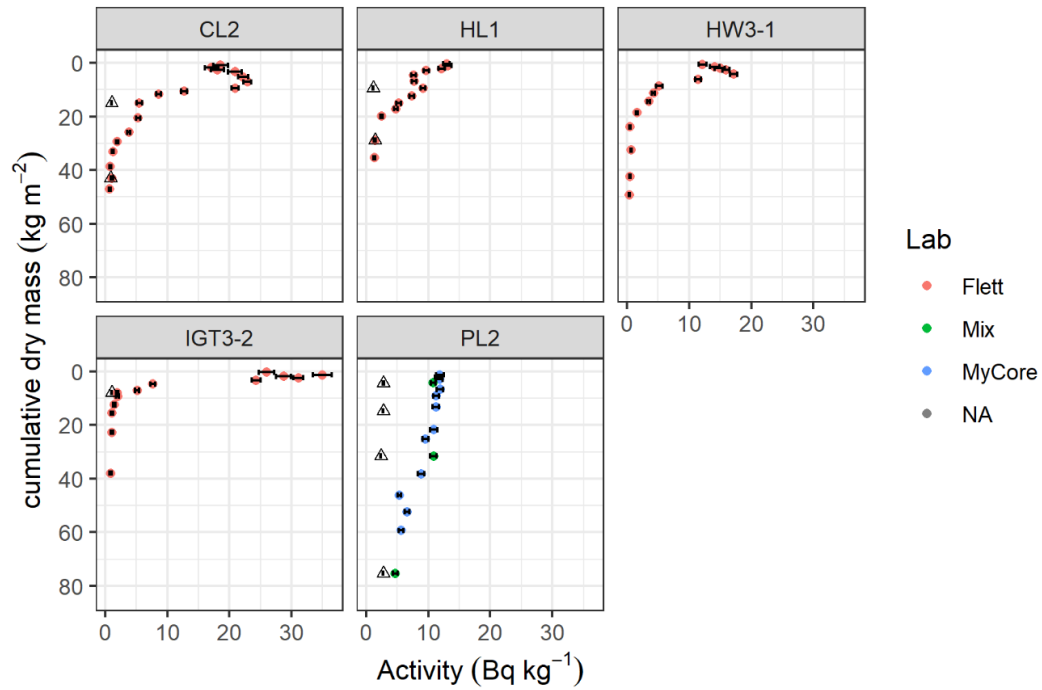


Figure 5.2: ²¹⁰Pb and ²²⁶Ra activity per depth in lakes. Point colors indicate the laboratory that analysed the sample.

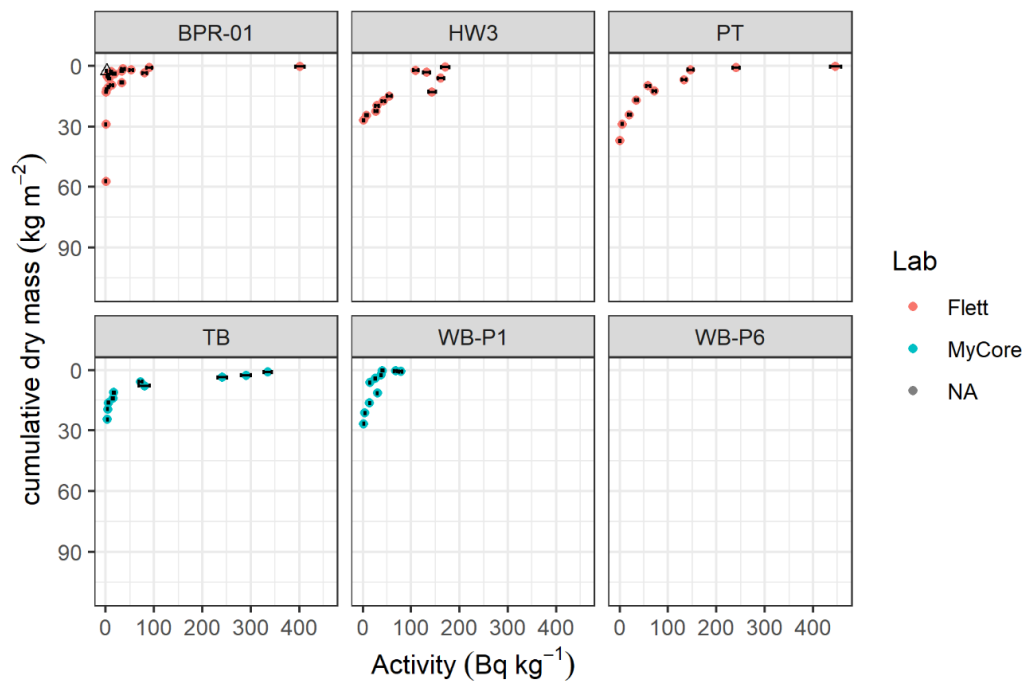


Figure 5.3: ²¹⁰Pb and ²²⁶Ra activity per depth in peat. Point colors indicate the laboratory that analysed the sample.

5.3.5 Flux calculation

The mass accumulation rate (sediment flux) approach is appropriate to evaluate anthropogenic pollution in lake sediment where there is a low concentration of analytes in the erosional source, and measures of excess mass accumulation rate should be used if the erosion rate is thought to have varied over time (Dunnington et al., 2020). The flux of each element to the lake sediment or the peat was estimated based on Eq. 5.1.

Eq.5.1 – Short-term flux estimation (for individual layer of peat or sediment)

$$f_m = \frac{\rho \times d \times [m]}{AR \times FF} \times 10,000$$

Where f_m is the flux of a metal m ($\mu\text{g m}^{-2} \text{yr}^{-1}$), ρ is the dry density of the sediment/peat layer (g cm^{-3}), d is the slice thickness (cm), $[m]$ is the metal m concentration ($\mu\text{g g}^{-1}$), AR is the median modelled vertical accumulation rate for the layer (yr cm^{-1}) obtained from the *Bacon* age-depth model and FF is a unitless focusing factor calculated for each lake representing the impact of sediment focusing in the deeper hollow of the lake bed. Specifically, the FF for each sediment core was estimated as the ratio of regional atmospheric ^{210}Pb fallout to the observed unsupported ^{210}Pb flux at the sediment-water interface (Blais and Kalff, 1995; Muir et al., 2009; Wiklund et al., 2017). For peat cores, the FF was set to 1 because catchment inputs from hydrological transport were assumed to be absent. We used a linear interpolation by depth to estimate the Pb and Al concentration in layers that were not analysed by ICP-MS.

The ^{210}Pb activity at the sediment-water interface was estimated using the intercept ($x=0$) of a linear regression model between ^{210}Pb activity and downcore dry sediment cumulative weight for the section where this relationship is linear. The local atmospheric ^{210}Pb deposition rate was estimated using equation 5.2 from Muir et al. (2009):

Eq. 5.2 – Estimation of regional ^{210}Pb deposition rate

$$\log 210\text{Pb} = 3.95 \pm 0.16 - 0.0352 \pm 0.0026 \times \textit{latitude}$$

Where ^{210}Pb is the atmospheric ^{210}Pb deposition rate ($\text{Bq m}^{-2} \text{ yr}^{-1}$) and latitude is the study site latitude in decimal degrees.

For both Pb and Hg, we estimated the average accumulation rate for four periods using core sections representative of those periods. The pre-industrial period (pre-1800) is the period preceding the use of fossil fuel and industrial release of Pb and Hg at a global scale. The average flux from the pre-industrial period was also used in the flux deconstruction to estimate background conditions. During the early industrial period (1800–1938), there was a gradual increase in anthropogenic activities releasing Pb and Hg globally, but not from local pollution sources in the study area, other than biomass burning by First Nations. During the late industrial period (1938–1999) there were active mines processing ore in Yellowknife, therefore the late-industrial period is marked by both long-range and local mining pollution sources. Finally, the recent period (2000–2016) represents the period between the cessation of ore roasting at Yellowknife to the date of core collection. The recent period also represents a period where Canadian Pb and Hg emissions to the atmosphere decreased substantially (E. and C. C. Canada ECCC, 2020; USEPA, 2020).

Core sections were delineated according to the median modelled age of the sediment or peat. The long-term average flux for each period were estimated using Eq. 5.3.

Eq.5.3 – Long-term average flux calculation

$$l f_{m,t} = \frac{\sum_{i=d_{min}}^{d_{max}} \rho_i \times [m_i] \times d / FF}{[AgeTop_{d_{min}} - AgeBot_{d_{max}}]}$$

Where $lf_{m,t}$ is the long-term flux for the metal m and for the period t , $dmin$ and $dmax$ are the minimum and maximum sediment depth where the median age is included within period t , and $AgeTop$ and $AgeBot$ are the modelled age at the top and bottom of the core section. The FF was not included for calculations with the peat cores (FF = 1).

We used a deconstruction approach for fluxes inspired by the method for lake sediments presented in Perry et al. (2005), in which the Hg flux to lake sediments was deconstructed into three components; background (pre-industrial), excess from catchment weathering and excess from anthropogenic sources. We used these same components for Hg flux deconstruction. When deconstructing the Pb fluxes, we considered an additional component which attributed a portion of the anthropogenic flux to local gold mining pollution from Giant Mine (see chapter 3 of this thesis). Element fluxes in the lake sediment and peat cores were deconstructed using equation 4.

Eq.4 – Flux deconstruction

$$F = F_B + F_L + F_M + F_A$$

F = Total flux for the period

F_B = pre-industrial flux. This flux represents the average long-term pre-industrial accumulation from natural sources. It is estimated from equation 3 on the pre-1800 portion of each core

F_L = lithogenic flux. The F_L component represents crustal metal input derived from weathering and erosion in the lake's catchment or aerial dust inputs. For peat, the lithogenic flux represented only aerial dust inputs. Al flux was selected as the most representative of conservative lithogenic element loading from the catchment (Boës et al., 2011). The F_L component was estimated from equation 5, using the lithogenic element (Al) flux and the crustal ratio of Al to Pb and Hg in the Canadian Precambrian Shield (Shaw et al., 1986).

Eq.5 – Estimation of flux from lithogenic sources

$$F_L = (f_{Al} - ltf_{Al,Pre-1800}) \times \frac{C_m}{C_{Al}}$$

Where F_L is the estimated lithogenic flux compared to the pre-industrial period, f_{Al} is the aluminum flux in a peat or sediment layer, $ltf_{Al,Pre-1800}$ is the long-term average pre-industrial aluminum flux in that core, $\frac{C_m}{C_{Al}}$ is the average ratio of crustal concentration of metal m to aluminum in the Canadian Precambrian Shield as estimated in Shaw et al. (1986).

F_M = Anthropogenic pollution specific to mining, estimated using Eq. 6 only for the reconstruction of Pb fluxes. The Hg flux attributable to local mining pollution could not be deconstructed separately because gaseous mercury has a longer atmospheric residence time than Sb and Pb, which were mostly emitted from the roaster stack as sulfide and Fe-oxide particulates (Bromstad et al., 2017; Houben et al., 2016).

Eq. 6 – Estimation of Pb flux from local mining pollution

$$F_M = (f_{Sb} - ltf_{Sb,Pre-1800}) \times 0.06132$$

Where f_{Sb} is the antimony flux observed in the section of interest, $ltf_{Sb,Pre-1800}$ is the long-term pre-industrial (pre-1800) Sb flux in the core estimated from Eq. 3, and 0.06132 is a constant representing the median ratio of Pb to Sb in dust samples from the ore roaster baghouse of Yellowknife's Giant Mine (INAC, 2007; SRK, 2002). The value is a conservative estimate that could slightly overestimate the contribution of mining Pb based on the results of recent stable Pb isotope measurements from Yellowknife Bay, where the median ratio was 0.049 (supplemental data available in the published version of chapter three of this thesis).

F_A = Excess anthropogenic flux, estimated by solving Eq. 4, represents anthropogenic pollution that is not accounted for by mining pollution (F_M). F_A includes long-range atmospheric deposition and legacy contamination remobilised from the catchment for lakes. For Hg fluxes only, F_A also potentially comprises local mining pollution, which could not be distinguished from long-range sources.

5.3.6 Charcoal accumulation rate

We measured macroscopic (>100 μm) charcoal accumulation rates in lakes and peat bogs as a proxy for wildfire influence. We followed the method described in chapter four of this thesis to prepare and analyse the samples. In short, charcoal particles were manually counted from a 1 cm^3 subsample of sediment or peat, pre-treated with bleach (6% sodium hypochlorite) and a deflocculant (5% sodium hexametaphosphate) for 24h. Charcoal accumulation rate (CHAR, # $\text{cm}^{-2} \text{yr}^{-1}$) was calculated from equation 7.

$$\text{Eq. 7 } \text{CHAR} = \frac{c}{(\text{AgeTop} - \text{AgeBot}) \times d}$$

Where c is the macroscopic charcoal concentration in a peat or sediment layer (# cm^{-3}), AgeTop and AgeBot are the median modelled age at the top and the bottom of the layer respectively, and d is the layer thickness in cm.

5.3.7 Smoothing of trends from different regions and types of archive

To provide a view of the general trend of anthropogenic Pb and Hg accumulation rate between ecoregions and types of environmental archive, we pooled all individual data points representing the modelled anthropogenic component (FA) of the fluxes by group (Taiga Plains, lakes of the Taiga Shield and peat bogs). We then applied a generalised additive model (GAM) to each subset of data. We used the *mgcv* package implemented in R to compute the smoothing and used cubic regression spline to penalize the basis coefficients in order to control the degree of smoothness (Simpson, 2018). A GAM is a not-parametric type of smoothing for time series that does not require an equal-time

spacing of data points. To avoid confidence interval extending below zero (negative flux), the confidence intervals were computed at a 95% level after a log-transformation of the y-values, and results were displayed on an exponential scale to reflect real values.

5.4 RESULTS

5.4.1 Age-depth models

The age-depth models for all cores are presented in Figures 5.4 and 5.5. The regional ^{210}Pb fallout estimated from ^{210}Pb inventories of the peat cores was $45 \pm 23 \text{ Bq m}^{-2} \text{ yr}^{-1}$, which is similar to the value predicted from the equation in Muir et al. (2009) ($56 \text{ Bq m}^{-2} \text{ yr}$). For comparability with previous studies, we used the Muir et al. (2009) value for regional ^{210}Pb fallout and focusing factor estimation in lake sediment. Lake sediment focusing factors were <1.5 (very low focusing) in all lakes except CL2 (FF = 3.3, low focusing) and PL2 (FF = 12.1, high focusing). The oldest lake sediment layer represented accumulation occurring between 323 BCE and 1413 CE, depending on the core (Figure 5.4), and peat cores reached back between 1264 BCE and 1854 CE, depending on the core (Figure 5.5). The median temporal resolution was 22 years/slice in peat cores (average = 34, sd = 44, n = 318) and 10 years/slice in the lake sediment cores (mean = 10, sd = 46, n = 360). In two peat cores (TB and BRP-01), the top 2 cm layers represent over 20 years of accumulation, which suggests a recent decrease in peat accumulation at these sites compared to the rest of the record.

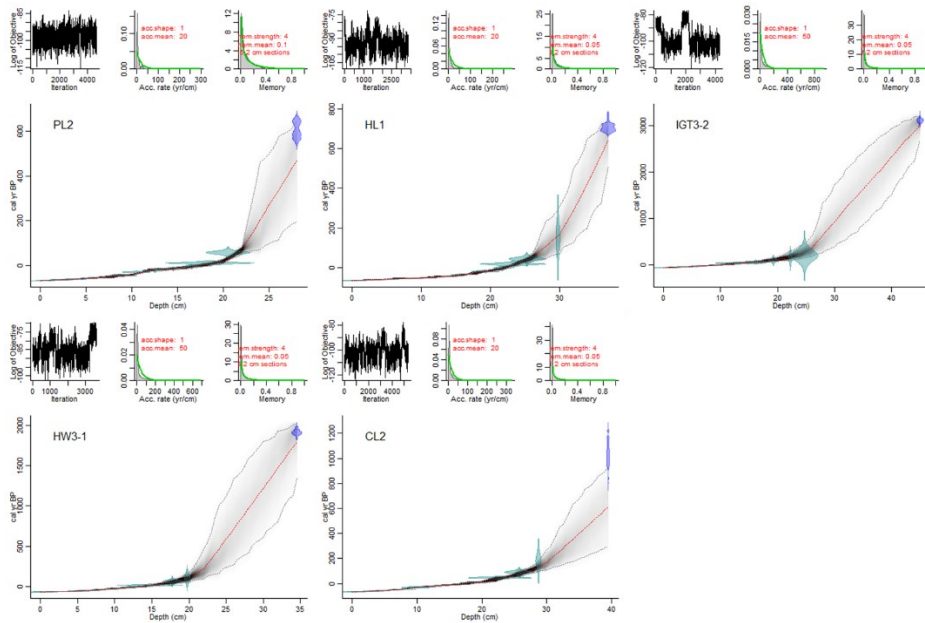


Figure 5.4: Bacon age-depth model for lakes. Light blue regions represent ^{210}Pb dates and dark blue regions represent ^{14}C dates.

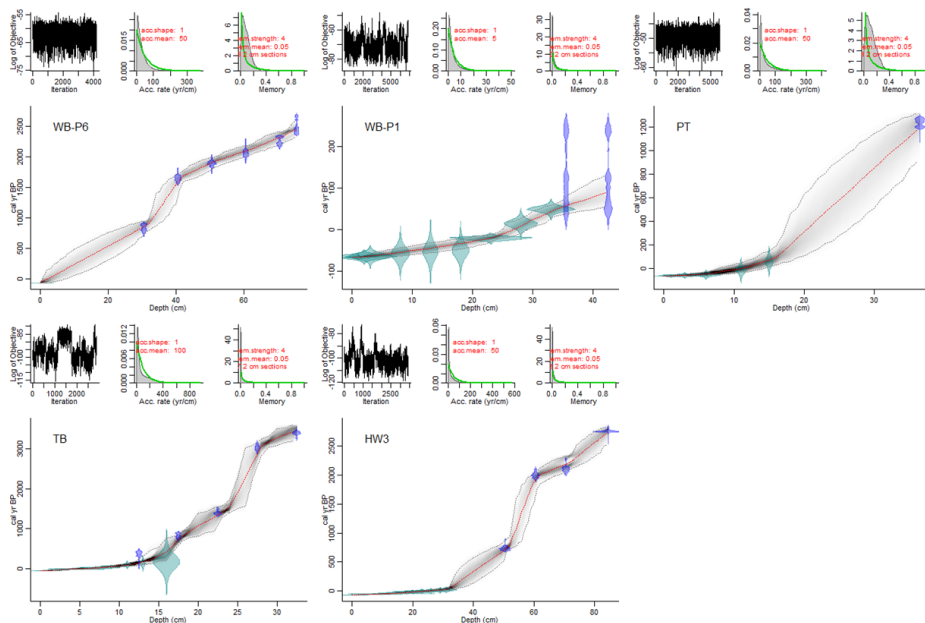


Figure 5.5: Bacon age-depth model for peatlands. Light blue regions represent ^{210}Pb dates and dark blue regions represent ^{14}C dates.

5.4.2 Concentrations of Pb and Hg in peat and lake sediments

Lead concentrations varied among peat cores (min=2.06 $\mu\text{g Pb g}^{-1}$, max 13.44, mean=6.19, n=172) but showed a similar trend of low historical concentrations during the pre-industrial period followed by a rise in Pb concentrations with industrialization (Figure 5.6). The Pb concentration of peat accumulated before 1800 (background) was similar among peat cores and showed little downcore variation (mean \pm sd = $0.26 \pm 0.15 \mu\text{g Pb g}^{-1}$, max= $0.98 \mu\text{g Pb g}^{-1}$, n=90). There was at least one peak in Pb concentration within the top 20 cm of all peat cores. We found the greatest differences in Pb concentrations between sites and the maximum Pb concentrations in peat typically accumulated in the late 1970s and early 1980s. Two sites had slow peat accumulation rates from the peak period (in the early 1980s) up to the peat surface (TB and BPR-01), leading to maximum concentrations near the surface (Figure 5.6a and 5.6f). The core collected at the City of Yellowknife (BRP-01) was the only core showing a distinct Pb peak in ca. 1950 (at $10 \mu\text{g Pb g}^{-1}$), coincident with the opening of Giant Mine, and it was the core with the greatest Pb concentration during that time (Figure 5.6a). Peat Pb concentrations were lowest throughout the record at the WB sites (WB-P1 and WB-P6, Figure 5.6c and 5.6d). The variations in peat bogs Pb concentrations reflected variation in Pb/Sc ratios (Figure 5.7), indicating an increase in non-lithogenic (excess) Pb source followed by a return to more lithogenic (natural) sources in recent years at most sites.

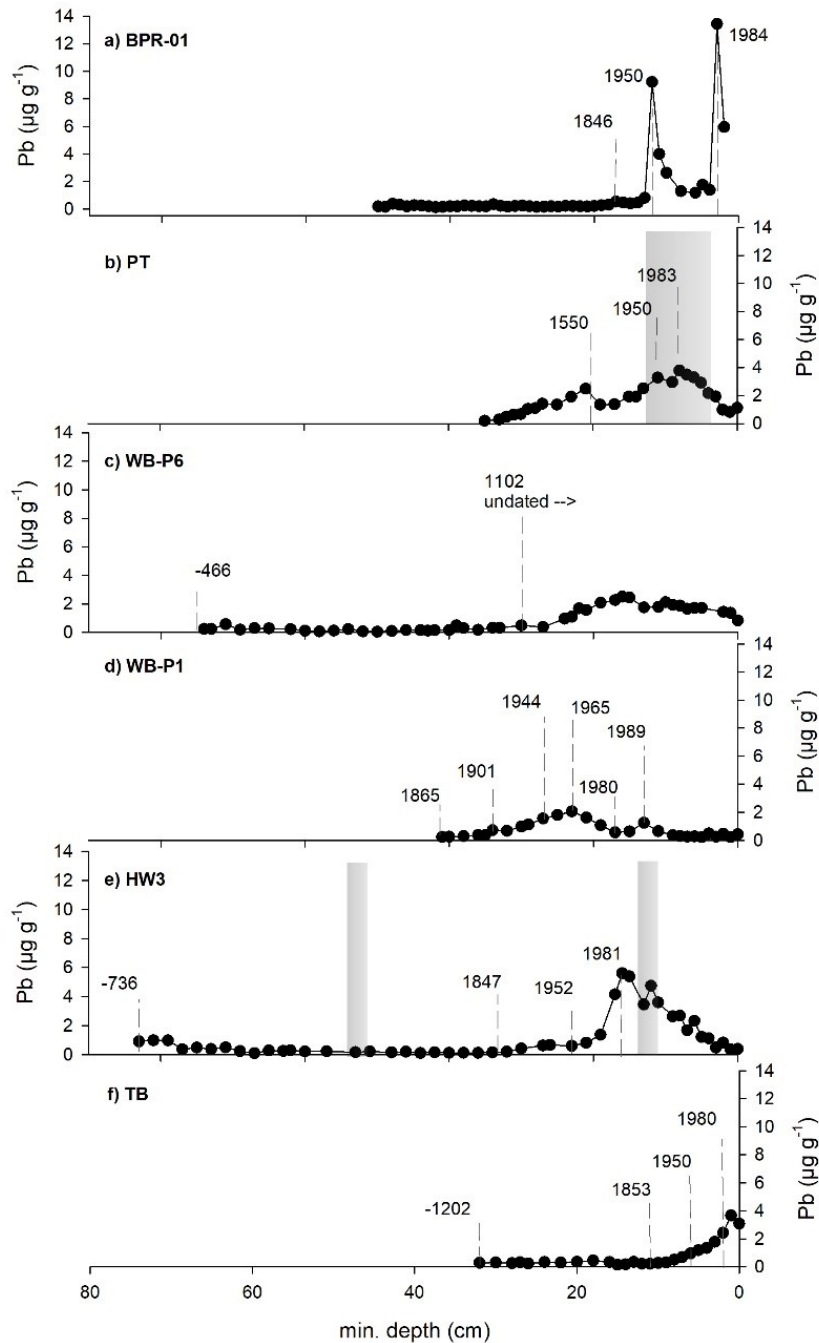


Figure 5.6: Pb concentration per depth in peat cores. Cores are organised from top to bottom by increasing distance to the City of Yellowknife and the local gold mines. Grey areas represent peat layers with ash content $>10\%$ (see Figure 5.13). Dashed lines represent the modelled age of selected layers.

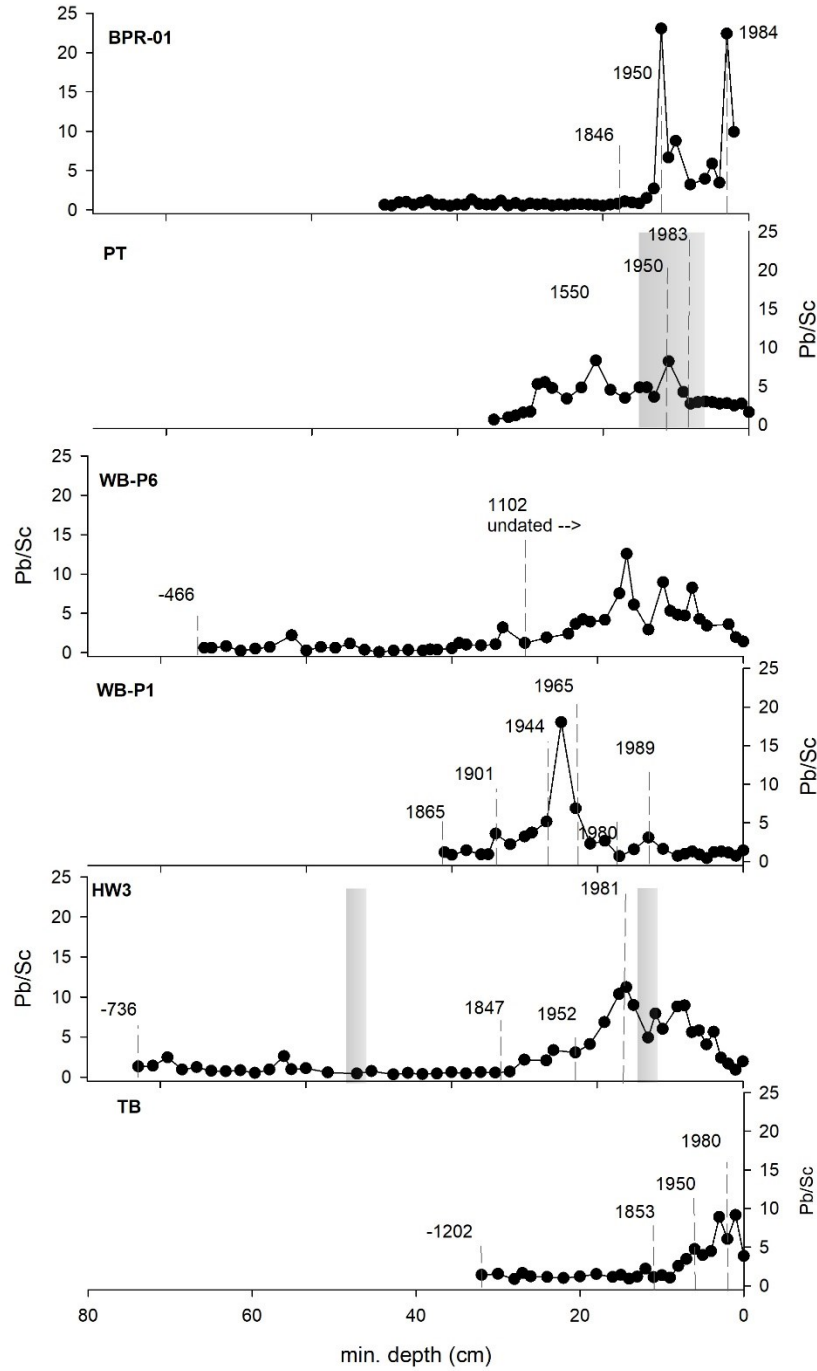


Figure 5.7: Lead (Pb) to scandium (Sc) ratio measured by ICP-MS against peat depth with age of certain peat layers in years (CE). Grey areas represent sections with high (>10%) ash content (Figure 5.13).

Lead concentrations were greater in lake sediments than in peat cores but the variation in Pb concentrations were relatively small in lake sediments (Figure 5.8) compared to the large changes observed in some peat cores (Figure 5.6). The Pb concentration in Taiga Plains lake sediment cores increased slightly from the bottom of the core (pre-industrial sediment) up to sediment accumulated in 1971 in CL2 (1969-1973, 95% CI) and in 1997 in HW3-1 (1995-1998, 95% CI) and then gradually decreased to pre-industrial concentrations (Figure 5.8a and 5.8b). During all time periods, the Pb concentrations of sediment in the Taiga Plains sites were lower than those from the Taiga Shield (Figure 5.8). In Taiga Shield lakes, changes in Pb concentration were relatively small ($\leq 15\%$ the background concentration) except in the lake located closest to the City of Yellowknife (IGT3-2), which had greater Pb concentrations in the top 12.5 cm of the core (Figure 5.8e), representing sediment accumulated after ~ 1928 C.E (1912-1943, 95% CI). The peak Pb concentration in the IGT3-2 sediment core was dated to 1964-1967 C.E (1954-1974, 95% CI).

The mean (\pm stdev) THg concentration of pre-industrial peat samples was 42 ± 15 ng g⁻¹ Hg (n= 172, max= 96 ng g⁻¹). There were clear sub-surface peaks in Hg concentration in all peat cores that corresponded to peat accumulated between 1950 and 1980 in dated cores (Figure 5.9). Surface peat Hg concentrations returned to pre-industrial concentrations in all peat cores except those with a slow peat accumulation rate after the 1980s (i.e., BPR-01, TB), in which case maximum Hg concentrations were found near the surface.

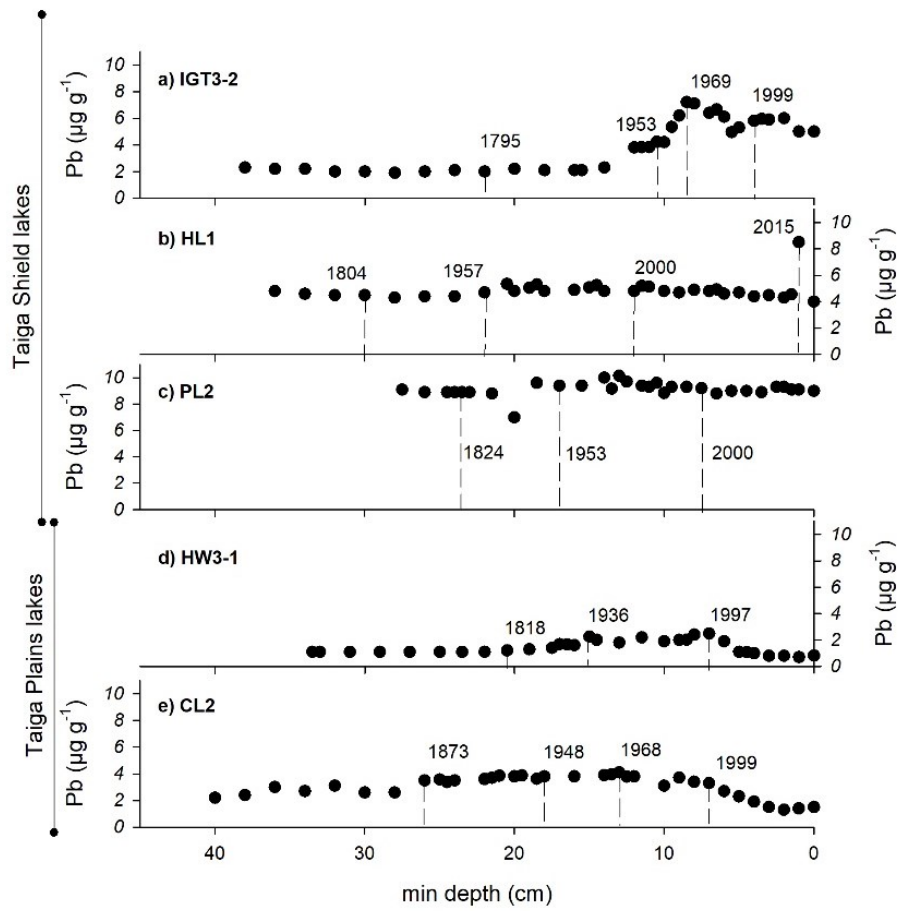


Figure 5.8: Pb concentration in lake sediment cores. Cores are organised from top to bottom by ecoregion and by increasing distance to the City of Yellowknife and the local gold mines. Dashed lines represent the modelled age of selected layers.

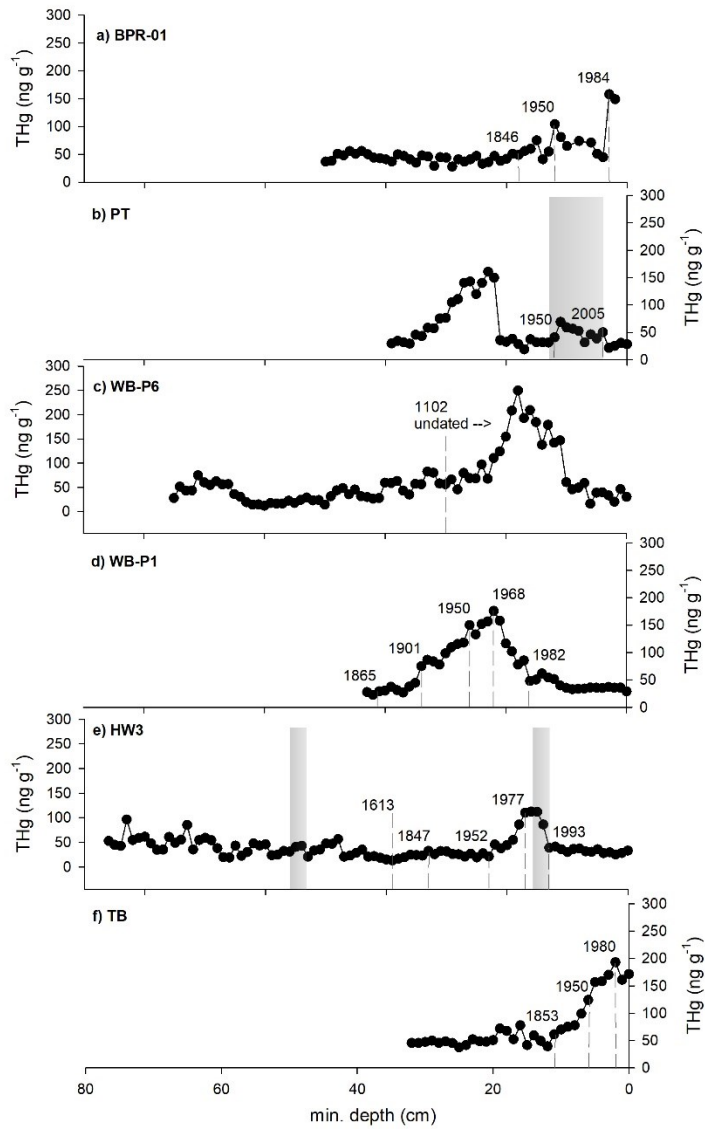


Figure 5.9: THg concentration per depth in peat cores. Cores are organised from top to bottom by increasing distance to the City of Yellowknife and the local gold mines. Grey areas represent peat layers with ash content >10% (see Figure 5.13). Dashed lines represent the modelled age of selected layers.

Lake sediment THg concentrations increased gradually over time at all sites (Figure 5.9) with a decline toward background concentrations starting in the late 1990s in Taiga Plains lakes only (Figure 5.9 and 5.9e). Mean (\pm stdev) THg concentration in pre-industrial sediment varied between $28 \pm 3 \text{ Hg g}^{-1}$ and $47 \pm 5 \text{ Hg g}^{-1}$, depending on the site (mean for all samples=39, min=23, max= 54, n=116). The THg concentration in pre-industrial lake sediment was greater in sediment at sites with more organic matter content, but the differences were not significant (Pearson r , $r = 0.77$, $p = 0.13$) which could be due to our low sample size ($n = 5$).

In the Taiga Shield lakes, the trend in sediment THg concentration differed between the three sites (Figure 5.9c, 5.9d and 5.9e). In PL2, THg concentration increased by only $\sim 20 \text{ ng g}^{-1}$ over the entire core and remained constant after $\sim 1998 \text{ C.E}$ (Figure 5.9c). Depth variation of sediment THg concentration in this lake was strongly correlated to organic matter content (Pearson, $r=0.93$, $p<0.001$). The trend in HL1 was similar to the PL2 trend except that the maximum increase in THg concentration was $\sim 40 \text{ ng g}^{-1}$ (Figure 5.9d) and the relationship to organic matter content was weaker but still significant (Pearson, $r=0.67$, $p<0.001$). The Taiga Shield site closest to Yellowknife (IGT3-2) had a distinct peak of THg concentration in sediment accumulated between 1948 and 1981, reaching a maximum at 133 ng g^{-1} (Figure 5.9e). Following this peak, sediment Hg concentration decreased but remained greater than in pre-industrial or early industrial sediment (Figure 5.9e). Contrary to the two other Taiga Shield sites, THg content was not correlated to organic matter concentration in IGT3-2 sediment (Pearson, $r=0.09$, $p>0.1$).

The magnitude of THg concentrations in sediment cores was similar for Taiga Plain lakes and Taiga Shield Lakes (Figure 5.9). In Taiga Plains lakes, there was no consistent relationship between sediment organic matter and sediment THg concentration, with one lake having a positive and the other a negative correlation between these variables (HW3-1: Pearson correlation, $r=0.28$, $p=0.02$; CL2:

Pearson correlation, $r = -0.39$, $p < 0.001$). Contrary to sediment cores from Taiga Shield lakes, Taiga Plain cores had declining THg concentrations in the sediment after 1975 (CL2, 1974-1977, 95% CI) and 1997 (HW3-1, 1995-1998, 95% CI).

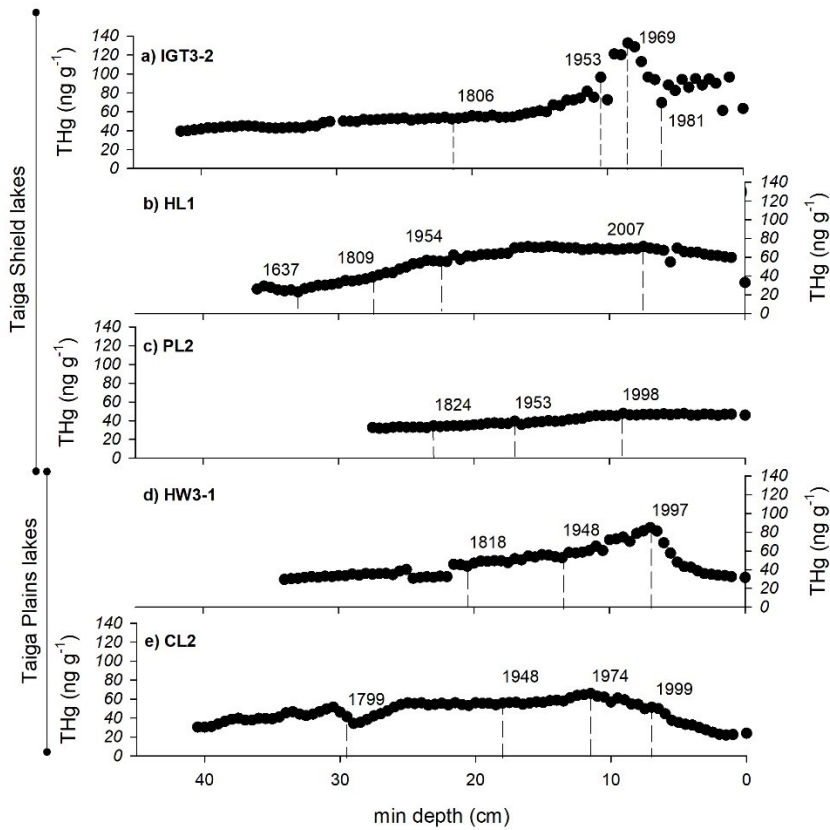


Figure 5.10: Mercury concentration per depth in lake sediment. Cores are organised from top to bottom by ecoregion and by increasing distance to the City of Yellowknife and the local gold mines. Dashed lines represent the modelled age of selected layers.

5.4.3 Assessment of peatland ombrotrophy

Peat bogs were mostly ombrotrophic as indicated by the Ca/Mg molar ratio in peat samples (Figure 5.11). The Ca/Mg molar ratio of peat samples was within the values reported for precipitation chemistry measurement at Snare Rapids hydro station, 140 km northwest of Yellowknife (ECCC, 2019). The Ca/Mg molar ratio and strontium content of the peat slightly increased with depth in all peat cores, but the scandium and aluminum concentrations did not, except for the bottom 10 cm of HW3 peat core and a large portion of the PT core (Figure 5.7). In these two sections, ash content is also $\geq 10\%$. We did not include the PT core and the bottom 10 cm of the HW3 core in our flux deconstruction because the aluminum, scandium and ash content indicated a possible contribution from surface or groundwater flow. Increasing Ca/Mg molar ratio with depth in peat could be due to the diffusion of Ca from the underlying mineral layers or to differences in peat decomposition and compression, but do not necessarily indicate minerotrophic status (Shotyk, 1996).

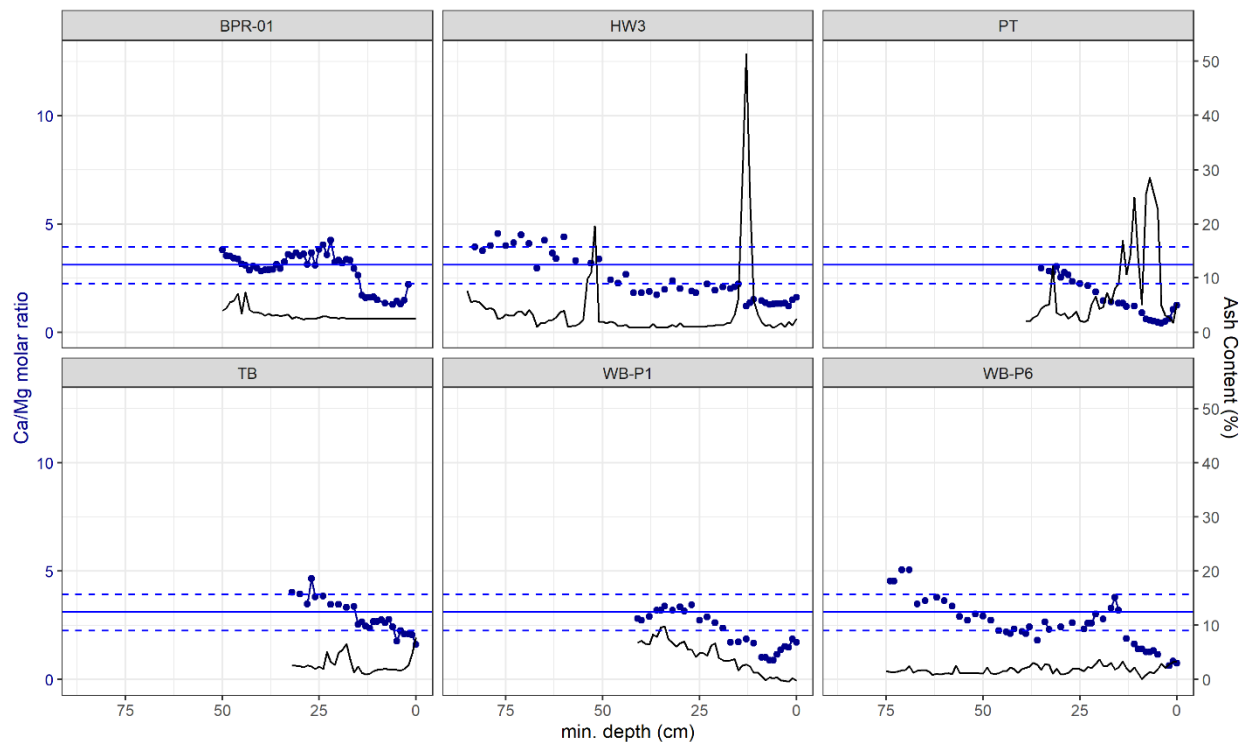


Figure 5.11: Ca/Mg molar ratio from ICP-MS measurement in peat samples (dark blue dots, left axis) and ash content in peat samples from loss-on-ignition at 550°C (full black line, right axis) plotted against peat depth. The horizontal blue lines indicate the average (full line), minimum and maximum (dashed lines) annual Ca/Mg molar ratio in precipitations at the Snare Rapids meteorological station between 2007-2016 (ECCC, 2019).

5.4.4 Lead fluxes

Average Pb fluxes in the pre-industrial period (pre-1800.) were very low in the Taiga Shield lakes ($21\text{--}97 \mu\text{g Pb m}^{-2} \text{ yr}^{-1}$), Taiga Plains lakes ($14\text{--}25 \mu\text{g Pb m}^{-2} \text{ yr}^{-1}$) and in peat bogs ($2\text{--}13 \mu\text{g Pb m}^{-2} \text{ yr}^{-1}$). During this period, the Pb accumulation rate in bogs (representing the atmospheric deposition rate) was 11–77% (median = 44%) of the Pb accumulation rate in lake sediment bog.

Between 1800 and 1938, Pb fluxes increased in all peat bogs (Figure 5.12a) and lake sediment cores (Figure 5.17a). However, only modest increases (<100 and $\leq 10 \mu\text{g Pb m}^{-2} \text{ yr}^{-1}$ in lakes and bogs respectively) occurred during the early industrial period (1800-1938) and prior to the onset of local emission sources during the late-industrial period (1938-2000). Over the last 200 years, differences in lithogenic input (FL) comprised the largest part of the Pb flux to two lakes and explained some of the inter-lake variability in total Pb accumulation rate for each time period (Figure 5.17a). Changes in

lithogenic input (F_L) were particularly important in Taiga Shield lakes (Figure 5.17a). Anthropogenic excess Pb (F_A) was the second most important deconstructed component of the Pb flux to lakes and local mining-derived Pb (F_M) accounted for the lowest amount of Pb deposited to lakes (Figure 5.17a). Detailed Pb fluxes of each core on a continuous time axis are provided in supplementary information for bogs (Figure 5.13 and 5.15) and lake sediment cores (Figure 5.14 and 5.16).

In bogs, long-range anthropogenic pollution (F_A) and mining pollution (F_M) accounted for the greatest changes in Pb fluxes accumulated during the late-industrial period (1938-2000) and the recent period (2000-2016). The average mining-derived Pb pollution flux (F_M) during the late-industrial period (1938-2000) decreased with distance from Giant Mine in the peat (Figure 5.12a) and lake sediment cores (Figure 5.17a). The greatest F_M for Pb was identified in the peatland BRP-01 (~2 km away from Giant Mine) and lower amounts were identified at sites further from the mines, including peatlands HW3 and WB-P1 (Figure 5.12a) and lake IGT3-2 (Figure 5.17a).

Compared to the late-industrial period, the total Pb flux and the anthropogenic Pb flux (F_A) decreased in recent years (2000-2016) in two of the three peat bogs with measurements for that time period (Figure 5.12a) and in Taiga Plains lakes (Figure 5.17a). However, the F_A flux for Pb, along with the lithogenic (F_L) flux continued to increase in Shield lakes over the same period.

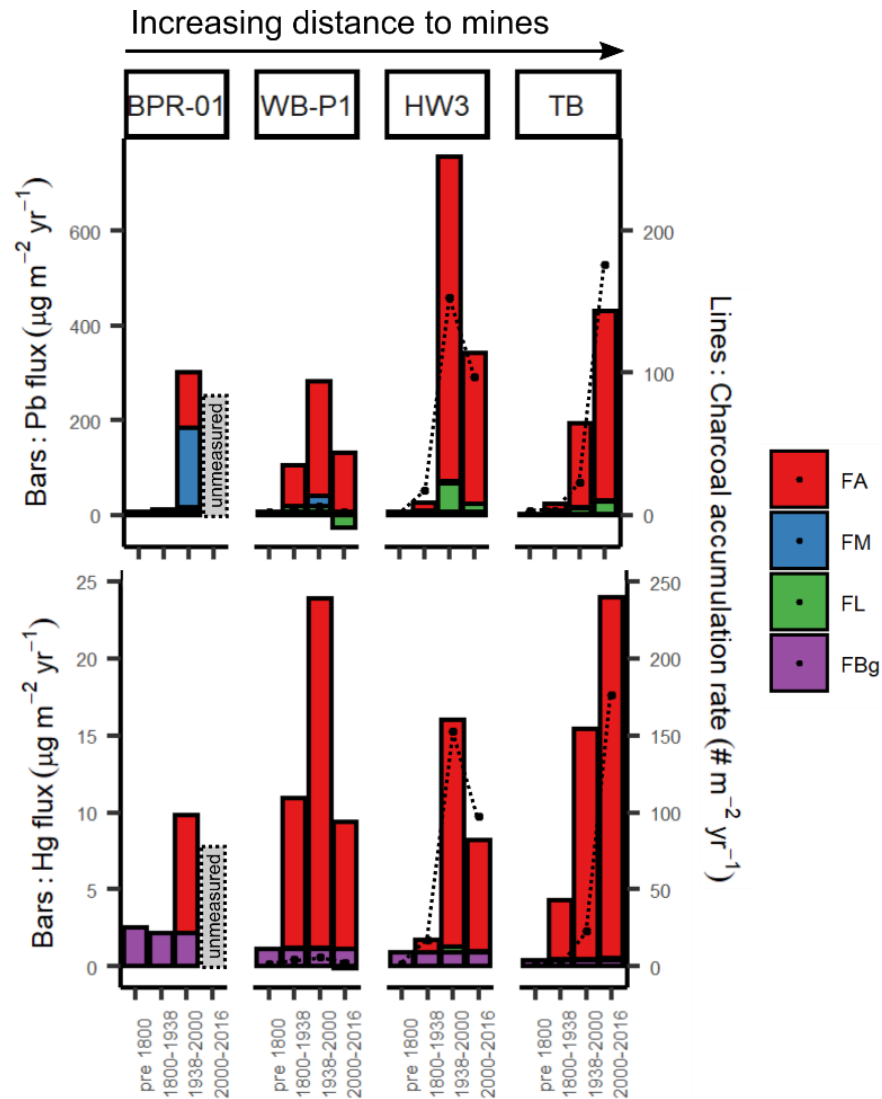


Figure 5.12: Average long-term Pb and Hg flux in peat bogs during four key periods (pre-1800; 1800-1938; 1938-2000; 2000-2016) estimated using equation 3 and organised from left to right by increasing distance to the City of Yellowknife and the local gold mines. Bar colors (and the legend) represent the result of long-term average flux deconstruction (see equation 5.4). The average macroscopic charcoal accumulation rate for each of these periods is indicated as a dashed line with the scale on the right side.

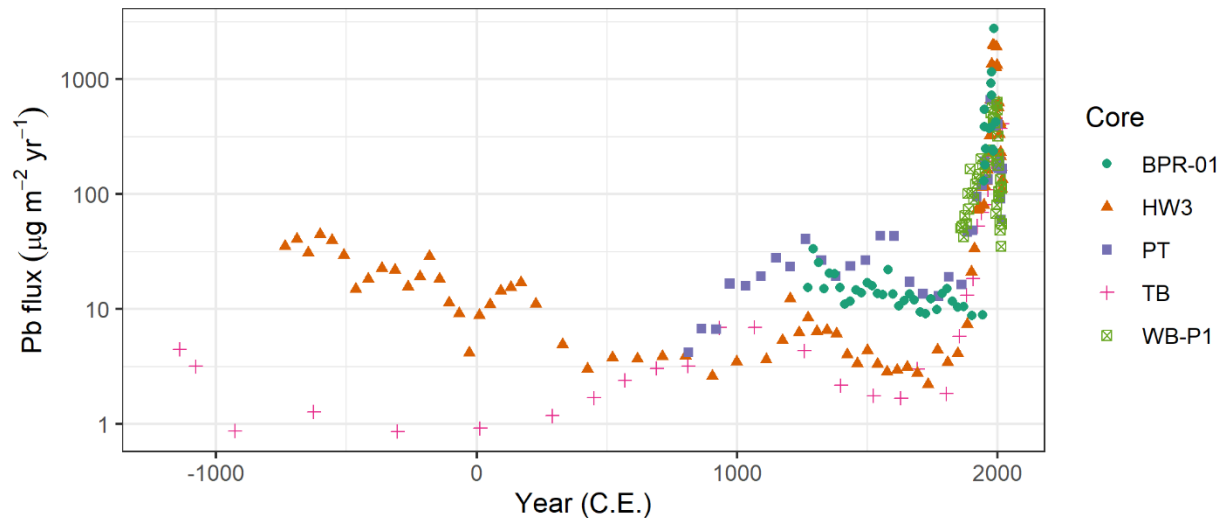


Figure 5.13: (a) Lead (Pb) flux in peatlands north of Great Slave Lake, NT, Canada since 0 CE. Notice the \log_{10} scale.

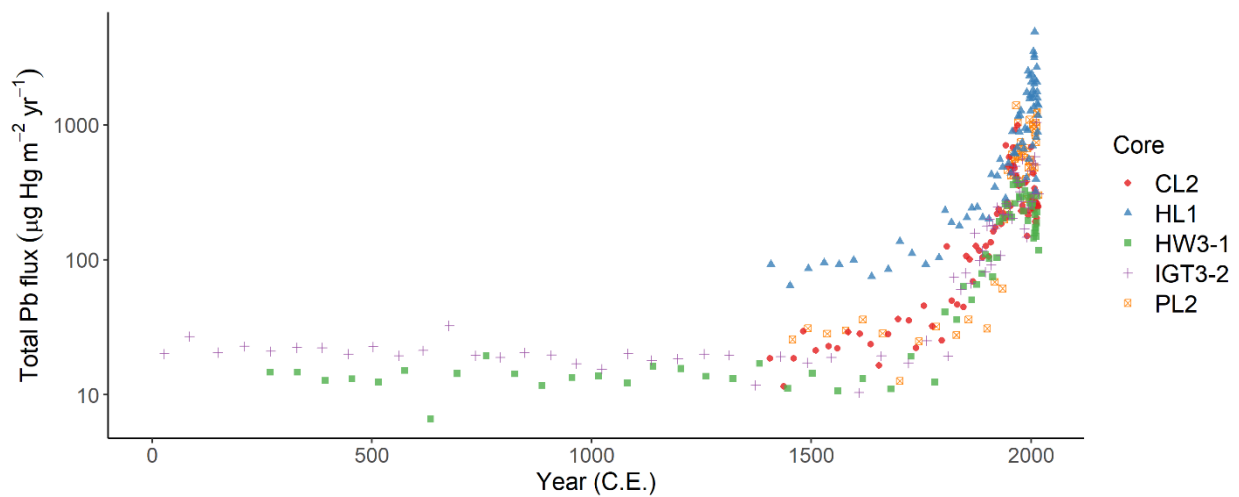


Figure 5.14: FF-corrected lead (Pb) flux in lake sediment of the Canadian Shield and Taiga Plains for the period 0 -2016 CE. Notice the \log_{10} scale.

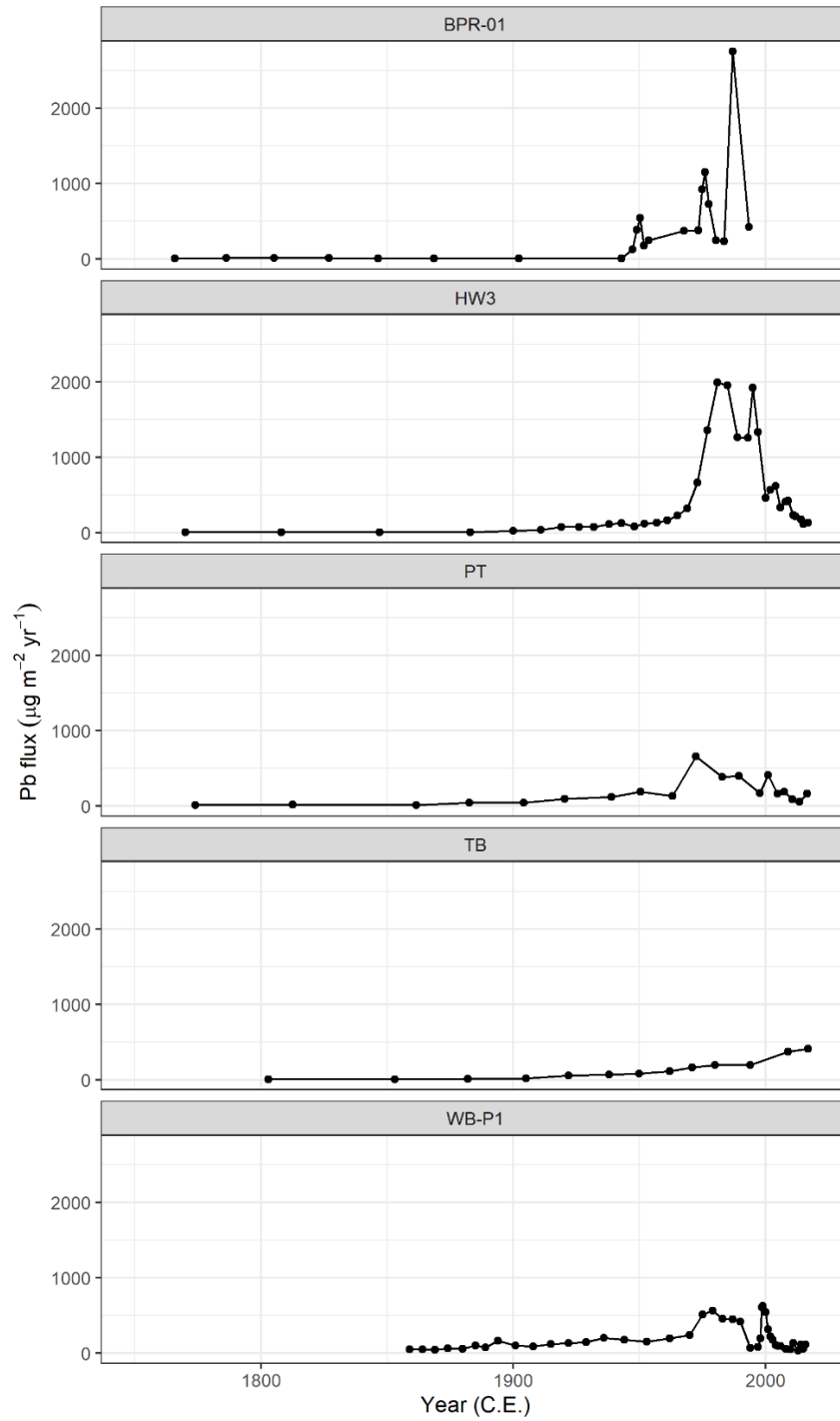


Figure 5.15: Lead (Pb) flux in peatlands north of Great Slave Lake, NT, Canada after the post-industrial era (>1800)

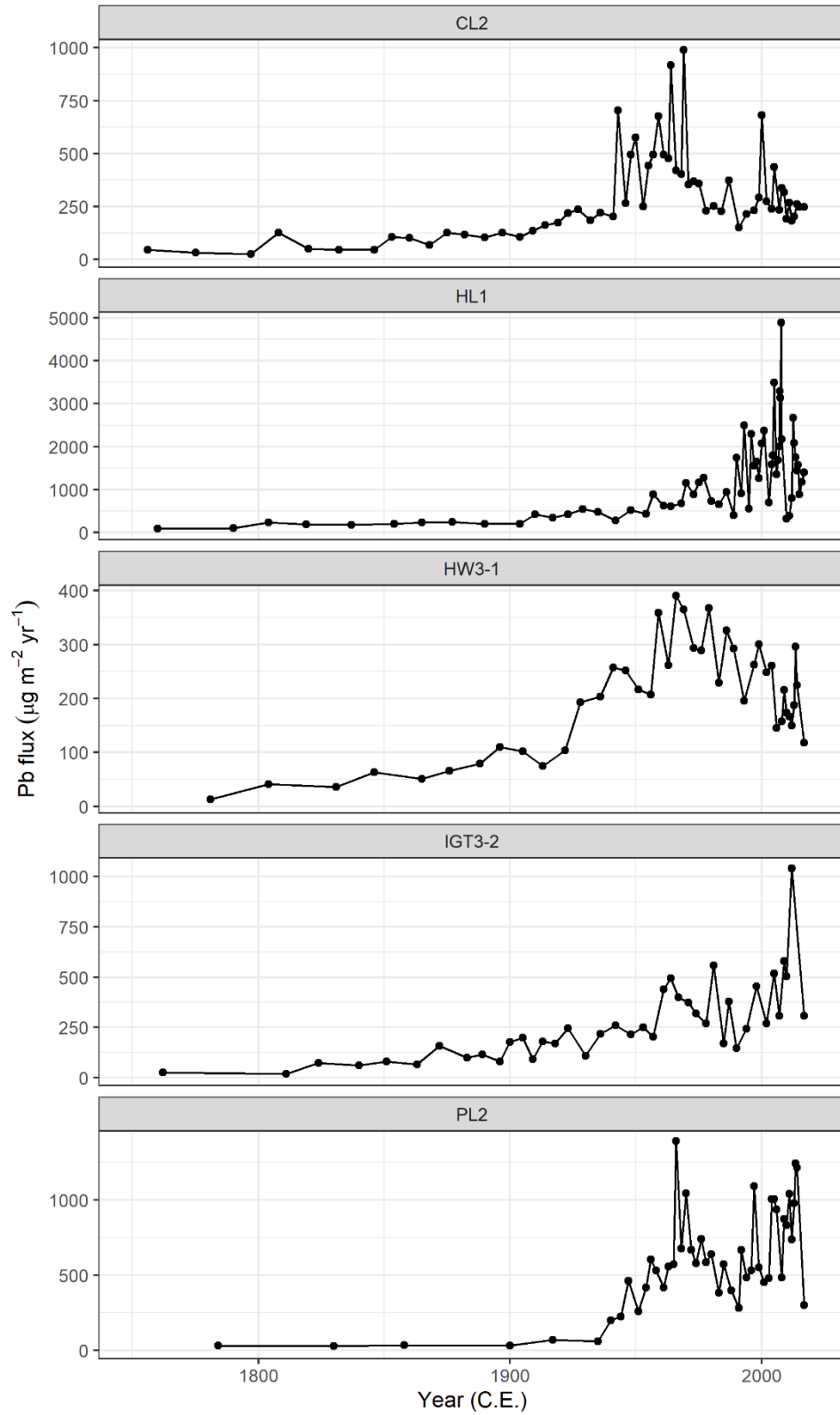


Figure 5.16: (a) FF-corrected lead (Pb) flux in lake sediment of the Taiga Shield and Taiga Plains for the period 1800 -2016 CE. Notice the variations in y-axis range.

5.4.5 Mercury fluxes

The average pre-industrial (pre-1800) Hg accumulation rate was low for bogs (0.38 to 2.50 $\mu\text{g Hg m}^{-2} \text{ yr}^{-1}$, mean = 1.0) and lakes (0.1 to 0.58 $\mu\text{g Hg m}^{-2} \text{ yr}^{-1}$, mean = 0.44). The differences in Hg accumulation rate between the two types of archives were exceptionally small during the pre-industrial period.

All peat and lake sediment cores showed a small increase in Hg flux during the early-industrial period (1800-1938) with a more substantial increase during the late-industrial (1938-2000) and most recent period (2000-2016) (Figures 5.12b and 5.17b). Detailed Hg fluxes for each core on a continuous time axis are provided in the for bogs in Figures 5.13 and 5.15 and lake sediment in Figure 5.14 and 5.16. The greatest anthropogenic flux (F_A) for Hg occurred during the late-industrial period (1938-2000) in most peatlands and in lakes of the Taiga Plains. The contribution from mining was not calculated separately for Hg fluxes and therefore, the F_A term includes possible local mining pollution. In the recent period (2000-2016), the anthropogenic Hg flux (F_A) and the lithogenic Hg flux (F_L) increased in Taiga Shield lakes but decreased in bogs (Figure 5.12a) and lakes of the Taiga Plains (Figure 5.17b).

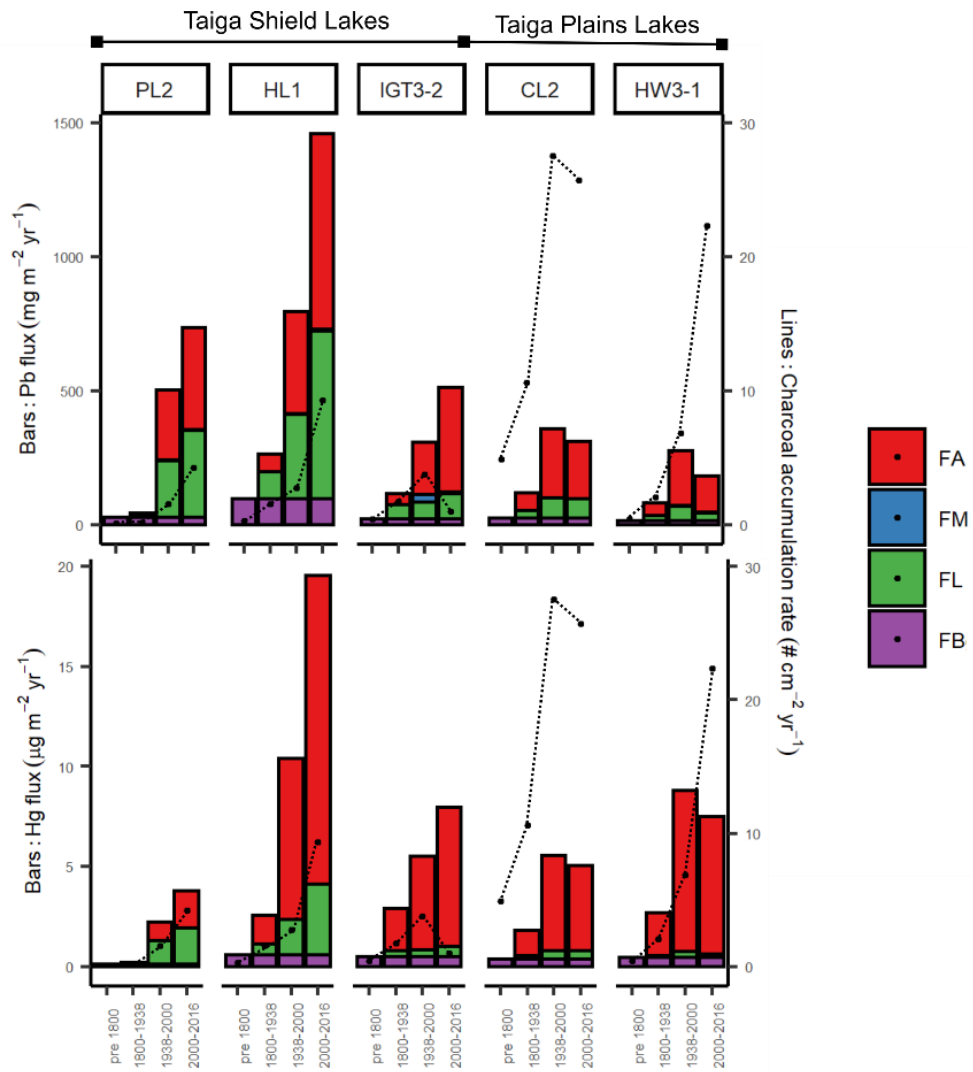


Figure 5.17: Average long-term Pb and Hg flux in lake sediment during four key periods (pre-1800; 1800-1938; 1938-2000; 2000-2016) organised by ecoregion and then by increasing distance to the City of Yellowknife and the mines from left to right. Bar colors (and the legend) represent the result of long-term average flux deconstruction (from equation 5.4) on the long-term average fluxes (from equation 5.3). The lines represent the average macroscopic charcoal accumulation rate for each of these periods and values are indicated on the secondary (right) y axis.

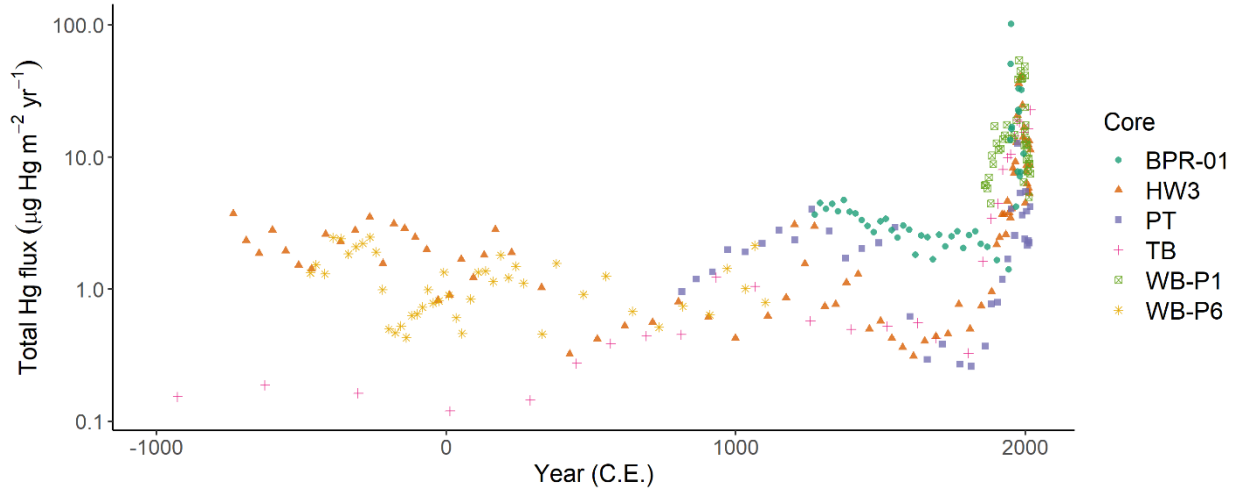


Figure 5.18: (a) Mercury (Hg) flux in peatlands north of Great Slave Lake, NT, Canada since 0 CE. Notice the \log_{10} scale.

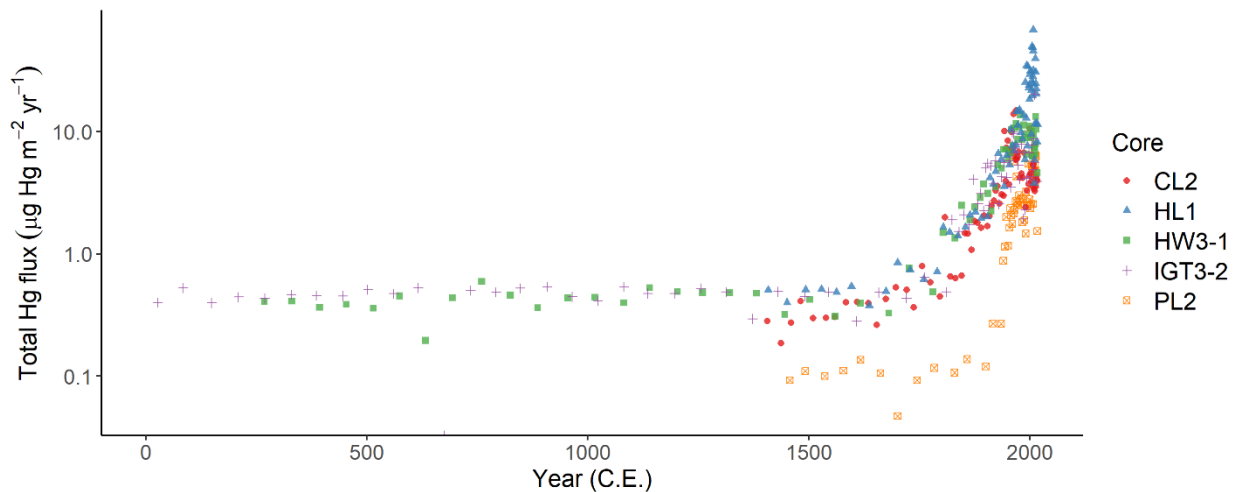


Figure 5.19: (a) FF-corrected mercury (Hg) flux in lake sediment of the Canadian Shield and Taiga Plains for the period 0 -2016 CE. Notice the \log_{10} scale. (b) FF-corrected Hg flux in lake sediment of the Canadian Shield and Taiga Plains for the period 1800 -2016 CE on a continuous (normal) scale.

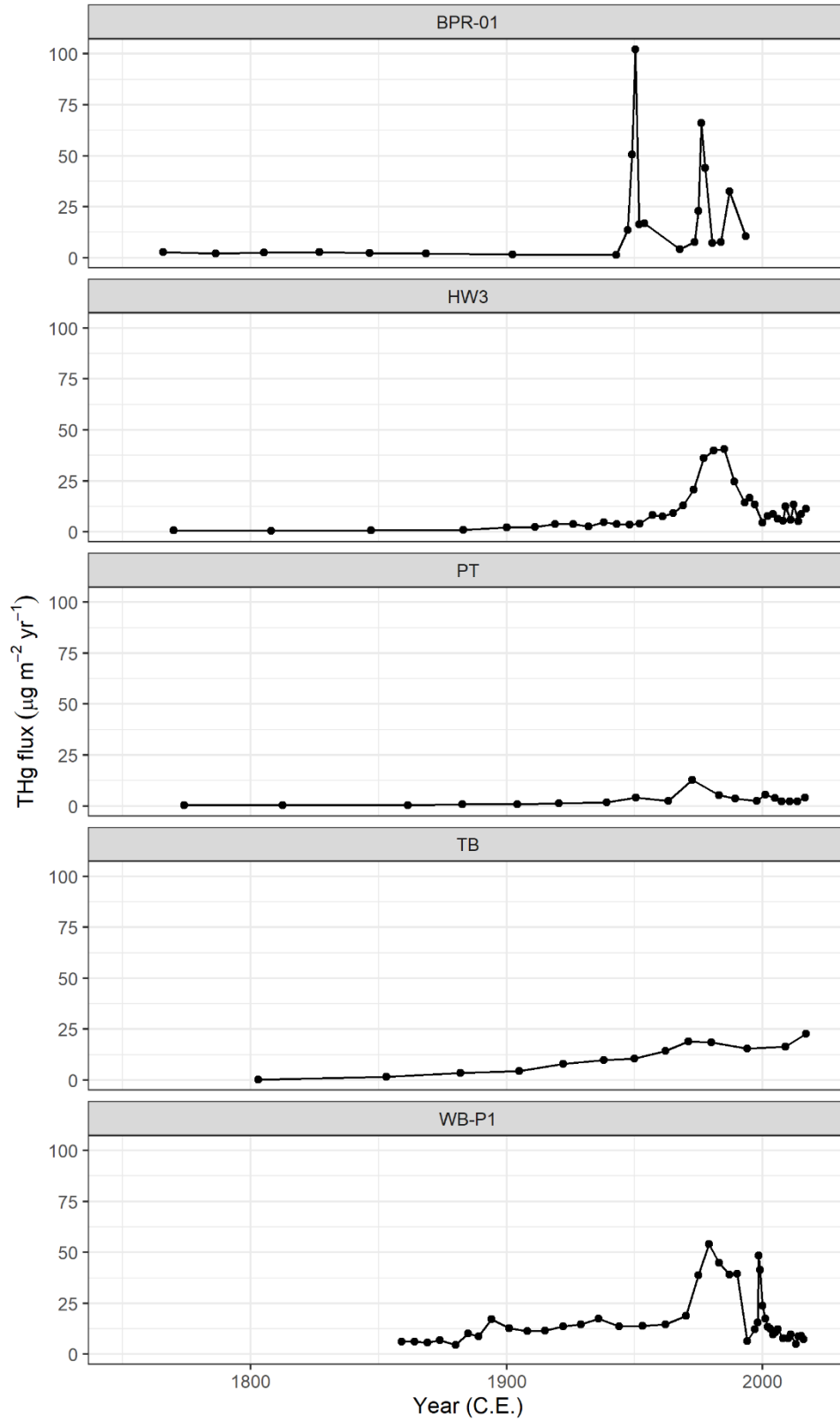


Figure 5.20: Total mercury (THg) flux in peatlands north of Great Slave Lake, NT, Canada after the post-industrial era (>1800).

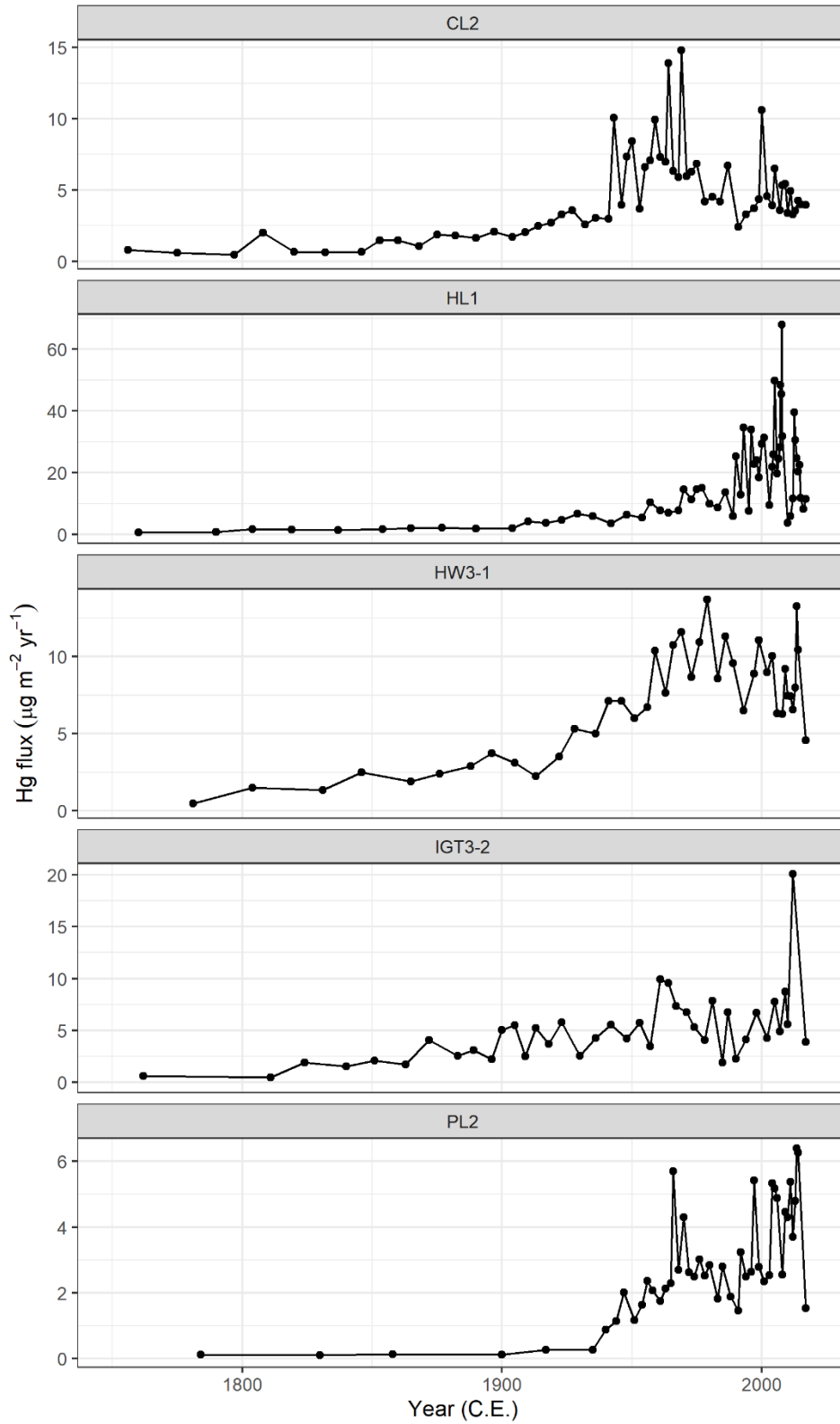


Figure 5.21: FF-corrected mercury (Hg) flux in lake sediment of the Canadian Shield and Taiga Plains for the period 1800 -2016 CE. Notice the variations in y-axis range.

5.4.6 Charcoal flux

Charcoal flux to the lakes and peatlands varied by period and by site but increased over the last 200 years in all bogs (Figure 5.12) and all lakes except IGT3-2 (Figures 5.17). Lakes in the Taiga Plains accumulated more charcoal particles than lakes of the Taiga Shield, especially during the period 1938-2000 (Figure 5.17).

In lake sediments, for any of the delineated periods, there were no significant correlations between the site-specific ($n = 5$) long-term charcoal accumulation rate and the long-term average accumulation rate of Pb (Pearson; pre-industrial $r=0.22, p=0.72$; early-industrial $r=0.04, p=0.95$; late-industrial $r=-0.35, p=0.57$; recent $r= -0.49, p=0.40$) or Hg (Pearson; pre-industrial $r=0.06, p=0.92$; early-industrial $r=-0.07, p=0.91$; late-industrial $r=-0.17, p=0.79$; recent $r= -0.01, p=0.99$).

In peat cores ($n=4$), there was also no correlation between the long-term average charcoal accumulation and the average Hg accumulation rate for any period (Pearson; pre-industrial $r=0.09, p=0.88$; early-industrial $r=-0.56, p=0.44$; late-industrial $r=-0.22, p=0.78$; recent $r= -0.79, p=0.21$). Charcoal accumulation was not correlated to Pb accumulation between peat bogs during the pre-industrial period (Pearson; pre-industrial $r=-0.31, p=0.62$) and the early-industrial period (Pearson, $r=0.37, p=0.63$), but there was a positive correlation between these variables during the late-industrial and recent periods (Pearson; late-industrial $r=0.96, p=0.04$; recent $r= 0.96, p=0.04$).

5.4.7 Anthropogenic Pb pollution accumulation rates in lakes sediment and peat bogs

Anthropogenic Pb pollution is identifiable in Taiga Plains lake sediment accumulated after ca. 1850 and in Taiga Shield lake sediment and peat accumulated after ca. 1900 (Figure 5.22b). Anthropogenic Pb accumulation rates peaked in the 1950s in Taiga Plains lake sediment and peaked in the 1990s for both lake sediment and bogs of the Taiga Shield (Figure 5.22). There was a marked decline in anthropogenic Pb accumulation rates in bogs after the 1990s whereas this flux increased in lake

sediments of the Taiga Shield and only declined marginally in lake sediments of the Taiga Plains (Figure 5.22).

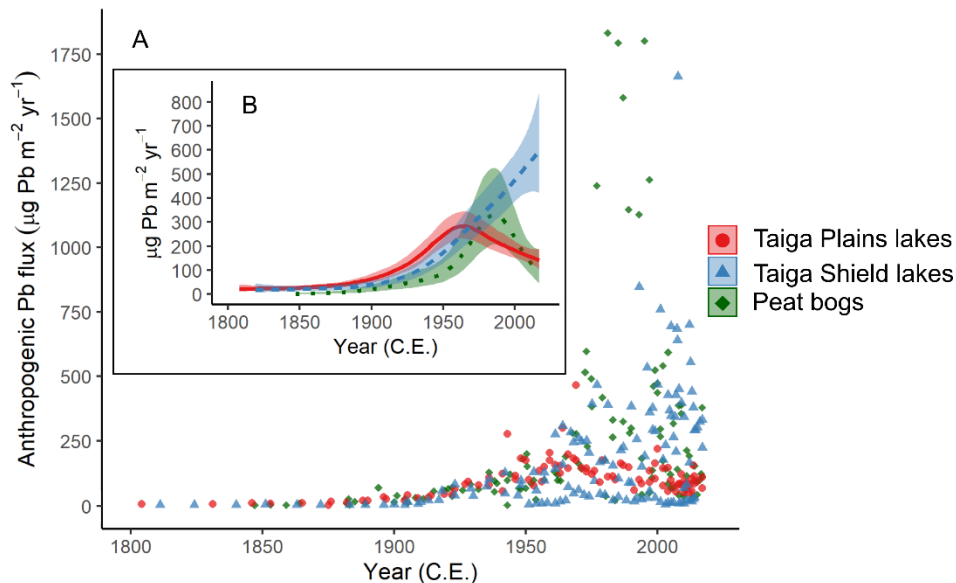


Figure 5.22: (A) Modelled fluxes of anthropogenic Pb (FA) in peat bogs (green diamonds), in Taiga Plains lakes (blue triangles) and in Taiga Shield lakes (red circles); (B) Generalised additive model (GAM) of anthropogenic Pb flux using data points from peat bogs (dotted green line), Taiga Plains lakes (dashed blue line) and in Taiga Shield lakes (red full line). The colored area represents the 95% CI for each GAM. The confidence intervals were estimated using a log10 transformation to avoid including negative flux values in the CI.

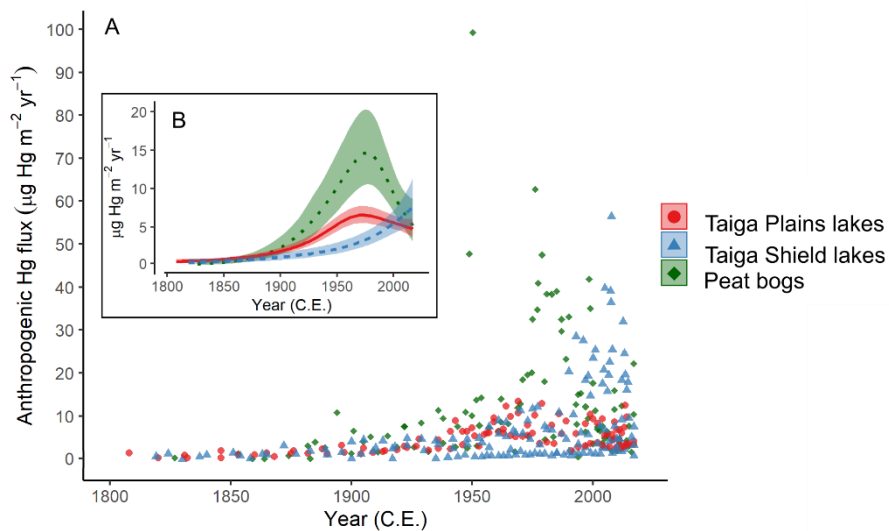


Figure 5.23: (A) Modelled fluxes of anthropogenic Hg (FA) in peat bogs (green diamonds), in Taiga Plains lakes (blue triangles) and in Taiga Shield lakes (red circles); (B) Generalised additive model

(GAM) of anthropogenic Hg flux using data points from peat bogs (dotted green line), Taiga Plains lakes (dashed blue line) and in Taiga Shield lakes (red full line). The colored area represents the 95% CI for each GAM. The confidence intervals were estimated using a log₁₀ transformation to avoid including negative flux values in the CI.

5.4.8 Anthropogenic Hg pollution accumulation rate in lakes sediment and peat bogs

Anthropogenic Hg pollution increased from the late 1800s onward in peat and lake sediment, with a more rapid increase in both types of archives starting in the early 1900s (Figure 5.23). The anthropogenic Hg flux modelled from bogs was consistently greater than the coeval lake sediment Hg flux from lakes of both ecoregions until the 1990s (Figure 5.23). The anthropogenic Hg accumulation rate peaked in the 1970s for bogs and lakes of the Taiga Plains but increased continuously over the same period in the Taiga Shield lakes (Figure 5.23).

5.5 DISCUSSION

This study used environmental archives from bogs and lake sediments to reconstruct atmospheric fluxes of Pb and Hg, and the environmental response of changing atmospheric fluxes to lakes. Our records of Pb and Hg fluxes to peatlands and lakes in northwestern Canada show a highly consistent pattern of low Pb and Hg deposition to these ecosystems in pre-industrial times. The accumulation rate of Pb and Hg in lakes and bogs are similar to other reports globally (Bindler, 2011; Bindler et al., 2001; Cooke et al., 2009; Drevnick et al., 2012; Pratte et al., 2018; Roos-Barraclough and Shotyk, 2003) suggesting a highly coherent global signature of these elements before the onset of large-scale anthropogenic release of these contaminants to the atmosphere.

Distinct differences were found in recent trends of Pb and Hg accumulation between lake sediments and peatlands around Yellowknife, NT, Canada. Lake sediment from the Taiga Shield recorded a continuous increase in Pb and Hg loading over the last two decades, whereas the accumulation rate of the same elements has declined in Taiga Plain lakes and steeply declined in bogs (Fig. 8). The peat records demonstrate the rapid and positive impact of environmental regulations on anthropogenic

emissions of atmospheric contaminants in North America. The continued loading of anthropogenic Pb and Hg to lake sediments and the different contaminant trajectories from the different ecoregions shows that the future state of Pb and Hg contamination in subarctic lakes will be modulated by catchment characteristics and their interactions with climate change.

5.5.1 Pre-industrial levels of Pb and Hg accumulation near Yellowknife (NT, Canada)

The pre-industrial (background) Hg accumulation rates calculated for peatlands in this study ($0.38 - 3.18 \mu\text{g m}^{-2} \text{y}^{-1}$, mean = $1.30 \mu\text{g m}^{-2} \text{y}^{-1}$) are similar to pre-industrial accumulation rates in peatlands of the Hudson Bay Lowlands ($1.51 \pm 0.56 \mu\text{g m}^{-2} \text{y}^{-1}$; Goacher, 2014), Southern Ontario, Canada ($1.4 \pm 1.0 \mu\text{g m}^{-2} \text{y}^{-1}$; Givelet and Roos-Barracough, 2003) and Maine, USA ($1.7 \pm 1.3 \mu\text{g m}^{-2} \text{y}^{-1}$, Roos-Barracough et al., 2006) and many remote European peatland records (Givelet et al. 2003; Fiona Roos-Barracough and Shotyck, 2003; Shotyck et al., 2005). Lake sediments accumulated Hg at a similar rate ($0.54 - 1.29 \mu\text{g m}^{-2} \text{y}^{-1}$, mean = $0.66 \mu\text{g m}^{-2} \text{y}^{-1}$) to peatlands during the pre-industrial period. Because of the study sites high latitude (62°N), continentality and distance to emission sources, pre-industrial Hg fluxes were below the average global background Hg flux in lake sediments ($3-3.5 \mu\text{g m}^{-2} \text{y}^{-1}$; Biester et al., 2007).

Similar to Hg, the natural background flux of Pb to peatlands in this study ($2 - 22 \mu\text{g m}^{-2} \text{y}^{-1}$, mean = $11 \mu\text{g m}^{-2} \text{y}^{-1}$) was low and consistent to values calculated for peat bogs of southern Quebec, Canada ($10 - 30 \mu\text{g m}^{-2} \text{yr}^{-1}$; Pratte et al., 2013), the Jura Mountain, Switzerland ($\sim 10 \mu\text{g Pb m}^{-2} \text{yr}^{-1}$; Shotyck et al., 1998) and Sweden ($10 \mu\text{g Pb m}^{-2} \text{yr}^{-1}$; Bindler, 2011). The pre-industrial Pb accumulation in Taiga Shield lakes ($21-97 \mu\text{g m}^{-2} \text{yr}^{-1}$, mean=28) was below the range of background Pb fluxes reported for Canadian Shield lakes ($250 \pm 120 \mu\text{g Pb m}^{-2} \text{yr}^{-1}$; Gallon et al., 2005). The background Pb flux and Pb concentration for Taiga Plains lakes ($14-25 \mu\text{g Pb m}^{-2} \text{yr}^{-1}$) is slightly lower than Shield lakes, likely because expansive bedrock outcrops in the Taiga Shield are more enriched in Pb than the

predominately till covered landscape of the Taiga Plains and catchment transport is more important in Taiga Shield lakes.

5.5.2 Long-term cumulative impact of pollution on Pb and Hg fluxes

The environmental archives around Yellowknife revealed that the area was affected by long-range pollution from the early 1800s onward, on which was superposed local pollution from mines between 1938 and 2000. The contamination level remained low in comparison to other contaminated sites near point-sources, but because background (pre-industrial) fluxes were extremely low, the anthropogenic flux ($90\text{--}400\ \mu\text{g Pb m}^{-2}\ \text{yr}^{-1}$) represented a large (4–166 fold) increase relative to pre-industrial conditions.

Between 1800 and 1938, fluxes of Pb and Hg increased above background values in bogs (mean = $4.8\ \mu\text{g Hg m}^{-2}\ \text{y}^{-1}$ and $41\ \mu\text{g Pb m}^{-2}\ \text{y}^{-1}$) and lake sediment (mean = $2.55\ \text{Hg m}^{-2}\ \text{yr}^{-1}$ and $114\ \mu\text{g Pb m}^{-2}\ \text{y}^{-1}$) (Figures 5.22 and 5.23) despite the absence of local anthropogenic sources for these elements in the area. Fluxes continued to increase in response to increasing deposition of long-range pollution and the appearance of local sources after the opening of gold mines in Yellowknife in 1938. During the period where mines were open in Yellowknife (1938–2000), the average fluxes of Pb and Hg continued to increase in Taiga Shield lakes (mean = $11.8\ \mu\text{g Hg m}^{-2}\ \text{yr}^{-1}$ and $898\ \mu\text{g Pb m}^{-2}\ \text{yr}^{-1}$) and were greater than in bogs ($1.7\text{--}10.9\ \mu\text{g Hg m}^{-2}\ \text{y}^{-1}$ and $10\text{--}105\ \mu\text{g Pb m}^{-2}\ \text{y}^{-1}$) and lakes of the Taiga Plains (mean = $7.2\ \mu\text{g Hg m}^{-2}\ \text{yr}^{-1}$ and $316\ \mu\text{g Pb m}^{-2}\ \text{yr}^{-1}$) (Figures 5.12 and 5.17). However, the magnitude of these fluxes was small in comparison to fluxes reported for lakes near important point-sources like smelters (Wiklund et al., 2017), and roughly half of the Pb flux estimates for a lake near coal-fired power plants in Alberta, Canada (Donahue et al., 2006). The Hg accumulation rate in this study was lower than accumulation rates in European peat bogs where deposition of $40\text{--}100\ \mu\text{g Hg m}^{-2}\ \text{yr}^{-1}$ have been commonly reported for the period 1950–1970 (Coggins et al., 2006).

Similar to Hg, the increase in Pb fluxes from 1800-1938 was relatively large compared to background conditions (8-10 fold greater in lakes and 6-80 fold greater in peat bogs), but remains low in comparison to Pb fluxes measured in lakes at close proximity (<2 km) to Giant Mine (Thienpont et al., 2016; Chapter 3 of this thesis). The maximum recorded Pb deposition rate in peatlands in this study ($\sim 2750 \mu\text{g Pb m}^{-2} \text{ yr}^{-1}$), although enriched by pollution from Giant Mine, was within the maximum reported flux for northern Alberta peat bogs near bituminous oil sands extraction plants, in 1967 ($\sim 1.4 - 9 \mu\text{g Pb m}^{-2} \text{ yr}^{-1}$) (Shotyk, et al., 2016). These north Albertan peat bogs also show similar recent Pb accumulation rates ($\sim 100-750 \mu\text{g Pb m}^{-2} \text{ yr}^{-1}$) to those in our study ($\sim 100-430 \mu\text{g Pb m}^{-2} \text{ yr}^{-1}$) (Shotyk et al., 2016). The maximum Pb flux recorded in peat bogs in this study was lower in magnitude than the maximum historical fluxes reported in most European bogs (Coggins et al., 2006; Shotyk et al., 1998).

5.5.3 Long-range atmospheric Hg pollution decreased in step with declining North American emissions

Our flux deconstruction approach indicates that atmospheric pollution (long-range and local) was the dominant driver of Hg accumulation in bogs from ~ 1880 onward and that atmospheric Hg deposition peaked during the 1970s. The post 1970s decline in atmospheric Hg deposition recorded by bogs corroborates findings from tree-ring reconstructions in the Mackenzie River Valley in the central Northwest Territories (Ghotra et al., 2020). Our bog records are also consistent with decreasing Hg concentrations in air (gaseous elemental Hg) and in precipitation measured at monitoring sites in southern Canada since the 1990s (Cole et al., 2014) as well as studies modelling Hg deposition based on anthropogenic emissions and atmospheric transport models (Zhang et al., 2016). The temporal trend of Hg accumulation is consistent with atmospheric Hg emissions from North-American sources (Streets et al., 2017) and the 91% decrease in Canadian atmospheric Hg emissions since 1990 (ECCC, 2020). The recent Hg flux estimated from the surface layer of peat bogs ($3 - 5.5 \mu\text{g Hg m}^{-2} \text{ yr}^{-1}$) is also in line with the recent accumulation of Hg in Sphagnum of northern Alberta ($5.7 - 6.1 \mu\text{g Hg m}^{-2} \text{ yr}^{-1}$).

¹Shotyk and Cuss, 2019). Despite the important decline in atmospheric Hg since the 1970s peak, the most recent (2000–2016) Hg flux to the bogs still represents a 5–40 fold increase compared to the pre-industrial accumulation rate. Overall, the declining trend in atmospheric Hg accumulation recorded by bogs of the Taiga Shield corroborate the 1.5 to 2.2% decline per year in atmospheric gaseous Hg observed across North America, Europe, and over the North Atlantic Ocean (Obrist et al., 2018).

5.5.4 The atmospheric deposition rate of Pb

The atmospheric deposition of anthropogenic Pb decreased rapidly following the gradual ban on leaded gasoline, the reduction of coal usage and the reduction of atmospheric pollution emissions from industrial activities since the 1980s. The anthropogenic Pb deposition rate in bogs followed the typical signature of leaded gasoline in North America (Gallon et al., 2005) and Europe (Bindler, 2011; Roos-Barraclough and Shotyk, 2003; Shotyk et al., 2002), with an increase in atmospheric deposition toward the end of the 1930s, a peak in the late 1980s and a decreasing trend thereafter. It should be noted that the long-range anthropogenic Pb pollution that reached the Yellowknife area is an exceedingly small amount ($\leq 1000 \mu\text{g m}^{-2} \text{yr}^{-1}$). To provide perspective, close-range atmospheric emissions from Giant Mine and the dumping of tailings and effluent has increased Pb accumulation by 10,000–40,000 $\mu\text{g m}^{-2} \text{yr}^{-1}$ for >40 years in Yellowknife Bay on Great Slave Lake (see chapter 3 of this thesis) and atmospheric deposition of Pb in the Adirondack Mountains of New York State peaked at 14,700 $\mu\text{g m}^{-2} \text{yr}^{-1}$ in the 1970s (Sarkar et al., 2015).

5.5.5 Trends in Pb and Hg accumulation

The decline in bog Pb accumulation rate in this study follows ice core records from Devon Island in the Canadian Arctic and from Greenland (Marx et al., 2016) and peat bog records from northern Alberta (Shotyk et al., 2016). This trend contrasts with an ice core record from the western Canadian Arctic suggesting increasing deposition of Pb over the same period (Marx et al., 2016; Osterberg et

al., 2008). Similarly, our reconstructions of atmospheric Hg deposition align with atmospheric Hg reconstruction from Mackenzie River tree-rings (Ghotra et al., 2020), showing a peak in the 1970s, but contrast with a recent tree-rings reconstructions from the western Canadian Arctic (Yukon) showing stable or increasing atmospheric Hg after the 1970s (Clackett et al., 2018, 2021). The Yellowknife area follows the continental Arctic trend in Pb and Hg accumulation rather than the western Canadian Arctic trend, which are respectively influenced by the Continental Polar and Arctic air masses and the Maritime Polar air mass, the former being more impacted by long-range influences from Asia (Dastoor et al., 2015). The Mackenzie River tree-rings reconstruction showed a new increase in atmospheric Hg concentration in the last 20 years (Ghotra et al., 2020), whereas there was no conclusive evidence of an increase in atmospheric Hg deposition in our bog records for the last 20 years. Only two of our ombrotrophic peat records (HW3 and WB-P1) had more than one sample dated post-2000, and Hg accumulation rate was slowly increasing in one (HW3) and slowly decreasing in the other (WB-P1) (Figure 5.20).

5.5.6 Legacy metals retained in Taiga Shield catchments continue to be delivered to subarctic lakes

Lake sediment records illustrated the persistence of Pb and Hg reservoirs in catchment soils. Across the study region there was a delay in the response of lake sediment archives to changes in Pb and Hg loading following North American reductions in anthropogenic emissions. Rates of Pb and Hg accumulation decreased slowly in Taiga Plains lakes and increased in Taiga Shield lakes compared to bog accumulation rates over the same period in this study and in northern Alberta (Shotyk et al., 2016).

Other studies have also demonstrated that a large portion of Hg and Pb accumulation in lakes can be derived from the long-term transport of legacy Pb and Hg from catchments (Kamman and Engstrom, 2002; Yang, 2015; Yang et al., 2018). Findings from an isotopically labelled Hg study on boreal forest vegetation showed that 50–80% of the annual wet Hg deposition was retained in above-ground

vegetation and soils with an half-life of 704 ± 52 days, causing a temporal delay between deposition and downward movement through the soil profile and into runoff (Graydon et al., 2009). For Pb, over 95% of the atmospherically deposited Pb can be retained in upland soils (Watmough and Dillon, 2007). The importance of catchment retention for the accumulation of Pb and Hg in lakes is hypothesised to be more important in lakes with more catchment influence, often identified from a larger catchment area: lake area ratio (Drevnick et al., 2012; Swain et al., 1992). Hence, the large impact of catchment retention in our study lakes is unexpected, as we analysed lakes with a relatively small catchment area. The small difference in Pb and Hg flux recorded in lake pre-industrial sediment and peat bogs also demonstrate how catchment contribution was historically not important compared to atmospheric deposition in the study lakes.

The lakes in this study were small and may not reflect processes occurring in larger lakes, where atmospheric deposition can represent the largest portion of Pb and Hg inputs. For example, in the Great Lakes sediment cores, Hg accumulation decreased uniformly in response to local, regional, and (inter)national management of Hg discharges to water and air (Drevnick et al., 2012). It remains unclear, however, if the decline in Hg accumulation observed in Great Lakes sediment between 2000–2010 reflected a recent cut in anthropogenic emissions (i.e. absence of temporal lag between emission reduction and lake accumulation rate) or decreases in Hg deposition that occurred decades earlier (Drevnick et al., 2012).

This is not the first study suggesting that the catchment transport of legacy Hg and Pb to lakes could increase in the future, independent from future atmospheric deposition rate (Klaminder et al., 2010; Mills et al., 2009). Future studies could investigate what are the catchment characteristics that contribute to the retention of legacy metals and those that contribute to the release of these metals to streams and lakes under different scenarios of climate change.

5.5.7 Impact of hydro-climatic changes

On the subarctic Canadian Shield, the delay between atmospheric deposition trends and lake sediment accumulation trends was more pronounced than in the Taiga Plains lakes and may be exacerbated by hydro-climatic changes that can alter catchment transport processes and the remobilization of legacy metals.

Yellowknife's average annual temperature and precipitation have increased by 2.5°C and 120 mm, respectively between 1943 and 2011 (Laing and Binyamin, 2013). In recent decades, the precipitation pattern is changing in the northwestern Canadian Shield, especially during fall, as precipitation now arrives more commonly as rain rather than snow (Spence et al., 2011), which has led to increased winter streamflow (Spence et al., 2014, 2015). It is apparent that lakes of the Taiga Shield and those of the Taiga Plains are not responding the same way to these changes in precipitation. Therefore, the difference in catchment characteristics is likely important to the response of lakes to diminishing atmospheric influence on contaminant loading in the last decades.

The Taiga Shield has shallow soils constrained within bedrock outcrops whereas the Taiga Plains soils are coarser, deeper and more easily drained (Wolfe, Kerr, et al., 2017; Wolfe, Morse, et al., 2017). The lower water storage capacity of the Taiga Shield catchments imply that they are more susceptible to variations in water table height and upper soil layer saturation (Spence and Woo, 2008). Saturated Shield soils are susceptible to release legacy metals since the presence of organic matter in the upper soil layer increases hydraulic conductivity and anthropogenic metals are typically accumulated in organic matter near the soil surface (Spence et al., 2015). The hydro-climatic changes responsible for increasing winter streamflow and solute transport in streams (Spence et al., 2014, 2015) may also be accelerating the transport of legacy contaminant from catchments toward subarctic Canadian Shield lakes. Other possible causes for greater catchment transport of Pb and Hg in Shield lakes include longer snow-free seasons and more important freshet events from snowmelt or heavy rains in

tributaries of small lakes (Gould et al., 2016; Vincent et al., 2013). Catchment retention is also evident, but less pronounced, in the Taiga Plains lakes, since the accumulation of anthropogenic Pb and Hg did not decrease as fast as it did in bog records and most recent bog accumulation rates are closer to background fluxes than lakes of either region in this study.

In this subarctic region, lakes and peatlands are snow covered for ~8 months of the year. The length of the growing/open water season is increasing due to climate warming. It is unclear how the changes in ice cover on the lakes and snow cover on the catchments and bogs are influencing the estimates of annual atmospheric deposition rates and the catchment contribution fluxes.

5.5.8 Mines, roads and wildfires

The impact of mining pollution on Pb fluxes in lakes and peatlands was limited to sites near the mines (Figure 5.24), that is consistent with previous estimates showing the local distribution of metal(loid) contamination decreased abruptly within 30 km of Giant Mine (Houben et al., 2016; Jamieson et al., 2017; Palmer et al., 2015; Chapter 3 of this thesis). The impact of the mines on Hg deposition is more uncertain, but the evidence points to a similar spatial and temporal footprint for Pb and Hg emitted by the mine.

The construction and use of roads near the study lakes beginning in the mid-1960s likely contributed to Pb and Hg accumulation in bogs and lakes since all sampling sites were within 500 m of a road. Lithogenic element accumulation increased sharply for a brief period around the 1960s in lakes and in bogs (Figure 5.25), indicative of dust input from blasting for road construction or from road usage. However, the road construction only had a temporary impact on fluxes, with a return toward pre-disturbance Al flux within ten years after the road construction in lakes and bogs (Figure 5.25). More important changes to Al flux in lakes occurred near the end of the 1990s that is unlikely to represent road influence given the timeline. The lithogenic flux, that could partly be caused by road influence,

was more important for Pb accumulation in lakes (Figure 5.12) than for Hg accumulation (Figure 5.17), because of the low concentration of Hg in crustal sources. It is possible, however, that the presence of roads in the lake's catchment facilitated catchment erosion and the transport of legacy metals to the lakes. The low contribution of lithogenic Hg to the total fluxes is not surprising since most Hg in the tundra environment is derived from gaseous Hg uptake by vegetation (Biester et al., 2007; Obrist et al., 2017).

The lake sediments showed two to four times more wildfire events occurring in the 60 years between 1955 and 2015 than in the 60 years between 1895 and 1955 (see chapter four of this thesis). This trend is part of broader-scale changes in fire regimes occurring over North America characterized by increases in the number of fires and the amount of hectares burned each year since 1959, especially in the central (most continental) Canadian ecozones (Hanes et al., 2019). Wildfires may have contributed to the remobilization of natural (lithogenic) and anthropogenic metals in the region (Kristensen & Taylor, 2012, chapter four and six of this thesis). Our recent research has shown that wildfires had a short-term impact on local atmospheric deposition of Pb and Hg (chapter four of this thesis). That research, involving a detailed analysis of the same lake sediment cores, showed that when wildfires were close enough to impact Pb and Hg loading in the study lakes, it constituted a small addition (median 5–10% of total flux) that lasted ≤ 2 years. Yet, it is possible that the cumulative impact of multiple wildfires, as well as the impact of wildfires occurring outside the source area of macroscopic charcoals (evaluated in chapter four of this thesis), may contribute to more Pb and Hg deposition than previously estimated. Wildfire-derived deposition possibly had a larger impact on bog reconstructions of atmospheric Pb deposition because the magnitude of Pb fluxes in bogs were lower. For instance, the only bog showing an increase in Pb accumulation rate between 2000 and 2016 compared to the period from 1938 to 2000 was the TB site, which is the one site showing the greatest relative increase in charcoal accumulation over the 2000–2016 period and is a site located near three massive wildfire

scars that occurred between 1998 and 2014 (GNWT, 2018). An alternative hypothesis for the unique trend at this site is the vertical migration of ^{210}Pb in the peat profile, which could lead to underestimating the age of recent peat layers and overestimating recent Hg and Pb fluxes (Biester et al., 2007; Cooke et al., 2020). The strong correlation between bogs' average long-term accumulation rates of Pb and charcoal particles during the late-industrial (1938–2000) and recent (2000–2016) periods warrants further investigation on the importance of wildfire activity for the reconstruction of metal accumulation from bog records.

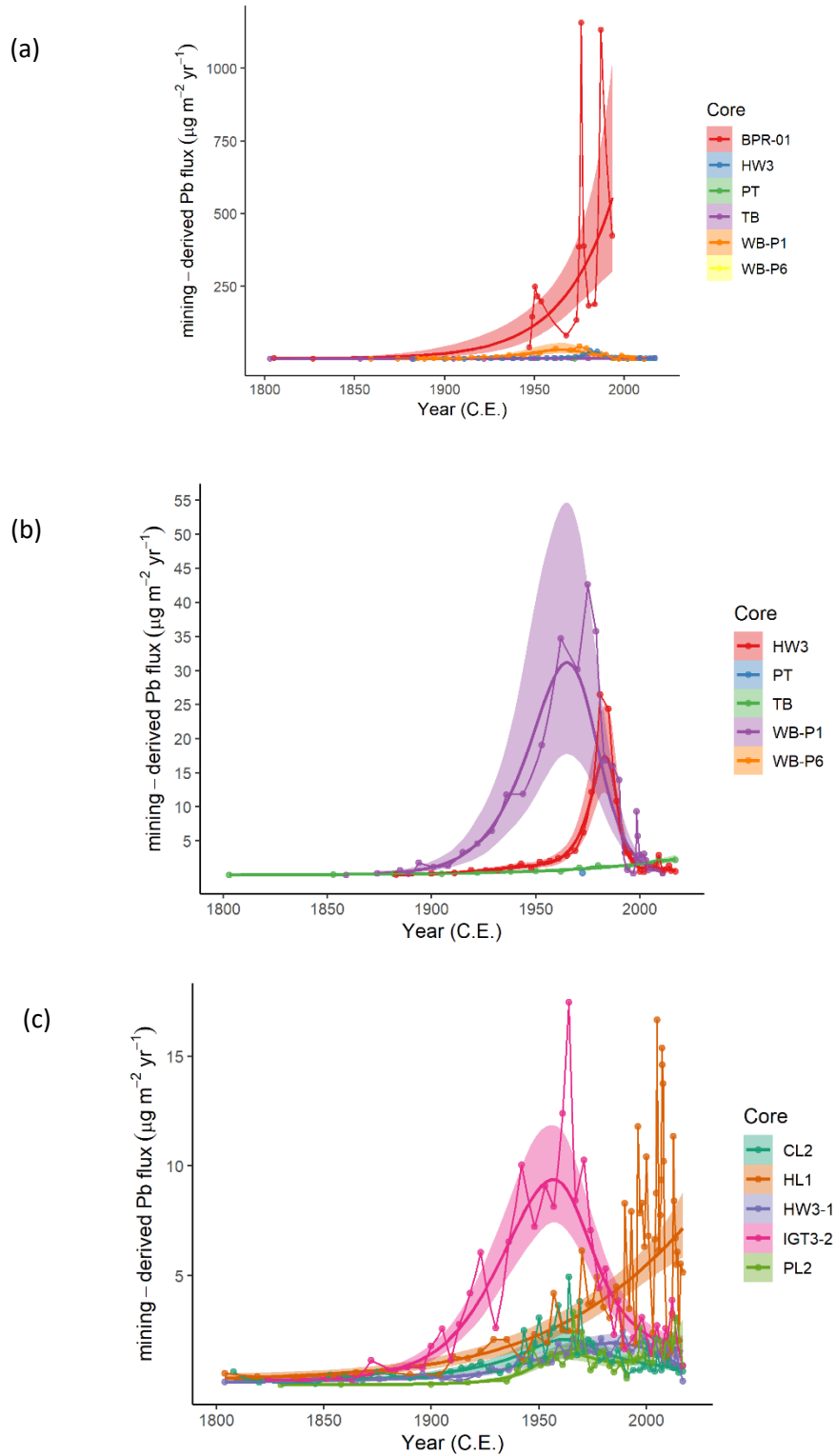


Figure 5.24: Mining-derived Pb flux in peatlands including the Giant Mine peatland (a) and excluding the Giant Mine peatland (b) and mining-derived Pb flux in lakes (c)

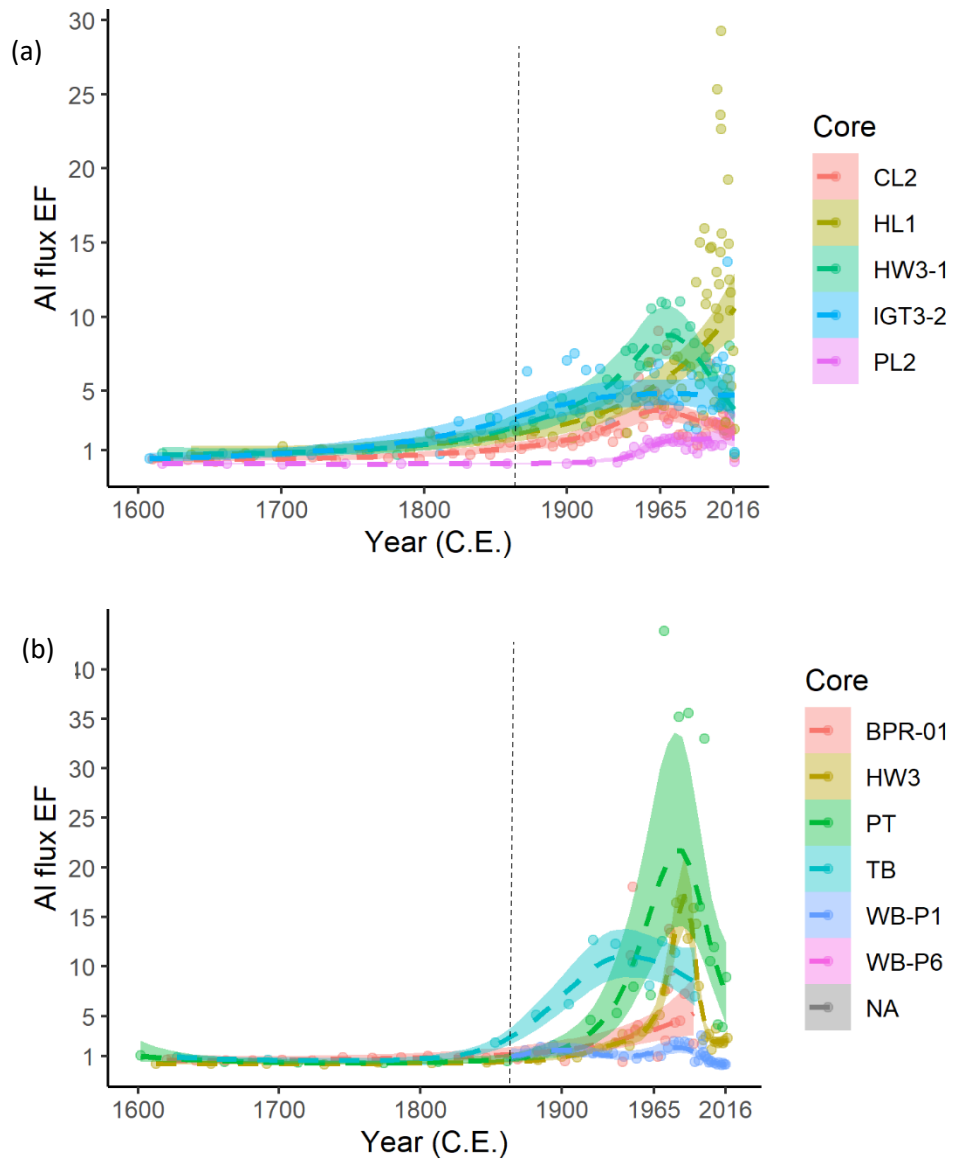


Figure 5.25: Aluminum flux enrichment in lakes (a) and peatlands (b). Enrichment factors are calculated by normalising fluxes to the pre-1800 Al accumulation rate in each core.

5.5.9 Combining peat cores and lake sediment

In this study, comparing bog and lake sediment archives allowed us to partly constrain atmospheric and catchment-based influences in the overall regional reconstruction of Pb and Hg fluxes. Combining the two types of archives in a common analysis provided more information than the mere sum of each record since each archive type is influenced by different accumulation processes (Biester et al., 2007; Cooke et al., 2020; Goodsite et al., 2013). Our analysis shows that carefully interpreted reconstructions from bogs assisted with the reconstruction of recent atmospheric trends in areas where catchment contributions to lake sediments are susceptible to have changed over time, such as the Canadian Arctic. Catchment influences in lake sediment can mask recent atmospheric trends, even when attempting to correct for variations in catchment contribution by using conservative lithogenic elements or flux deconstruction approaches. On the other hand, peat records have an inherent coarse temporal resolution because each 1 cm peat slice represents many years of accumulation, but it is hard to cut thinner peat slices in a consistent way.

5.6 CONCLUSIONS

This study explored how the individual and cumulative impacts of long-range anthropogenic pollution, local mining pollution, and catchment transport processes have affected Pb and Hg accumulation in small subarctic lakes. We show that lake sediment and bogs showed an unequivocally rapid response to increasing atmospheric pollution from local and global industrial activities, but did not all respond in the same way to the reduction in North American emissions from these same sources. The Taiga Shield lakes were particularly slow to recover, showing increases in Pb and Hg accumulation rates despite decreasing atmospheric deposition in the region. As the anthropogenic metal accumulation in Taiga Shield lakes was no longer driven by atmospheric deposition, the recent increase in lake metal accumulation must have arisen from an external factor affecting catchment contributions. Since anthropogenic Pb and Hg pollution is now ubiquitous across the world's

watersheds, it is becoming increasingly hard to distinguish in environmental archives the impact of contemporary deposition from the remobilization of legacy pollution, especially when natural processes (e.g. weathering and erosion) are changing simultaneously in response to climate. The findings in this study provide a perspective on the future recovery of subarctic lakes from anthropogenic Pb and Hg pollution which is applicable beyond the local context, given the global distribution of these pollutants. We recommend that paleoenvironmental studies aiming at reconstructing Pb and Hg cycling combine nearby lake sediment and peat archives whenever possible to deconstruct the cumulative impacts of sources and processes on metal deposition in terrestrial and aquatic environments. One crucial research question for the near future will be to identify the catchment characteristics contributing to the retention of legacy metals and those that will influence the release of these elements to aquatic ecosystems under different scenarios of climate change.

6 WILDFIRE IMPACT ON THE CATCHMENT TRANSPORT OF METALS TO SUBARCTIC MONTANE LAKES

6.1 PREFACE

More metals were transported to lakes in watersheds affected by wildfires than in undisturbed watershed because of changes in catchment soil properties following the fires. Wildfires may therefore change the rate of transport of metals in the lakes' catchment, including legacy contaminants emitted in the last centuries. This chapter will follow-up on the findings from chapter five showing that catchment retention is delaying the response of subarctic lakes to diminishing atmospheric deposition of metals, and show that wildfires may further impact the transport of natural and anthropogenic metals from burned catchments. Moreover, this study offers a rare view of decadal changes in the levels and accumulation rates of metals in subarctic montane lakes affected by wildfires that are severe, large and have a short return interval. In the current context where wildfire events of this type are predicted to become more frequent in the near future (and arguably already are), quantifying the impacts of these events on metal transport to lakes is important to predict changes at larger scale.

6.2 INTRODUCTION

Wildfire occurrence and severity will increase in many regions, including North-western Canada, in response to climate warming and the interplay between precipitation and temperature variables (Coogan et al., 2019; Krawchuk et al., 2009). Some models predict a small increase in the near-future annual burned area in Yukon, Canada (Kitzberger et al., 2017), and the fire return interval is already short in the Southern Yukon boreal forest dominated by lodgepole pines (Prince et al., 2018) . The impact of burned catchments on boreal lake geochemistry typically lasts two to three decades (Dijkstra et al., 2013; Dunnette et al., 2014), and includes greater loading of terrestrial organic matter (Dunnette et al., 2014; Leys et al., 2016; Pompeani et al., 2020), nutrients (especially phosphorus) (Paterson et al., 2002; Philibert et al., 2003; Waters et al., 2019), and metal(loid)s (Abraham et al., 2017; Chapter 4 of

this thesis). These changes can have ecological consequences on lake ecosystems including invertebrates (Garcia et al., 2007; Harper et al., 2019; Pretty et al., 2020) and fish (Garcia & Carignan, 2005; Kelly et al., 2006; Spencer et al., 2003). The release of legacy natural and anthropogenic metal contaminants from catchment soils and biomass (remobilization) by wildfire has been observed in lake sediment (Odigie et al., 2015; Odigie & Flegal, 2014) and fly ashes samples (Isley & Taylor, 2020; Wu et al., 2017). Yet, there is still little data to help us predict what the future impact of wildfires will be on the accumulation rate of metal contaminants in lakes.

The impact of wildfires on lake geochemistry should vary by physiographic region according to factors such as vegetation, hydrology, soil and topography (Harper et al., 2019; Pereira & Úbeda, 2010; Pompeani et al., 2020; Shakesby, 2011). The burn conditions, including fuel load, fire severity and extent, may also modulate the impact of wildfires on lakes geochemical fluxes and the reactivity of the elements released by wildfires (Cerrato et al., 2016; Webster et al., 2016a). More intense wildfires burn at higher temperatures, and consume more plant biomass and organic soils, therefore mobilising a wider range of elements (Bodí et al., 2014; Campos et al., 2015; Kohlenberg et al., 2018; Nzihou & Stanmore, 2013). Some elements are also volatilised by wildfires under gaseous (e.g., Hg) (Campos et al., 2015; Kohlenberg et al., 2018) or particulate forms (Bodí et al., 2014; Chapter 4 of this thesis). Severe wildfires may surpass ecological thresholds preventing the recovery of soils and vegetation (McLauchlan et al., 2020; Stevens-Rumann & Morgan, 2019). For example, a short fire-return interval of severe wildfires inhibits the regeneration of subalpine lodgepole pine (*Pinus contorta* Douglas) forests (Turner et al., 2019) and subarctic black spruce (*Picea mariana* Miller) forests (Brown & Johnstone, 2012). The impact of particularly severe wildfires or those with a short return interval on lake sediment geochemistry has been little investigated so far. Moreover, most paleolimnological analysis of wildfires in lake sediment have looked at the impact of fires over the Holocene, with little distinction between ancient fires and the recent ones. Since the geochemical cycling of multiple metal(loid)s elements was

disturbed by human activities in the last century, an analysis of the impact of recent wildfires on lakes sediment is necessary to evaluate if recent wildfires have a greater geochemical impact than ancient fires.

We measured the impact of two large wildfires that occurred approximately 20 and 40 years ago on sedimentation rates and metal loading in three lakes located 50-80 km from the historical mining town of Whitehorse, Yukon, Canada. The lakes catchments have a moderately steep topography and a large section of one lake catchment (Little Fox Lake) has never recovered ecologically from the wildfire events. This study is a rare opportunity to examine the long-term (decadal) impact of a severe wildfire on lake sediment geochemistry in a context where background levels of metal loading are high because of natural geological conditions and the legacy of mining pollution.

6.2.1 Historical wildfire activity in the study area

Severe fires occurred in the study area in 1958 (1342 km² burned) and 1998 (439 km² burned) (Figure 6.1) (Yukon Wildland Fire Management, 2014). Vegetation has only poorly recovered from the 1998 fire and the thick organic soils layers found in unburned areas offers a striking contrast with the bare mineral soils in adjacent burned slopes (Figure 6.2). Lakes catchments were affected to a varying degree by the 1958 and 1998 fires (Table 6.1). All of the Little Braeburn Lake catchment was affected by the 1958 but this catchment was spared by the 1998 fire. Fire maps indicate that Little Braeburn catchment was burned up to the shore by the 1958 fire (Figure 6.1), but the field investigation revealed no ash layer directly around the lake, suggesting that a buffer of soil and vegetation resisted the fire. Previous investigations of the 1958 wildfire have reported an uneven stand-age structure following the fire, indicative of a low intensity fire that affected the forest unevenly (Marcantonio, 2007). The Little Fox Lake catchment was partially affected by the 1958 fire (42% of the catchment area) and almost entirely affected by the 1998 fire (99% area), including a 159 km² area that burned twice over the 20 years period. There were signs of the fire directly around the lake shore, including ash and

charcoal in the nearby soil profiles. The Fox lake catchment was only partially affected by the 1958 and 1998 fires (43 and 20% area respectively), and most of the lake shore remained untouched by both fire events. Previous investigations of fire history in the area based on dendrochronology and lake sediment analysis revealed the occurrence of severe wildfires in the area in ca. 1760, 1775, 1835 and 1920 (Marcantonio, 2007).

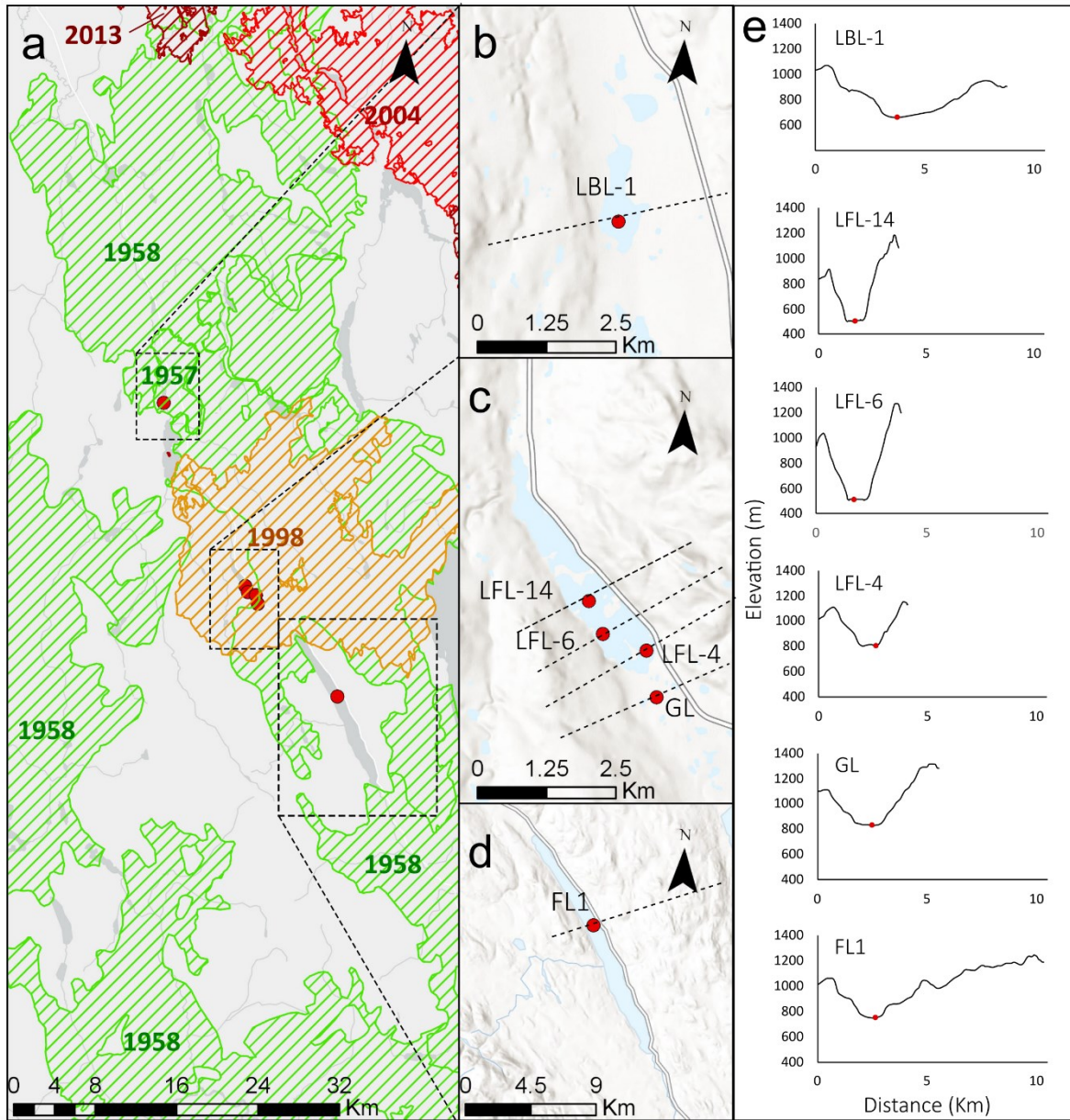


Figure 6.1: (a) Location of lake sediment core sampled in 2018. The colored polygons are the wildfire scar with the year of the fire event indicated. Second panel is a close-up view of Little Braeburn Lake (b), Little Fox Lake and GL (small wetland pond barely visible on this map), (c) and Fox Lake with surface shadowing to indicate topography with dashed line indicating the orientation of the profiles presented in (e). (e) Topographic cross-section of the valley crossing the sampling locations for each lake sediment cores.

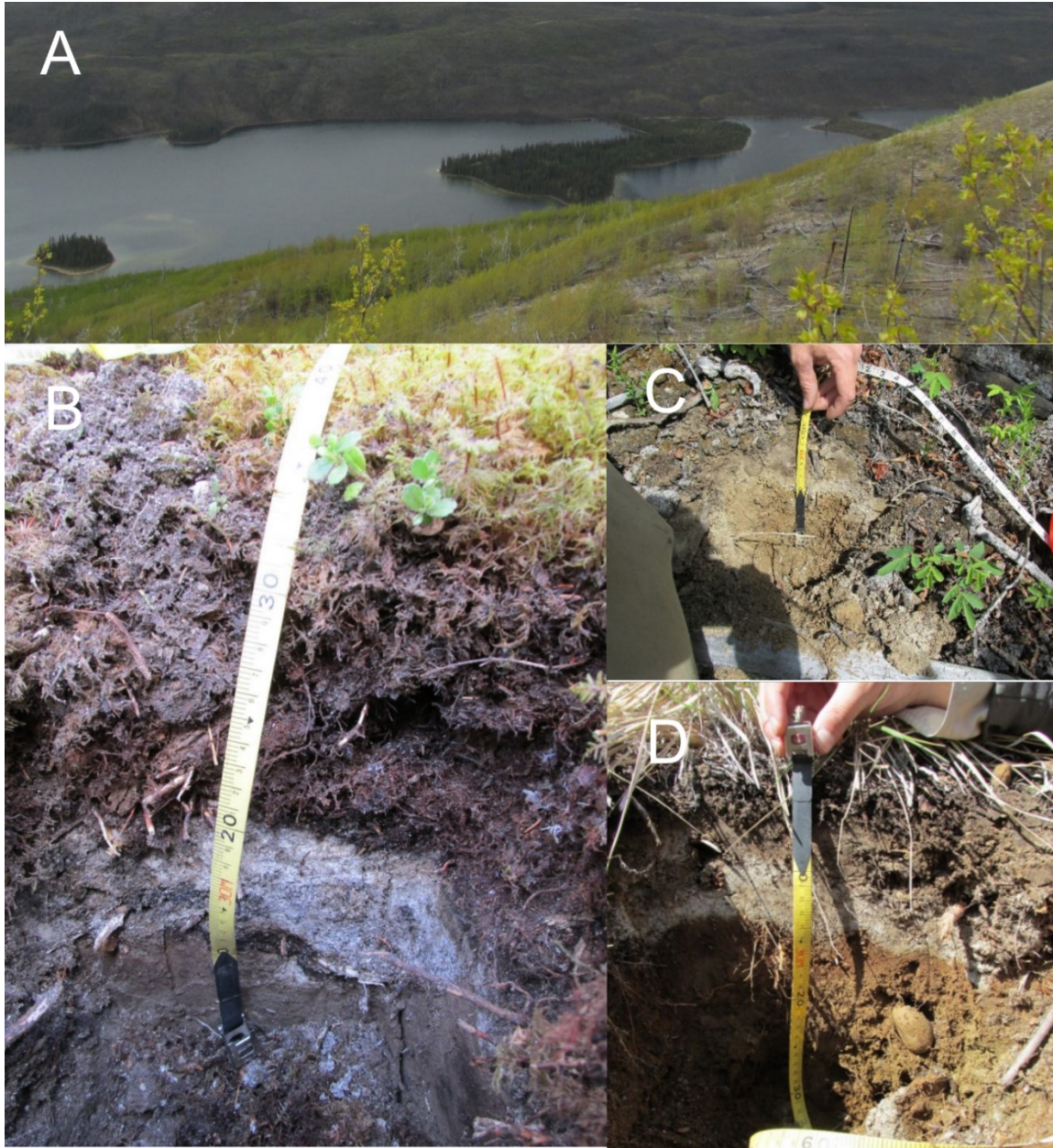


Figure 6.2: (a) view of two side of the Little Fox Lake catchment: the East side (West-South facing slope; bottom of the picture) burned twice and has little vegetation cover 20 years after the second fire event; the West side (North-East facing slope; top of the picture) burned in 1958 and vegetation recovery is evident; (b) thick (>15 cm) organic soil layer with a moss cover at the bottom of a slope that burned once in 1958; (c and d) thin organic soil layer (~5 cm) at the bottom of a slope burned twice in 1958 and 1998 near Little Fox Lake.

6.3 METHODS

6.3.1 Sampling procedures

Sediment cores were collected from a canoe in July 2018 using a UWITEC gravity corer. A total of 22 cores were collected from the deepest sections of each lake based on and handheld depth finder. Six of these cores, from four different lakes were selected for analysis, and we selected the cores from each lake that were longest and most likely to be undisturbed based on the appearance of the sediment-water interface at the time of collection. Analyzed core lengths varied between 20.5 and 33cm. Sediments were extruded from coring tubes on the same day as they were recovered from the lake and sliced into 5 mm increments except for the uppermost water sediment interface, which was sampled at a 1cm interval. Sediment samples were enclosed in whirl pack bags and weighed to obtain wet weights. Sediment samples were frozen in the field and shipped back to Carleton University, Ottawa, Canada where they were kept at 4°C until further processed. At Carleton, a 1 cm³ sub-sample of homogenized sediment from each interval of the cores were set aside for charcoal analysis. The remaining samples was freeze-dried and weighed again to obtain dry weights. Sediment density was calculated from the dry weight of the sediment divided by the volume of the sample, taking into consideration the 1 cm³ previously extracted for charcoal analysis.

6.3.2 Charcoal analysis

The 1 cm³ fresh sub-samples set aside for charcoal analysis were treated in 11% sodium hypochlorite (industrial bleach) at room temperature for 24h to make charcoal particles more distinguishable from mineral and uncharred organic matter. The solution was then filtered with a 150 µm mesh to remove smaller particles and retain macroscopic charcoals. The sediments coarser than 150 µm were carefully distributed on the mesh to avoid overlapping of particles and photographed with a Leica Si9 dissection microscope using the LAS EZ (Leica®) software at a magnification of six times. Photos were then analyzed using *Image J* software (Rasband, 1997-2018) to determine the count and surface area of

charcoal in each sample. Within *Image J*, the image brightness was manually adjusted to ensure that the charcoal were recognized by the software and distinguished from any remaining uncharred organic matter. The charcoal of each sub-sample was quantified based on three characteristics: abundance ($\#/cm^3$), cumulative area (mm^2/cm^3), and mean size of charcoal ($mm^2/ unit$). Mean charcoal size was acquired by dividing cumulative area by the abundance of the subsample. Prior to any image analysis, *Image J* was calibrated to the scope resolution ($mm/pixel$) using a 0.5 mm diameter machined pencil lead.

6.3.3 Core chronology

Chronologies for the sediment cores were developed using radiogenic lead (^{210}Pb) and the Constant Rate of Supply (CRS) model (Appleby & Oldfield, 1978). The ^{210}Pb activity was measured by alpha spectrometry in 12-15 sediment slices per core. The ^{210}Pb activity in sediment layers was interpolated following a log-linear relationship with cumulative dry sediment weight ($g\ cm^{-2}$). We used the mean of three measurements of ^{226}Ra activity by alpha spectrometry per core to estimate the supported ^{210}Pb activity in the sediment core. Measurements were conducted at Flett Research Ltd (Winnipeg MB, Canada).

6.3.4 Geochemical analysis

The dry sediment samples were analyzed for 37 elements by ICP-MS concentration and for mercury concentration in four cores using a DMA. The Hg concentrations in cores LFL-14 and LFL-6 were obtained with ICP-MS measurements only. We compared ICP-MS and DMA measurements for Hg in the four cores where both measures were obtained to ensure comparability between results (see SI). The sediment samples Hg concentration measured by both analysis ($n=103$), had $6\pm 4\%$ RSD (mean \pm standard) between methods and the differences between obtained concentrations were not significantly different (paired t-test, $p=0.78$).

For the ICP-MS measurements, sediments were digested by aqua regia and analyzed by ICP-MS following the Bureau Veritas Minerals (BVM) method AQ250. DMA measurements were conducted on a DMA-80 evo Direct Mercury Analyzer (Milestone Inc., CT, USA) on freeze-dried samples without prior digestion. A complete QA/QC analysis comprising the measurement of analytical blanks (n=6), sediment samples duplicates (n=5), standard reference material (n=8) and in-house standards (n=12) is presented in supplementary information for each analyzed element.

6.3.5 Ordination for elements concentration

We used a Principal Component Analysis (PCA) to identify the elements concentration that varied the most in lake sediments following the 1958 and 1998 wildfires and to identify regional trends in sediment metal concentration (not due to wildfires). The elements preferentially transported to lakes following the wildfires would score orthogonally to a principal component that varies distinctly in the lakes most affected by wildfire (i.e., Little Fox Lake) and with a timing that is consistent with the wildfire history. Regional trends in metal accumulation (e.g., from atmospheric deposition) are identified from principal components co-varying simultaneously in each lake, independent from wildfire exposure.

The PCA was performed on the combined data set of ICP-MS and DMA measurements along with measurements of organic matter and carbonate concentration for each layer where all these measurements were performed and above detection limit (n=67). In total, 29 elements were included in the PCA (organic matter, CaCO₃, Hg, Pb, Cd, Mo, Cu, Zn, Ag, Ni, Co, Mn, Fe, As, Sr, Sb, V, Ca, P, Cr, Mg, Ba, Ti, Al, Na, K, Sc, S, Se). The data was standardized (Z-scored) and the PCA was calculated using *SigmaPlot 14.0*. The principal components (PCs) with a eigenvalue over one are presented in the results.

6.3.6 Modelling of excess Pb, Hg and Cd

We modelled the excess Pb, Cd and Hg (from anthropogenic contaminants) in modern (post-1850) sediments using linear regressions in pre-industrial (pre-1850) sediments between the element of interest, a conservative lithogenic elements (Ti, Al, Fe or Cu) and, for Hg only, sediment organic matter. We assumed that in pre-industrial sediments, Pb and Cd were entirely derived from catchment erosion and that Hg was derived from catchment erosion and the uptake of dissolved Hg⁰ by algae. The excess concentration of Pb, Cd or Hg in sediment samples was obtained by solving Eq. 6.1.

$$\text{Eq. 6.1} \quad [Pb, Cd, Hg] = [modelled Pb, Cd, Hg] + [excess Pb, Cd, Hg]$$

Where $[Pb, Cd, Hg]$ is the concentration of Pb, Cd or Hg in a sediment sample, $[modelled Pb, Cd]$ is the predicted concentration of Pb, Cd or Hg from catchment erosion and lake production (for Hg) that is estimated from Eq.6.2 for Pb and Cd and from Eq. 6.3 for Hg. The $[excess Pb, Cd]$ is the excess concentration of Pb, Cd or Hg in the sediment sample obtained by re-arranging and solving Eq. 6.1.

$$\text{Eq. 6.2} \quad [modelled Pb, Cd] = a + b_{litho}[m_{litho}]$$

Where a and b_{litho} are, respectively, the intercept and coefficient of a linear regression between the concentration of Pb or Cd and the conservative lithogenic element that has the greatest correlation coefficient with Pb or Cd (between Ti, Al, Sc, Fe or Cu) in pre-industrial sediment. The m_{litho} variable is the concentration of the chosen conservative lithogenic element in the sediment sample. Regressions were computed for each individual core and therefore, the value a and b_{litho} varies by core (Table 6.2 and 6.3).

For Hg, we added the impact of variation in lake organic matter production to the model and the excess concentration in sediment samples was obtained by solving Eq. 6.3.

$$\text{Eq. 6.3} \quad [\textit{modelled Hg}] = a + b_{Litho}[m_{litho}] + b_{OM}[OM]$$

Where a is the intercept of a multiple linear regression with the concentration of a conservative lithogenic element in ppm (m_{litho}) and organic matter from loss-on-ignition in % (OM), b_{Litho} and b_{OM} are the regression coefficients for the predicting variables. Regressions were computed for each individual core and therefore, the values for a , b_{Litho} and b_{LOI} varies by core (Table 6.1). The values of the intercepts, variable coefficients, coefficient of determination (R^2) and p-value are presented in Table 6.1 for Hg, Table 6.2 for Pb and Table 6.3 for Cd.

Table 6.1: Intercepts \pm standard error, coefficients \pm standard error, R and p-values for linear regressions predicting the concentration of Hg (in ng g^{-1}) in the pre-industrial sediment of each lake. The Element used to estimate erosional input of the model (for Eq. 6.3) are indicated in the b_{Litho} column with units in parentheses.

Lake	Core	a intercept	b_{Litho}			b_{OM}		Regression	
			Element (unit)	coefficient	p	coefficient	p	R	p
Fox Lake	FL	37.8 ± 21.8	Ti (ppm)	110 ± 187	0.57	3.35 ± 0.90	0.004	0.77	0.01
Little Braeburn Lake	LBL	-59.5 ± 55.3	Al (%)	45.3 ± 24.6	0.08	6.04 ± 1.01	<0.001	0.79	<0.001
Little Fox Lake	LFL-4	-9.77 ± 27.2	Al (%)	78.4 ± 22.1	0.001	-0.38 ± 0.73	0.60	0.56	0.005
	LFL-6	-7.592 ± 28.0	Ti (ppm)	1510 ± 412	0.001	0.93 ± 1.28	0.47	0.62	0.002
	LFL-14	2.8 ± 15.7	Ti (ppm)	1744 ± 267	<0.001	0.90 ± 0.95	0.35	0.79	<0.001

Table 6.2: Intercepts \pm standard error, coefficients \pm standard error, R and p-values for linear regressions predicting the concentration of Pb (in $\mu\text{g g}^{-1}$) in the pre-industrial sediment of each lake. The Element used to estimate erosional input of the model (for Eq. 6.2) are indicated in the b_{Litho} column with units in parentheses.

Lake	Core	a intercept	b_{Litho}			Regression	
			Element (unit)	coefficient	p	R	p
Fox Lake	FL	6.14 ± 1.20	Sc (ppm)	0.53 ± 0.18	0.01	0.64	0.01
Little Braeburn Lake	LBL	-3.59 ± 2.27	Al (%)	9.8 ± 1.3	<0.001	0.92	<0.001
Little Fox Lake	LFL-4	0.12 ± 3.15	Al (%)	7.37 ± 2.46	0.01	0.63	0.01
	LFL-6	-2.71 ± 1.19	Al (%)	8.91 ± 0.82	<0.001	0.90	<0.001
	LFL-14	-3.21 ± 1.03	Al (%)	10.02 ± 0.68	<0.001	0.90	<0.001

Table 6.3: Intercepts \pm standard error, coefficients \pm standard error, R and p-values for linear regressions predicting the concentration of Cd (in $\mu\text{g g}^{-1}$) in the pre-industrial sediment of each lake. The Element used to estimate erosional input of the model (for Eq. 6.2) are indicated in the b_{Litho} column with units in parentheses.

Lake	Core	a	b_{Litho}		Regression	
		intercept	Element (unit)	coefficient	R	p
Fox Lake	FL	458 ± 194	Cu (%)	14.7 ± 32.9	0.78	<0.001
Little Braeburn Lake	LBL	266 ± 442	Fe (%)	0.018 ± 0.014	0.37	0.21
Little Fox Lake	LFL-4	16.7 ± 64.5	Cu (%)	7.58 ± 1.12	0.80	<0.001
	LFL-6	27.4 ± 168	Cu (%)	8.62 ± 2.99	0.49	0.008
	LFL-14	-0.49 ± 0.11	Al (%)	0.70 ± 0.07	0.85	<0.001

We also evaluated the proportion of Pb, Cd or Hg concentration that was predicted by variation in erosion-derived element (m_{litho}) using Eq. 6.4 and by variation in sediment organic matter (OM) using Eq. 6.5.

$$\text{Eq. 6.4} \quad [Pb, Cd, Hg \text{ from erosion}] = \frac{b_{litho}[m_{litho}]}{[Pb, Cd, Hg] - a} \times [Pb, Cd, Hg]$$

$$\text{Eq. 6.5} \quad [Hg \text{ from OM}] = \frac{b_{OM}[OM]}{[Hg] - a} \times [Hg]$$

6.3.7 Geochemical fluxes calculation

The fluxes of each analyzed element, including organic matter and carbonates (excluding charcoals), were calculated following equation 6.6:

Eq.6.6

$$f_m = \frac{SR \times [m]}{FF}$$

Where f_m is the flux of a metal m ($\mu\text{g m}^{-2} \text{yr}^{-1}$), $[m]$ is the metal m concentration ($\mu\text{g g}^{-1}$), SR is the modelled sedimentation rate (or mass accumulation rate) for the layer ($\text{g m}^{-2} \text{yr}^{-1}$) obtained from the CRS model and FF is the sediment focusing factor (Blais & Kalff, 1995; Lehman, 1975), estimated as

the ratio of regional atmospheric ^{210}Pb fallout to the observed unsupported ^{210}Pb flux at the sediment-water interface (Blais & Kalff, 1995; Muir et al., 2009; Wiklund et al., 2017). The local atmospheric ^{210}Pb deposition rate was estimated using the value from the formula developed by Muir et al. (2009).

In Eq. 6.6, $[m]$ can be substituted for the specific concentration predicted by catchment erosion (from Eq. 6.4), sediment organic matter (from Eq. 6.5) or excess (from solving Eq. 6.1) to obtain the corresponding component flux.

6.4 RESULTS

6.4.1 Fire exposure in each lake

Spikes in charcoal accumulation rates (CHAR) agreed with the known fire history of the area, but the magnitude of CHAR was 10-50 times in Little Fox Lake than in Fox Lake or Little Braeburn Lake. The small CHAR observed in Fox Lake (Figure 6.3a) agreed with the limited burned area in this lake's catchment indicated in the historical fire maps (Figure 6.1). In contrast, the small CHAR observed in the Little Braeburn Lake sediment was surprising since historical fire maps suggested that all of Little Braeburn Lake catchment burned between 1957 and 1958. For sure, the Little Braeburn Lake's catchment was not burned during the 1998 and yet, this fire event was recorded in Little Braeburn Lake sediment as a peak in CHAR of similar magnitude to the 1957-1958 wildfire (Figure 6.3c). The short duration of the CHAR peaks in the Little Braeburn Lake sediment are typical of primary charcoal transport (atmospherically deposited) rather than catchment transport (Higuera et al., 2007; Peters & Higuera, 2007). Therefore, Fox Lake and Little Braeburn Lake likely received primary charcoals from wildfire fallouts during both the 1957-1958 and 1998 wildfires, but little to no charcoals from catchment surface erosion. Little Fox Lake contrasts with Fox Lake and Little Braeburn Lake because the magnitude and aspect of peaks in CHAR clearly indicate that charcoals were mostly transported by catchment erosion in the years following the fire. Using macroscopic charcoals as a proxy for the

presence of wildfire-derived material in lake sediment, Little Fox Lake shows the greatest exposure to wildfires by far, followed by Little Braeburn Lake where CHAR is low but a large catchment surface was affected and Fox Lake is a control site with negligible fire impact.

Table 6.4: Lake surface area with lake catchment area and surface burned during the 1957-1958 and 1998 fires.

Lake	Lake surface (km ²)	Direct watershed size excluding lake area (km ²)	Watershed area: Lake area ratio	Water depth at coring location (m)	Burned area 1957-1958			Burned area 1998		
					km ²	(%) Watershed affected	(%) Lake shore affected	km ²	(%) Watershed affected	(%) Lake shore affected
LBL	0.71	70	98	22	70	100	100%*	0	0	0%
LFL	1.13	376	333		159	42	0%	372	99	100%
	(4)			26						
	(6)			17						
	(14)			26						
GL	0.01	unknown	unknown	6	-	100	100%	-	100	100%
FL	14.55	910	63	44	296	33	5%	118	13	3%

*Historical fire maps suggest the lake shore burned but field investigation revealed no sign of a fire event in the lake shore soil profiles.

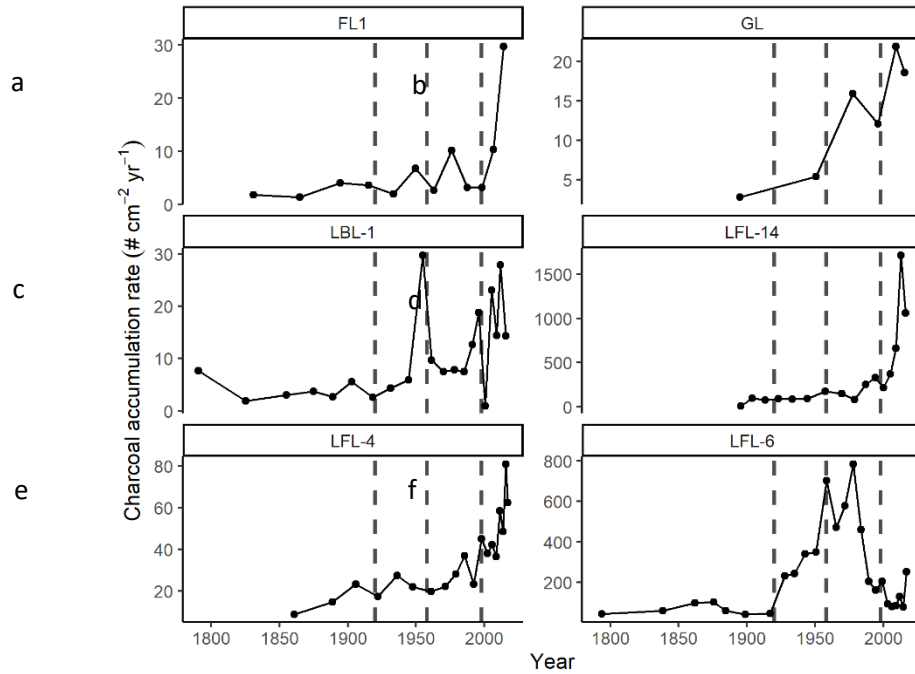


Figure 6.3: Focusing-factor-corrected charcoal accumulation rates in lake sediment cores FL1 (a), LBL1 (b), LFL-4 (c), GL (d), LFL-14 (e) and LFL-6 (f). The vertical dashed lines represent the years of major fires in the study area (1920, 1957 and 1998). Note the large difference in y-axis scales between lakes.

6.4.2 Variation in sedimentation rate

Sedimentation rates were similar between sediment cores from the earliest modelled period (~1850) until the early 20th century ($60 \pm 35 \text{ g m}^{-2} \text{ yr}^{-1}$), after which sedimentation rates doubled in Little Fox Lake and Fox Lake but remained constant in Little Braeburn Lake (Figure 6.4). The 1957-1958 wildfires triggered a small increase in Little Braeburn Lake sedimentation rate (Figure 6.4), that was mostly associated with greater organic matter accumulation rate in this lake. The 1958 wildfire also initiated an important increase in Little Fox Lake sedimentation rate (Figure 6.4). The following wildfire (in 1998) severely affected the Little Fox Lake catchment and caused further increase in this lake's sedimentation rates that persisted for the remaining of the sediment record (Figure 6.4). To the contrary, sedimentation rate in Little Braeburn Lake (unaffected by the 1998 wildfire) continued to increase following the pre-wildfire rate and Fox Lake sedimentation rate slightly decreased over the same period (Figure 6.4). Compared to the pre-1900 sedimentation rate, the recent sedimentation rate is about two and three folds higher in Little Braeburn Lake and Fox Lake respectively ($120\text{-}175 \text{ g m}^{-2} \text{ yr}^{-1}$). In contrast, in Little Fox Lake, with the largest burned area in the catchment for both fire events, sedimentation rates are five to eight folds higher ($300\text{-}500 \text{ g m}^{-2} \text{ yr}^{-1}$).

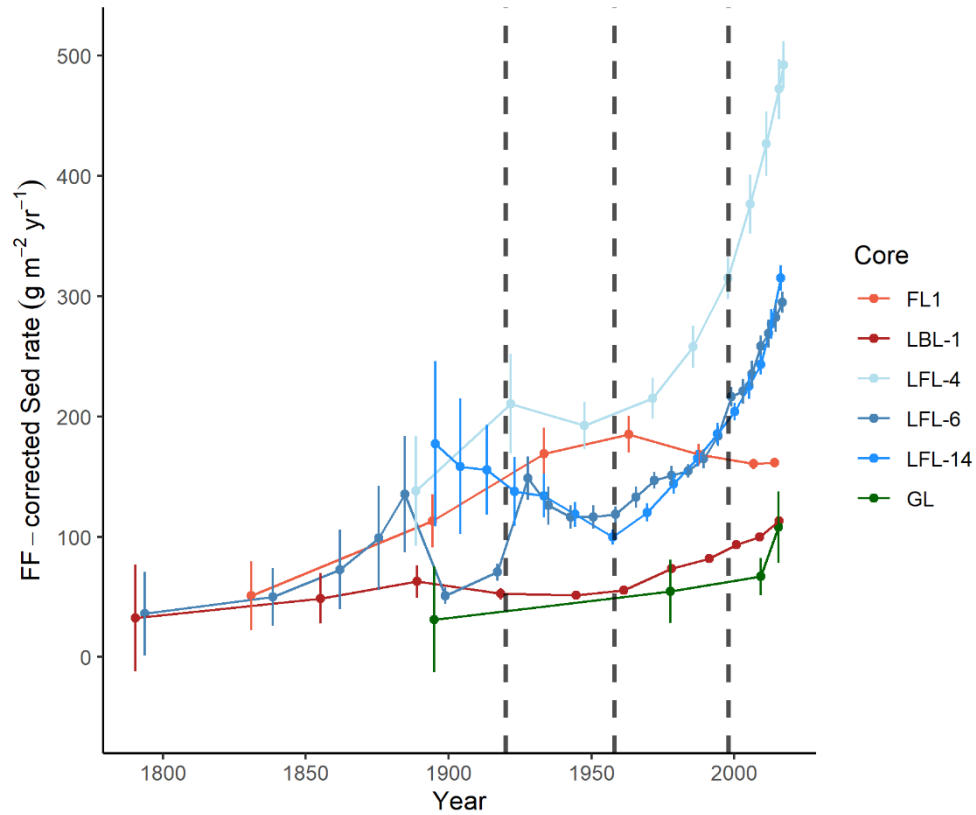


Figure 6.4: Modelled sedimentation rate (CRS model) and uncertainties against time in each core. The vertical dashed lines represent the occurrence of known wildfires events in the study area.

6.4.3 Principal component analysis for sediment geochemistry

The principal component analysis returned five significant (eigenvalues > 1) components together explaining 86% of the variation in sediment concentration of the 29 studied elements. We focused on the first four components of this analysis for our interpretation, which represented 77% of the variation in sediment composition. The PC1 was scoring positively for a large range of base metals including (Co < Al < Ag < Zn < Fe) and had no important negatively scoring elements (Table 6.5). The PC2 loading was positively scoring for organic matter and metals preferentially binding to organic matter (rather than oxy-hydroxides) in lake sediments (Feyte et al., 2010) (Cd < Hg < Se < Sr), and scored negatively for the terrigenous metals Ti (Table 6.5). The PC2 vary both by site and over time (Figure 6.5 and 6.6). The PC2 increased with time in Little Fox Lake and Little Braeburn Lake, whereas it remained stable in Grayling Lake and decreased with time in Fox Lake (Figure 6.6). The PC3 does not vary significantly with sediment age in each core and separates sediment records by site (Figure 6.7). The PC3 component scored positively for CaCO₃, Ca, K and Sc, and negatively for Ni, Mn, As and Sb (Table 6.5). The PC4 scored positively for Cu, Sc and S and negatively for Pb, Sr and Ca (Table 6.5). The PC4 component scores are similar between sites and follow a common decreasing trend from ca. 1920 onward (Figure 6.6). The PC5 was scoring positively for redox-sensitive elements in lake sediments (Outridge & Wang, 2015) and negatively, Hg, Sc, organic matter, that are particularly stable in lake sediments (Table 6.5).

Table 6.5: Components loading for PCA. Values over 0.5 and under -0.5 are highlighted in green and red respectively.

	PC1	PC2	PC3	PC4	PC5
Org.M.	-0.24	0.74	0.26	0.23	-0.45
CaCO3	0.01	0.29	0.56	-0.01	0.33
Mo	0.05	0.47	0.14	0.05	0.74
Cu	0.23	0.45	0.05	0.67	-0.42
Pb	0.53	0.22	-0.04	-0.57	-0.10
Zn	0.84	0.39	0.23	0.08	0.09
Ag	0.83	0.38	-0.23	-0.03	-0.07
Ni	0.69	-0.14	-0.53	0.23	-0.24
Co	0.89	0.07	0.06	0.21	0.28
Mn	0.69	0.17	-0.56	-0.14	0.02
Fe	0.80	-0.16	-0.03	0.19	0.48
As	0.16	0.01	-0.54	0.32	0.63
Sr	0.37	0.55	0.08	-0.66	0.05
Cd	0.25	0.79	0.28	0.40	-0.17
Sb	0.59	0.09	-0.55	0.32	-0.26
V	0.86	-0.37	-0.13	0.16	0.04
Ca	-0.17	0.49	0.54	-0.50	0.08
P	0.71	0.21	-0.47	-0.38	-0.09
Cr	0.78	-0.43	0.29	-0.03	-0.11
Mg	0.78	-0.52	0.23	-0.15	-0.06
Ba	0.78	0.25	-0.12	-0.38	0.07
Ti	-0.04	-0.80	0.47	0.11	0.09
Al	0.85	-0.30	0.31	0.23	0.03
Na	0.32	-0.48	0.45	-0.29	-0.08
K	0.64	-0.38	0.61	-0.02	0.03
Sc	0.42	-0.27	0.57	0.49	-0.28
S	-0.33	0.39	0.04	0.48	0.63
Se	0.51	0.63	0.47	0.00	0.17
Hg_Best	0.29	0.77	0.24	0.07	-0.32

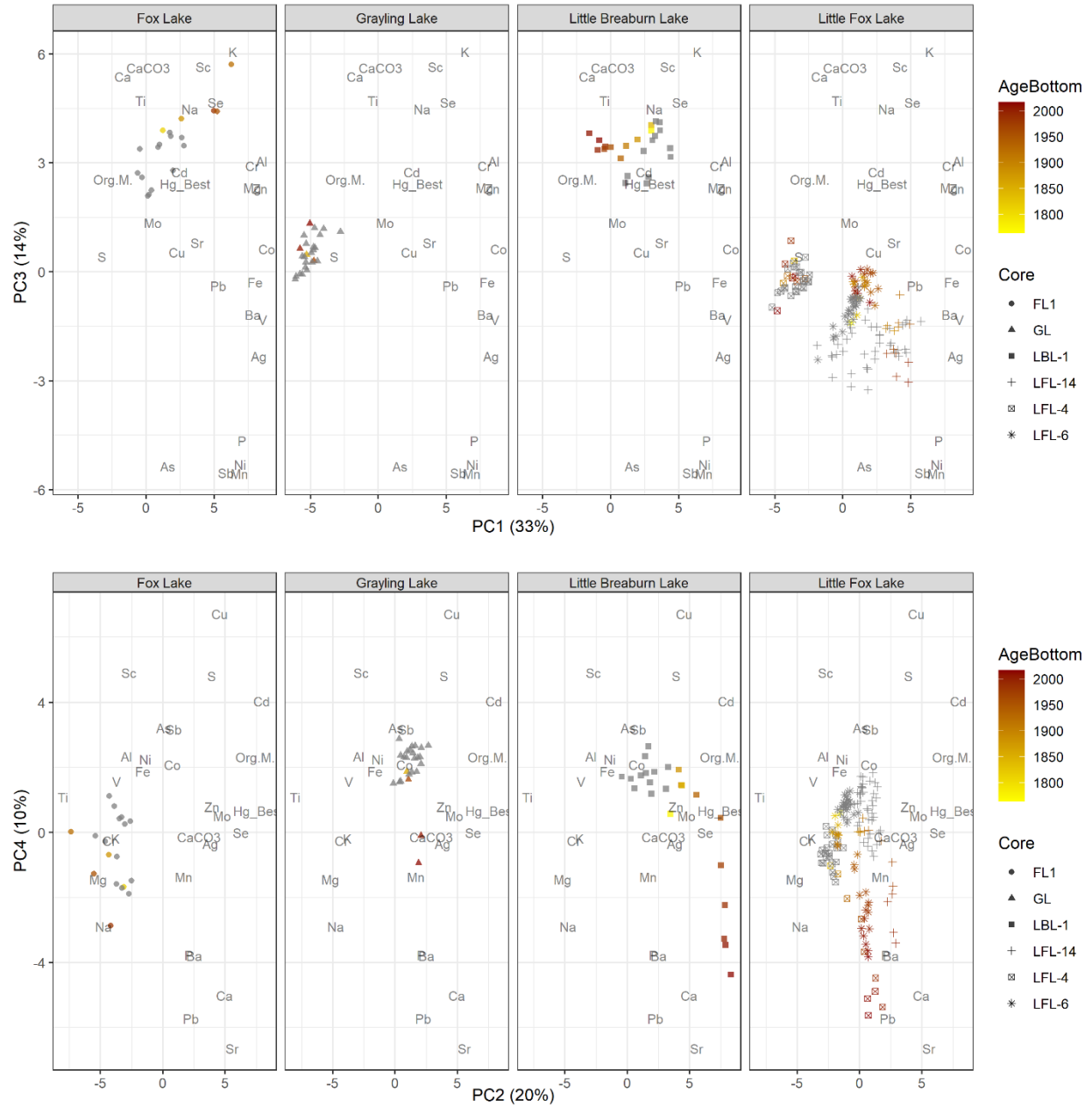


Figure 6.5: Principal components scores for sediment samples plotted as (a) PC1 vs. PC2 and (b) PC3 vs. PC4. Word labels are the component loading scores for elements (multiplied by 10), points shape indicates different cores and color indicates the modelled age of the sediment layers, correspond to undated layers at the bottom of the cores, which correspond to pre-industrial samples.

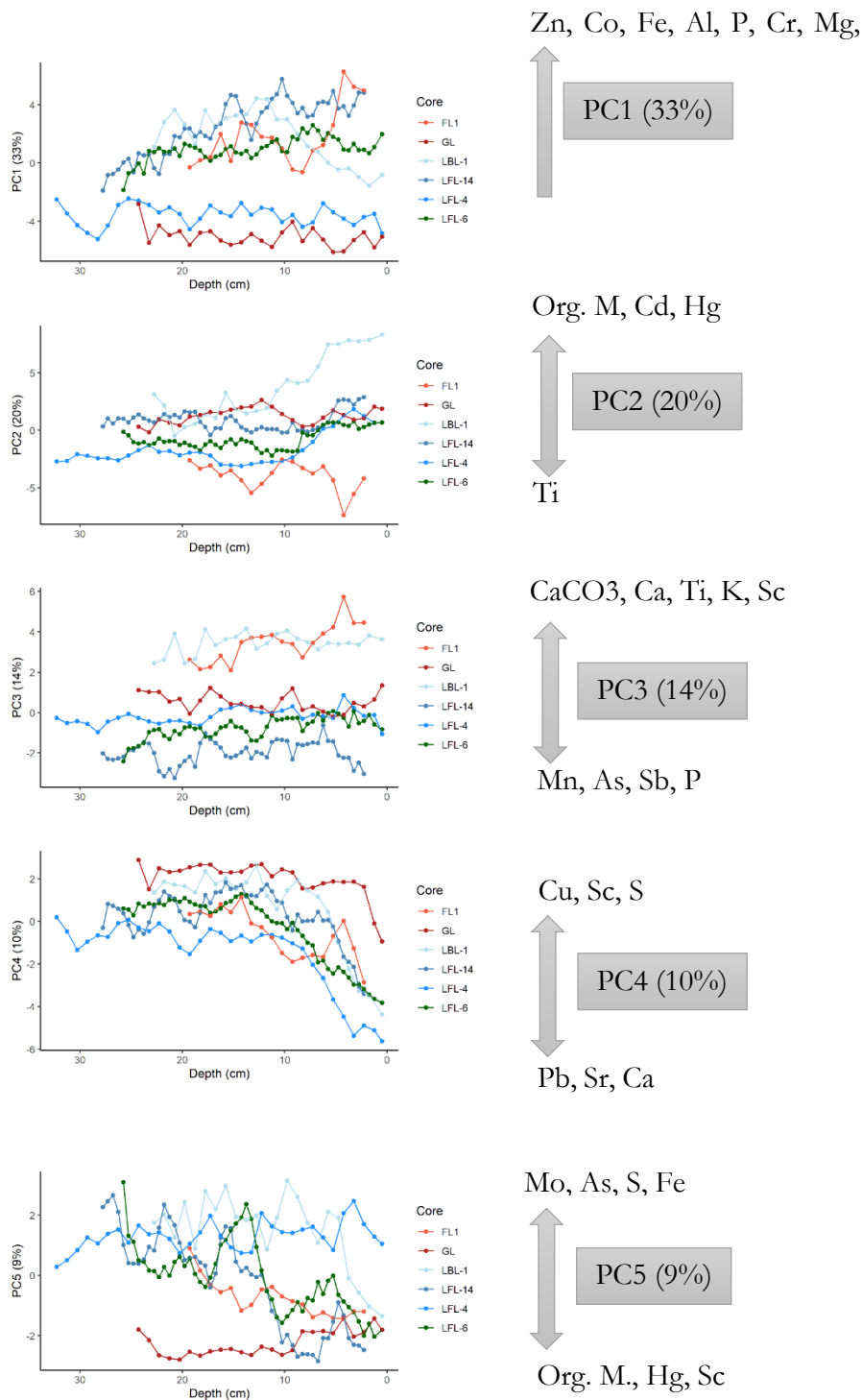


Figure 6.6: Principal components scores for sediment metal concentration and organic matter (Org. M.), by site and **by sediment depth**. Elements indicated on the right side of the graphs are the most important component loadings orthogonal to this principal component, with negatively scoring elements in the low y-axis values (below the arrow) and positively scoring elements in the high y-axis values (above the arrow).

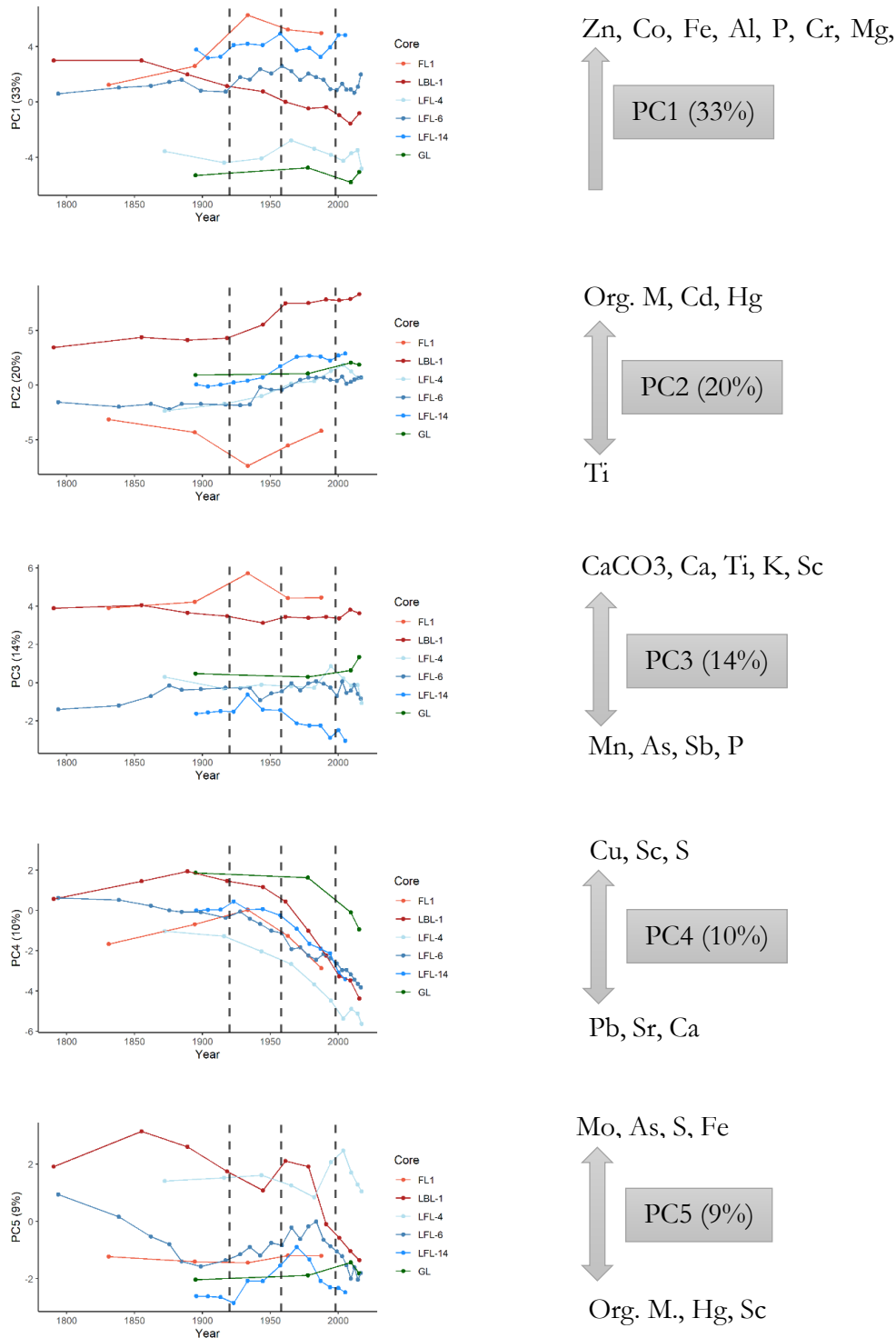


Figure 6.7: Principal components scores for sediment metal concentration and organic matter (Org. M.), by site and **by sediment age**. The dashed lines represent the years of occurrence of known fire events (1958 and 1998). Elements indicated on the right side of the graphs are the most important component loadings orthogonal to this principal component, with negatively scoring elements in the low y-axis values (below arrow) and positively scoring elements in the high y-axis values (above arrow).

From our interpretation, PC1 and PC3 represents the loading of the main mineral constituents from catchment soils (feldspar, other aluminosilicates and carbonates; Ti, Al, Fe, Sc, Ag, Zn, Ni, Cr, Mg, Ca, Na, CaCO₃), PC2 represents the loading of organic matter and associated constituents (from catchment and in-lake production; OM, Hg, Cd, Se, Sr) and PC4 represents the impact of regional atmospheric deposition (Pb, Sr, Ca, Ba). In Little Fox Lake, the occurrence of wildfires corresponds to a marked decrease in PC4 indicating particularly important concentration of Pb, Sr, Ba, Mn and Ca and lower concentration of terrigenous metals (Al, Ti, Sc, Cu, Fe). In Little Fox Lake and Little Braeburn Lake, post-wildfire samples also have higher PC2 scores (Figure 6.7), indicating greater concentration of organic matter, Cd and Hg.

6.4.4 Concentration of Hg, Pb and Cd in lake sediment

There were variations in sediment metal concentrations occurring both in the dated and undated portion of each core (Figure 6.8) and these variations confirmed trends observed in the PCA. The concentration of Hg in lake sediment has increased by 40-100 ng g⁻¹, representing a 40-80% increase over time compared to baseline concentration (Figure 6.8). There was a clear sub-surface peak in Pb concentration in Fox Lake and Little Fox Lake (not Little Braeburn Lake), with Pb concentrations remaining 7-10 mg g⁻¹ above background value (75-120% increase) until the end of the record in 2018. The concentration of Cd increased by 0.2 mg g⁻¹ (20% increase) in Little Braeburn Lake and one core from Little Fox Lake (LFL-14) but remained stable or slightly decreased in Fox Lake and two other cores from Little Fox Lake (Figure 6.8). Elements that scored with high positive on PC5 (Mn, Mo, As, S, Fe) had high concentration near the surface (top 1.5 cm) of core FL1, likely has a result of post-deposition mobilisation by changes in redox conditions because these are redox-sensitive elements.

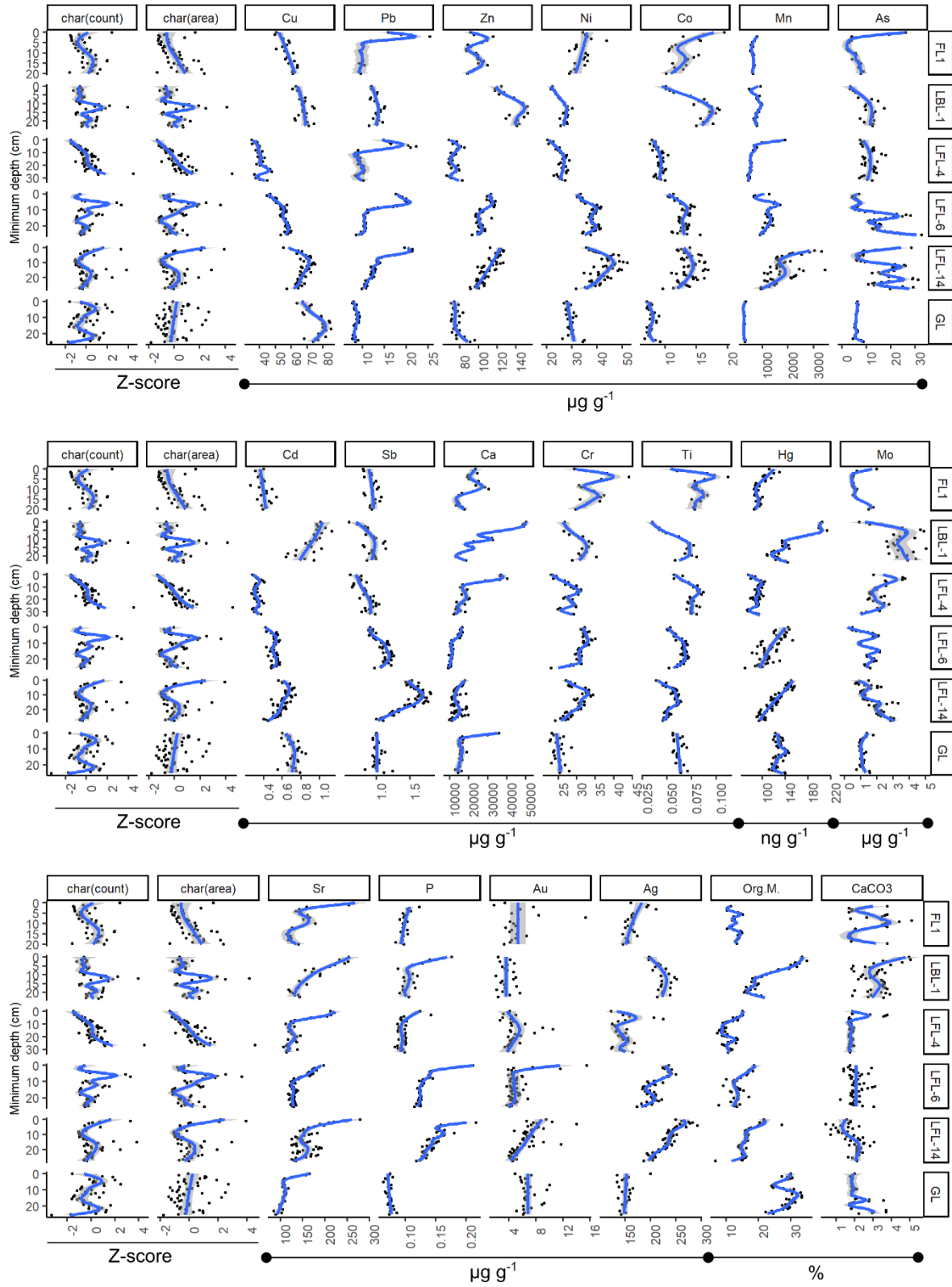


Figure 6.8: Element concentration profile by depth in each Yukon lake sediment core with charcoal concentration normalised (z-scored) by core.

The sediment concentrations of Cu, Pb, Zn and As was high compared to reported concentration of these elements in bedrock samples from nearby boreholes (Table 6.4). Some sediment samples from Little Fox Lake and Little Braeburn Lake were over the CCME Interim Sediment Quality Guideline for Cr, Hg, Cd and Zn but concentrations were always below the Probable Effect Level reported by the CCME.

Table 6.6: Mean \pm standard deviation of concentration of selected metals in each core compared to reported values for rock samples from a few nearby boreholes (Yukon Geological Survey, 2020)

Lake sediment cores	Cu (ppm)	Pb (ppm)	Zn (ppm)	As (ppm)	Cd (ppm)	Cr (ppm)	THg (ppb)
FL1	57.52 \pm 4.2 (63.8)	11.78 \pm 4.23 (25.34)	97.94 \pm 8.25 (115.4)	6.73 \pm 5.79 (26)	0.39 \pm 0.06 (0.54)	34.28 \pm 3.63 (44.1)	96.52 \pm 10.75 (129.87)
GL	75.67 \pm 6.08 (84.91)	8.45 \pm 0.48 (9.36)	76.81 \pm 6.08 (95.5)	5.98 \pm 0.84 (8.8)	0.71 \pm 0.07 (0.85)	25.05 \pm 1.49 (28.5)	128.72 \pm 8.09 (146.06)
LBL-1	67.27 \pm 3.79 (74.62)	13.18 \pm 0.99 (15.06)	138.1 \pm 11.12 (152.7)	9.95 \pm 3.76 (17.2)	0.92 \pm 0.12 (1.13)	30.4 \pm 2.63 (35.3)	156.74 \pm 32.87 (213.32)
LFL-14	66.92 \pm 4.1 (74.95)	13.57 \pm 3.2 (21.39)	109.85 \pm 10.1 (126.9)	16.53 \pm 7.31 (31.1)	0.6 \pm 0.08 (0.74)	29.87 \pm 2.52 (34.4)	121.73 \pm 19.8 (156)
LFL-4	40.59 \pm 3.11 (47.64)	11.39 \pm 3.97 (22.25)	73.68 \pm 4.53 (84.6)	10.94 \pm 2.73 (17.8)	0.33 \pm 0.04 (0.41)	27.65 \pm 2.2 (31.1)	89.39 \pm 7.09 (104)
LFL-6	54.43 \pm 3.62 (59.69)	13.34 \pm 4.13 (20.79)	105.46 \pm 6.67 (117.8)	12.74 \pm 7.19 (32.5)	0.51 \pm 0.04 (0.57)	31.21 \pm 1.9 (35)	114.63 \pm 18.62 (153)
Boreholes (rock type)	Cu (ppm)	Pb (ppm)	Zn (ppm)	As (ppm)	Cd (ppm)	Cr (ppm)	THg (ppb)
06MC115-1 (rhyolite)	-	13	40	7	-	20	-
06GGA158-1 (dacite)	10	27	250	-	-	40	-
CDB-10-102 (quartz monzonite)	1	14	24	0.5	-	10	-
15PS- 087 (granite)	0	15	60	-	-	40	-
15PS- 090 (granodiorite)	0	10	40	-	-	40	-
CDB-10-101 (granodiorite)	4	8	36	0.8	-	10	-
14-SI-167-1 (andesite)	-	11	80	16	-	30	-
17EB-111-1 (volcanic matrix)	50	0	60	0	-	200	-
17EB-178-1 (volcanic matrix)	50	0	100	0	-	660	-
16EB-474-1 (gabbro)	170	6	80	0	-	230	-

6.4.5 Changes in geochemical fluxes after wildfires

Most metals analysed in this study had increasing fluxes over time in lake sediments, especially over the last 60 years (Figure 6.9), and mostly in response to increasing sedimentation rates (Figure 6.4). For the elements most strongly associated with PC2 and PC4 (including Cd, Hg, Pb, Ca and Sr), increasing fluxes were also attributable to a widespread increase in the concentration of these elements in the sediments. Other metals tended to decrease in concentration following wildfire, and that dampened the fluxes of these metals caused by greater sedimentation rates.

The pre-industrial (pre-1850) fluxes of Pb, Hg and Cd were small and comparable between all sites (Figure 6.9). The 1958 wildfire is concurrent with excess metal fluxes to the lakes of $11 \pm 10 \mu\text{g Hg m}^{-2} \text{yr}^{-1}$ (max $29 \mu\text{g Hg m}^{-2} \text{yr}^{-1}$), $1.8 \pm 1.1 \text{ mg Pb m}^{-2} \text{yr}^{-1}$ (max $2.9 \text{ mg Pb m}^{-2} \text{yr}^{-1}$), $57 \pm 66 \mu\text{g Cd m}^{-2} \text{yr}^{-1}$ (max $187 \mu\text{g Cd m}^{-2} \text{yr}^{-1}$) and $19 \pm 15 \text{ mg Ag m}^{-2} \text{yr}^{-1}$ (max $42 \text{ mg Ag m}^{-2} \text{yr}^{-1}$). The 1998 fire had a larger impact on metal fluxes, being concurrent with excess fluxes of $25 \pm 18 \mu\text{g Hg m}^{-2} \text{yr}^{-1}$ (max $58 \mu\text{g Hg m}^{-2} \text{yr}^{-1}$), $3.2 \pm 1.7 \text{ mg Pb m}^{-2} \text{yr}^{-1}$ (max $5.1 \text{ mg Pb m}^{-2} \text{yr}^{-1}$), $107 \pm 102 \mu\text{g Cd m}^{-2} \text{yr}^{-1}$ (max $306 \mu\text{g Cd m}^{-2} \text{yr}^{-1}$) and $32 \pm 17 \text{ mg Ag m}^{-2} \text{yr}^{-1}$ (max $55 \text{ mg Ag m}^{-2} \text{yr}^{-1}$).

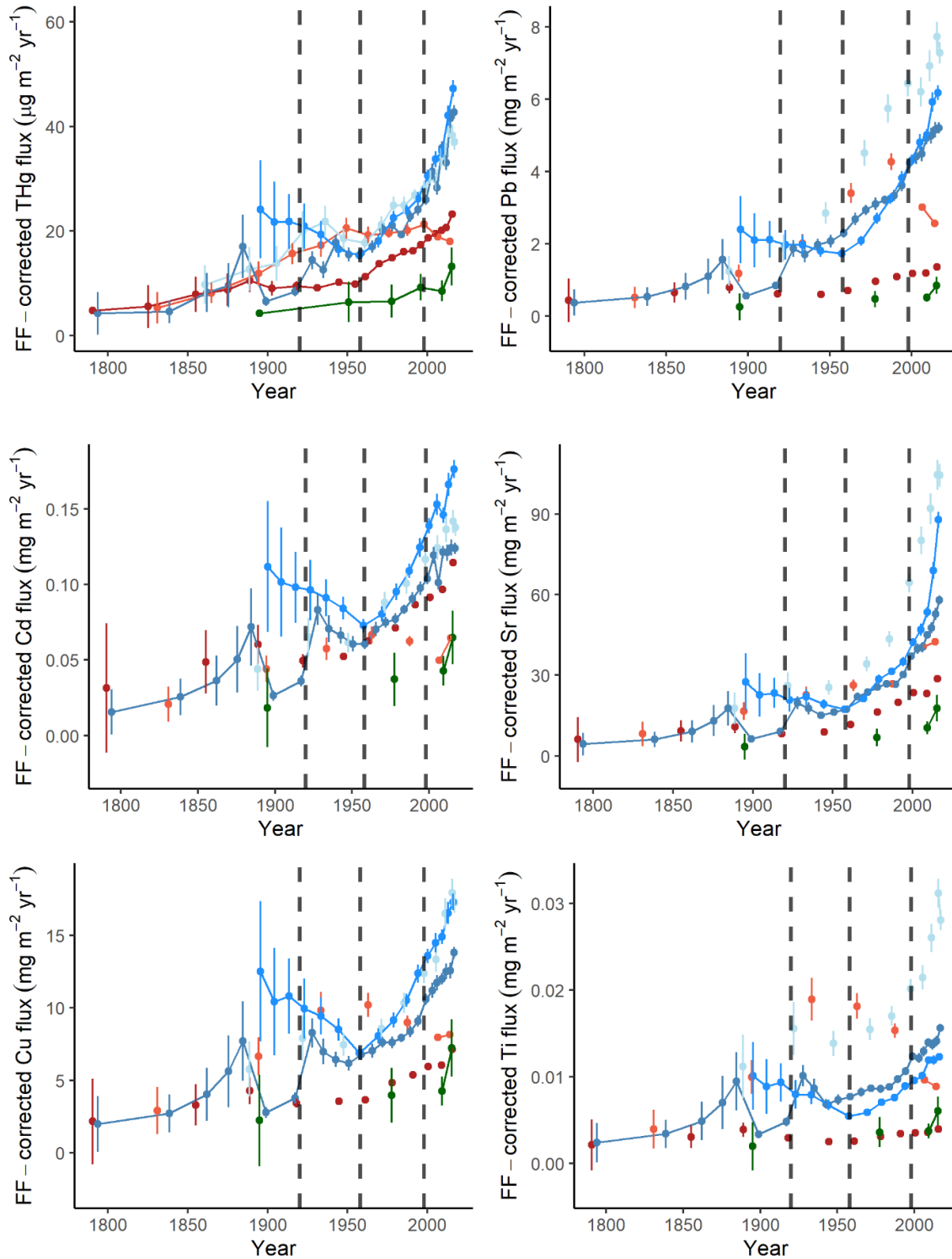


Figure 6.9 Modelled fluxes corrected for sediment focusing and uncertainties for six metals. Vertical dashed lines represent the occurrence of known wildfire events in the study area in 1920, 1958 and 1998.

The greatest increase in all analysed metals accumulation rate over time, including Hg, Pb and Cd, occurred in Little Fox Lake (Figure 6.8). The timing of the variation, as well as the co-occurring changes in charcoal accumulation rate, clearly demonstrates that the increase in metal accumulation rate was initially caused by the occurrence of the two wildfires. However, Little Fox Lake sedimentation rate and metal accumulation rate continued to increase over the twenty years that followed the fire instead of gradually returning toward pre-fire accumulation rate. In contrast, Fox Lake had no visible increase in metal accumulation that co-occurred with wildfires (Figure 6.9).

The accumulation rate of Pb in the most recent section of the records (2008-2018) was three to five times greater in Little Fox Lake ($5-8 \text{ mg Pb m}^{-2} \text{ yr}^{-1}$) than in Fox Lake ($2-3 \text{ mg Pb m}^{-2} \text{ yr}^{-1}$) and Little Braeburn Lake ($1-2 \text{ mg Pb m}^{-2} \text{ yr}^{-1}$). Similarly, the recent Hg accumulation rates in Little Fox Lake ($40 \mu\text{g Hg m}^{-2} \text{ yr}^{-1}$) were twice the accumulation rate in Fox Lake and Little Braeburn Lake ($\sim 20 \mu\text{g Hg m}^{-2} \text{ yr}^{-1}$). The same was true for most metal elements, i.e., accumulation rates were 2-5 times greater in Little Fox Lake compared to Fox Lake and Little Braeburn Lake.

6.4.6 Modelling of excess Hg, Pb and Cd in the sediments

Most variations in Hg, Pb and Cd metal fluxes that were associated with wildfire events were caused by erosional fluxes (Figures 6.10 to 6.12). Excess fluxes, i.e., those not predicted by changes in lithogenic (erosional) fluxes or organic matter inputs (for Hg) also contributed to a significant proportion of the increase in the accumulation rate of Hg (Figure 6.10) and Pb (Figure 6.11) but were very small for Cd (Figure 6.12). Excess Hg fluxes increased in Fox Lake and Little Fox Lake but not in Little Braeburn Lake, were most of the increase in Hg accumulation rate could be predicted from changes in organic matter accumulation (Figure 6.10). The excess Hg and Pb flux was similar in Fox Lake and Little Fox Lake until the 1958 wildfire, after which Hg fluxes increased faster in Little Fox lake and than in Fox Lake (Figure 6.10) and Pb increased in Little Fox Lake whereas they decreased in Fox Lake (Figure 6.11).

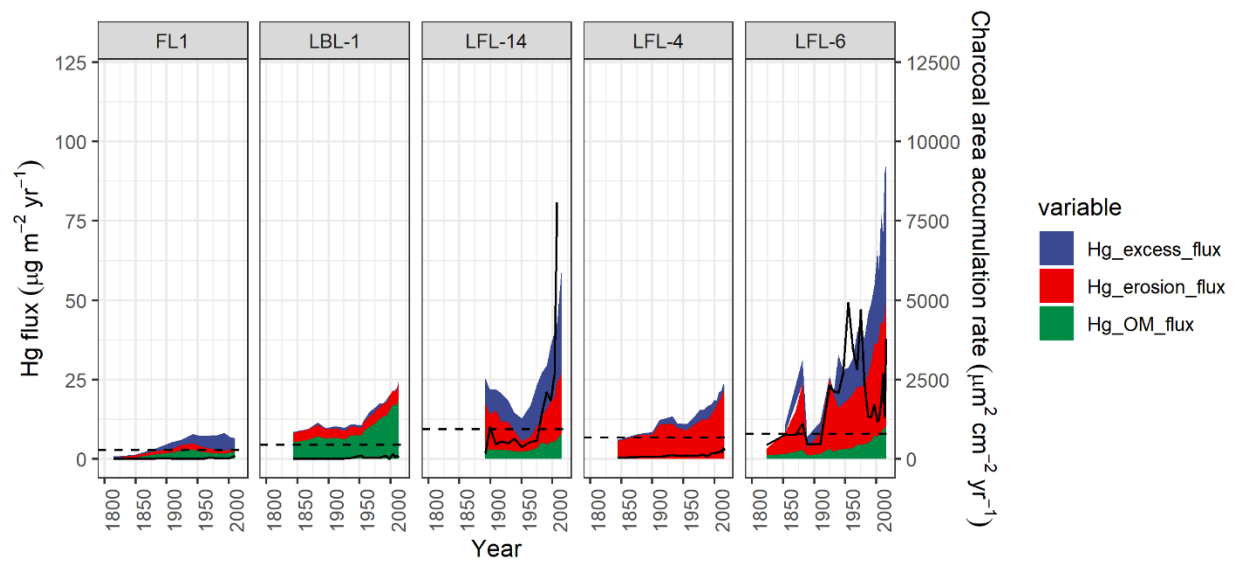


Figure 6.10: Deconstructed fluxes of Hg in each lake sediment following equation 6.1 and 6.3. The full black line represents the charcoal accumulation rate in each core and follows the secondary y-axis scale (right side). The dashed line represents the long-term pre-industrial baseline flux based on the oldest modelled sedimentation rate and average pre-industrial Hg concentration in each core.

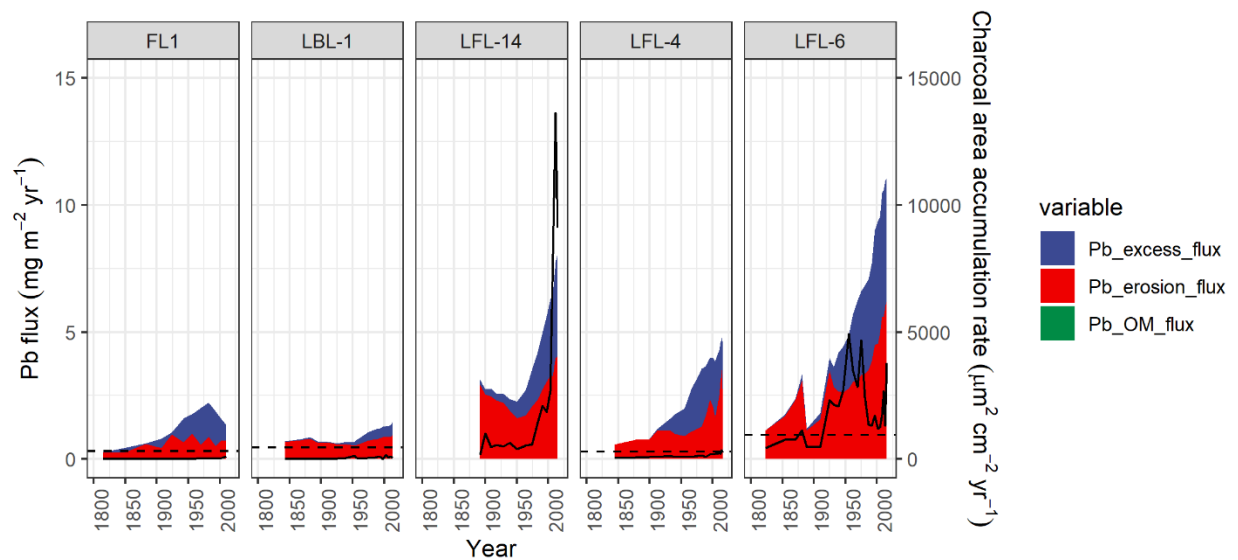


Figure 6.11: Deconstructed fluxes of Pb in each lake sediment following equation 6.1 and 6.2. The full black line represents the charcoal accumulation rate in each core and follows the secondary y-axis scale (right side). The dashed line represents the long-term pre-industrial baseline flux based on the oldest modelled sedimentation rate and average pre-industrial Pb concentration in each core.

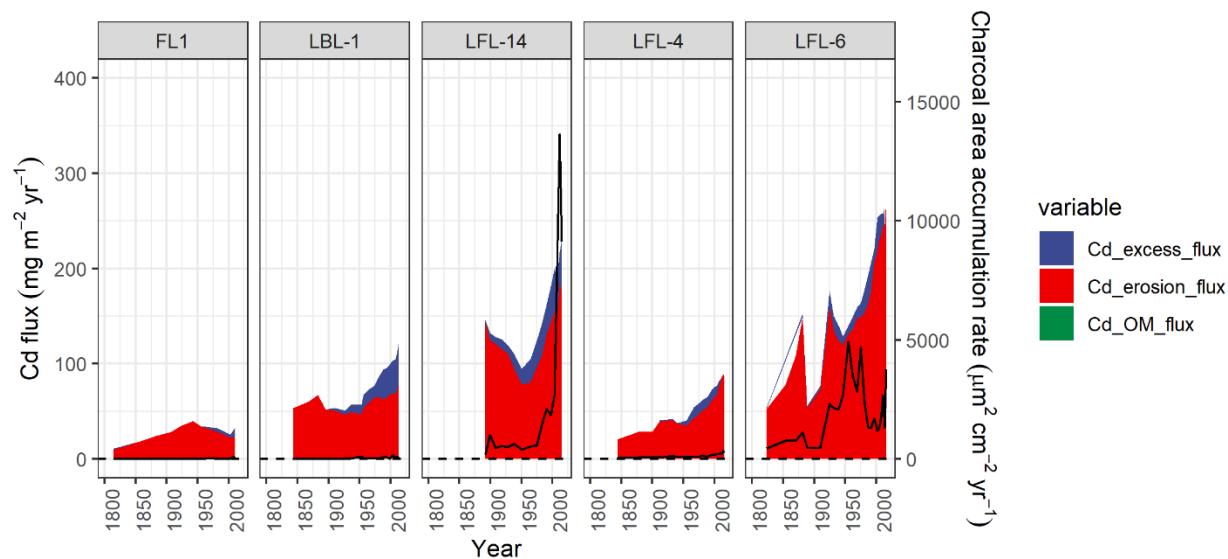


Figure 6.12: Deconstructed fluxes of Cd in each lake sediment following equation 6.1 and 6.2. The full black line represents the charcoal accumulation rate in each core and follows the secondary y-axis scale (right side). The dashed line represents the long-term pre-industrial baseline flux based on the oldest modelled sedimentation rate and average pre-industrial Cd concentration in each core.

Some excess fluxes of Cd are present after 1950 at all sites but the fluxes are exceedingly small compared to natural inputs from catchment erosion (Figure 6.12). Excess Cd is more important in Little Braeburn Lake than other lakes (Figure 6.12).

6.5 DISCUSSION

6.5.1 Geochemical impact of wildfires in lakes with minor exposure

Fox Lake and Little Braeburn Lake had only minor exposure to wildfire events during the 20-21st century, i.e., they received little to no particulate inputs attributable to the erosion of burned catchments but may have received atmospheric deposition from wildfires fallouts or leachates from burned soil. In fox Lake, we identified no change in lake sediment metal concentration or accumulation rate co-occurring with wildfires. In Little Braeburn Lake, the light impact of the 1957-1958 wildfire may have primed organic matter production, with minor consequences on the accumulation rate and concentration of Hg and Cd in the sediment. However, the changes in organic

matter production in Little Braeburn Lake may be climate-driven rather than consequential to the wildfire.

The absence of geochemical impact from the 1958 and 1998 wildfires in the Fox Lake sediment was expected because of the relatively small size of the burned area (13-33% of the watershed area) in the lake's catchment and the absence of burned shore on the lake, together limiting the transport of terrestrial material by erosion. Changes in sediment accumulation rate at the beginning of the twentieth century occurred before the occurrence of the 1958 fire (Figures 6.4 and 6.9) and may be attributable to the economic development of the area, past forestry operations, and the enlargement of the road that now corresponds to the Klondike highway. Because of the stable sedimentation rate, the surrounding geology, the small change in organic matter accumulation over time and the similarity in metal accumulation pattern before the wildfires, Fox Lake is the best control site to evaluate the impact of catchment transport caused by the wildfires in Little Fox Lake's catchment.

In the Little Braeburn Lake catchment, the extensive development of the organic soil layer, the size of the mature trees and the small magnitude of charcoal accumulation are evidence that the 1957-1958 fires were not severe stand-replacing wildfires. The lighter slopes around the Little Braeburn Lake watershed (Figure 6.1) and the different local geology at this site may be limiting the runoff in this watershed compared to the Little Fox Lake and Fox Lake watersheds, and therefore this area may maintain conditions less conducive to severe wildfires (e.g., moisture level) and may simultaneously experience reduced erosion from wildfire of any severity. Little Braeburn Lake was necessarily exposed to atmospheric fallouts from the wildfires. In chapter four of this thesis, wildfire fallouts strictly from atmospheric transport caused a ≤ 2 years increases in the lakes sediment accumulation rate of multiple metals, including Hg (mean \pm sd $0.1 \pm 1 \mu\text{g m}^{-2} \text{yr}^{-1}$, max $2.6 \mu\text{g m}^{-2} \text{yr}^{-1}$) and Pb (mean \pm sd, $32 \pm 107 \mu\text{g m}^{-2} \text{yr}^{-1}$, max $307 \mu\text{g m}^{-2} \text{yr}^{-1}$). These increases are small compared to the magnitude of Hg and Pb

fluxes in Little Braeburn Lake and would not stand out from the accumulation record in this lake. The primary impact of the 1957-1958 wildfire around Little Braeburn Lake may have been to promote the accumulation of organic matter, leading to higher levels (2-3 folds) in this lake than in sediment than Little Fox Lake (more seriously affected by the fires) or Fox Lake (not affected). The organic matter loading that succeeded the fire could be caused by autochthonous (in-lake) production, catchment transport of terrestrial organic matter or a mix of both. The autochthonous production hypothesis is favored in the case of Little Braeburn Lake because of the lack of evidence for increased catchment transport following the fire. The release of limiting nutrients (N, P, K) from the catchment during the combustion of biomass is commonly reported in surface water and groundwater affected by wildfires (Bayley et al., 1992; Leys et al., 2016; Shakesby, 2011; Spencer et al., 2003), and these elements may also be transported atmospherically (Lindaas et al., 2021) as ashes and charred organic matter (Bodí et al., 2014; Pelletier, Chételat, Blarquez, et al., 2020; Raison et al., 1985) or in soluble or fine particulates form from ground and surface water flow (Ice et al., 2004; Neary et al., 1999; Smith et al., 2011). Nutrients transported from wildfires may then prime in-lake production for decades (Pompeani et al., 2020). The impact of phosphorus addition is of particular interest since this element is the most common limiting nutrient in boreal lakes (Schindler, 1977; Schindler et al., 2008) and is one of the primary constituents of wildfire ash (Bodí et al., 2014; Certini, 2005; Harper et al., 2019). However, it is also possible that the observed increase in organic matter accumulation in Little Braeburn Lake is climate-driven more than nutrient-driven. Lakes algae production has increase in temperate latitudes in Canada in some lakes where no eutrophication occurred in response to longer summers, more ice-free days and changes in the thermal stratification and salinity of lakes (Smol, 2016).

As a result of greater biomass production, metals that have a greater affinity for organic matter like Hg and Cd have become more abundant in the sediment of Little Braeburn Lake than in the other study lakes (Figure 6.10). It is unclear if this trend is related to algal scavenging, a hypothesised process

where increase the productivity of algae cause the acquisition of more atmospheric Hg, leading to greater sediment Hg accumulation rate (Outridge et al., 2007; 2019). However, the scavenging hypothesis cannot explain the greater Cd accumulation rate observed in Little Braeburn Lake (figure 6.9) because Cd does not have an important gaseous phase in the atmosphere and therefore should not be acquired in excess by algae. For algal scavenging to impact Cd accumulation in the sediment, there would need to be a source of dissolved Cd in the water column that can replenish the Cd acquired by algae, otherwise Cd would become depleted in the water column and the accumulation rate in the sediment would reduce over time. It is likely that Hg and Cd accumulation increased in this lake independently from organic matter production and created a strong spurious correlation with these variables.

6.5.2 Geochemical impact of wildfires in lakes with major exposure

In Little Fox Lake (LFL), both the 1958 and 1998 fires increased sedimentation rate and sediment metal loading in response to the important loss of vegetation in this catchment that accelerated soil erosion rates. The cumulative impact of the two wildfires culminated in a four-to-six-fold increase in the accumulation rate of Pb, Ca, Ba, Sr, Ag, Hg, Se and P in the lake sediment and the concentration of these element in the sediment was greater post-wildfires. The accumulation rate of every other analysed metal was also two to four times greater during the two decades that followed the 1998 wildfire.

The main difference between this lake and the other study sites is the obvious lack of vegetation and soil recovery that was caused by the severity of the 1998 fire (Figure 6.2). A large section of the lake's catchment was affected by both the 1958 and 1998 wildfires and show shallow (≤ 5 cm thick) or non-existent organic soil along the Eastern slope of the catchment. As a result, while the sedimentation rate and metal loading in all studied lakes were similar before the two wildfires, today the most severely burned lake (Little Fox Lake) has two to five times greater sedimentation rate and metal fluxes than

the other lakes. Severe or frequent wildfires can impede the normal vegetation recovery past a certain threshold (McLauchlan et al., 2020; Stevens-Rumann & Morgan, 2019) and such threshold shifts have frequently been inferred for similar ecosystems as the study area such as in Wyoming subalpine lodgepole pine forests (Turner et al., 2019) and Yukon subarctic black spruce forests (Brown & Johnstone, 2012). In Little Fox lake, the minor vegetation recovery 20 years after the wildfire indicate that this threshold was exceeded and that this was the main driver for the important multi-decadal impact observed in this lake. However, other factors such as steeper topography and different catchment geology may have contributed to the increase the wildfire impacts in this lake.

Topography

There are steeper slopes in the Little Fox Lake valley section than in the Little Braeburn section of the valley (Figure 6.1). Steep slopes facilitate soil drainage, leading to drier surface soil conditions that can increase available fuel load and favorize more severe wildfires (Bassett et al., 2017). Burned soil in steeper slopes is also eroded faster because of accelerated unsaturated flow (Ebel, 2013) and greater peak surface flow during storm events (Ice et al., 2004; Shakesby, 2011). Lower slopes may also limit wildfire-driven erosion by allowing more organic soil to build up in low-relief areas, that are capable of retaining sediments and leachates (Johnston, 1991). In comparison to wet organic soils around Little Braeburn Lake, colluvial soils in steep slopes around Little Fox lake are coarser and more easily drained.

Catchment geology and buffering capacity

The lack of buffering capacity from carbonate rocks in the Little Fox Lake catchment may also have contributed to greater wildfire impact in this lake compared to Little Braeburn Lake, where the surrounding geology is dominated by calcareous greywacke and argillaceous limestone. Carbonates could buffer the acid leachates from fire ash (Certini, 2005), and the lack of buffering capacity in the

Little Fox Lake catchment soil may be a factor that inhibited vegetation regrowth and facilitated metal transport.

6.5.3 Impact of the timber harvest in the burned catchment

In long-term lake sediment reconstructions, the typical geochemical impact of wildfires to Colorado alpine lakes typically lasted for 20-30 years following fire events during the Holocene (Dunnette et al., 2014; Leys et al., 2016; Pompeani et al., 2020). In this study, the fire return interval at Little Fox Lake was twenty years, explaining why we saw no sign of recovery between fire events. There was an unexpected trend in Little Fox Lake sedimentation rate and metal accumulation where these variables increase with time after the 1998 wildfire and this may be caused by a timber harvest operation that occurred in the lake's catchment between 2010 and 2018 (Yukon Government, 2012). These operations have likely further disturbed the fragile barren soil in the burned catchment, and that may have facilitated catchment erosion and inhibited vegetation regrowth.

6.5.4 Deposition and remobilisation of long-range and regional contaminants in subarctic Canadian lakes

The impact of wildfires on Hg, Cd and Pb loading in the study lakes surpassed the impact of long-range and regional contaminant emissions. Most Hg, Cd and Pb accumulating in the sediment of the study lakes were of catchment soil origin and wildfires primarily increased the transport of catchment (natural) Pb, Cd and Hg. However, the impact of long-range contaminants is superimposed on the impact of wildfires in the case of Hg and Pb. The atmospheric deposition of Pb and Hg in the West Coast of Yukon is primarily sourced from East Asia because of the trans-Pacific atmospheric transport (Durnford et al., 2010; Osterberg et al., 2008) but regional sources must also have contributed, including the City of Whitehorse and all the mining operations from the Klondike era onward.

Ice cores records from Mt. Logan, Yukon (~270 km West of the study sites) showed that the atmospheric Pb concentration in Western Yukon peaked during the 1980s and decreased thereafter

but was on the rise again in 2008 when cores were analysed (Osterberg et al., 2008). In this study, the excess Pb accumulation rate (attributable to long-range Pb contamination) followed the expected trend in atmospheric deposition in the lake unaffected by wildfire (Fox Lake) but increased continuously in the lake that was severely affected by two wildfires (Little Fox Lake) (Figure 6.13).

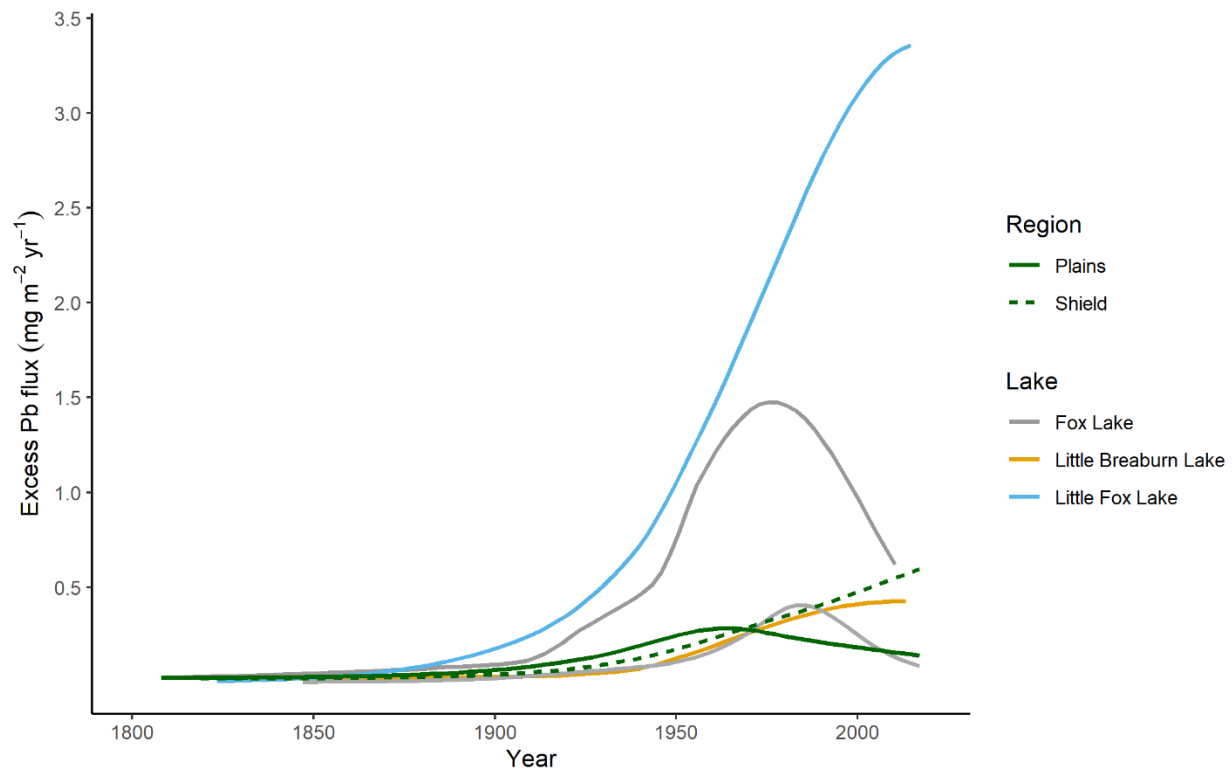


Figure 6.13: Generalised additive model of excess Pb flux from 1800 to 2018 in sites from chapter five and chapter six.

The observed excess Pb fluxes were several folds over the excess fluxes measured in the Taiga Plains, Taiga Shield lake sediment and bog records (Figure 6.13) or records of atmospheric deposition in northern Alberta bogs (Shotyk et al., 2016), which could be explained by the importance of the regional development in that area during the Klondike era compared to the southern Northwest Territories and northern Alberta.

Two large-scale tree-rings reconstructions have recently shown that atmospheric Hg concentration in Yukon have continuously increased since the 19th century (Clackett et al., 2018, 2021). In this study, the excess Hg accumulation was more in line with the variations in atmospheric Hg concentration in Fox Lake than in Little Fox Lake, where it increased exponentially with time after the 1998 fire (Figure 6.14a). The trend in excess Hg in Little Fox Lake is comparable to the trend in excess Pb in this lake or the trend in excess Hg and Pb the Taiga Shield Lakes presented in chapter five of this thesis (Figure 6.14a).

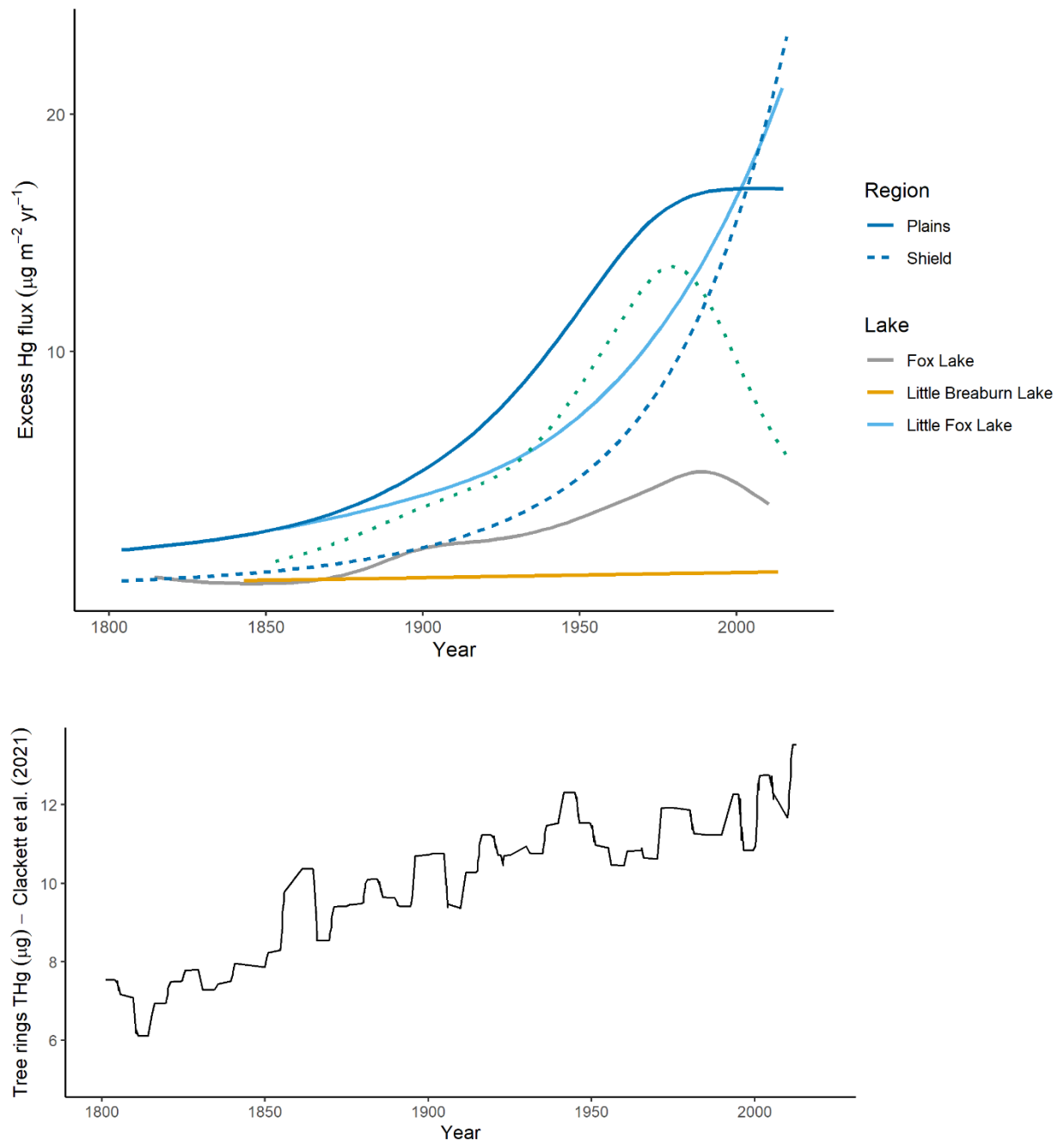


Figure 6.14: (a) Generalised additive model of excess Hg flux from 1800 to 2018 in sites from chapter five and chapter six.;(b) Tree-rings THg concentration from North-western Yukon (Clackett et al., 2021).

The impacts of wildfire and anthropogenic pollution (regional and long ranged) can be distinguished by comparing the fluxes in Fox Lake to those in Little Fox Lake. Both lakes had similar increases in Pb and Hg accumulation rates before the 1998 fire and must therefore respond in similar way to changes in atmospheric deposition. The increases in excess Pb and Hg accumulation preceding the 1998 wildfire corresponds to the timing of increasing Pb and Hg pollution at global scale (Bindler, 2011; Marx et al., 2016; Streets et al., 2017). Wildfires accelerated the transport of legacy Hg and Pb to Little Fox Lake, creating an impact similar to the hydrological changes in the Taiga Shield lakes. Our results demonstrate that wildfires constitute an important pathway for the transport of anthropogenic Pb and Hg to subarctic lakes. One implication of this finding is that the future loading of Hg and Pb in northern lakes will not entirely depend on our ability to control the atmospheric emissions of these contaminants. While there are clearly ongoing sources of excess Pb and Hg in the regional atmospheric deposition of southern Yukon, wildfires exacerbate the impact of this deposition and of previous legacy deposition in lakes. The recent atmospheric deposition of Pb from regional and long-range source in the study area is $\sim 0.6 \text{ mg m}^{-2} \text{ yr}^{-1}$ (based on Fox Lake and Grayling Lake) but the fast erosion in the burned catchment of Little Fox Lake funnels this deposition to Little Fox Lake and the rate of excess Pb accumulation in this lake is six times the atmospheric deposition rate. Similarly, while in unburned catchment we recorded a recent anthropogenic excess of $\sim 5 \text{ } \mu\text{g m}^{-2} \text{ yr}^{-1}$, the impact of the burned catchment caused an increase of $>20 \text{ } \mu\text{g m}^{-2} \text{ yr}^{-1}$.

6.5.5 Distribution of metals released by wildfires in lakes with a complex bathymetry

We used multiple cores to model the metal(loid) accumulation in Little Fox Lake, which has a complex bathymetry composed of multiple sub-basins. Interestingly, we observed a different pattern of charcoal accumulation in the different sub-basins of this lake and the differences were linked to the proximity of the sub-basin to the burned catchment during each fire event. Cores from the West basin of the lake recorded the fires occurring in the corresponding catchment section and cores from the

East basins did the same. Although the pattern of charcoal accumulation differed between the lake sub-basins, the changes in metal(loid) accumulation caused by the wildfire were consistent throughout the lake and led to similar metal(loid) accumulation rates (Figure 6.9), independent from macroscopic charcoal accumulation rates. Therefore, metal(loid) and P transported from burned catchments were not adsorbed to charcoal particles in lake sediment and must have been transported independently from charcoal. Fire ash analysis revealed that at high temperature ($>580^{\circ}\text{C}$), fire releases metals in the forms of oxides that may be weakly adsorbed to charred organic matter particulate or may be found in mineral and highly mobile form (Bodí et al., 2014). The observation that metal(loid) transport was not restricted by lakebed topography suggests that metal(loid)s released by wildfires are susceptible to be transported long distances downstream if they are washed into a stream instead of a lake and that they are susceptible to be transported to downstream lakes in an open or connected surface water system. This is in agreement with studies on metal(loid) analysis of stream systems near burned catchments (Burton et al., 2016; Smith et al., 2011; Stein et al., 2012).

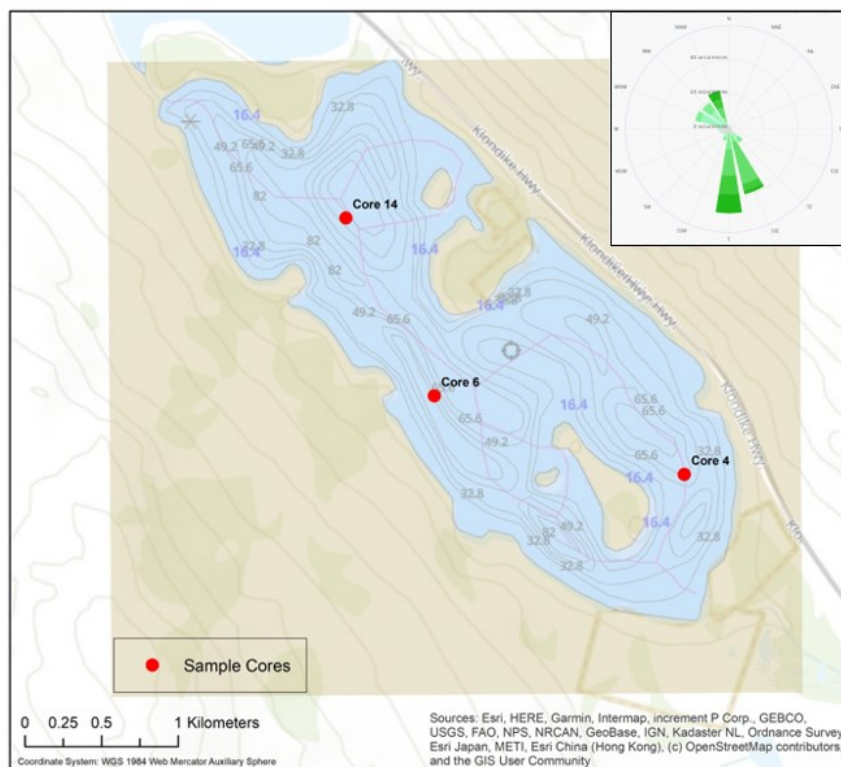


Figure 6.15: From Sarah Sinon Honor thesis (Carleton, 2020). Location of sample cores in Little Fox Lake (LFL) overplotted on lake bathymetry. Depths isolines are in feet. The upper-right corner wind rose shows the mean annual wind direction weighted by frequency at the nearest meteorological station.

6.5.6 A proposed conceptual chart of wildfire impacts on lakes metal loading

Based on the existing literature and the results of this study, I conceptualise four ways in which lakes metal loading may be affected by wildfires. These impacts are laid on a continuum, from minor atmospheric inputs related to fallouts from wildfire plume to the important impact caused by severely burned catchment after stand-replacing wildfires. However, it is unlikely that lakes metal loading responds linearly to fire severity because the largest impacts of wildfires on metal loading are related to catchment erosion processes, which in-turn is most affected by catchment vegetation cover. There are fire severity thresholds after which vegetation recovery becomes especially difficult (Jin et al., 2012; Meng et al., 2015), and the future catchment erosion (and metal loading) in northern lakes will partly depend on the propensity of wildfires to exceed these thresholds in the future.

- 1) Wildfires occurring outside of lakes catchments: particulate emissions comprise in wildfires plumes transport a fraction of metals consumed in the burning biomass (see chapter four of this thesis) and a part of this material is deposited in lakes along the path of the wildfire plumes. However, the depositional fluxes from wildfire plumes are very small because a large proportion of metal released from burned vegetation is accumulated in ash that remains in soils and particles small enough to remain in suspension plumes are spread over large region, especially for species with a long residence time like Hg⁰.
- 2) Wildfires of minor severity inside lakes catchments: The fire far from being severe enough to exceed the ecosystem resilience and may be a small crown fire. The fire does not consume enough surface organic matter to influence lake sedimentation rate. However, phosphorous released from the biomass combustion can reach the lake by atmospheric transport or groundwater flow, which can prime the accumulation of organic matter in the water column, and in turn accelerate the biotic accumulation of metal(loid) elements susceptible to algal scavenging such as Hg. This impact was observed at Little Braeburn Lake.
- 3) Wildfires of moderate severity inside lake catchment: An initial increase in metal accumulation rate is rapid and temporally coherent with the wildfire event. Sedimentation rate and metal(loid) fluxes peak and then return to pre-disturbance conditions. The recovery is initially rapid, but return to pre-disturbance condition takes up to 20 years (Dunnette et al., 2014). This pattern is expected in partially burned catchment (consisting an easily erodible stock of fine particulates and charred material) and some loss of surface vegetation, causing a short-term increase in organic/inorganic terrestrial material transport to the lakes following the wildfires. The return to pre-disturbance conditions is related to vegetation recovery and organic soil aggradation (gradually limiting the catchment erosion rate) and the depletion of partially

burned material in the catchment. The atmospheric deposition of ash and secondary transport of this ash also account for some of the metal accumulation in lake following the fire. Most wildfires occurring during the Holocene likely impacted lakes in this way.

- 4) Wildfires of extreme severity inside lakes catchment: This type of impact is associated with more severe events or fire events with a short return interval. In this type of events, a large fraction of soil organic layer is consumed during the wildfire. An increase in sedimentation rate and metal(loid) flux is temporally coherent with the wildfire event but may not peak in the first year of the event. The impact of the wildfire on lake sedimentation and metal(loid) loading can grow with time as acid leachates liberated from ashes transport metal elements to the lake. Moreover, the small amount of organic matter left at the soil surface rapidly decompose and is not replaced by new organic matter, which slowly releases the metal(loid) elements adsorbed to it or incorporated within it. Vegetation recovery in the catchment is slow or non-existent, leading to a net loss of organic matter in the catchment over time, a decrease in soil stability and increasing erosion over time. This impact was observed in Little Fox Lake.

6.6 CONCLUSION

In the four subarctic study lakes, we observed a range of impacts of wildfires on sedimentation rate, organic matter and metal(loid) loading, from mild to severe. Large changes in catchment erosion followed two severe wildfires in Little Fox lake and this greater erosion accelerated the transport of both natural and anthropogenically-released metals from the catchment to the lake. The lack of vegetation and soil recovery observed in the Little Fox Lake catchment is the hallmark of a short fire-return interval (20 years) and a high fire severity (in 1998) and logging operations have exacerbated the problem past 2010. However, it is obvious that large multi-decadal impacts like those observed at Little Fox Lake would not be possible in a milder topography, where erosion is slower.

There was a clear impact of long-range and regional Pb and Hg contamination in the sediment of every studied lake, but this impact was largely exacerbated by the occurrence of wildfires in Little Fox lake. This has large implications for any Arctic and subarctic lakes in catchment that has a minimum of relief, because wildfire frequency and intensity will increase with time (Coogan et al., 2019). This will create multiple situations like Little Fox Lake where severe stand-replacing wildfire will accelerate terrestrial erosion rate and carry terrestrial contaminants toward streams and lakes. In areas where atmospheric deposition has decreased in response to recent regulations of anthropogenic emissions, wildfire will delay the recovery of aquatic ecosystem toward pre-industrial levels of contaminants. In areas where external contaminants sources are actively depositing contaminants to this day, like in Western Yukon that still receives Pb and Hg from Asian sources (Bao et al., 2015; Strode et al., 2008), wildfires will exacerbates the funneling effect of lake catchments for these atmospheric contaminants. Subarctic lakes catchments are changing rapidly in response to climate change and other processes are already impacting the release of natural metals and legacy contaminants from their soils, like changes in precipitation patterns (discussed in chapter 5 of this thesis) and permafrost thaw (Vonk et al., 2015). The impact of severe wildfires is an additional way in which subarctic lakes geochemistry will change in the future in response to climate change.

Our study showed that wildfire severity, catchment topography, and the resulting ecological setting in terms of catchment soils and vegetation recovery are critical factors controlling wildfire impacts on lake sedimentation rate and metal(loid) loading. A future increase in wildfire severity subarctic Canada may have important consequences for sediment geochemistry at local scales, and trace element cycling at larger scale. Contaminants release by wildfires will also occur in more remote, northern regions of the Arctic as climate warming continue and affect areas where wildfire have not been occurring over the last millennia (McCarty et al., 2020). Since the Arctic has been a sink for global atmospheric Pb and Hg for centuries to millennia, the occurrence of wildfires in these new regions will release

anthropogenic contaminants and add to the existing pressure from other environmental pressures such as permafrost thaw (also facilitated by wildfires: Gibson et al., 2018), changes in precipitation patterns (chapter five of this thesis) and changes in lake productivity (that could affect Hg accumulation). The impact of wildfires on the release of legacy contaminants from (sub)Arctic catchments should continue to be investigated in different geophysical regions and in areas where multiple climatic pressures may intersect. For example, areas affected by changes in precipitations, permafrost thaw and wildfires simultaneously may experience an especially rapid release of contaminants to aquatic ecosystems that should be measured.

Another interesting follow-up on the conclusion of this chapter is knowing how long can the release of legacy contaminants can persists in subarctic Canada once atmospheric deposition have decreased. For example, decades have past since Pb emissions in Canada and the USA have dropped, and yet Pb from anthropogenic sources is actively deposited at the surface of lake sediment in Southern Yukon and the Northwest Territories (chapter three and five of this thesis). At one point in time, this anthropogenic Pb will become depleted in subarctic catchment catchment and lake accumulation should resume to be entirely constituted of natural Pb from catchment soil weathering. The timing for this is highly unclear and will depend on the total inventory of anthropogenic contaminants in subarctic soils, the distribution of these in soil profiles and the future catchments flow and erosion rates. Recent mapping effort for anthropogenic Hg in soils has been conducted in Alaska (Perryman et al., 2020) and a similar investigation on the northern Canadian Territories, and for different contaminants (e.g., Hg, Pb , Cd) would be greatly beneficial to our ability to predict future areas of concern. This is particularly true if the risk of future climate-induced pressures such as wildfires, permafrost thaw and precipitation patterns can also be mapped with an efficient precision and cross-analysed with legacy contaminants mapping.

7 CONCLUSION

7.1 CONCLUDING STATEMENT

This thesis provides novel insights on the cumulative and individual impacts of multiple sources of metal contamination to subarctic Canadian lakes that changed over time. The research quantifies the impacts of different human emission sources and natural processes on the transport of metals to lakes and the effectiveness of historical environmental policies (e.g., reduction in atmospheric Pb and Hg emissions) at limiting metal loading in different ecoregions of the Northwest Territories and Yukon. Environmental archives have been crucial at informing environmental policies in the past by showing anthropogenic impacts in long time series, and could therefore play an equally important role in evaluating the efficiency of past regulations and informing future ones. Here I demonstrated that it is crucial that climatic changes that can affect catchment erosion and wildfires should weight in our expectations of future lake recovery from anthropogenic contamination, and that these effects will vary by ecoregion in subarctic Canada. The climate impacts evaluated in this thesis (wildfires in chapter four and six, precipitations in chapter five) had the common consequence of accelerating the transport of metals from catchments to aquatic environments, including legacy contaminants emitted locally (e.g., mining pollution in chapter three and four) and long-range contaminants (e.g., long-range Pb and Hg in chapter five). It is crucial that climate change is explicitly considered in setting objectives for acceptable levels of human metal emissions and that future research continue to investigate the bioavailability and toxicity of legacy contaminants released to aquatic environments and monitor metal concentration in biota of sensitive areas (e.g., those affected by severe wildfire like Little Fox Lake).

In recent decades, great advancements in the paleoecological modelling of geochemical data have improved our ability to quantify the influence of natural processes and isolate human impacts in reconstruction from lake sediments and peatlands. New paleoenvironmental data that informs future environmental regulation processes should make the best possible use of these new methods,

including those developed in this thesis to model the impact of processes like wildfires and catchment transport. These methods include combining archives from a variety of ecoregions, combining different types of natural archives in the same analysis, combining new indicators (e.g., charcoals) and metal fluxes in sediment and peat reconstructions, the use of stable isotopes to quantify individual sources of contamination in sediments and new statistical approaches developed by other disciplines such as applied mathematics and economy (e.g., the Superposed epoch analysis or GAM of multiple cores). These methods build up on a growing body of literature that are continuously making the interpretation of paleoenvironmental record more precise and informative. Paleoenvironmental science will also remain relevant in future years by applying these techniques to the study of new emerging contaminants (e.g., some POPs, PAHs and microplastics). Methods developed for trace metal contaminants, such as baseline background determination, source partitioning of fluxes using tracers, combining multiple archives and spatial-temporal reconstruction from multiple records are easily transferable to some other environmental contaminants.

The processes investigated in this thesis, namely point-source pollution from mining, wildfires, catchment erosion and long-range pollution are all predicted to continue growing in near future and affect new areas. For example, Arctic wildfires are now occurring in areas where they have been almost inexistant during at least the last three millennia (Hu et al., 2015; Mack et al., 2011; McCarty et al., 2020). These tundra fires will impact Arctic lakes by releasing legacy metals from Arctic catchments, which is one more pressure on Arctic ecosystems that are already fragilized by multiple environmental changes caused by global climate warming.

7.2 SUGGESTIONS FOR FUTURE RESEARCH

Based on the findings of my research and the uncertainties that could not be addressed, I recommend that future studies continue to explore the transport mechanisms and temporal trend of accumulation

for legacy metals in different types of northern environments. Specifically for lakes, it is important to better understand the watershed characteristics that promote the sequestration of metals in subarctic soils and those that influence the stability of these elements in soils. It is becoming apparent that the release of metal from a lake's catchments will be impacted by increasing temperature, changes in precipitation patterns and extreme weather leading to more frequent and severe wildfires. Future studies should aim at measuring and modelling the interactions between region-specific climate change, catchment characteristics and sites contamination history to better identify the areas where legacy contaminants could be released in the largest proportion. Mapping the distribution of contaminants in (sub)Arctic soils (like it is done for soil organic carbon in carbon cycling studies) could allow to quantify the risk that these contaminants will be transported to aquatic ecosystems in response to region-specific climate trends.

Another important aspect of legacy metal transport (not addressed in this thesis) is the bioavailability of those released elements. Evaluating the extent of bioaccumulation and biomagnification of these elements and monitoring how biota respond to their presence is of paramount importance to evaluate future ecological risks.

The impact of wildfires on the transport and transformation of legacy metals is understudied in Canada and the extent to which findings from other regions and climates (e.g., California, Australia) are applicable to the northern Canadian landscape. Post-wildfire metal accumulation rates in lakes should be evaluated for a wide variety of geophysical regions and at varying proximity to pollution sources. Moreover, wildfire-associated processes causing changes in lakes metal accumulation highlighted in this thesis could also impact the cycling of other contaminants such as POPs, radionuclides and nanoparticles. New research should investigate how recent wildfires may accelerate the accumulation of these elements in lakes.

The approaches presented in the thesis are building up on a wide existing body of literature dedicated to attribution science in paleoenvironmental data. The new combinations of analytes (e.g., metals and macroscopic charcoals), environmental archives (lake sediment and peat bogs) and ecoregions (Taiga Plains and Taiga Shield) in the same analysis brought forward new ways to quantify individual processes. This research shows that when archives, analysis and study regions are combined with care, paleoenvironmental analyses have the power to isolate and quantify the impact of multiple individual sources and processes in geochemical records.

8 BIBLIOGRAPHY

- Abraham, J., Dowling, K., & Florentine, S. (2017). Risk of post-fire metal mobilization into surface water resources: A review. *Science of The Total Environment*, 599–600, 1740–1755.
<https://doi.org/10.1016/j.scitotenv.2017.05.096>
- Adams, J. B., Mann, M. E., & Ammann, C. M. (2003). Proxy evidence for an El Niño-like response to volcanic forcing. *Nature*, 426(6964), 274–278. <https://doi.org/10.1038/nature02101>
- Adrian, R., O'Reilly, C. M., Zagarese, H., Baines, S. B., Hessen, D. O., Keller, W., Livingstone, D. M., Sommaruga, R., Straile, D., Van Donk, E., Weyhenmeyer, G. A., & Winder, M. (2009). Lakes as sentinels of climate change. *Limnology and Oceanography*, 54(6), 2283–2297.
<http://www.ncbi.nlm.nih.gov/pmc/articles/PMC2854826/>
- Alaee, M., Muir, D., Cannon, C., & Helm, P. (2003). Canadian Arctic Contaminants Assessment Report II: Sources, occurrence, trends and pathways in the physical environment. In 2003.
<http://caid.ca/CanArtCon5.2003.pdf>
- Ali, H., & Khan, E. (2019). Trophic transfer, bioaccumulation, and biomagnification of non-essential hazardous heavy metals and metalloids in food chains/webs—Concepts and implications for wildlife and human health. In *Human and Ecological Risk Assessment* (Vol. 25, Issue 6, pp. 1353–1376). Taylor and Francis Inc.
<https://doi.org/10.1080/10807039.2018.1469398>
- Ali, H., Khan, E., & Ilahi, I. (2019). Environmental chemistry and ecotoxicology of hazardous heavy metals: Environmental persistence, toxicity, and bioaccumulation. In *Journal of Chemistry* (Vol. 2019). Hindawi Limited. <https://doi.org/10.1155/2019/6730305>
- AMAP/UNEP. (2013). *Technical Background Report for the Global Mercury Assessment 2013*. Arctic

Monitoring and Assessment Programme, Oslo, Norway/UNEP Chemicals Branch, Geneva, Switzerland. <https://oarchive.arctic-council.org/handle/11374/732>

Andrade, C. F., Jamieson, H. E., Kyser, T. K., Praharaj, T., & Fortin, D. (2010). Biogeochemical redox cycling of arsenic in mine-impacted lake sediments and co-existing pore waters near Giant Mine, Yellowknife Bay, Canada. *Applied Geochemistry*, 25(2), 199–211. <https://doi.org/10.1016/j.apgeochem.2009.11.005>

Appleby, P. G., & Oldfield, F. (1978). The calculation of lead-210 dates assuming a constant rate of supply of unsupported ^{210}Pb to the sediment. *CATENA*, 5(1), 1–8. [https://doi.org/10.1016/S0341-8162\(78\)80002-2](https://doi.org/10.1016/S0341-8162(78)80002-2)

Aryal, R., Beecham, S., Sarkar, B., Chong, M. N., Kinsela, A., Kandasamy, J., & Vigneswaran, S. (2017). Readily Wash-Off Road Dust and Associated Heavy Metals on Motorways. *Water, Air, and Soil Pollution*, 228(1), 1–12. <https://doi.org/10.1007/s11270-016-3178-3>

Audry, S., Pokrovsky, O. S., Shirokova, L. S., Kirpotin, S. N., & Dupré, B. (2011). Organic matter mineralization and trace element post-depositional redistribution in Western Siberia thermokarst lake sediments. *Biogeosciences*, 8(11), 3341–3358. <https://doi.org/10.5194/bg-8-3341-2011>

Azcue, J. M., Mudroch, A., Rosa, F., Hall, G. E. M., Jackson, T. A., & Reynoldson, T. (1995). Trace elements in water, sediments, porewater, and biota polluted by tailings from an abandoned gold mine in British Columbia, Canada. *Journal of Geochemical Exploration*, 52(1), 25–34. [https://doi.org/10.1016/0375-6742\(94\)00028-A](https://doi.org/10.1016/0375-6742(94)00028-A)

Babos, H. B., Black, S., Pluskowski, A., Brown, A., Rohrssen, M., & Chappaz, A. (2019). Evidence for the onset of mining activities during the 13th century in Poland using lead isotopes from

lake sediment cores. *Science of the Total Environment*, 683, 589–599.

<https://doi.org/10.1016/j.scitotenv.2019.05.177>

Bacardit, M., & Camarero, L. (2010). Modelling Pb, Zn and As transfer from terrestrial to aquatic ecosystems during the ice-free season in three Pyrenean catchments. *Science of the Total Environment*, 408(23), 5854–5861. <https://doi.org/10.1016/j.scitotenv.2010.07.088>

Balshi, M. S., David, M. A., Paul, D., Mike, F., John, W., & Jerry, M. (2008). Assessing the response of area burned to changing climate in western boreal North America using a Multivariate Adaptive Regression Splines (MARS) approach. *Global Change Biology*, 15(3), 578–600. <https://doi.org/10.1111/j.1365-2486.2008.01679.x>

Bao, K., Shen, J., Wang, G., & Roux, G. (2015). Atmospheric Deposition History of Trace Metals and Metalloids for the Last 200 Years Recorded by Three Peat Cores in Great Hinggan Mountain, Northeast China. *Atmosphere*, 6(3), 380–409. <https://doi.org/10.3390/atmos6030380>

Bárcena, J. F., Claramunt, I., García-Alba, J., Pérez, M. L., & García, A. (2017). A method to assess the evolution and recovery of heavy metal pollution in estuarine sediments: Past history, present situation and future perspectives. *Marine Pollution Bulletin*, 124(1), 421–434. <https://doi.org/10.1016/j.marpolbul.2017.07.070>

Barrett, K. L. (2017). Exploring Community Levels of Lead (Pb) and Youth Violence. *Sociological Spectrum*, 37(4), 205–222. <https://doi.org/10.1080/02732173.2017.1319307>

Barrie, L. A., Gregor, D., Hargrave, B., Lake, R., Muir, D., Shearer, R., Tracey, B., & Bidleman, T. (1992). Arctic contaminants: sources, occurrence and pathways. *Science of the Total Environment*, 122(1–2), 1–74. [https://doi.org/10.1016/0048-9697\(92\)90245-N](https://doi.org/10.1016/0048-9697(92)90245-N)

Barrie, L. A., & Schemenauer, R. S. (1989). Wet Deposition of Heavy Metals. In *Control and Fate of*

Atmospheric Trace Metals (pp. 203–231). Springer Netherlands. https://doi.org/10.1007/978-94-009-2315-7_10

Bassett, M., Leonard, S. W. J., Chia, E. K., Clarke, M. F., & Bennett, A. F. (2017). Interacting effects of fire severity, time since fire and topography on vegetation structure after wildfire. *Forest Ecology and Management*, 396, 26–34. <https://doi.org/10.1016/j.foreco.2017.04.006>

Bayley, S. E., Schindler, D. W., Beaty, K. G., Parker, B. R., & Stainton, M. P. (1992). Effects of Multiple Fires on Nutrient Yields from Streams Draining Boreal Forest and Fen Watersheds: Nitrogen and Phosphorus. *Canadian Journal of Fisheries and Aquatic Sciences*, 49(3), 584–596. <https://doi.org/10.1139/f92-068>

Beliveau, A., Lucotte, M., Davidson, R., Paquet, S., Mertens, F., Passos, C. J., & Romana, C. A. (2017). Reduction of soil erosion and mercury losses in agroforestry systems compared to forests and cultivated fields in the Brazilian Amazon. *Journal of Environmental Management*, 203, 522–532. <https://doi.org/10.1016/j.jenvman.2017.07.037>

Berg, T., Røyset, O., Steinnes, E., & Vadset, M. (1995). Atmospheric trace element deposition: Principal component analysis of ICP-MS data from moss samples. *Environmental Pollution*, 88(1), 67–77. [https://doi.org/10.1016/0269-7491\(95\)91049-Q](https://doi.org/10.1016/0269-7491(95)91049-Q)

Biester, H., Bindler, R., Martinez-Cortizas, A., & Engstrom, D. R. (2007). Modeling the Past Atmospheric Deposition of Mercury Using Natural Archives. *Environmental Science & Technology*, 41(14), 4851–4860. <https://doi.org/10.1021/es0704232>

Bindler, R. (2011). Contaminated lead environments of man: reviewing the lead isotopic evidence in sediments, peat, and soils for the temporal and spatial patterns of atmospheric lead pollution in Sweden. *Environmental Geochemistry and Health*, 33(4), 311–329. <https://doi.org/10.1007/s10653->

- Bindler, R., Renberg, I., John Anderson, N., Appleby, P. G., Emteryd, O., & Boyle, J. (2001). Pb isotope ratios of lake sediments in West Greenland: inferences on pollution sources. *Atmospheric Environment*, *35*(27), 4675–4685. [https://doi.org/10.1016/S1352-2310\(01\)00115-7](https://doi.org/10.1016/S1352-2310(01)00115-7)
- Bindler, R., Renberg, I., & Klaminder, J. (2008). Bridging the gap between ancient metal pollution and contemporary biogeochemistry. *Journal of Paleolimnology*, *40*(3), 755–770. <https://doi.org/10.1007/s10933-008-9208-4>
- Birch, G. F., Taylor, S. E., & Matthai, C. (2001). Small-scale spatial and temporal variance in the concentration of heavy metals in aquatic sediments: a review and some new concepts. *Environmental Pollution*, *113*(3), 357–372. [https://doi.org/10.1016/S0269-7491\(00\)00182-2](https://doi.org/10.1016/S0269-7491(00)00182-2)
- Bird, G., Brewer, P. A., Macklin, M. G., Nikolova, M., Kotsev, T., Mollov, M., & Swain, C. (2010). Quantifying sediment-associated metal dispersal using Pb isotopes: Application of binary and multivariate mixing models at the catchment-scale. *Environmental Pollution*, *158*(6), 2158–2169. <https://doi.org/10.1016/j.envpol.2010.02.020>
- Biswas, A., Blum, J. D., Klaue, B., & Keeler, G. J. (2007). Release of mercury from Rocky Mountain forest fires. *Global Biogeochemical Cycles*, *21*(1). <https://doi.org/10.1029/2006GB002696>
- Biswas, B., Qi, F., Biswas, J., Wijayawardena, A., Khan, M., & Naidu, R. (2018). The Fate of Chemical Pollutants with Soil Properties and Processes in the Climate Change Paradigm—A Review. *Soil Systems*, *2*(3), 51. <https://doi.org/10.3390/soilsystems2030051>
- Blaauw, M., & Christen, J. A. (2011). Flexible paleoclimate age-depth models using an autoregressive gamma process. *Bayesian Analysis*, *6*(3), 457–474. <https://doi.org/10.1214/ba/1339616472>
- Blais, J., & Kalff, J. (1995). The influence of lake morphometry on sediment focusing. *Limnology and*

Oceanography, 40(3), 582–588. <https://doi.org/10.4319/lo.1995.40.3.0582>

Blais, Jules M., & Kalff, J. (1993). Atmospheric loading of Zn, Cu, Ni, Cr, and Pb to lake sediments:

The role of catchment, lake morphometry, and physico-chemical properties of the elements.

Biogeochemistry, 23(1), 1–22. <https://doi.org/10.1007/BF00002920>

Blarquez, O., Vanniere, B., Marlon, J. R., Daniau, A.-L., Power, M. J., Brewer, S., & Bartlein, P. J.

(2014). paleofire: An R package to analyse sedimentary charcoal records from the Global

Charcoal Database to reconstruct past biomass burning. *Computers & Geosciences*, 72, 255–261.

<https://doi.org/10.1016/j.cageo.2014.07.020>

Bodí, M. B., Martin, D. A., Balfour, V. N., Santín, C., Doerr, S. H., Pereira, P., Cerdà, A., & Mataix-

Solera, J. (2014). Wildland fire ash: Production, composition and eco-hydro-geomorphic

effects. *Earth-Science Reviews*, 130, 103–127. <https://doi.org/10.1016/j.earscirev.2013.12.007>

Boës, X., Rydberg, J., Martinez-Cortizas, A., Bindler, R., & Renberg, I. (2011). Evaluation of

conservative lithogenic elements (Ti, Zr, Al, and Rb) to study anthropogenic element

enrichments in lake sediments. *Journal of Paleolimnology*, 46(1), 75–87.

<https://doi.org/10.1007/s10933-011-9515-z>

Bollhofer, A., & Rosman, K. J. R. (2001). Isotopic source signatures for atmospheric lead: The

Northern Hemisphere. *Geochimica Et Cosmochimica Acta*, 65(11), 1727–1740.

[https://doi.org/10.1016/S0016-7037\(00\)00630-X](https://doi.org/10.1016/S0016-7037(00)00630-X)

Borrelli, P., Robinson, D. A., Fleischer, L. R., Lugato, E., Ballabio, C., Alewell, C., Meusburger, K.,

Modugno, S., Schütt, B., Ferro, V., Bagarello, V., Oost, K. Van, Montanarella, L., & Panagos,

P. (2017). An assessment of the global impact of 21st century land use change on soil erosion.

Nature Communications, 8(1), 1–13. <https://doi.org/10.1038/s41467-017-02142-7>

- Bouchard, F., Turner, K. W., MacDonald, L. A., Deakin, C., White, H., Farquharson, N., Medeiros, A. S., Wolfe, B. B., Hall, R. I., Pienitz, R., & Edwards, T. W. D. (2013). Vulnerability of shallow subarctic lakes to evaporate and desiccate when snowmelt runoff is low. *Geophysical Research Letters*, *40*(23), 6112–6117. <https://doi.org/10.1002/2013GL058635>
- Boudreau, B. P. (1999). Metals and models: Diagenetic modelling in freshwater lacustrine sediments. In *Journal of Paleolimnology* (Vol. 22, Issue 3, pp. 227–251). Springer Netherlands. <https://doi.org/10.1023/A:1008144029134>
- Boyle, J. (2001). Redox remobilization and the heavy metal record in lake sediments: a modelling approach. *Journal of Paleolimnology*, *26*(4), 423–431. <https://doi.org/10.1023/A:1012785525239>
- Boyle, J., Chiverrell, R., & Schillereff, D. (2015). Lacustrine Archives of Metals from Mining and Other Industrial Activities—A Geochemical Approach. In *Environmental Contaminants* (pp. 121–159). Springer, Dordrecht. https://link-springer-com.proxy.library.carleton.ca/chapter/10.1007/978-94-017-9541-8_7
- Bradl, H. B. (2005). Chapter 1 Sources and origins of heavy metals. *Interface Science and Technology*, *6*(C), 1–27. [https://doi.org/10.1016/S1573-4285\(05\)80020-1](https://doi.org/10.1016/S1573-4285(05)80020-1)
- Brännvall, M.-L., Bindler, R., Renberg, I., Emteryd, O., Bartnicki, J., & Billström, K. (1999). The Medieval Metal Industry Was the Cradle of Modern Large-Scale Atmospheric Lead Pollution in Northern Europe. *Environmental Science & Technology*, *33*(24), 4391–4395. <https://doi.org/10.1021/es990279n>
- Brännvall, M.-L., Bindler, R., Emteryd, O., & Renberg, I. (2001). Four thousand years of atmospheric lead pollution in northern Europe: a summary from Swedish lake sediments. *Journal of Paleolimnology*, *25*(4), 421–435. <https://doi.org/10.1023/A:1011186100081>

- Bromstad, M. J., Wrye, L. A., & Jamieson, H. E. (2017). The characterization, mobility, and persistence of roaster-derived arsenic in soils at Giant Mine, NWT. *Applied Geochemistry*, *82*, 102–118. <https://doi.org/10.1016/j.apgeochem.2017.04.004>
- Brown, C. D., & Johnstone, J. F. (2012). Once burned, twice shy: Repeat fires reduce seed availability and alter substrate constraints on *Picea mariana* regeneration. *Forest Ecology and Management*, *266*, 34–41. <https://doi.org/10.1016/j.foreco.2011.11.006>
- Burke, M. P., Hogue, T. S., Ferreira, M., Mendez, C. B., Navarro, B., Lopez, S., & Jay, J. A. (2010). The Effect of Wildfire on Soil Mercury Concentrations in Southern California Watersheds. *Water, Air, and Soil Pollution*, *212*(1–4), 369–385. <https://doi.org/10.1007/s11270-010-0351-y>
- Burke, S. M., Zimmerman, C. E., Branfireun, B. A., Koch, J. C., & Swanson, H. K. (2018). Patterns and controls of mercury accumulation in sediments from three thermokarst lakes on the Arctic Coastal Plain of Alaska. *Aquatic Sciences*, *80*(1), 1. <https://doi.org/10.1007/s00027-017-0553-0>
- Burton, C. A., Hoefen, T. M., Plumlee, G. S., Baumberger, K. L., Backlin, A. R., Gallegos, E., & Fisher, R. N. (2016). Trace Elements in Stormflow, Ash, and Burned Soil following the 2009 Station Fire in Southern California. *PLoS One*, *11*(5), e0153372. <https://doi.org/10.1371/journal.pone.0153372>
- Butcher, J. B., Nover, D., Johnson, T. E., & Clark, C. M. (2015). Sensitivity of lake thermal and mixing dynamics to climate change. *Climatic Change*, *129*(1–2), 295–305. <https://doi.org/10.1007/s10584-015-1326-1>
- Caldwell, C. A., Canavan, C. M., & Bloom, N. S. (2000). Potential effects of forest fire and storm flow on total mercury and methylmercury in sediments of an arid-lands reservoir. *The Science of the Total Environment*, *260*(1–3), 125–133. <http://www.ncbi.nlm.nih.gov/pubmed/11032121>

- Callaghan, T. V., Bergholm, F., Christensen, T. R., Jonasson, C., Kokfelt, U., & Johansson, M. (2010). A new climate era in the sub-Arctic: Accelerating climate changes and multiple impacts. *Geophysical Research Letters*, *37*(14). <https://doi.org/10.1029/2009GL042064>
- Callender, E. (2003). Heavy Metals in the Environment-Historical Trends. *Treatise on Geochemistry*, *9*, 612. <https://doi.org/10.1016/B0-08-043751-6/09161-1>
- Callender, Edward, & Granina, L. (1997). Geochemical mass balances of major elements in Lake Baikal. *Limnology and Oceanography*, *42*(1), 148–155. <https://doi.org/10.4319/lo.1997.42.1.0148>
- Campos, I., Vale, C., Abrantes, N., Keizer, J. J., & Pereira, P. (2015). Effects of wildfire on mercury mobilisation in eucalypt and pine forests. *CATENA*, *131*, 149–159. <https://doi.org/10.1016/j.catena.2015.02.024>
- Canadian Environmental Assessment Act*, (2012) (testimony of Government of Canada). <https://laws-lois.justice.gc.ca/eng/acts/C-15.21/>
- Canadian Hydrographic Service. (2005). *Canadian Hydrographic Service Chart 6369 [map]. (1:31 680)*.
- Carcaillet, C., Bergeron, Y., Richard, P. J. H., Fréchette, B., Gauthier, S., & Prairie, Y. T. (2001). Change of fire frequency in the eastern Canadian boreal forests during the Holocene: does vegetation composition or climate trigger the fire regime? *Journal of Ecology*, *89*(6), 930–946. <https://doi.org/10.1111/j.1365-2745.2001.00614.x>
- Carignan, J., & Gariépy, C. (1995). Isotopic composition of epiphytic lichens as a tracer of the sources of atmospheric lead emissions in southern Québec, Canada. *Geochimica et Cosmochimica Acta*, *59*(21), 4427–4433. [https://doi.org/10.1016/0016-7037\(95\)00302-G](https://doi.org/10.1016/0016-7037(95)00302-G)
- Carignan, J., & Sonke, J. (2010). The effect of atmospheric mercury depletion events on the net deposition flux around Hudson Bay, Canada. *Atmospheric Environment*, *44*(35), 4372–4379.

<https://doi.org/10.1016/j.atmosenv.2010.07.052>

Carrie, J., Wang, F., Sanei, H., Macdonald, R. W., Outridge, P. M., & Stern, G. A. (2010). Increasing Contaminant Burdens in an Arctic Fish, Burbot (*Lota lota*), in a Warming Climate.

Environmental Science & Technology, 44(1), 316–322. <https://doi.org/10.1021/es902582y>

Catalan, J., Pla-Rabés, S., Wolfe, A. P., Smol, J. P., Rühland, K. M., Anderson, N. J., Kopáček, J., Stuchlík, E., Schmidt, R., Koinig, K. A., Camarero, L., Flower, R. J., Heiri, O., Kamenik, C., Korhola, A., Leavitt, P. R., Psenner, R., & Renberg, I. (2013). Global change revealed by palaeolimnological records from remote lakes: a review. *Journal of Paleolimnology*, 49(3), 513–535.

<https://doi.org/10.1007/s10933-013-9681-2>

CCME, C. C. of M. of the E. (2002). *Canadian environmental quality guidelines* (Vol. 2). Canadian Council of Ministers of the Environment.

Cerrato, J. M., Blake, J. M., Hirani, C., Clark, A. L., Ali, A.-M. S., Artyushkova, K., Peterson, E., & Bixby, R. J. (2016). Wildfires and water chemistry: effect of metals associated with wood ash.

Environmental Science-Processes & Impacts, 18(8), 1078–1089.

<https://doi.org/10.1039/c6em00123h>

Certini, G. (2005). Effects of fire on properties of forest soils: a review. *Oecologia*, 143(1), 1–10.

<https://doi.org/10.1007/s00442-004-1788-8>

Chen, B., Stein, A. F., Maldonado, P. G., Sanchez de la Campa, A. M., Gonzalez-Castanedo, Y., Castell, N., & de la Rosa, J. D. (2013). Size distribution and concentrations of heavy metals in atmospheric aerosols originating from industrial emissions as predicted by the HYSPLIT model. *Atmospheric Environment*, 71, 234–244. <https://doi.org/10.1016/j.atmosenv.2013.02.013>

Chen, C., Amirbahman, A., Fisher, N., Harding, G., Lamborg, C., Nacci, D., & Taylor, D. (2008).

- Methylmercury in marine ecosystems: Spatial patterns and processes of production, bioaccumulation, and biomagnification. In *EcoHealth* (Vol. 5, Issue 4, pp. 399–408). Springer.
<https://doi.org/10.1007/s10393-008-0201-1>
- Chen, C. Y., Driscoll, C. T., Eagles-Smith, C. A., Eckley, C. S., Gay, D. A., Hsu-Kim, H., Keane, S. E., Kirk, J. L., Mason, R. P., Obrist, D., Selin, H., Selin, N. E., & Thompson, M. R. (2018). A Critical Time for Mercury Science to Inform Global Policy. *Environmental Science & Technology*, *52*(17), 9556–9561. <https://doi.org/10.1021/acs.est.8b02286>
- Chen, J., Hintelmann, H., Zheng, W., Feng, X., Cai, H., Wang, Z., Yuan, S., & Wang, Z. (2016). Isotopic evidence for distinct sources of mercury in lake waters and sediments. *Chemical Geology*, *426*(Supplement C), 33–44. <https://doi.org/10.1016/j.chemgeo.2016.01.030>
- Chen, L., Wang, H. H., Liu, J. F., Tong, Y. D., Ou, L. B., Zhang, W., Hu, D., Chen, C., & Wang, X. J. (2014). Intercontinental transport and deposition patterns of atmospheric mercury from anthropogenic emissions. *Atmospheric Chemistry and Physics*, *14*(18), 10163–10176.
<https://doi.org/10.5194/acp-14-10163-2014>
- Cheney, C. L., Eccles, K. M., Kimpe, L. E., Thienpont, J. R., Korosi, J. B., & Blais, J. M. (2020). Determining the effects of past gold mining using a sediment palaeotoxicity model. *Science of the Total Environment*, *718*, 137308. <https://doi.org/10.1016/j.scitotenv.2020.137308>
- Cheng, H., & Hu, Y. (2010). Lead (Pb) isotopic fingerprinting and its applications in lead pollution studies in China: A review. *Environmental Pollution*, *158*(5), 1134–1146.
<https://doi.org/10.1016/j.envpol.2009.12.028>
- Chételat, J., Amyot, M., Arp, P., Blais, J. M., Depew, D., Emmerton, C. A., Evans, M., Gamberg, M., Gantner, N., Girard, C., Graydon, J., Kirk, J., Lean, D., Lehnher, I., Muir, D., Nasr, M., J.

- Poulain, A., Power, M., Roach, P., ... van der Velden, S. (2015). Mercury in freshwater ecosystems of the Canadian Arctic: Recent advances on its cycling and fate. *Science of The Total Environment*, 509–510, 41–66. <https://doi.org/10.1016/j.scitotenv.2014.05.151>
- Chételat, J., Amyot, M., C G Muir, D., Black, J., Richardson, M., Evans, M., & Palmer, M. (2017). *Arsenic, antimony, and metal concentrations in water and sediment of Yellowknife Bay; Northwest Territories Geological Survey Open File 2017-05*.
- Chételat, J., Braune, B., Stow, J., & Tomlinson, S. (2015). Special issue on mercury in Canada's North: Summary and recommendations for future research. *Science of The Total Environment*, 509–510(Supplement C), 260–262. <https://doi.org/10.1016/j.scitotenv.2014.06.063>
- Chételat, J., Cott, P. A., Rosabal, M., Houben, A., McClelland, C., Belle Rose, E., & Amyot, M. (2019). Arsenic bioaccumulation in subarctic fishes of a mine-impacted bay on Great Slave Lake, Northwest Territories, Canada. *PLOS ONE*, 14(8), e0221361. <https://doi.org/10.1371/journal.pone.0221361>
- Child, A. W., Moore, B. C., Vervoort, J. D., & Beutel, M. W. (2018). Tracking long-distance atmospheric deposition of trace metal emissions from smelters in the upper Columbia River valley using Pb isotope analysis of lake sediments. *Environmental Science and Pollution Research*, 25(6), 5501–5513. <https://doi.org/10.1007/s11356-017-0914-1>
- Chow, T. J., & Earl, J. L. (1972). Lead Isotopes in North American Coals. *Science*, 176(4034), 510–511. <https://doi.org/10.1126/science.176.4034.510>
- Chrastny, V., Sillerova, H., Vitkova, M., Francova, A., Jehlicka, J., Kocourkova, J., Aspholm, P. E., Nilsson, L. O., Berglen, T. F., Jensen, H. K. B., & Komarek, M. (2018). Unleaded gasoline as a significant source of Pb emissions in the Subarctic. *Chemosphere*, 193, 230–236.

<https://doi.org/10.1016/j.chemosphere.2017.11.031>

Christophoridis, C., & Fytianos, K. (2006). Conditions Affecting the Release of Phosphorus from Surface Lake Sediments. *Journal of Environmental Quality*, 35(4), 1181–1192.

<https://doi.org/10.2134/jeq2005.0213>

Chuan, M. C., Shu, G. Y., & Liu, J. C. (1996). Solubility of heavy metals in a contaminated soil: Effects of redox potential and pH. *Water, Air, and Soil Pollution*, 90(3–4), 543–556.

<https://doi.org/10.1007/BF00282668>

Ci, Z., Peng, F., Xue, X., & Zhang, X. (2020). Permafrost Thaw Dominates Mercury Emission in Tibetan Thermokarst Ponds. *Environmental Science and Technology*, 54(9), 5456–5466.

<https://doi.org/10.1021/acs.est.9b06712>

Ciszewski, D., & Grygar, T. M. (2016). A Review of Flood-Related Storage and Remobilization of Heavy Metal Pollutants in River Systems. *Water, Air, and Soil Pollution*, 227(7), 1–19.

<https://doi.org/10.1007/s11270-016-2934-8>

Clackett, S. P., Porter, T. J., & Lehnerr, I. (2018). 400-Year Record of Atmospheric Mercury from Tree-Rings in Northwestern Canada. *Environmental Science and Technology*, 52(17), 9625–9633.

<https://doi.org/10.1021/acs.est.8b01824>

Clackett, S. P., Porter, T. J., & Lehnerr, I. (2021). The tree-ring mercury record of Klondike gold mining at Bear Creek, central Yukon. *Environmental Pollution*, 268, 115777.

<https://doi.org/10.1016/j.envpol.2020.115777>

Cliff, R. A., Hanser, A., & Hofmann, A. W. (1996). Evaluation of a 202pb _ 205pb Double Spike for High-Precision Lead Isotope Analysis. *Earth Processes: Reading the Isotopic Code*, 95, 429.

Cole, A., Steffen, A., Eckley, C., Narayan, J., Pilote, M., Tordon, R., Graydon, J., St. Louis, V., Xu,

- X., & Branfireun, B. (2014). A Survey of Mercury in Air and Precipitation across Canada: Patterns and Trends. *Atmosphere*, 5(3), 635–668. <https://doi.org/10.3390/atmos5030635>
- Coleman Wasik, J. K., Engstrom, D. R., Mitchell, C. P. J., Swain, E. B., Monson, B. A., Balogh, S. J., Jeremiason, J. D., Branfireun, B. A., Kolka, R. K., & Almendinger, J. E. (2015). The effects of hydrologic fluctuation and sulfate regeneration on mercury cycling in an experimental peatland. *Journal of Geophysical Research G: Biogeosciences*, 120(9), 1697–1715. <https://doi.org/10.1002/2015JG002993>
- Connan, O., Maro, D., Hébert, D., Roupsard, P., Goujon, R., Letellier, B., & Le Cavelier, S. (2013). Wet and dry deposition of particles associated metals (Cd, Pb, Zn, Ni, Hg) in a rural wetland site, Marais Vernier, France. *Atmospheric Environment*, 67, 394–403. <https://doi.org/10.1016/j.atmosenv.2012.11.029>
- Contaminants in Canada's North: State of Knowledge and Regional Highlights (2017) - Science.gc.ca.* (n.d.). Retrieved November 18, 2020, from http://www.science.gc.ca/eic/site/063.nsf/eng/h_97661.html
- Coogan, S. C. P., Robinne, F.-N., Jain, P., & Flannigan, M. D. (2019). Scientists' warning on wildfire — a Canadian perspective. *Canadian Journal of Forest Research*, 49(9), 1015–1023. <https://doi.org/10.1139/cjfr-2019-0094>
- Cooke, C. A., Balcom, P. H., Biester, H., & Wolfe, A. P. (2009). Over three millennia of mercury pollution in the Peruvian Andes. *Proceedings of the National Academy of Sciences*, 106(22), 8830–8834. <https://doi.org/10.1073/pnas.0900517106>
- Cooke, C. A., Martínez-Cortizas, A., Bindler, R., & Sexauer Gustin, M. (2020). Environmental archives of atmospheric Hg deposition – A review. *Science of the Total Environment*, 709, 134800.

<https://doi.org/10.1016/j.scitotenv.2019.134800>

Cott, P. A., Zajdlik, B. A., Palmer, M. J., & McPherson, M. D. (2016). Arsenic and mercury in lake whitefish and burbot near the abandoned Giant Mine on Great Slave Lake. *Journal of Great Lakes Research*, 42(2), 223–232. <https://doi.org/10.1016/j.jglr.2015.11.004>

Couillard, Y., Cattaneo, A., Gallon, C., & Courcelles, M. (2008). Sources and chronology of fifteen elements in the sediments of lakes affected by metal deposition in a mining area. *Journal of Paleolimnology*, 40(1), 97–114. <https://doi.org/10.1007/s10933-007-9146-6>

Courtney Mustaphi, C. J., Davis, E. L., Perreault, J. T., & Pisaric, M. F. J. (2015). Spatial variability of recent macroscopic charcoal deposition in a small montane lake and implications for reconstruction of watershed-scale fire regimes. *Journal of Paleolimnology*, 54(1), 71–86. <https://doi.org/10.1007/s10933-015-9838-2>

Cousens, B., Facey, K., & Falck, H. (2002). Geochemistry of the late Archean Banting Group, Yellowknife greenstone belt, Slave Province, Canada: Simultaneous melting of the upper mantle and juvenile mafic crust. In *Canadian Journal of Earth Sciences* (Vol. 39, Issue 11, pp. 1635–1656). NRC Research Press Ottawa, Canada . <https://doi.org/10.1139/e02-070>

Cousens, B., Falck, H., Ootes, L., Jackson, V., Mueller, W., Corcoran, P., Finnigan, C., van Hees, C. F., & Alcazar, A. (2006). 9. REGIONAL CORRELATIONS, TECTONIC SETTINGS, AND STRATIGRAPHIC SOLUTIONS IN THE YELLOWKNIFE GREENSTONE BELT AND ADJACENT AREAS FROM GEOCHEMICAL AND SM-ND ISOTOPIC ANALYSES OF VOLCANIC AND PLUTONIC ROCKS.

Cousens, B. L. (2000). Geochemistry of the Archean Kam group, yellowknife Greenstone Belt, Slave Province, Canada. *Journal of Geology*, 108(2), 181–197. <https://doi.org/10.1086/314397>

- Cousens, B. L., Falck, H., van Hees, E. H., Farrell, S., & Ootes, L. (2006). Pb isotopic compositions of sulphide minerals from the Yellowknife gold camp: Metal sources and timing of mineralization. *Geological Association of Canada Mineral Deposits Division*, 286–300.
- Couture, R.-M., Gobeil, C., & Tessier, A. (2008). Chronology of Atmospheric Deposition of Arsenic Inferred from Reconstructed Sedimentary Records. *Environmental Science & Technology*, 42(17), 6508–6513. <https://doi.org/10.1021/es800818j>
- Crusius, J., & Anderson, R. F. (1995). Evaluating the mobility of ^{137}Cs , $^{239+240}\text{Pu}$ and ^{210}Pb from their distributions in laminated lake sediments. *Journal of Paleolimnology*, 13(2), 119–141. <https://doi.org/10.1007/BF00678102>
- Csavina, J., Field, J., Taylor, M. P., Gao, S., Landázuri, A., Betterton, E. A., & Sáez, A. E. (2012). A review on the importance of metals and metalloids in atmospheric dust and aerosol from mining operations. In *Science of the Total Environment* (Vol. 433, pp. 58–73). Elsevier. <https://doi.org/10.1016/j.scitotenv.2012.06.013>
- Cumming, G. L., & Tsong, F. (1975). Variations in the isotopic composition of volatilized lead and the age of the western granodiorite, Yellowknife, Northwest Territories. *Canadian Journal of Earth Sciences*, 12(4), 558–573.
- Cuvier, A., Pourcelot, L., Probst, A., Prunier, J., & Le Roux, G. (2016). Trace elements and Pb isotopes in soils and sediments impacted by uranium mining. *Science of the Total Environment*, 566–567, 238–249. <https://doi.org/10.1016/j.scitotenv.2016.04.213>
- Dastoor, A., Ryzhkov, A., Durnford, D., Lehnerr, I., Steffen, A., & Morrison, H. (2015). Atmospheric mercury in the Canadian Arctic. Part II: Insight from modeling. In *Science of the Total Environment* (Vols. 509–510, pp. 16–27). Elsevier.

<https://doi.org/10.1016/j.scitotenv.2014.10.112>

- Davidson, C. I., Chu, L., Grimm, T. C., Nasta, M. A., & Qamoos, M. P. (1981). Wet and dry deposition of trace elements onto the Greenland ice sheet. *Atmospheric Environment (1967)*, *15*(8), 1429–1437. [https://doi.org/10.1016/0004-6981\(81\)90349-8](https://doi.org/10.1016/0004-6981(81)90349-8)
- Davies, S. J., Lamb, H. F., & Roberts, S. J. (2015). *Micro-XRF Core Scanning in Palaeolimnology: Recent Developments* (pp. 189–226). Springer, Dordrecht. https://doi.org/10.1007/978-94-017-9849-5_7
- Davis, R. B., Anderson, D. S., Dixit, S. S., Appleby, P. G., & Schauffler, M. (2006). Responses of two New Hampshire (USA) lakes to human impacts in recent centuries. *Journal of Paleolimnology*, *35*(4), 669–697. <https://doi.org/10.1007/s10933-005-4505-7>
- de Paiva Magalhães, D., da Costa Marques, M. R., Baptista, D. F., & Buss, D. F. (2015). Metal bioavailability and toxicity in freshwaters. In *Environmental Chemistry Letters* (Vol. 13, Issue 1, pp. 69–87). Springer Verlag. <https://doi.org/10.1007/s10311-015-0491-9>
- Dean, W. E. (1974). Determination of Carbonate and Organic Matter in Calcareous Sediments and Sedimentary Rocks by Loss on Ignition: Comparison With Other Methods. *Journal of Sedimentary Research*, *44*(1). <http://archives.datapages.com/data/sepm/journals/v42-46/data/044/044001/0242.htm>
- DeLong, S. B., Youberg, A. M., DeLong, W. M., & Murphy, B. P. (2018). Post-wildfire landscape change and erosional processes from repeat terrestrial lidar in a steep headwater catchment, Chiricahua Mountains, Arizona, USA. *Geomorphology*, *300*, 13–30. <https://doi.org/10.1016/j.geomorph.2017.09.028>
- Demers, J. D., Blum, J. D., & Zak, D. R. (2013). Mercury isotopes in a forested ecosystem:

- Implications for air-surface exchange dynamics and the global mercury cycle. *Global Biogeochemical Cycles*, 27(1), 222–238. <https://doi.org/10.1002/gbc.20021>
- Diaz-Somoano, M., Kylander, M. E., Lopez-Anton, M. A., Suarez-Ruiz, I., Martinez-Tarazona, M. R., Ferrat, M., Kober, B., & Weiss, D. J. (2009). Stable Lead Isotope Compositions In Selected Coals From Around The World And Implications For Present Day Aerosol Source Tracing. *Environmental Science & Technology*, 43(4), 1078–1085. <https://doi.org/10.1021/es801818r>
- Dietze, E., Brykała, D., Schreuder, L. T., Jazdzewski, K., Blarquez, O., Brauer, A., Dietze, M., Obremaska, M., Ott, F., Pieńczewska, A., Schouten, S., Hopmans, E. C., & Słowiński, M. (2019). Human-induced fire regime shifts during 19th century industrialization: A robust fire regime reconstruction using northern Polish lake sediments. *PLOS ONE*, 14(9), e0222011. <https://doi.org/10.1371/journal.pone.0222011>
- Dijkstra, J. A., Buckman, K. L., Ward, D., Evans, D. W., Dionne, M., & Chen, C. Y. (2013). Experimental and Natural Warming Elevates Mercury Concentrations in Estuarine Fish. *PLOS ONE*, 8(3), e58401. <https://doi.org/10.1371/journal.pone.0058401>
- Donahue, W. F., Allen, E. W., & Schindler, D. W. (2006). Impacts of coal-fired power plants on trace metals and polycyclic aromatic hydrocarbons (PAHs) in lake sediments in central Alberta, Canada. *Journal of Paleolimnology*, 35(1), 111–128. <https://doi.org/10.1007/s10933-005-7878-8>
- Dong, S., Gonzalez, R. O., Harrison, R. M., Green, D., North, R., Fowler, G., & Weiss, D. (2017). Isotopic signatures suggest important contributions from recycled gasoline, road dust and non-exhaust traffic sources for copper, zinc and lead in PM10 in London, United Kingdom. *Atmospheric Environment*, 165, 88–98. <https://doi.org/10.1016/j.atmosenv.2017.06.020>
- Douglas, T. A., & Blum, J. D. (2019). Mercury Isotopes Reveal Atmospheric Gaseous Mercury

Deposition Directly to the Arctic Coastal Snowpack. *Environmental Science and Technology Letters*, 6(4), 235–242. <https://doi.org/10.1021/acs.estlett.9b00131>

Drevnick, P. E., Cooke, C. A., Barraza, D., Blais, J. M., Coale, K. H., Cumming, B. F., Curtis, C. J., Das, B., Donahue, W. F., Eagles-Smith, C. A., Engstrom, D. R., Fitzgerald, W. F., Furl, C. V., Gray, J. E., Hall, R. I., Jackson, T. A., Laird, K. R., Lockhart, W. L., Macdonald, R. W., ... Wolfe, B. B. (2016). Spatiotemporal patterns of mercury accumulation in lake sediments of western North America. *Science of the Total Environment*, 568, 1157–1170. <https://doi.org/10.1016/j.scitotenv.2016.03.167>

Drevnick, P. E., Engstrom, D. R., Driscoll, C. T., Swain, E. B., Balogh, S. J., Kamman, N. C., Long, D. T., Muir, D. G. C., Parsons, M. J., Rolffhus, K. R., & Rossmann, R. (2012). Spatial and temporal patterns of mercury accumulation in lacustrine sediments across the Laurentian Great Lakes region. *Environmental Pollution*, 161, 252–260. <https://doi.org/10.1016/j.envpol.2011.05.025>

Driscoll, C. T., Mason, R. P., Chan, H. M., Jacob, D. J., & Pirrone, N. (2013). Mercury as a Global Pollutant: Sources, Pathways, and Effects. *Environmental Science & Technology*, 47(10), 4967–4983. <https://doi.org/10.1021/es305071v>

Dunnette, P. V, Higuera, P. E., McLauchlan, K. K., Derr, K. M., Briles, C. E., & Keefe, M. H. (2014). Biogeochemical impacts of wildfires over four millennia in a Rocky Mountain subalpine watershed. *New Phytologist*, 203(3), 900–912. <https://doi.org/10.1111/nph.12828>

Dunnington, D. W., Gregory, B. R. B., Spooner, I. S., White, C. E., & Gagnon, G. A. (2020). Evaluating the performance of calculated elemental measures in sediment archives. *Journal of Paleolimnology*, 64(2), 155–166. <https://doi.org/10.1007/s10933-020-00123-3>

- Dunnington, D. W., White, H., Spooner, I. S., Mallory, M. L., White, C., O'Driscoll, N. J., & McLellan, N. R. (2017). A paleolimnological archive of metal sequestration and release in the Cumberland Basin Marshes, Atlantic Canada. *FACETS*. <https://doi.org/10.1139/facets-2017-0004>
- Durnford, D, Dastoor, A., Figueras-Nieto, D., & Ryjkov, A. (2010). Long range transport of mercury to the Arctic and across Canada. *Atmospheric Chemistry & Physics*, *10*(13), 6063–6086. <https://doi.org/10.5194/acp-10-6063-2010>
- Durnford, D, Dastoor, A., Ryzhkov, A., Poissant, L., Pilote, M., & Figueras-Nieto, D. (2012). How relevant is the deposition of mercury onto snowpacks? - Part 2: A modeling study. *Atmospheric Chemistry and Physics*, *12*(19), 9251–9274. <https://doi.org/10.5194/acp-12-9251-2012>
- Durnford, Dorothy, & Dastoor, A. (2011). The behavior of mercury in the cryosphere: A review of what we know from observations. *Journal of Geophysical Research: Atmospheres*, *116*(D6), D06305. <https://doi.org/10.1029/2010JD014809>
- Ebel, B. A. (2013). Simulated unsaturated flow processes after wildfire and interactions with slope aspect. *Water Resources Research*, *49*(12), 8090–8107. <https://doi.org/10.1002/2013WR014129>
- ECCC, E. and C. C. C. (2019). *Canadian Air and Precipitation Monitoring Network (CAPMoN), Data files: AtmosphericPrecipitationChemistry-MajorIons-CAPMoN-AllSites-2007.csv (2007-2016)*. <https://doi.org/10.18164/72bef1bc-709a-4d57-99ea-6969b9728335>
- ECCC, E. and C. C. Canada. (2020). *Canada's Air Pollutant Emissions Inventory Report 2020*. <https://www.canada.ca/en/environment-climate-change/services/air-pollution/publications/emissions-inventory-report-2020.html>
- Eckley, C. S., Eagles-Smith, C., Tate, M. T., Kowalski, B., Danchy, R., Johnson, S. L., &

- Krabbenhoft, D. P. (2018). Stream Mercury Export in Response to Contemporary Timber Harvesting Methods (Pacific Coastal Mountains, Oregon, USA). *Environmental Science & Technology*, 52(4), 1971–1980. <https://doi.org/10.1021/acs.est.7b05197>
- Egozcue, J. J., Pawlowsky-Glahn, V., Mateu-Figueras, G., & Barceló-Vidal, C. (2003). Isometric Logratio Transformations for Compositional Data Analysis. *Mathematical Geology*, 35(3), 279–300. <https://doi.org/10.1023/A:1023818214614>
- Ek, A. S., & Renberg, I. (2001). Heavy metal pollution and lake acidity changes caused by one thousand years of copper mining at Falun, central Sweden. *Journal of Paleolimnology*, 26(1), 89–107. <https://doi.org/10.1023/A:1011112020621>
- Elbaz-Poulichet, F., Nagy, A., Cserny, T., & Pomogyi, P. (1996). Biogeochemistry of trace metals (Mn, Sr, Rb, Ba, Cu, Zn, Pb and Cd) in a River-Wetland-Lake system (Balaton Region, Hungary). *Aquatic Geochemistry*, 2(4), 379–402. <https://doi.org/10.1007/bf00115978>
- Engstrom, D. R., & Rose, N. L. (2013). A whole-basin, mass-balance approach to paleolimnology. *Journal of Paleolimnology*, 49(3), 333–347. <https://doi.org/10.1007/s10933-012-9675-5>
- Enrico, M., Le Roux, G., Heimbürger, L.-E., Van Beek, P., Souhaut, M., Chmeleff, J., & Sonke, J. E. (2017). Holocene Atmospheric Mercury Levels Reconstructed from Peat Bog Mercury Stable Isotopes. *Environmental Science & Technology*, 51(11), 5899–5906. <https://doi.org/10.1021/acs.est.6b05804>
- Enrico, M., Roux, G. Le, Maruszczak, N., Heimbürger, L.-E., Claustres, A., Fu, X., Sun, R., & Sonke, J. E. (2016). Atmospheric Mercury Transfer to Peat Bogs Dominated by Gaseous Elemental Mercury Dry Deposition. *Environmental Science & Technology*, 50(5), 2405–2412. <https://doi.org/10.1021/acs.est.5b06058>

- Evans, M., Muir, D., Brua, R. B., Keating, J., & Wang, X. (2013). Mercury Trends in Predatory Fish in Great Slave Lake: The Influence of Temperature and Other Climate Drivers. *Environmental Science & Technology*, 47(22), 12793–12801. <https://doi.org/10.1021/es402645x>
- Fawcett, S. E., Jamieson, H. E., Nordstrom, D. K., & McCleskey, R. B. (2015). Arsenic and antimony geochemistry of mine wastes, associated waters and sediments at the Giant Mine, Yellowknife, Northwest Territories, Canada. *Applied Geochemistry*, 62, 3–17. <https://doi.org/10.1016/j.apgeochem.2014.12.012>
- Ferrat, M., Weiss, D. J., Spiro, B., & Large, D. (2012). The inorganic geochemistry of a peat deposit on the eastern Qinghai-Tibetan Plateau and insights into changing atmospheric circulation in central Asia during the Holocene. *Geochimica et Cosmochimica Acta*, 91, 7–31. <https://doi.org/10.1016/j.gca.2012.05.028>
- Feyte, S., Gobeil, C., Tessier, A., & Cossa, D. (2012). Mercury dynamics in lake sediments. *Geochimica et Cosmochimica Acta*, 82, 92–112. <https://doi.org/10.1016/j.gca.2011.02.007>
- Feyte, S., Tessier, A., Gobeil, C., & Cossa, D. (2010). In situ adsorption of mercury, methylmercury and other elements by iron oxyhydroxides and organic matter in lake sediments. *Applied Geochemistry*, 25(7), 984–995. <https://doi.org/10.1016/j.apgeochem.2010.04.005>
- Finley, B. D., Swartzendruber, P. C., & Jaffe, D. A. (2009). Particulate mercury emissions in regional wildfire plumes observed at the Mount Bachelor Observatory. *Atmospheric Environment*, 43(38), 6074–6083. <https://doi.org/10.1016/j.atmosenv.2009.08.046>
- Fitzgerald, W. F., Engstrom, D. R., Lamborg, C. H., Tseng, C.-M., Balcom, P. H., & Hammerschmidt, C. R. (2005). Modern and Historic Atmospheric Mercury Fluxes in Northern Alaska: Global Sources and Arctic Depletion. *Environmental Science & Technology*, 39(2), 557–568.

<https://doi.org/10.1021/es049128x>

Fitzgerald, W. F., Engstrom, D. R., Mason, R. P., & Nater, E. A. (1998). The Case for Atmospheric Mercury Contamination in Remote Areas. *Environmental Science & Technology*, 32(1), 1–7.

<https://doi.org/10.1021/es970284w>

Flannigan, M. D., Logan, K. A., Amiro, B. D., Skinner, W. R., & Stocks, B. J. (2005). Future Area Burned in Canada. *Climatic Change*, 72(1–2), 1–16. <https://doi.org/10.1007/s10584-005-5935-y>

Flynn, W. (1968). Determination of Low Levels of Polonium-210 in Environmental Materials.

Analytica Chimica Acta, 43(2), 221-. [https://doi.org/10.1016/S0003-2670\(00\)89210-7](https://doi.org/10.1016/S0003-2670(00)89210-7)

Foster, I. D. L., & Charlesworth, S. M. (1996). Heavy metals in the hydrological cycle: Trends and explanation. *Hydrological Processes*, 10(2), 227–261. [https://doi.org/10.1002/\(SICI\)1099-1085\(199602\)10:2<227::AID-HYP357>3.0.CO;2-X](https://doi.org/10.1002/(SICI)1099-1085(199602)10:2<227::AID-HYP357>3.0.CO;2-X)

Fraser, A., Dastoor, A., & Ryjkov, A. (2018). How important is biomass burning in Canada to mercury contamination? *Atmospheric Chemistry and Physics*, 18(10), 7263–7286.

<https://doi.org/https://doi.org/10.5194/acp-18-7263-2018>

French, N. H. F., Graham, J., Whitman, E., & Bourgeau-Chavez, L. L. (2020). Quantifying surface severity of the 2014 and 2015 fires in the Great Slave Lake area of Canada. *International Journal of Wildland Fire*, 29(10), 892. <https://doi.org/10.1071/WF20008>

French, N. H. F., Jenkins, L. K., Loboda, T. V., Flannigan, M., Jandt, R., Bourgeau-Chavez, L. L., & Whitley, M. (2015). Fire in arctic tundra of Alaska: past fire activity, future fire potential, and significance for land management and ecology. *International Journal of Wildland Fire*, 24(8), 1045.

<https://doi.org/10.1071/WF14167>

Friedli, H R, Radke, L. F., Lu, J. Y., Banic, C. M., Leitch, W. R., & MacPherson, J. I. (2003).

Mercury emissions from burning of biomass from temperate North American forests: laboratory and airborne measurements. *Atmospheric Environment*, 37(2), 253–267.
[https://doi.org/10.1016/S1352-2310\(02\)00819-1](https://doi.org/10.1016/S1352-2310(02)00819-1)

Friedli, Hans R, Radke, L. F., & Lu, J. Y. (2001). Mercury in smoke from biomass fires. *Geophysical Research Letters*, 28(17), 3223–3226. <https://doi.org/10.1029/2000GL012704>

Furl, C. V., & Meredith, C. A. (2011). Mercury accumulation in sediment cores from three Washington state lakes: Evidence for local deposition from a coal-fired power plant. *Archives of Environmental Contamination and Toxicology*, 60(1), 26–33. <https://doi.org/10.1007/s00244-010-9530-5>

Gabrielli, P., & Vallelonga, P. (2015). Contaminant Records in Ice Cores. In J M Blais, M. R. Rosen, & J. P. Smol (Eds.), *Environmental Contaminants: Using Natural Archives to Track Sources and Long-Term Trends of Pollution* (Vol. 18, pp. 393–430). Springer.

Gallon, C., Tessier, A., Gobeil, C., & Alfaro-De La Torre, M. C. (2004). Modeling diagenesis of lead in sediments of a Canadian Shield lake 1. *Geochimica et Cosmochimica Acta*, 68(17), 3531–3545.
<https://doi.org/10.1016/j.gca.2004.02.013>

Gallon, C., Tessier, A., Gobeil, C., & Beaudin, L. (2005). Sources and chronology of atmospheric lead deposition to a Canadian Shield lake: Inferences from Pb isotopes and PAH profiles. *Geochimica et Cosmochimica Acta*, 69(13), 3199–3210. <https://doi.org/10.1016/j.gca.2005.02.028>

Gallon, C., Tessier, A., Gobeil, C., & Carignan, R. (2006). Historical Perspective of Industrial Lead Emissions to the Atmosphere from a Canadian Smelter. *Environmental Science & Technology*, 40(3), 741–747. <https://doi.org/10.1021/es051326g>

Galloway, J. M., Palmer, M., Jamieson, H. E., Patterson, R. T., Nasser, N., Falck, H., Macumber, A.

- L., Goldsmith, S. A., Sanei, H., Normandeau, P., Hadlari, T., Roe, H. M., Neville, L. A., & Lemay, D. (2015). Geochemistry of lakes across ecozones in the Northwest Territories and implications for the distribution of arsenic in the Yellowknife region. Part 1: Sediments. In *Part 1: Sediments: Vol. Open File* (Issue 1 .zip file). <https://doi.org/10.4095/296954>
- Galloway, J. M., Swindles, G. T., Jamieson, H. E., Palmer, M., Parsons, M. B., Sanei, H., Macumber, A. L., Timothy Patterson, R., & Falck, H. (2018). Organic matter control on the distribution of arsenic in lake sediments impacted by ~65years of gold ore processing in subarctic Canada. *The Science of the Total Environment*, 622–623, 1668–1679. <https://doi.org/10.1016/j.scitotenv.2017.10.048>
- Galloway, J. N., Thornton, J. D., Norton, S. A., Volchok, H. L., & McLean, R. A. N. (1982). Trace metals in atmospheric deposition: A review and assessment. *Atmospheric Environment* (1967), 16(7), 1677–1700. [https://doi.org/10.1016/0004-6981\(82\)90262-1](https://doi.org/10.1016/0004-6981(82)90262-1)
- Garcia, E., & Carignan, R. (1999). Impact of wildfire and clear-cutting in the boreal forest on methyl mercury in zooplankton. *Canadian Journal of Fisheries and Aquatic Sciences*, 56(2), 339–345. <https://doi.org/10.1139/cjfas-56-2-339>
- Garcia, E., & Carignan, R. (2005). Mercury concentrations in fish from forest harvesting and fire-impacted Canadian Boreal lakes compared using stable isotopes of nitrogen. *Environmental Toxicology and Chemistry*, 24(3), 685–693. <https://doi.org/10.1897/04-065R.1>
- Garcia, E., Carignan, R., & Lean, D. R. S. (2007). Seasonal and inter-annual variations in methyl mercury concentrations in zooplankton from boreal lakes impacted by deforestation or natural forest fires. *Environmental Monitoring and Assessment*, 131(1–3), 1–11. <https://doi.org/10.1007/s10661-006-9442-z>

- Ghotra, A., Lehnherr, I., Porter, T. J., & Pisaric, M. F. J. (2020). Tree-Ring Inferred Atmospheric Mercury Concentrations in the Mackenzie Delta (NWT, Canada) Peaked in the 1970s but Are Increasing Once More. *Cite This: ACS Earth Space Chem*, 2020, 457–466.
<https://doi.org/10.1021/acsearthspacechem.0c00003>
- Gibson, C. M., Chasmer, L. E., Thompson, D. K., Quinton, W. L., Flannigan, M. D., & Olefeldt, D. (2018). Wildfire as a major driver of recent permafrost thaw in boreal peatlands. *Nature Communications*, 9(1). <https://doi.org/10.1038/s41467-018-05457-1>
- Giesler, R., Clemmensen, K. E., Wardle, D. A., Klaminder, J., & Bindler, R. (2017). Boreal Forests Sequester Large Amounts of Mercury over Millennial Time Scales in the Absence of Wildfire. *Environmental Science & Technology*, 51(5), 2621–2627. <https://doi.org/10.1021/acs.est.6b06369>
- Givelet N, Roos-Barracough F, S. W. (2003). Predominant anthropogenic sources and rates of atmospheric mercury accumulation in southern Ontario recorded by peat cores from three bogs: compari... - PubMed - NCBI. *J Environ Monit.*, 5(6), 935–949. <https://www.ncbi.nlm.nih.gov/myaccess.library.utoronto.ca/pubmed/14710936>
- Givelet, N., Le Roux, G., Cheburkin, A., Chen, B., Frank, J., Goodsite, M. E., Kempter, H., Krachler, M., Noernberg, T., Rausch, N., Rheinberger, S., Roos-Barracough, F., Sapkota, A., Scholz, C., & Shotyk, W. (2004). Suggested protocol for collecting, handling and preparing peat cores and peat samples for physical, chemical, mineralogical and isotopic analyses. *Journal of Environmental Monitoring*, 6(5), 481–492. <https://doi.org/10.1039/b401601g>
- Goacher, W. (2014). Peat as an Archive of Remote Mercury Deposition in the Hudson Bay Lowlands, Ontario, Canada. *Electronic Thesis and Dissertation Repository*.
<https://ir.lib.uwo.ca/etd/2320>

- Gobeil, C., Macdonald, R. W., Smith, J. N., & Beaudin, L. (2001). Atlantic water flow pathways revealed by lead contamination in Arctic basin sediments. *Science*, *293*(5533), 1301–1304.
<https://doi.org/10.1126/science.1062167>
- Gobeil, Charles, Tessier, A., & Couture, R.-M. (2013). Upper Mississippi Pb as a mid-1800s chronostratigraphic marker in sediments from seasonally anoxic lakes in Eastern Canada. *Geochimica Et Cosmochimica Acta*, *113*, 125–135. <https://doi.org/10.1016/j.gca.2013.02.023>
- Goldman, C. R., Jassby, A. D., Amezaga, E. de, & de Amezaga, E. (1990). Forest fires, atmospheric deposition and primary productivity at Lake Tahoe, California-Nevada. *SIL Proceedings, 1922-2010*, *24*(1), 499–503. <https://doi.org/10.1080/03680770.1989.11898787>
- Goodsite, M. E., Outridge, P. M., Christensen, J. H., Dastoor, A., Muir, D., Travnikov, O., & Wilson, S. (2013). How well do environmental archives of atmospheric mercury deposition in the Arctic reproduce rates and trends depicted by atmospheric models and measurements? *Science of The Total Environment*, *452–453*, 196–207.
<https://doi.org/10.1016/j.scitotenv.2013.02.052>
- Gordon, J., Quinton, W., Branfireun, B. A., & Olefeldt, D. (2016). Mercury and methylmercury biogeochemistry in a thawing permafrost wetland complex, Northwest Territories, Canada. *Hydrological Processes*, *30*(20), 3627–3638. <https://doi.org/10.1002/hyp.10911>
- Gouin, T., MacKay, D., Jones, K. C., Harner, T., & Meijer, S. N. (2004). Evidence for the “grasshopper” effect and fractionation during long-range atmospheric transport of organic contaminants. *Environmental Pollution*, *128*(1–2), 139–148.
<https://doi.org/10.1016/j.envpol.2003.08.025>
- Gould, G. K., Liu, M., Barber, M. E., Cherkauer, K. A., Robichaud, P. R., & Adam, J. C. (2016). *The*

effects of climate change and extreme wildfire events on runoff erosion over a mountain watershed.

<https://doi.org/10.1016/j.jhydrol.2016.02.025>

Government of NWT with permission from Environment and Natural Resources, N. (2019). *Fire History*. <http://www.geomatics.gov.nt.ca/data.aspx?node=data>

Graydon, J. A., St. Louis, V. L., Hintelmann, H., Lindberg, S. E., Sandilands, K. A., Rudd, J. W. M., Kelly, C. A., Tate, M. T., Krabbenhoft, D. P., & Lehnherr, I. (2009). Investigation of uptake and retention of atmospheric Hg(II) by boreal forest plants using stable Hg isotopes. *Environmental Science and Technology*, 43(13), 4960–4966. <https://doi.org/10.1021/es900357s>

Gregory, B. R. B., Patterson, R. T., Reinhardt, E. G., Galloway, J. M., & Roe, H. M. (2019). An evaluation of methodologies for calibrating Itrax X-ray fluorescence counts with ICP-MS concentration data for discrete sediment samples. *Chemical Geology*, 521, 12–27. <https://doi.org/10.1016/j.chemgeo.2019.05.008>

Gross, B. H., Kreutz, K. J., Osterberg, E. C., McConnell, J. R., Handley, M., Wake, C. P., & Yalcin, K. (2012). Constraining recent lead pollution sources in the North Pacific using ice core stable lead isotopes. *Journal of Geophysical Research: Atmospheres*, 117(D16). <https://doi.org/10.1029/2011JD017270>

Guilizzoni, P. (2012). Palaeolimnology: an introduction. *Limnology of Rivers and Lakes-Encyclopedia of Life Support Systems (EOLSS)*, *Eols Publ. Accessed on January, 15, 2013.*

Guzman-Rangel, G., Martínez-Villegas, N., & Smolders, E. (2020). The labile fractions of metals and arsenic in mining-impacted soils are explained by soil properties and metal source characteristics. *Journal of Environmental Quality*, 49(2), 417–427. <https://doi.org/10.1002/jeq2.20055>

- Häder, D. P., Villafaña, V. E., & Helbling, E. W. (2014). Productivity of aquatic primary producers under global climate change. In *Photochemical and Photobiological Sciences* (Vol. 13, Issue 10, pp. 1370–1392). Royal Society of Chemistry. <https://doi.org/10.1039/c3pp50418b>
- Halbach, K., Mikkelsen, O., Berg, T., & Steinnes, E. (2017). The presence of mercury and other trace metals in surface soils in the Norwegian Arctic. *Chemosphere*, *188*, 567–574. <https://doi.org/10.1016/j.chemosphere.2017.09.012>
- Hanes, C. C., Wang, X., Jain, P., Parisien, M. A., Little, J. M., & Flannigan, M. D. (2019). Fire-regime changes in Canada over the last half century. *Canadian Journal of Forest Research*, *49*(3), 256–269. <https://doi.org/10.1139/cjfr-2018-0293>
- Hans Wedepohl, K. (1995). The composition of the continental crust. *Geochimica et Cosmochimica Acta*, *59*(7), 1217–1232. [https://doi.org/10.1016/0016-7037\(95\)00038-2](https://doi.org/10.1016/0016-7037(95)00038-2)
- Hansson, S. V., Claustres, A., Probst, A., De Vleeschouwer, F., Baron, S., Galop, D., Mazier, F., & Le Roux, G. (2017). Atmospheric and terrigenous metal accumulation over 3000 years in a French mountain catchment: Local vs distal influences. *Anthropocene*, *19*, 45–54. <https://doi.org/10.1016/j.ancene.2017.09.002>
- Harper, A. R., Santin, C., Doerr, S. H., Froyd, C. A., Albini, D., Otero, X. L., Viñas, L., & Pérez-Fernández, B. (2019). Chemical composition of wildfire ash produced in contrasting ecosystems and its toxicity to *Daphnia magna*. *International Journal of Wildland Fire*, *28*(10), 726. <https://doi.org/10.1071/WF18200>
- Hawryshyn, J., Ruehland, K. M., Quinlan, R., & Smol, J. P. (2012). Long-term water quality changes in a multiple-stressor system: a diatom-based paleolimnological study of Lake Simcoe (Ontario, Canada). *Canadian Journal of Fisheries and Aquatic Sciences*, *69*(1), 24–40.

<https://doi.org/10.1139/F2011-134>

- Haynes, K. M., Kane, E. S., Potvin, L., Lilleskov, E. A., Kolka, R. K., & Mitchell, C. P. J. (2017a). Gaseous mercury fluxes in peatlands and the potential influence of climate change. *Atmospheric Environment*, *154*, 247–259. <https://doi.org/10.1016/j.atmosenv.2017.01.049>
- Haynes, K. M., Kane, E. S., Potvin, L., Lilleskov, E. A., Kolka, R. K., & Mitchell, C. P. J. (2017b). Mobility and transport of mercury and methylmercury in peat as a function of changes in water table regime and plant functional groups. *Global Biogeochemical Cycles*, *31*(2), 233–244. <https://doi.org/10.1002/2016GB005471>
- Heiri, O., Lotter, A. F., & Lemcke, G. (2001). Loss on ignition as a method for estimating organic and carbonate content in sediments: reproducibility and comparability of results. *Journal of Paleolimnology*, *25*(1), 101–110. <https://doi.org/10.1023/A:1008119611481>
- Hermanns, Y. M., Cortizas, A. M., Arz, H., Stein, R., & Biester, H. (2013). Untangling the influence of in-lake productivity and terrestrial organic matter flux on 4,250 years of mercury accumulation in Lake Hambre, Southern Chile. *Journal of Paleolimnology*, *49*(4), 563–573. <https://doi.org/10.1007/s10933-012-9657-7>
- Hermanson, M. H. (1993). Historical accumulation of atmospherically derived pollutant trace metals in the arctic as measured in dated sediment cores. *Water Science and Technology*, *28*(8–9), 33–41. <https://doi.org/10.2166/wst.1993.0601>
- Higuera, P. E., Brubaker, L. B., Anderson, P. M., Hu, F. S., & Brown, T. A. (2009). Vegetation mediated the impacts of postglacial climate change on fire regimes in the south-central Brooks Range, Alaska. *Ecological Monographs*, *79*(2), 201–219. <https://doi.org/10.1890/07-2019.1>
- Higuera, P. E., Chipman, M. L., Barnes, J. L., Urban, M. A., & Hu, F. S. (2011). Variability of tundra

- fire regimes in Arctic Alaska: Millennial-scale patterns and ecological implications. *Ecological Applications*, 21(8), 3211–3226. <https://doi.org/10.1890/11-0387.1>
- Higuera, P. E., Gavin, D. G., Bartlein, P. J., & Hallett, D. J. (2011). Peak detection in sediment–charcoal records: impacts of alternative data analysis methods on fire-history interpretations. *International Journal of Wildland Fire*, 19(8), 996–1014. <https://doi.org/10.1071/WF09134>
- Hillman, A. L., Abbott, M. B., Valero-Garces, B. L., Morellon, M., Barreiro-Lostres, F., & Bain, D. J. (2017). Lead pollution resulting from Roman gold extraction in northwestern Spain. *Holocene*, 27(10), 1465–1474. <https://doi.org/10.1177/0959683617693903>
- Hocking, D., Kuchar, P., Plambeck, J. A., & Smith, R. A. (1978). The Impact of Gold Smelter Emissions on Vegetation and Soils of a Sub-Arctic Forest-Tundra Transition Ecosystem. *Journal of the Air Pollution Control Association*, 28(2), 133–137. <https://doi.org/10.1080/00022470.1978.10470580>
- Hojdová, M., Navrátil, T., Rohovec, J., Žák, K., Vaněk, A., Chrastný, V., Bače, R., & Svoboda, M. (2011). Changes in Mercury Deposition in a Mining and Smelting Region as Recorded in Tree Rings. *Water, Air, & Soil Pollution*, 216(1–4), 73–82. <https://doi.org/10.1007/s11270-010-0515-9>
- Holmes, C. D., Jacob, D. J., Corbitt, E. S., Mao, J., Yang, X., Talbot, R., & Slemr, F. (2010). Global atmospheric model for mercury including oxidation by bromine atoms. *Atmos. Chem. Phys.*, 10(24), 12037–12057. <https://doi.org/10.5194/acp-10-12037-2010>
- Hong, S., Candelone, J.-P. P., Patterson, C. C., & Boutron, C. F. (1994). Greenland Ice Evidence of Hemispheric Lead Pollution Two Millennia Ago by Greek and Roman Civilizations. *Science*, 265(5180), 1841–1843. <https://doi.org/10.1126/science.265.5180.1841>

- Houben, A. J., D'Onofrio, R., Kokelj, S. V., & Blais, J. M. (2016). Factors Affecting Elevated Arsenic and Methyl Mercury Concentrations in Small Shield Lakes Surrounding Gold Mines near the Yellowknife, NT, (Canada) Region. *PLoS ONE*, *11*(4), e0150960.
<https://doi.org/10.1371/journal.pone.0150960>
- Houle, D., Marty, C., Augustin, F., Dermont, G., & Gagnon, C. (2020). Impact of Climate Change on Soil Hydro-Climatic Conditions and Base Cations Weathering Rates in Forested Watersheds in Eastern Canada. *Frontiers in Forests and Global Change*, *3*, 111.
<https://doi.org/10.3389/ffgc.2020.535397>
- Hu, F. S., Higuera, P. E., Duffy, P., Chipman, M. L., Rocha, A. V., Young, A. M., Kelly, R., & Dietze, M. C. (2015). Arctic tundra fires: natural variability and responses to climate change. *Frontiers in Ecology and the Environment*, *13*(7), 369–377. <https://doi.org/10.1890/150063>
- Hu, F. S., Higuera, P. E., Walsh, J. E., Chapman, W. L., Duffy, P. A., Brubaker, L. B., & Chipman, M. L. (2010). Tundra burning in Alaska: Linkages to climatic change and sea ice retreat. *Journal of Geophysical Research: Biogeosciences*, *115*(G4). <https://doi.org/10.1029/2009JG001270>
- Hughes, M. K. (1981). Cycling of trace metals in ecosystems. In *Effect of heavy metal pollution on plants* (pp. 95–118). Springer.
- Hutchinson, T. C., Aufreiter, S., & Hancock, R. G. V. (1982). Arsenic pollution in the Yellowknife Area from gold smelter activities. *Journal of Radioanalytical Chemistry*, *71*(1–2), 59–73.
<https://doi.org/10.1007/BF02516141>
- Hwang, H. M., Fiala, M. J., Park, D., & Wade, T. L. (2016). Review of pollutants in urban road dust and stormwater runoff: part 1. Heavy metals released from vehicles. In *International Journal of Urban Sciences* (Vol. 20, Issue 3, pp. 334–360). Routledge.

<https://doi.org/10.1080/12265934.2016.1193041>

Ice, G. G., Neary, D. G., & Adams, P. W. (2004). Effects of Wildfire on Soils and Watershed Processes. *Journal of Forestry*, 102(6), 16–20.

INAC, (Indian and Northern Affairs Canada). (2007). *Giant Mine Remediation Plan. Report of the Giant Mine Remediation Project Team.*

INAC, Indian and Northern Affairs Canada. (1984). The Whitehorse Copper Belt - A Compilation - Publication Details - Yukon Geological Survey. In *Open File 1984*.
<http://data.geology.gov.yk.ca/Reference/42011#InfoTab>

INAC, Indigenous and Northern Affairs Canada. (2013). *History of Giant Mine*. <https://www.aadnc-aandc.gc.ca/eng/1100100027388/1100100027390>

Isley, C. F., & Taylor, M. P. (2020). Atmospheric remobilization of natural and anthropogenic contaminants during wildfires. *Environmental Pollution*, 267, 115400.
<https://doi.org/10.1016/j.envpol.2020.115400>

Ito de Lima, C. A., de Almeida, M. G., Pestana, I. A., Bastos, W. R., Nery do Nascimento Recktenvald, M. C., Magalhaes de Souza, C. M., & Pedrosa, P. (2017). Impact of Land Use on the Mobility of Hg Species in Different Compartments of a Tropical Watershed in Brazil. *Archives of Environmental Contamination and Toxicology*, 73(4), 578–592.
<https://doi.org/10.1007/s00244-017-0449-y>

Jamieson, H.E., Maitland, K. M., Oliver, J. T., & Palmer, M. J. (2017). Regional distribution of arsenic in near-surface soils in the Yellowknife area; *Northwest Territories Geological Survey; NWT Open File*.

Jamieson, Heather E. (2014). The Legacy of Arsenic Contamination from Mining and Processing

Refractory Gold Ore at Giant Mine, Yellowknife, Northwest Territories, Canada. *Reviews in Mineralogy and Geochemistry*, 79(1), 533–551. <https://doi.org/10.2138/rmg.2014.79.12>

Jarsjö, J., Andersson-Sköld, Y., Fröberg, M., Pietronó, J., Borgström, R., Löf, Å., & Kleja, D. B. (2020). Projecting impacts of climate change on metal mobilization at contaminated sites: Controls by the groundwater level. *Science of the Total Environment*, 712, 135560. <https://doi.org/10.1016/j.scitotenv.2019.135560>

Jensen, A. M., Scanlon, T. M., & Riscassi, A. L. (2017). Emerging investigator series: the effect of wildfire on streamwater mercury and organic carbon in a forested watershed in the southeastern United States. *Environmental Science: Processes & Impacts*, 19(12), 1505–1517. <https://doi.org/10.1039/C7EM00419B>

Ji, X., Abakumov, E., Antcibor, I., Tomashunas, V., Knoblauch, C., Zubzycki, S., & Pfeiffer, E. M. (2019). Influence of Anthropogenic Activities on Metals in Arctic Permafrost: A Characterization of Benchmark Soils on the Yamal and Gydan Peninsulas in Russia. *Archives of Environmental Contamination and Toxicology*, 76(4), 540–553. <https://doi.org/10.1007/s00244-019-00607-y>

Jin, Y., Randerson, J. T., Goetz, S. J., Beck, P. S. A., Loranty, M. M., & Goulden, M. L. (2012). The influence of burn severity on postfire vegetation recovery and albedo change during early succession in North American boreal forests. *Journal of Geophysical Research: Biogeosciences*, 117(1), 1036. <https://doi.org/10.1029/2011JG001886>

Johnson, E.A., Miyanishi, K., & Weir, J. M. H. (1998). Wildfires in the western Canadian boreal forest: Landscape patterns and ecosystem management. *Journal of Vegetation Science*, 9(4), 603–610. <https://doi.org/10.2307/3237276>

- Johnson, Edward A. (1992). Fire and Vegetation Dynamics: Studies from the North American Boreal Forest. In *Cambridge Studies in Ecology*. Cambridge University Press.
<https://doi.org/DOI:10.1017/CBO9780511623516>
- Johnson, K. P., Blum, J. D., Keeler, G. J., & Douglas, T. A. (2008). Investigation of the deposition and emission of mercury in arctic snow during an atmospheric mercury depletion event. *Journal of Geophysical Research: Atmospheres*, 113(D17), D17304. <https://doi.org/10.1029/2008JD009893>
- Johnston, C. A. (1991). Sediment and nutrient retention by freshwater wetlands: Effects on surface water quality. *Critical Reviews in Environmental Control*, 21(5–6), 491–565.
<https://doi.org/10.1080/10643389109388425>
- Kamman, N. C., & Engstrom, D. R. (2002). Historical and present fluxes of mercury to Vermont and New Hampshire lakes inferred from 210Pb dated sediment cores. *Atmospheric Environment*, 36(10), 1599–1609. [https://doi.org/10.1016/S1352-2310\(02\)00091-2](https://doi.org/10.1016/S1352-2310(02)00091-2)
- Kelly, E. N., Schindler, D. W., Louis, V. L. S., Donald, D. B., & Vladicka, K. E. (2006). Forest fire increases mercury accumulation by fishes via food web restructuring and increased mercury inputs. *Proceedings of the National Academy of Sciences*, 103(51), 19380–19385.
<https://doi.org/10.1073/pnas.0609798104>
- Kelly, R., Chipman, M. L., Higuera, P. E., Stefanova, I., Brubaker, L. B., & Hu, F. S. (2013). Recent burning of boreal forests exceeds fire regime limits of the past 10,000 years. *Proceedings of the National Academy of Sciences of the United States of America*, 110(32), 13055–13060.
<https://doi.org/10.1073/pnas.1305069110>
- Kemp, A. C., Sommerfield, C. K., Vane, C. H., Horton, B. P., Chenery, S., Anisfeld, S., & Nikitina, D. (2012). Use of lead isotopes for developing chronologies in recent salt-marsh sediments.

Quaternary Geochronology, 12, 40–49. <https://doi.org/10.1016/j.quageo.2012.05.004>

Kerr, D. E. (2006). Surficial geology and exploration geochemistry, Yellowknife area. *Gold in the Yellowknife Greenstone Belt; Northwest Territories: Results of the EXTECH III Multidisciplinary Research Project*, 301–324.

Kirk, J., & Gleason, A. (2015). Tracking Long-range Atmospheric Transport of Contaminants in Arctic Regions Using Lake Sediments. In *Environmental Contaminants* (pp. 223–262). Springer, Dordrecht. https://link-springer-com.proxy.library.carleton.ca/chapter/10.1007/978-94-017-9541-8_10

Kirk, J. L., Lehnherr, I., Andersson, M., Braune, B. M., Chan, L., Dastoor, A. P., Durnford, D., Gleason, A. L., Loseto, L. L., Steffen, A., & St Louis, V. L. (2012). Mercury in Arctic marine ecosystems: Sources, pathways and exposure. *Environmental Research*, 119, 64–87. <https://doi.org/10.1016/j.envres.2012.08.012>

Kirk, J. L., Muir, D. C. G., Antoniades, D., Douglas, M. S. V., Evans, M. S., Jackson, T. A., Kling, H., Lamoureux, S., Lim, D. S. S., Pienitz, R., Smol, J. P., Stewart, K., Wang, X., & Yang, F. (2011). Response to Comment on Climate Change and Mercury Accumulation in Canadian High and Subarctic Lakes. *Environmental Science & Technology*, 45(15), 6705–6706. <https://doi.org/10.1021/es202053c>

Kitzberger, T., Falk, D. A., Westerling, A. L., & Swetnam, T. W. (2017). Direct and indirect climate controls predict heterogeneous early-mid 21st century wildfire burned area across western and boreal North America. *PLOS ONE*, 12(12), e0188486. <https://doi.org/10.1371/journal.pone.0188486>

Klaminder, J., Bindler, R., Emteryd, O., & Renberg, I. (2005). Uptake and recycling of lead by boreal

- forest plants: Quantitative estimates from a site in northern Sweden. *Geochimica Et Cosmochimica Acta*, 69(10), 2485–2496. <https://doi.org/10.1016/j.gca.2004.11.013>
- Klaminder, Jonatan, Bindler, R., Laudon, H., Bishop, K., Emteryd, O., & Renberg, I. (2006). Flux rates of atmospheric lead pollution within soils of a small catchment in Northern Sweden and their implications for future stream water quality. *Environmental Science and Technology*, 40(15), 4639–4645. <https://doi.org/10.1021/es0520666>
- Klaminder, Jonatan, Hammarlund, D., Kokfelt, U., Vonk, J. E., & Bigler, C. (2010). Lead Contamination of Subarctic Lakes and Its Response to Reduced Atmospheric Fallout: Can the Recovery Process Be Counteracted by the Ongoing Climate Change? *Environmental Science & Technology*, 44(7), 2335–2340. <https://doi.org/10.1021/es903025z>
- Klemt, W. H., Kay, M. L., Wiklund, J. A., Wolfe, B. B., & Hall, R. I. (2020). Assessment of vanadium and nickel enrichment in Lower Athabasca River floodplain lake sediment within the Athabasca Oil Sands Region (Canada). *Environmental Pollution*, 114920. <https://doi.org/10.1016/j.envpol.2020.114920>
- Kohlenberg, A. J., Turetsky, M. R., Thompson, D. K., Branfireun, B. A., & Mitchell, C. P. J. (2018). Controls on boreal peat combustion and resulting emissions of carbon and mercury. *Environmental Research Letters*, 13(3), 35005. <https://doi.org/10.1088/1748-9326/aa9ea8>
- Kokfelt, U., RoséN, P., Schoning, K., Christensen, T. R., Förster, J., Karlsson, J., Reuss, N., Rundgren, M., Callaghan, T. V., Jonasson, C., & Hammarlund, D. (2009). Ecosystem responses to increased precipitation and permafrost decay in subarctic Sweden inferred from peat and lake sediments. *Global Change Biology*, 15(7), 1652–1663. <https://doi.org/10.1111/j.1365-2486.2009.01880.x>

Kolka, R K. (2012). Effects of fire and fuels management on water quality in eastern North America.

In: LaFayette, Russell; Brooks, Maureen T.; Potyondy, John P.; Audin, Lisa; Krieger, Suzanne L.; Trettin, Carl C. Eds. 2012. Cumulative Watershed Effects of Fuel Management in the Eastern United States. Gen. Tech. Rep. SRS-161. Asheville, NC: U.S. Departm, 161, 282–293.

<https://www.fs.usda.gov/treearch/pubs/41101>

Kolka, Randall K, Sturtevant, B. R., Miesel, J. R., Singh, A., Wolter, P. T., Fraver, S., DeSutter, T.

M., & Townsend, P. A. (2017). Emissions of forest floor and mineral soil carbon, nitrogen and mercury pools and relationships with fire severity for the Pagami Creek Fire in the Boreal Forest of northern Minnesota. *International Journal of Wildland Fire*, 26(4), 296.

<https://doi.org/10.1071/WF16128>

Komárek, M., Ettler, V., Chrástný, V., & Mihaljevič, M. (2008). Lead isotopes in environmental sciences: A review. *Environment International*, 34(4), 562–577.

<https://doi.org/10.1016/j.envint.2007.10.005>

Korosi, J. B., Griffiths, K., Smol, J. P., & Blais, J. M. (2018). Trends in historical mercury deposition inferred from lake sediment cores across a climate gradient in the Canadian High Arctic.

Environmental Pollution, 241, 459–467. <https://doi.org/10.1016/j.envpol.2018.05.049>

Krawchuk, M. A., Moritz, M. A., Parisien, M.-A., Van Dorn, J., & Hayhoe, K. (2009). Global Pyrogeography: the Current and Future Distribution of Wildfire. *PLoS ONE*, 4(4), e5102.

<https://doi.org/10.1371/journal.pone.0005102>

Kristensen, Louise J, & Taylor, M. P. (2012). Fields and Forests in Flames: Lead and Mercury

Emissions from Wildfire Pyrogenic Activity. *Environmental Health Perspectives*, 120(2), a56–a57.

<https://doi.org/10.1289/ehp.1104672>

- Kristensen, Louise J, Taylor, M. P., Odigie, K. O., Hibdon, S. A., & Flegal, A. R. (2014). Lead isotopic compositions of ash sourced from Australian bushfires. *Environmental Pollution*, *190*, 159–165. <https://doi.org/10.1016/j.envpol.2014.03.025>
- Kristensen, Louise Jane, Taylor, M. P., & Flegal, A. R. (2017). An odyssey of environmental pollution: The rise, fall and remobilisation of industrial lead in Australia. *Applied Geochemistry*, *83*, 3–13. <https://doi.org/10.1016/j.apgeochem.2017.02.007>
- Kumar, A., Wu, S., Huang, Y., Liao, H., & Kaplan, J. O. (2018). Mercury from wildfires: Global emission inventories and sensitivity to 2000–2050 global change. *Atmospheric Environment*, *173*, 6–15. <https://doi.org/10.1016/j.atmosenv.2017.10.061>
- Kumar, S. P., & Patterson, E. (2009). Assessment of metal concentration in the sediment cores of Manakudy estuary, south west coast of India. *Indian Journal of Marine Sciences*, *38*(2), 235–248. <https://www-scopus-com.proxy.library.carleton.ca/record/display.uri?eid=2-s2.0-69749118040&origin=inward&txGid=a2836e778a437ab930fa65ae32dfef2f>
- Kurek, J., Kirk, J. L., Muir, D. C. G., Wang, X., Evans, M. S., & Smol, J. P. (2013). Legacy of a half century of Athabasca oil sands development recorded by lake ecosystems. *Proceedings of the National Academy of Sciences*, *110*(5), 1761. <https://doi.org/10.1073/pnas.1217675110>
- Laing, J., & Binyamin, J. (2013). Climate Change Effect on Winter Temperature and Precipitation of Yellowknife, Northwest Territories, Canada from 1943 to 2011. *American Journal of Climate Change*, *02*(04), 275–283. <https://doi.org/10.4236/ajcc.2013.24027>
- Landers, D. H., Gubala, C., Verta, M., Lucotte, M., Johansson, K., Vlasova, T., & Lockhart, W. L. (1998). Using lake sediment mercury flux ratios to evaluate the regional and continental dimensions of mercury deposition in arctic and boreal ecosystems. *Atmospheric Environment*,

32(5), 919–928. [https://doi.org/10.1016/S1352-2310\(97\)00116-7](https://doi.org/10.1016/S1352-2310(97)00116-7)

Laperriere, L., Fallu, M.-A., Hausmann, S., Pienitz, R., & Muir, D. (2008). Paleolimnological evidence of mining and demographic impacts on Lac Dauriat, schefferville (subarctic Quebec, Canada). *Journal of Paleolimnology*, 40(1), 309–324. <https://doi.org/10.1007/s10933-007-9162-6>

Lehman, J. T. (1975). Reconstructing the rate of accumulation of lake sediment: The effect of sediment focusing. *Quaternary Research*, 5(4), 541–550. [https://doi.org/10.1016/0033-5894\(75\)90015-0](https://doi.org/10.1016/0033-5894(75)90015-0)

Lehnherr, I. (2014). Methylmercury biogeochemistry: A review with special reference to Arctic aquatic ecosystems. In *Environmental Reviews* (Vol. 22, Issue 3, pp. 229–243). National Research Council of Canada. <https://doi.org/10.1139/er-2013-0059>

Leys, B., Higuera, P. E., McLauchlan, K. K., & Dunnette, P. V. (2016). Wildfires and geochemical change in a subalpine forest over the past six millennia. *Environmental Research Letters*, 11(12), 125003. <https://doi.org/10.1088/1748-9326/11/12/125003>

Lima, A. L., Bergquist, B. A., Boyle, E. A., Reuer, M. K., Dudas, F. O., Reddy, C. M., & Eglinton, T. I. (2005). High-resolution historical records from Pettaquamscutt River basin sediments: 2. Pb isotopes reveal a potential new stratigraphic marker. *Geochimica Et Cosmochimica Acta*, 69(7), 1813–1824. <https://doi.org/10.1016/j.gca.2004.10.008>

Lindaas, J., Pollack, I. B., Garofalo, L. A., Pothier, M. A., Farmer, D. K., Kreidenweis, S. M., Campos, T. L., Flocke, F., Weinheimer, A. J., Montzka, D. D., Tyndall, G. S., Palm, B. B., Peng, Q., Thornton, J. A., Permar, W., Wielgasz, C., Hu, L., Ottmar, R. D., Restaino, J. C., ... Fischer, E. V. (2021). Emissions of Reactive Nitrogen From Western U.S. Wildfires During Summer 2018. *Journal of Geophysical Research: Atmospheres*, 126(2).

<https://doi.org/10.1029/2020jd032657>

Liu, R., Wang, Q., Lu, X., Fang, F., & Wang, Y. (2003). Distribution and speciation of mercury in the peat bog of Xiaoxing'an Mountain, northeastern China. *Environmental Pollution*, *124*(1), 39–46. [https://doi.org/10.1016/S0269-7491\(02\)00432-3](https://doi.org/10.1016/S0269-7491(02)00432-3)

Liu, X., Jiang, S., Zhang, P., & Xu, L. (2012a). Effect of recent climate change on Arctic Pb pollution: A comparative study of historical records in lake and peat sediments. *Environmental Pollution*, *160*(1), 161–168. <https://doi.org/10.1016/j.envpol.2011.09.019>

Liu, X., Jiang, S., Zhang, P., & Xu, L. (2012b). Effect of recent climate change on Arctic Pb pollution: A comparative study of historical records in lake and peat sediments. *Environmental Pollution*, *160*, 161–168. <https://doi.org/10.1016/j.envpol.2011.09.019>

Lockhart, W. L., Macdonald, R. W., Outridge, P. M., Wilkinson, P., DeLaronde, J. B., & Rudd, J. W. M. (2000). Tests of the fidelity of lake sediment core records of mercury deposition to known histories of mercury contamination. *Science of The Total Environment*, *260*(1–3), 171–180. [https://doi.org/10.1016/S0048-9697\(00\)00561-1](https://doi.org/10.1016/S0048-9697(00)00561-1)

Loiko, S. V., Pokrovsky, O. S., Raudina, T. V., Lim, A., Kolesnichenko, L. G., Shirokova, L. S., Vorobyev, S. N., & Kirpotin, S. N. (2017). Abrupt permafrost collapse enhances organic carbon, CO₂, nutrient and metal release into surface waters. *Chemical Geology*, *471*, 153–165. <https://doi.org/10.1016/j.chemgeo.2017.10.002>

Löwemark, L., Bloemsa, M., Croudace, I., Daly, J. S., Edwards, R. J., Francus, P., Galloway, J. M., Gregory, B. R. B., Steven Huang, J. J., Jones, A. F., Kylander, M., Luo, Y., Maclachlan, S., Ohlendorf, C., Patterson, R. T., Pearce, C., Profe, J., Reinhardt, E. G., Stranne, C., ... Turner, J. N. (2019). Practical guidelines and recent advances in the Itrax XRF core-scanning

- procedure. *Quaternary International*, 514, 16–29. <https://doi.org/10.1016/j.quaint.2018.10.044>
- Luo, X., Bing, H., Luo, Z., Wang, Y., & Jin, L. (2019). Impacts of atmospheric particulate matter pollution on environmental biogeochemistry of trace metals in soil-plant system: A review. In *Environmental Pollution* (Vol. 255, p. 113138). Elsevier Ltd.
<https://doi.org/10.1016/j.envpol.2019.113138>
- MacDonald, L. A., Wiklund, J. A., Elmes, M. C., Wolfe, B. B., & Hall, R. I. (2016). Paleolimnological assessment of riverine and atmospheric pathways and sources of metal deposition at a floodplain lake (Slave River Delta, Northwest Territories, Canada). *Science of The Total Environment*, 544(Supplement C), 811–823. <https://doi.org/10.1016/j.scitotenv.2015.11.173>
- Macdonald, R. W., Harner, T., & Fyfe, J. (2005). Recent climate change in the Arctic and its impact on contaminant pathways and interpretation of temporal trend data. *Science of The Total Environment*, 342(1), 5–86. <https://doi.org/10.1016/j.scitotenv.2004.12.059>
- Mack, M. C., Bret-Harte, M. S., Hollingsworth, T. N., Jandt, R. R., Schuur, E. A. G., Shaver, G. R., & Verbyla, D. L. (2011). Carbon loss from an unprecedented Arctic tundra wildfire. *Nature*, 475(7357), 489–492. <https://doi.org/10.1038/nature10283>
- MacMillan, G. A., Girard, C., Chételat, J., Laurion, I., & Amyot, M. (2015). High Methylmercury in Arctic and Subarctic Ponds is Related to Nutrient Levels in the Warming Eastern Canadian Arctic. *Environmental Science and Technology*, 49(13), 7743–7753.
<https://doi.org/10.1021/acs.est.5b00763>
- Makepeace, D. K., Smith, D. W., & Stanley, S. J. (1995). Urban Stormwater Quality: Summary of Contaminant Data. *Critical Reviews in Environmental Science and Technology*, 25(2), 93–139.
<https://doi.org/10.1080/10643389509388476>

- Makinen, J., Kauppila, T., Loukola-Ruskeeniemi, K., Mattila, J., & Miettinen, J. (2010). Impacts of point source and diffuse metal and nutrient loading on three northern boreal lakes. *Journal of Geochemical Exploration*, 104(1–2), 47–60. <https://doi.org/10.1016/j.gexplo.2009.11.007>
- Mamun, A. Al, Cheng, I., Zhang, L., Dabek-Zlotorzynska, E., & Charland, J. P. (2020). Overview of size distribution, concentration, and dry deposition of airborne particulate elements measured worldwide. In *Environmental Reviews* (Vol. 28, Issue 1, pp. 77–88). Canadian Science Publishing. <https://doi.org/10.1139/er-2019-0035>
- Marcantonio, F., Zimmerman, A., Xu, Y. F., & Canuel, E. (2002). A Pb isotope record of mid-Atlantic US atmospheric Pb emissions in Chesapeake Bay sediments. *Marine Chemistry*, 77(2–3), 123–132. [https://doi.org/10.1016/S0304-4203\(01\)00081-0](https://doi.org/10.1016/S0304-4203(01)00081-0)
- Marcantonio, R. (2007). *A 1200-year record of forest fire history from macroscopic charcoal preserved in lake sediment, south-central Yukon Territory* [Carleton University]. <https://doi.org/https://doi.org/10.22215/etd/2007-07664>
- Mariet, A.-L., Monna, F., Gimbert, F., Bégeot, C., Cloquet, C., Belle, S., Millet, L., Rius, D., & Walter-Simonnet, A.-V. (2018). Tracking past mining activity using trace metals, lead isotopes and compositional data analysis of a sediment core from Longemer Lake, Vosges Mountains, France. *Journal of Paleolimnology*, 60(3), 399–412. <https://doi.org/10.1007/s10933-018-0029-9>
- Marlon, J. R., Bartlein, P. J., Gavin, D. G., Long, C. J., Anderson, R. S., Briles, C. E., Brown, K. J., Colombaroli, D., Hallett, D. J., Power, M. J., Scharf, E. A., & Walsh, M. K. (2012). Long-term perspective on wildfires in the western USA. *Proceedings of the National Academy of Sciences*, 109(9), E535–E543. <https://doi.org/10.1073/pnas.1112839109>
- Marx, S. K., Rashid, S., & Stromsoe, N. (2016). Global-scale patterns in anthropogenic Pb

- contamination reconstructed from natural archives. In *Environmental Pollution* (Vol. 213, pp. 283–298). Elsevier Ltd. <https://doi.org/10.1016/j.envpol.2016.02.006>
- Mataix-Solera, J., Cerda, A., Arcenegui, V., Jordan, A., & Zavala, L. M. (2011). Fire effects on soil aggregation: A review. *Earth-Science Reviews*, *109*(1–2), 44–60. <https://doi.org/10.1016/j.earscirev.2011.08.002>
- Matilainen, T. (1995). Involvement of bacteria in methylmercury formation in anaerobic lake waters. *Water, Air, & Soil Pollution*, *80*(1–4), 757–764. <https://doi.org/10.1007/BF01189727>
- McCarty, J. L., Smith, T. E. L., & Turetsky, M. R. (2020). Arctic fires re-emerging. In *Nature Geoscience* (Vol. 13, Issue 10, pp. 658–660). Nature Research. <https://doi.org/10.1038/s41561-020-00645-5>
- McComb, J. (2014). Understanding Biogeochemical Cycling of Trace Elements and Heavy Metals in Estuarine Ecosystems. *Journal of Bioremediation & Biodegradation*, *05*(03). <https://doi.org/10.4172/2155-6199.1000e148>
- McConnell, J. R., & Edwards, R. (2008). Coal burning leaves toxic heavy metal legacy in the Arctic. *Proceedings of the National Academy of Sciences of the United States of America*, *105*(34), 12140–12144. <https://doi.org/10.1073/pnas.0803564105>
- McGuire, K. J., McDonnell, J. J., Weiler, M., Kendall, C., McGlynn, B. L., Welker, J. M., & Seibert, J. (2005). The role of topography on catchment-scale water residence time. *Water Resources Research*, *41*(5), 1–14. <https://doi.org/10.1029/2004WR003657>
- McLauchlan, K. K., Higuera, P. E., Miesel, J., Rogers, B. M., Schweitzer, J., Shuman, J. K., Tepley, A. J., Varner, J. M., Veblen, T. T., Adalsteinsson, S. A., Balch, J. K., Baker, P., Batllori, E., Bigio, E., Brando, P., Cattau, M., Chipman, M. L., Coen, J., Crandall, R., ... Watts, A. C.

- (2020). Fire as a fundamental ecological process: Research advances and frontiers. In *Journal of Ecology* (Vol. 108, Issue 5, pp. 2047–2069). Blackwell Publishing Ltd.
<https://doi.org/10.1111/1365-2745.13403>
- Meng, R., Dennison, P. E., Huang, C., Moritz, M. A., & D'Antonio, C. (2015). Effects of fire severity and post-fire climate on short-term vegetation recovery of mixed-conifer and red fir forests in the Sierra Nevada Mountains of California. *Remote Sensing of Environment*, 171, 311–325. <https://doi.org/10.1016/j.rse.2015.10.024>
- Mielke, H. W., & Zahran, S. (2012). The urban rise and fall of air lead (Pb) and the latent surge and retreat of societal violence. *Environment International*, 43(1), 48–55.
<https://doi.org/10.1016/j.envint.2012.03.005>
- Miller, J. R., Lechler, P. J., Mackin, G., Germanoski, D., & Villarroel, L. F. (2007). Evaluation of particle dispersal from mining and milling operations using lead isotopic fingerprinting techniques, Rio Pilcomayo Basin, Bolivia. *Science of The Total Environment*, 384(1), 355–373.
<https://doi.org/10.1016/j.scitotenv.2007.05.029>
- Mills, R. B., Paterson, A. M., Blais, J. M., Lean, D. R. S., Smol, J. P., & Mierle, G. (2009). Factors influencing the achievement of steady state in mercury contamination among lakes and catchments of south-central Ontario. *Canadian Journal of Fisheries and Aquatic Sciences*, 66(2), 187–200. <https://doi.org/10.1139/F08-204>
- Millspaugh, S. H., & Whitlock, C. (1995). A 750-year fire history based on lake sediment records in central Yellowstone National Park, USA. *The Holocene*, 5(3), 283–292.
<https://doi.org/10.1177/095968369500500303>
- Moreno, C. E., Fjeld, E., & Lydersen, E. (2016). The effects of wildfire on mercury and stable

- isotopes ($\delta^{15}\text{N}$, $\delta^{13}\text{C}$) in water and biota of small boreal, acidic lakes in southern Norway. *Environmental Monitoring and Assessment*, 188(3), 1–23. <https://doi.org/10.1007/s10661-016-5148-z>
- Mudroch, A., Joshi, S. R., Sutherland, D., Mudroch, P., & Dickson, K. M. (1989). Geochemistry of sediments in the back bay and Yellowknife Bay of the Great Slave Lake. *Environmental Geology and Water Sciences*, 14(1), 35–42. <https://doi.org/10.1007/BF01740583>
- Muir, D C G, Wang, X., Yang, F., Nguyen, N., Jackson, T. A., Evans, M. S., Douglas, M., Köck, G., Lamoureux, S., Pienitz, R., Smol, J. P., Vincent, W. F., & Dastoor, A. (2009). Spatial Trends and Historical Deposition of Mercury in Eastern and Northern Canada Inferred from Lake Sediment Cores. *Environmental Science & Technology*, 43(13), 4802–4809. <https://doi.org/10.1021/es8035412>
- Muir, Derek C.G., Shearer, R. G., Oostdam, J. Van, Donaldson, S. G., & Furgal, C. (2005). Contaminants in Canadian arctic biota and implications for human health: Conclusions and knowledge gaps. In *Science of the Total Environment* (Vols. 351–352, pp. 539–546). Elsevier. <https://doi.org/10.1016/j.scitotenv.2005.08.030>
- Muller, H. R., & Muheim, G. (1969). Recording sensory action potentials of the finger nerves by use of a special needle electrode. *Electroencephalography and Clinical Neurophysiology*, 27(1), 108. <https://www-scopus-com.proxy.library.carleton.ca/record/display.uri?eid=2-s2.0-0014544783&origin=inward&txGid=6757912a4035d723d668db8feb43f749>
- Muller, J., Kylander, M., Martinez-Cortizas, A., Wüst, R. A. J., Weiss, D., Blake, K., Coles, B., & Garcia-Sanchez, R. (2008). The use of principle component analyses in characterising trace and major elemental distribution in a 55 kyr peat deposit in tropical Australia: Implications to paleoclimate. *Geochimica et Cosmochimica Acta*, 72(2), 449–463.

<https://doi.org/10.1016/j.gca.2007.09.028>

Murakami, M., Nakajima, F., & Furumai, H. (2008). The sorption of heavy metal species by sediments in soakaways receiving urban road runoff. *Chemosphere*, *70*(11), 2099–2109.

<https://doi.org/10.1016/j.chemosphere.2007.08.073>

Murozumi, M., Chow, T., & Patterson, C. (1969). Chemical Concentrations of Pollutant Lead Aerosols, Terrestrial Dusts and Sea Salts in Greenland and Antarctic Snow Strata. *Geochimica Et Cosmochimica Acta*, *33*(10), 1247-+. [https://doi.org/10.1016/0016-7037\(69\)90045-3](https://doi.org/10.1016/0016-7037(69)90045-3)

Naharro, R., Esbrí, J. M., Amorós, J. Á., García-Navarro, F. J., & Higuera, P. (2018). Assessment of mercury uptake routes at the soil-plant-atmosphere interface. *Geochemistry: Exploration, Environment, Analysis*, *19*(2), 146–154. <https://doi.org/10.1144/geochem2018-019>

Nappi, A., Drapeau, P., & Savard, J. P. L. (2004). Salvage logging after wildfire in the boreal forest: Is it becoming a hot issue for wildlife? In *Forestry Chronicle* (Vol. 80, Issue 1, pp. 67–74). Canadian Institute of Forestry. <https://doi.org/10.5558/tfc80067-1>

Neary, D. G., Klopatek, C. C., DeBano, L. F., & Ffolliott, P. F. (1999). Fire effects on belowground sustainability: a review and synthesis. *Forest Ecology and Management*, *122*(1), 51–71.

[https://doi.org/10.1016/S0378-1127\(99\)00032-8](https://doi.org/10.1016/S0378-1127(99)00032-8)

Nelson, S. J., Johnson, K. B., Kahl, J. S., Haines, T. A., & Fernandez, I. J. (2007). Mass Balances of Mercury and Nitrogen in Burned and Unburned Forested Watersheds at Acadia National Park, Maine, USA. *Environmental Monitoring and Assessment*, *126*(1–3), 69–80.

<https://doi.org/10.1007/s10661-006-9332-4>

Nguyen-Xuan, T., Bergeron, Y., Simard, D., Fyles, J. W., & Pare, D. (2000). The importance of forest floor disturbance in the early regeneration patterns of the boreal forest of western and

- central quebec: A wildfire versus logging comparison. *Canadian Journal of Forest Research*, 30(9), 1353–1364. <https://doi.org/10.1139/x00-067>
- Norton, S. A. (1986). A review of the chemical record in lake sediment of energy related air pollution and its effects on lakes. *Water, Air, and Soil Pollution*, 30(1–2), 331–345. <https://doi.org/10.1007/BF00305204>
- Norton, S. A., Dillon, P. J., Evans, R. D., Mierle, G., & Kahl, J. S. (1990). The History of Atmospheric Deposition of Cd, Hg, and Pb in North America: Evidence from Lake and Peat Bog Sediments. In *Acidic Precipitation* (pp. 73–102). Springer, New York, NY. https://link-springer-com.proxy.library.carleton.ca/chapter/10.1007/978-1-4612-4454-7_4
- Nosrati, K., & Collins, A. L. (2019). Investigating the importance of recreational roads as a sediment source in a mountainous catchment using a fingerprinting procedure with different multivariate statistical techniques and a Bayesian un-mixing model. *Journal of Hydrology*, 569, 506–518. <https://doi.org/10.1016/j.jhydrol.2018.12.019>
- Nzihou, A., & Stanmore, B. (2013). The fate of heavy metals during combustion and gasification of contaminated biomass-A brief review. In *Journal of Hazardous Materials* (Vols. 256–257, pp. 56–66). Elsevier. <https://doi.org/10.1016/j.jhazmat.2013.02.050>
- Obrist, D., Agnan, Y., Jiskra, M., Olson, C. L., Colegrove, D. P., Hueber, J., Moore, C. W., Sonke, J. E., & Helmig, D. (2017). Tundra uptake of atmospheric elemental mercury drives Arctic mercury pollution. *Nature*, 547(7662), 201–204. <https://doi.org/10.1038/nature22997>
- Obrist, D., Kirk, J. L., Zhang, L., Sunderland, E. M., Jiskra, M., & Selin, N. E. (2018). A review of global environmental mercury processes in response to human and natural perturbations: Changes of emissions, climate, and land use. *Ambio*, 47(2), 116–140.

<https://doi.org/10.1007/s13280-017-1004-9>

Obrist, D., Moosmüller, H., Schürmann, R., Chen, L.-W. A., & Kreidenweis, S. M. (2008).

Particulate-Phase and Gaseous Elemental Mercury Emissions During Biomass Combustion: Controlling Factors and Correlation with Particulate Matter Emissions. *Environmental Science & Technology*, 42(3), 721–727. <https://doi.org/10.1021/es071279n>

Obrist, D., Pearson, C., Webster, J., Kane, T., Lin, C.-J., Aiken, G. R., & Alpers, C. N. (2016). A synthesis of terrestrial mercury in the western United States: Spatial distribution defined by land cover and plant productivity. *Science of The Total Environment*, 568(Supplement C), 522–535.

<https://doi.org/10.1016/j.scitotenv.2015.11.104>

Odigie, K. O., & Flegal, A. R. (2011). Pyrogenic Remobilization of Historic Industrial Lead

Depositions. *Environmental Science & Technology*, 45(15), 6290–6295.

<https://doi.org/10.1021/es200944w>

Odigie, K. O., & Flegal, A. R. (2014). Trace Metal Inventories and Lead Isotopic Composition

Chronicle a Forest Fire's Remobilization of Industrial Contaminants Deposited in the Angeles National Forest. *PLOS ONE*, 9(9), e107835. <https://doi.org/10.1371/journal.pone.0107835>

Odigie, K. O., Khanis, E., Hibdon, S. A., Jana, P., Araneda, A., Urrutia, R., & Flegal, A. R. (2015).

Remobilization of trace elements by forest fire in Patagonia, Chile. *Regional Environmental Change*, 16(4), 1089–1096. <https://doi.org/10.1007/s10113-015-0825-y>

Odigie, K. O., Khanis, E., Hibdon, S. A., Jana, P., Araneda, A., Urrutia, R., & Flegal, A. R. (2016).

Remobilization of trace elements by forest fire in Patagonia, Chile. *Regional Environmental Change*, 16(4), 1089–1096. <https://doi.org/10.1007/s10113-015-0825-y>

Oris, F., Ali, A. A., Asselin, H., Paradis, L., Bergeron, Y., & Finsinger, W. (2014). Charcoal

dispersion and deposition in boreal lakes from 3 years of monitoring: Differences between local and regional fires. *Geophysical Research Letters*, 41(19), 6743–6752.

<https://doi.org/10.1002/2014GL060984>

Osterberg, E., Mayewski, P., Kreutz, K., Fisher, D., Handley, M., Sneed, S., Zdanowicz, C., Zheng, J., Demuth, M., Waskiewicz, M., & Bourgeois, J. (2008). Ice core record of rising lead pollution in the North Pacific atmosphere. *Geophysical Research Letters*, 35(5), L05810.

<https://doi.org/10.1029/2007GL032680>

Outridge, P. M., MacDonald, R. W., Wang, F., Stern, G. A., & Dastoor, A. P. (2008). A mass balance inventory of mercury in the Arctic Ocean. In *Environmental Chemistry* (Vol. 5, Issue 2, pp. 89–111). CSIRO PUBLISHING. <https://doi.org/10.1071/EN08002>

Outridge, P M, Hermanson, M. H., & Lockhart, W. L. (2002). Regional variations in atmospheric deposition and sources of anthropogenic lead in lake sediments across the Canadian Arctic. *Geochimica et Cosmochimica Acta*, 66(20), 3521–3531. [https://doi.org/10.1016/S0016-7037\(02\)00955-9](https://doi.org/10.1016/S0016-7037(02)00955-9)

Outridge, P M, Rausch, N., Percival, J. B., Shotyk, W., & McNeely, R. (2011). Comparison of mercury and zinc profiles in peat and lake sediment archives with historical changes in emissions from the Flin Flon metal smelter, Manitoba, Canada. *Science of The Total Environment*, 409(3), 548–563. <https://doi.org/10.1016/j.scitotenv.2010.10.041>

Outridge, P M, Stern, G. A., Hamilton, P. B., & Sanei, H. (2019). Algal scavenging of mercury in preindustrial Arctic lakes. *Limnology and Oceanography*, 64(4), 1558–1571.

<https://doi.org/10.1002/lno.11135>

Outridge, Peter M, & Wang, F. (2015). The Stability of Metal Profiles in Freshwater and Marine

Sediments. In Jules M Blais, M. R. Rosen, & J. P. Smol (Eds.), *Environmental Contaminants* (pp. 35–60). Springer Netherlands. http://link.springer.com/chapter/10.1007/978-94-017-9541-8_3

Outridge, Sanei, H., Stern, Hamilton, & Goodarzi, F. (2007). Evidence for Control of Mercury Accumulation Rates in Canadian High Arctic Lake Sediments by Variations of Aquatic Primary Productivity. *Environmental Science & Technology*, *41*(15), 5259–5265.
<https://doi.org/10.1021/es070408x>

Pacyna, J. M., & Keeler, G. J. (1995). Sources of Mercury in the Arctic. In *Mercury as a Global Pollutant* (pp. 621–632). Springer Netherlands. https://doi.org/10.1007/978-94-011-0153-0_68

Paerl, H. W., & Huisman, J. (2009). Climate change: A catalyst for global expansion of harmful cyanobacterial blooms. In *Environmental Microbiology Reports* (Vol. 1, Issue 1, pp. 27–37). Environ Microbiol Rep. <https://doi.org/10.1111/j.1758-2229.2008.00004.x>

Palmer, M., Galloway, J., Jamieson, H., Patterson, R. T., Falck, H., & Kokelj, S. V. (2015). The concentration of arsenic in lake waters of the Yellowknife area. *Yellowknife, NT: NWT Open File*, *6*.

Palmer, M. J., Chételat, J., Richardson, M., Jamieson, H. E., & Galloway, J. M. (2019). Seasonal variation of arsenic and antimony in surface waters of small subarctic lakes impacted by legacy mining pollution near Yellowknife, NT, Canada. *Science of the Total Environment*, *684*, 326–339.
<https://doi.org/10.1016/j.scitotenv.2019.05.258>

Parnell, A. C., Phillips, D. L., Bearhop, S., Semmens, B. X., Ward, E. J., Moore, J. W., Jackson, A. L., Grey, J., Kelly, D. J., & Inger, R. (2013). Bayesian stable isotope mixing models. *Environmetrics*, *24*(6), 387–399. <https://doi.org/10.1002/env.2221>

- Parnell, A., & Inger, R. (2016). Simmr: a stable isotope mixing model. *R Package Version 0.3*. R.
- Paterson, A. M., Morimoto, D. S., Cumming, B. F., Smol, J. P., & Szeicz, J. M. (2002). A paleolimnological investigation of the effects of forest fire on lake water quality in northwestern Ontario over the past ca. 150 years. *Canadian Journal of Botany*, *80*(12), 1329–1336. <https://doi.org/10.1139/b02-117>
- Peikertova, P., & Filip, P. (2016). Influence of the Automotive Brake Wear Debris on the Environment - A Review of Recent Research. *SAE International Journal of Materials and Manufacturing*, *9*(1), 133–146. <http://www.jstor.org/stable/26268813>
- Pelletier, N., Chételat, J., Blarquez, O., & Vermaire, J. C. (2020). Paleolimnological assessment of wildfire-derived atmospheric deposition of trace metal (loid)s and major ions to subarctic lakes (Northwest Territories, Canada). *Journal of Geophysical Research: Biogeosciences*. <https://doi.org/10.1029/2020jg005720>
- Pelletier, N., Chételat, J., Cousens, B., Zhang, S., Stepner, D., Muir, D. C. G., & Vermaire, J. C. (2020). Lead contamination from gold mining in Yellowknife Bay (Northwest Territories), reconstructed using stable lead isotopes. *Environmental Pollution*, *259*. <https://doi.org/10.1016/j.envpol.2019.113888>
- Pennington, W., Cambray, R., & Fisher, E. (1973). Observations on Lake Sediments Using Fallout Cs-137 as a Tracer. *Nature*, *242*(5396), 324–326. <https://doi.org/10.1038/242324a0>
- Percival, J. B., & Outridge, P. M. (2013). A test of the stability of Cd, Cu, Hg, Pb and Zn profiles over two decades in lake sediments near the Flin Flon Smelter, Manitoba, Canada. *Science of The Total Environment*, *454–455*, 307–318. <https://doi.org/10.1016/j.scitotenv.2013.03.011>
- Pereira, P., & Úbeda, X. (2010). Spatial distribution of heavy metals released from ashes after a

wildfire. *Journal of Environmental Engineering and Landscape Management*, 18(1), 13–22.

<https://doi.org/10.3846/jeelms.2010.02>

Pereira, P., Úbeda, X., & Martin, D. A. (2012). Fire severity effects on ash chemical composition and water-extractable elements. *Geoderma*, 191, 105–114.

<https://doi.org/10.1016/j.geoderma.2012.02.005>

Perez-Rodriguez, M., Silva-Sanchez, N., Kylander, M. E., Bindler, R., Mighall, T. M., Edward Schofield, J., Edwards, K. J., & Martinez Cortizas, A. (2018). Industrial-era lead and mercury contamination in southern Greenland implicates North American sources. *Science of the Total Environment*, 613, 919–930. <https://doi.org/10.1016/j.scitotenv.2017.09.041>

Perry, E, Norton, S. A., Kamman, N. C., Lorey, P. M., & Driscoll, C. T. (2005). Deconstruction of historic mercury accumulation in lake sediments, northeastern United States. *Ecotoxicology*, 14(1–2), 85–99. <https://doi.org/10.1007/s10646-004-6261-2>

Perry, Ethan, Norton, S. A., Kamman, N. C., Lorey, P. M., & Driscoll, C. T. (2005). Deconstruction of historic mercury accumulation in lake sediments, northeastern United States. *Ecotoxicology*, 14(1–2), 85–99. <https://doi.org/10.1007/s10646-004-6261-2>

Perryman, C. R., Wirsing, J., Bennett, K. A., Brennick, O., Perry, A. L., Williamson, N., & Ernakovich, J. G. (2020). Heavy metals in the Arctic: Distribution and enrichment of five metals in Alaskan soils. *PLOS ONE*, 15(6), e0233297.

<https://doi.org/10.1371/journal.pone.0233297>

Peters, M. E., & Higuera, P. E. (2007). Quantifying the source area of macroscopic charcoal with a particle dispersal model. *Quaternary Research*, 67(2), 304–310.

<https://doi.org/10.1016/j.yqres.2006.10.004>

- Philibert, A., Prairie, Y. T., & Carcaillet, C. (2003). 1200 years of fire impact on biogeochemistry as inferred from high resolution diatom analysis in a kettle lake from the Picea mariana-moss domain (Quebec, Canada). *Journal of Paleolimnology*, *30*(2), 167–181.
<https://doi.org/10.1023/A:1025526200880>
- Pirrone, N., Cinnirella, S., Feng, X., Finkelman, R. B., Friedli, H. R., Leaner, J., Mason, R., Mukherjee, A. B., Stracher, G. B., Streets, D. G., & Telmer, K. (2010). Global mercury emissions to the atmosphere from anthropogenic and natural sources. *Atmospheric Chemistry and Physics*, *10*(13), 5951–5964. <https://doi.org/10.5194/acp-10-5951-2010>
- Pisaric, M. F. J. (2002). Long-distance transport of terrestrial plant material by convection resulting from forest fires. *Journal of Paleolimnology*, *28*(3), 349–354.
<https://doi.org/10.1023/A:1021630017078>
- Pisaric, M., Moser, K., Prince, T., Ceci, M., Sia, M., & Warren, E. (2018). Fire and vegetation history during the Holocene epoch in the North Slave Region, Northwest Territories, Canada. *EGUGA*, 7783. <https://ui.adsabs.harvard.edu/abs/2018EGUGA..20.7783P/abstract>
- Pompeani, D. P., McLauchlan, K. K., Chileen, B. V., Calder, W. J., Shuman, B. N., & Higuera, P. E. (2020). The biogeochemical consequences of late Holocene wildfires in three subalpine lakes from northern Colorado. *Quaternary Science Reviews*, *236*, 106293.
<https://doi.org/10.1016/j.quascirev.2020.106293>
- Popoola, L. T., Adebajo, S. A., & Adeoye, B. K. (2018). Assessment of atmospheric particulate matter and heavy metals: a critical review. In *International Journal of Environmental Science and Technology* (Vol. 15, Issue 5, pp. 935–948). Center for Environmental and Energy Research and Studies. <https://doi.org/10.1007/s13762-017-1454-4>

- Porter, C., Morin, P., Howat, I., Noh, M.-J., Bates, B., Peterman, K., Keesey, S., Schlenk, M., Gardiner, J., Tomko, K., Willis, M., Kelleher, C., Cloutier, M., Husby, E., Foga, S., Nakamura, H., Platson, M., Wethington Jr., M., Williamson, C., ... Bojesen, M. A.-N. S. F. A.-N. S. F. (2019). *ArcticDEM* (V1 ed.). Harvard Dataverse. <https://doi.org/doi:10.7910/DVN/OHHUKH>
- Pratte, S., Bao, K., Shen, J., Mackenzie, L., Klamt, A.-M., Wang, G., & Xing, W. (2018). Recent atmospheric metal deposition in peatlands of northeast China: A review. *Science of The Total Environment*, 626, 1284–1294. <https://doi.org/https://doi.org/10.1016/j.scitotenv.2018.01.183>
- Pratte, S., Mucci, A., & Garneau, M. (2013). Historical records of atmospheric metal deposition along the St. Lawrence Valley (eastern Canada) based on peat bog cores. *Atmospheric Environment*, 79, 831–840. <https://doi.org/10.1016/j.atmosenv.2013.07.063>
- Pretty, T. J., Chanyi, C.-M., Kuhn, C., & Gray, D. K. (2020). Factors influencing the structure of macroinvertebrate communities in subarctic lakes affected by wildfires. *Canadian Journal of Fisheries and Aquatic Sciences*. <https://doi.org/10.1139/cjfas-2020-0141>
- Prince, T. J., Pisaric, M. F. J., & Turner, K. W. (2018). Postglacial Reconstruction of Fire History Using Sedimentary Charcoal and Pollen From a Small Lake in Southwest Yukon Territory, Canada. *Frontiers in Ecology and Evolution*, 6(DEC), 209. <https://doi.org/10.3389/fevo.2018.00209>
- Programme (AMAP), A. M. and A. (2011). *AMAP Assessment 2011: Mercury in the Arctic*. Arctic Monitoring and Assessment Programme (AMAP). <https://oaarchive.arctic-council.org/handle/11374/701>
- Programme (UNEP), U. N. E. (2013). *Global Mercury Assessment 2013: Sources, emissions, releases, and*

environmental transport. <http://wedocs.unep.org/handle/20.500.11822/7984>

- Pryor, S. C., Larsen, S. E., Sørensen, L. L., & Barthelmie, R. J. (2008). Particle fluxes above forests: Observations, methodological considerations and method comparisons. *Environmental Pollution*, *152*(3), 667–678. <https://doi.org/10.1016/j.envpol.2007.06.068>
- Quenea, K., Lamy, I., Winterton, P., Bermond, A., & Dumat, C. (2009). Interactions between metals and soil organic matter in various particle size fractions of soil contaminated with waste water. *Geoderma*, *149*(3–4), 217–223. <https://doi.org/10.1016/j.geoderma.2008.11.037>
- Quinton, W. I., Hayashi, M., & Chasmer, L. E. (2011). Permafrost-thaw-induced land-cover change in the Canadian subarctic: implications for water resources. *Hydrological Processes*, *25*(1), 152–158. <https://doi.org/10.1002/hyp.7894>
- R Core Development Team. (2020). *R: A language and environment for statistical computing*. R Foundation for Statistical Computing. <http://www.r-project.org/>
- Raison, R. J., Khanna, P. K., & Woods, P. V. (1985). Mechanisms of element transfer to the atmosphere during vegetation fires. *Canadian Journal of Forest Research*, *15*(1), 132–140. <https://doi.org/10.1139/x85-022>
- Ranalli, A. J., & Stevens, M. R. (2004). *Streamwater Quality Data from the 2002 Hayman, Hinman, and Missionary Ridge Wildfires, Colorado, 2003*. US Geological Survey.
- Rantala, M. V., Luoto, T. P., & Nevalainen, L. (2016). Temperature controls organic carbon sequestration in a subarctic lake. *Scientific Reports*, *6*(1), 1–11. <https://doi.org/10.1038/srep34780>
- Renberg, I., Brännvall, M.-L., Bindler, R., & Emteryd, O. (2002). Stable lead isotopes and lake sediments—a useful combination for the study of atmospheric lead pollution history. *Science of*

- The Total Environment*, 292(1), 45–54. [https://doi.org/10.1016/S0048-9697\(02\)00032-3](https://doi.org/10.1016/S0048-9697(02)00032-3)
- Renberg, Ingemar, Bindler, R., & Brännvall, M.-L. (2001). Using the historical atmospheric lead-deposition record as a chronological marker in sediment deposits in Europe. *The Holocene*, 11(5), 511–516. <https://doi.org/10.1191/095968301680223468>
- Renberg, Ingemar, Persson, M. W., & Emteryd, O. (1994). Pre-industrial atmospheric lead contamination detected in Swedish lake sediments. *Nature*, 368(6469), 323–326. <https://doi.org/10.1038/368323a0>
- Reyes, F. R., & Lougheed, V. L. (2015). Rapid nutrient release from permafrost thaw in arctic aquatic ecosystems. *Arctic, Antarctic, and Alpine Research*, 47(1), 35–48. <https://doi.org/10.1657/AAAR0013-099>
- Rhoades, C. C., Chow, A. T., Covino, T. P., Feghel, T. S., Pierson, D. N., & Rhea, A. E. (2019). The Legacy of a Severe Wildfire on Stream Nitrogen and Carbon in Headwater Catchments. *Ecosystems*, 22(3), 643–657. <https://doi.org/10.1007/s10021-018-0293-6>
- Rieuwerts, J. S., Thornton, I., Farago, M. E., & Ashmore, M. R. (2015). *Chemical Speciation & Bioavailability Factors influencing metal bioavailability in soils: preliminary investigations for the development of a critical loads approach for metals*. <https://doi.org/10.3184/095422998782775835>
- Riva, M. A., Lafranconi, A., D’Orso, M. I., & Cesana, G. (2012). Lead poisoning: Historical aspects of a paradigmatic “occupational and environmental disease.” In *Safety and Health at Work* (Vol. 3, Issue 1, pp. 11–16). Elsevier Science B.V. <https://doi.org/10.5491/SHAW.2012.3.1.11>
- Roberts, S., Kirk, J. L., Wiklund, J. A., Muir, D. C. G., Keating, J., Yang, F., Gleason, A., Lawson, G., Wang, X., & Evans, M. (2020). Sources of atmospheric metal(loid) pollution recorded in Thompson Manitoba lake sediment cores within the Canadian boreal biome. *Science of the Total*

- Environment*, 732, 139043. <https://doi.org/10.1016/j.scitotenv.2020.139043>
- Rohbock, E. (1982). *ATMOSPHERIC REMOVAL OF AIRBORNE METALS BY WET AND DRY DEPOSITION*. 159–171. https://doi.org/10.1007/978-94-009-7864-5_16
- Roos-Barraclough, F., Givelet, N., Cheburkin, A. K., Shotyk, W., & Norton, S. A. (2006). Use of Br and Se in peat to reconstruct the natural and anthropogenic fluxes of atmospheric Hg: A 10000-year record from Caribou Bog, Maine. *Environmental Science and Technology*, 40(10), 3188–3194. <https://doi.org/10.1021/es051945p>
- Roos-Barraclough, F., Martínez-Cortizas, A., García-Rodeja, E., & Shotyk, W. (2002). A 14 500 year record of the accumulation of atmospheric mercury in peat: Volcanic signals, anthropogenic influences and a correlation to bromine accumulation. *Earth and Planetary Science Letters*, 202(2), 435–451. [https://doi.org/10.1016/S0012-821X\(02\)00805-1](https://doi.org/10.1016/S0012-821X(02)00805-1)
- Roos-Barraclough, Fiona, & Shotyk, W. (2003). Millennial-scale records of atmospheric mercury deposition obtained from ombrotrophic and minerotrophic peatlands in the Swiss Jura mountains. *Environmental Science and Technology*, 37(2), 235–244. <https://doi.org/10.1021/es0201496>
- Rose, N. L., Yang, H., Turner, S. D., & Simpson, G. L. (2012). An assessment of the mechanisms for the transfer of lead and mercury from atmospherically contaminated organic soils to lake sediments with particular reference to Scotland, UK. *Geochimica et Cosmochimica Acta*, 82, 113–135. <https://doi.org/10.1016/j.gca.2010.12.026>
- Rosen, M. R. (2015). *The Influence of Hydrology on Lacustrine Sediment Contaminant Records* (pp. 5–33). Springer, Dordrecht. https://doi.org/10.1007/978-94-017-9541-8_2
- Rothenberg, S. E., Kirby, M. E., Bird, B. W., DeRose, M. B., Lin, C.-C., Feng, X., Ambrose, R. F., &

- Jay, J. A. (2010). The impact of over 100 years of wildfires on mercury levels and accumulation rates in two lakes in southern California, USA. *Environmental Earth Sciences*, *60*(5), 993–1005.
<https://doi.org/10.1007/s12665-009-0238-7>
- Rouse, W. R., Douglas, M. S. V., Hecky, R. E., Hershey, A. E., Kling, G. W., Lesack, L., Marsh, P., McDonald, M., Nicholson, B. J., Roulet, N. T., & Smol, J. P. (1997). Effects of climate change on the freshwaters of arctic and subarctic North America. *Hydrological Processes*, *11*(8), 873–902.
[https://doi.org/10.1002/\(SICI\)1099-1085\(19970630\)11:8<873::AID-HYP510>3.0.CO;2-6](https://doi.org/10.1002/(SICI)1099-1085(19970630)11:8<873::AID-HYP510>3.0.CO;2-6)
- Rydberg, J, & Martinez-Cortizas, A. (2014). Geochemical assessment of an annually laminated lake sediment record from northern Sweden: a multi-core, multi-element approach. *Journal of Paleolimnology*, *51*(4), 499–514. <https://doi.org/10.1007/s10933-014-9770-x>
- Rydberg, Johan, Gälman, V., Renberg, I., Bindler, R., Lambertsson, L., & Martínez-Cortizas, A. (2008). Assessing the Stability of Mercury and Methylmercury in a Varved Lake Sediment Deposit. *Environmental Science & Technology*, *42*(12), 4391–4396.
<https://doi.org/10.1021/es7031955>
- Rydberg, Johan, Klaminder, J., Rosén, P., Bindler, R., Rosen, P., & Bindler, R. (2010). Climate driven release of carbon and mercury from permafrost mires increases mercury loading to sub-arctic lakes. *Science of the Total Environment*, *408*(20), 4778–4783.
<https://doi.org/10.1016/j.scitotenv.2010.06.056>
- Rydberg, Johan, Lindborg, T., Sohlenius, G., Reuss, N., Olsen, J., & Laudon, H. (2016). The Importance of Eolian Input on Lake-Sediment Geochemical Composition in the Dry Proglacial Landscape of Western Greenland. *Arctic, Antarctic, and Alpine Research*, *48*(1), 93–109.
<https://doi.org/10.1657/AAAR0015-009>

- Saaristo, M., Brodin, T., Balshine, S., Bertram, M. G., Brooks, B. W., Ehlman, S. M., McCallum, E. S., Sih, A., Sundin, J., Wong, B. B. M., & Arnold, K. E. (2018). Direct and indirect effects of chemical contaminants on the behaviour, ecology and evolution of wildlife. *Proceedings of the Royal Society B: Biological Sciences*, *285*(1885), 20181297. <https://doi.org/10.1098/rspb.2018.1297>
- Sabin, L. D., Lim, J. H., Stolzenbach, K. D., & Schiff, K. C. (2005). Contribution of trace metals from atmospheric deposition to stormwater runoff in a small impervious urban catchment. *Water Research*, *39*(16), 3929–3937. <https://doi.org/10.1016/j.watres.2005.07.003>
- Sahoo, G. B., & Schladow, S. G. (2008). Impacts of climate change on lakes and reservoirs dynamics and restoration policies. *Sustainability Science*, *3*(2), 189–199. <https://doi.org/10.1007/s11625-008-0056-y>
- Sanchez-Cabeza, J.-A., Carolina Ruiz-Fernandez, A., Feliciano Ontiveros-Cuadras, J., Perez Bernal, L. H., & Olid, C. (2014). Monte Carlo uncertainty calculation of Pb-210 chronologies and accumulation rates of sediments and peat bogs. *Quaternary Geochronology*, *23*, 80–93. <https://doi.org/10.1016/j.quageo.2014.06.002>
- Sankey, J. B., Glenn, N. F., Germino, M. J., Gironella, A. I. N., & Thackray, G. D. (2010). Relationships of aeolian erosion and deposition with LiDAR-derived landscape surface roughness following wildfire. *Geomorphology*, *119*(1), 135–145. <https://doi.org/10.1016/j.geomorph.2010.03.013>
- Sarkar, S., Ahmed, T., Swami, K., Judd, C. D., Bari, A., Dutkiewicz, V. A., & Husain, L. (2015a). History of atmospheric deposition of trace elements in lake sediments, 1880 to 2007. *Journal of Geophysical Research: Atmospheres*, *120*(11), 5658–5669. <https://doi.org/10.1002/2015JD023202>
- Sarkar, S., Ahmed, T., Swami, K., Judd, C. D., Bari, A., Dutkiewicz, V. A., & Husain, L. (2015b).

- History of atmospheric deposition of trace elements in lake sediments, ~1880 to 2007. *Journal of Geophysical Research: Atmospheres*, 120(11), 5658–5669. <https://doi.org/10.1002/2015JD023202>
- Saulnier, I., & Mucci, A. (2000). Trace metal remobilization following the resuspension of estuarine sediments: Saguenay Fjord, Canada. *Applied Geochemistry*, 15(2), 191–210. [https://doi.org/10.1016/S0883-2927\(99\)00034-7](https://doi.org/10.1016/S0883-2927(99)00034-7)
- Schillereff, D. N., Chiverrell, R. C., Macdonald, N., Hooke, J. M., & Welsh, K. E. (2016). Quantifying system disturbance and recovery from historical mining-derived metal contamination at Brotherswater, northwest England. *Journal of Paleolimnology*, 56(2–3), 205–221. <https://doi.org/10.1007/s10933-016-9907-1>
- Schindler, D. W. (1977). Evolution of phosphorus limitation in lakes. *Science*, 195(4275), 260–262. <https://doi.org/10.1126/science.195.4275.260>
- Schindler, D. W. (2009). Lakes as sentinels and integrators for the effects of climate change on watersheds, airsheds, and landscapes. *Limnology and Oceanography*, 54(6), 2349–2358. https://doi.org/10.4319/lo.2009.54.6_part_2.2349
- Schindler, David W., Hecky, R. E., Findlay, D. L., Stainton, M. P., Parker, B. R., Paterson, M. J., Beaty, K. G., Lyng, M., & Kasian, S. E. M. (2008). Eutrophication of lakes cannot be controlled by reducing nitrogen input: Results of a 37-year whole-ecosystem experiment. *Proceedings of the National Academy of Sciences of the United States of America*, 105(32), 11254–11258. <https://doi.org/10.1073/pnas.0805108105>
- Schindler, David W., & Smol, J. P. (2006). Cumulative effects of climate warming and other human activities on freshwaters of Arctic and subarctic North America. *Ambio*, 35(4), 160–168. [https://doi.org/10.1579/0044-7447\(2006\)35\[160:CEOCWA\]2.0.CO;2](https://doi.org/10.1579/0044-7447(2006)35[160:CEOCWA]2.0.CO;2)

- Schroeder, W. H., & Munthe, J. (1998). Atmospheric mercury - An overview. *Atmospheric Environment*, 32(5), 809–822. [https://doi.org/10.1016/S1352-2310\(97\)00293-8](https://doi.org/10.1016/S1352-2310(97)00293-8)
- Schuster, P. F., Krabbenhoft, D. P., Naftz, D. L., Cecil, L. D., Olson, M. L., Dewild, J. F., Susong, D. D., Green, J. R., & Abbott, M. L. (2002). Atmospheric Mercury Deposition during the Last 270 Years: A Glacial Ice Core Record of Natural and Anthropogenic Sources. *Environmental Science & Technology*, 36(11), 2303–2310. <https://doi.org/10.1021/es0157503>
- Schuster, P. F., Striegl, R. G., Aiken, G. R., Krabbenhoft, D. P., Dewild, J. F., Butler, K., Kamark, B., & Dornblaser, M. (2011). Mercury Export from the Yukon River Basin and Potential Response to a Changing Climate. *Environmental Science & Technology*, 45(21), 9262–9267. <https://doi.org/10.1021/es202068b>
- Schwefel, R., Gaudard, A., Wüest, A., & Bouffard, D. (2016). Effects of climate change on deepwater oxygen and winter mixing in a deep lake (Lake Geneva): Comparing observational findings and modeling. *Water Resources Research*, 52(11), 8811–8826. <https://doi.org/10.1002/2016WR019194>
- Shakesby, R. A. (2011). Post-wildfire soil erosion in the Mediterranean: Review and future research directions. *Earth-Science Reviews*, 105(3), 71–100. <https://doi.org/10.1016/j.earscirev.2011.01.001>
- Shakesby, R. A., & Doerr, S. H. (2006). Wildfire as a hydrological and geomorphological agent. *Earth-Science Reviews*, 74(3–4), 269–307. <https://doi.org/10.1016/j.earscirev.2005.10.006>
- Shaw, D. M., Cramer, J. J., Higgins, M. D., & Truscott, M. G. (1986). Composition of the Canadian Precambrian shield and the continental crust of the earth. *Geological Society Special Publication*, 24, 275–282. <https://doi.org/10.1144/GSL.SP.1986.024.01.24>

- Sherman, L. S., Blum, J. D., Dvonch, J. T., Gratz, L. E., & Landis, M. S. (2015). The use of Pb, Sr, and Hg isotopes in Great Lakes precipitation as a tool for pollution source attribution. *The Science of the Total Environment*, 502, 362–374. <https://doi.org/10.1016/j.scitotenv.2014.09.034>
- Shotyk, W., Blaser, P., Grünig, A., & Cheburkin, A. K. (2000). A new approach for quantifying cumulative, anthropogenic, atmospheric lead deposition using peat cores from bogs: Pb in eight Swiss peat bog profiles. *Science of the Total Environment*, 249(1–3), 281–295. [https://doi.org/10.1016/S0048-9697\(99\)00523-9](https://doi.org/10.1016/S0048-9697(99)00523-9)
- Shotyk, W., Goodsite, M. E., Roos-Barraclough, F., Givelet, N., Le Roux, G., Weiss, D., Cheburkin, A. K., Knudsen, K., Heinemeier, J., van Der Knaap, W. O., Norton, S. A., & Lohse, C. (2005). Accumulation rates and predominant atmospheric sources of natural and anthropogenic Hg and Pb on the Faroe Islands. *Geochimica et Cosmochimica Acta*, 69(1), 1–17. <https://doi.org/10.1016/j.gca.2004.06.011>
- Shotyk, W., Weiss, D., Appleby, P. G., Cheburkin, A. K., Frei, R., Gloor, M., Kramers, J. D., Reese, S., & Van Der Knaap, W. O. (1998). History of atmospheric lead deposition since 12,370 14C yr BP from a peat bog, jura mountains, Switzerland. *Science*, 281(5383), 1635–1640. <https://doi.org/10.1126/science.281.5383.1635>
- Shotyk, W., Weiss, D., Heisterkamp, M., Cheburkin, A. K., Appleby, P. G., & Adams, F. C. (2002). New peat bog record of atmospheric lead pollution in Switzerland: Pb concentrations, enrichment factors, isotopic composition, and organolead species. *Environmental Science and Technology*, 36(18), 3893–3900. <https://doi.org/10.1021/es010196i>
- Shotyk, W., Weiss, D., Kramers, J. D., Frei, R., Cheburkin, A. K., Gloor, M., & Reese, S. (2001). Geochemistry of the peat bog at Etang de la Gruère, Jura Mountains, Switzerland, and its record of atmospheric pb and lithogenic trace metals (Sc, Ti, Y, Zr, and REE) since 12,370 14C

yr bp. *Geochimica et Cosmochimica Acta*, 65(14), 2337–2360. [https://doi.org/10.1016/S0016-7037\(01\)00586-5](https://doi.org/10.1016/S0016-7037(01)00586-5)

Shotyk, William. (1996). Peat bog archives of atmospheric metal deposition: Geochemical evaluation of peat profiles, natural variations in metal concentrations, and metal enrichment factors. In *Environmental Reviews* (Vol. 4, Issue 2, pp. 149–183). National Research Council of Canada. <https://doi.org/10.1139/a96-010>

Shotyk, William, Appleby, P. G., Bicalho, B., Davies, L., Froese, D., Grant-Weaver, I., Krachler, M., Magnan, G., Mullan-Boudreau, G., Noernberg, T., Pelletier, R., Shannon, B., van Bellen, S., & Zacccone, C. (2016). Peat bogs in northern Alberta, Canada reveal decades of declining atmospheric Pb contamination. *Geophysical Research Letters*, 43(18), 9964–9974. <https://doi.org/10.1002/2016GL070952>

Shotyk, William, Appleby, P. G., Bicalho, B., Davies, L. J., Froese, D., Grant-Weaver, I., Magnan, G., Mullan-Boudreau, G., Noernberg, T., Pelletier, R., Shannon, B., van Bellen, S., & Zacccone, C. (2017). Peat Bogs Document Decades of Declining Atmospheric Contamination by Trace Metals in the Athabasca Bituminous Sands Region. *Environmental Science & Technology*, 51(11), 6237–6249. <https://doi.org/10.1021/acs.est.6b04909>

Shotyk, William, Bicalho, B., Cuss, C. W., Duke, M. J. M., Noernberg, T., Pelletier, R., Steinnes, E., & Zacccone, C. (2016). Dust is the dominant source of “heavy metals” to peat moss (*Sphagnum fuscum*) in the bogs of the Athabasca Bituminous Sands region of northern Alberta. *Environment International*, 92–93, 494–506. <https://doi.org/10.1016/j.envint.2016.03.018>

Shotyk, William, & Cuss, C. W. (2019). Atmospheric Hg accumulation rates determined using *Sphagnum* moss from ombrotrophic (rain-fed) bogs in the Athabasca Bituminous Sands region of northern Alberta, Canada. *Ecological Indicators*, 107.

<https://doi.org/10.1016/j.ecolind.2019.105626>

- Simon, L. (2014). Potentially harmful elements in agricultural soils. In *PHEs, Environment and Human Health: Potentially Harmful Elements in the Environment and the Impact on Human Health* (pp. 85–150). Springer Netherlands. https://doi.org/10.1007/978-94-017-8965-3_3
- Simonetti, A., Gariépy, C., & Carignan, J. (2003). Tracing sources of atmospheric pollution in Western Canada using the Pb isotopic composition and heavy metal abundances of epiphytic lichens. *Atmospheric Environment*, *37*(20), 2853–2865. [https://doi.org/10.1016/S1352-2310\(03\)00210-3](https://doi.org/10.1016/S1352-2310(03)00210-3)
- Simpson, G. L. (2018). Modelling Palaeoecological Time Series Using Generalised Additive Models. *Frontiers in Ecology and Evolution*, *6*(OCT), 149. <https://doi.org/10.3389/fevo.2018.00149>
- Singh, S. M., Sharma, J., Gawas-Sakhalkar, P., Upadhyay, A. K., Naik, S., Pedneker, S. M., & Ravindra, R. (2013). Atmospheric deposition studies of heavy metals in Arctic by comparative analysis of lichens and cryoconite. *Environmental Monitoring and Assessment*, *185*(2), 1367–1376. <https://doi.org/10.1007/s10661-012-2638-5>
- Skierszkan, E. K., Irvine, G., Doyle, J. R., Kimpe, L. E., & Blais, J. M. (2013). Is there widespread metal contamination from in-situ bitumen extraction at Cold Lake, Alberta heavy oil field? *Science of the Total Environment*, *447*, 337–344. <https://doi.org/10.1016/j.scitotenv.2012.12.097>
- Smith, H. G., Sheridan, G. J., Lane, P. N. J., Nyman, P., & Haydon, S. (2011). Wildfire effects on water quality in forest catchments: A review with implications for water supply. *Journal of Hydrology*, *396*(1–2), 170–192. <https://doi.org/10.1016/j.jhydrol.2010.10.043>
- Smol, J. P. (2010). The power of the past: using sediments to track the effects of multiple stressors on lake ecosystems. *Freshwater Biology*, *55*, 43–59. <https://doi.org/10.1111/j.1365->

- Smol, J. P. (2016). Arctic and Sub-Arctic shallow lakes in a multiple-stressor world: a paleoecological perspective. *Hydrobiologia*, 778(1), 253–272. <https://doi.org/10.1007/s10750-015-2543-3>
- Soerensen, A. L., Jacob, D. J., Schartup, A. T., Fisher, J. A., Lehnherr, I., St Louis, V. L., Heimbürger, L. E., Sonke, J. E., Krabbenhoft, D. P., & Sunderland, E. M. (2016). A mass budget for mercury and methylmercury in the Arctic Ocean. *Global Biogeochemical Cycles*, 30(4), 560–575. <https://doi.org/10.1002/2015GB005280>
- Spence, C., Kokelj, S. A., Kokelj, S. V., & Hedstrom, N. (2014). The process of winter streamflow generation in a subarctic Precambrian Shield catchment. *Hydrological Processes*, 28(14), 4179–4190. <https://doi.org/10.1002/hyp.10119>
- Spence, C., Kokelj, S. V., Kokelj, S. A., McCluskie, M., & Hedstrom, N. (2015). Evidence of a change in water chemistry in Canada's subarctic associated with enhanced winter streamflow. *Journal of Geophysical Research: Biogeosciences*, 120(1), 113–127. <https://doi.org/10.1002/2014JG002809>
- Spence, C., Kokelj, S. V., & Ehsanzadeh, E. (2011). Precipitation trends contribute to streamflow regime shifts in northern Canada. *Cold Regions Hydrology in a Changing Climate*, Edited by: Yang, D., Marsh, P., and Gelfan, A., LAHS Publication, Int Assoc Hydrological Sciences, Wallingford, 3–8.
- Spence, C., & Woo, M. K. (2008). Hydrology of the northwestern subarctic Canadian shield. In *Cold Region Atmospheric and Hydrologic Studies. The Mackenzie GEWEX Experience* (Vol. 2, pp. 235–256). Springer Berlin Heidelberg. https://doi.org/10.1007/978-3-540-75136-6_13
- Spencer, C. N., Gabel, K. O., & Hauer, F. R. (2003). Wildfire effects on stream food webs and nutrient dynamics in Glacier National Park, USA. *Forest Ecology and Management*, 178(1), 141–

153. [https://doi.org/10.1016/S0378-1127\(03\)00058-6](https://doi.org/10.1016/S0378-1127(03)00058-6)

Sprague, D. D., & Vermaire, J. C. (2018a). Legacy Arsenic Pollution of Lakes Near Cobalt, Ontario, Canada: Arsenic in Lake Water and Sediment Remains Elevated Nearly a Century After Mining Activity Has Ceased. *Water Air and Soil Pollution*, 229(3), 87. <https://doi.org/10.1007/s11270-018-3741-1>

Sprague, D. D., & Vermaire, J. C. (2018b). The landscape-scale relationship between lake sediment geochemistry and catchment bedrock composition from the Temagami and Gowganda areas of Northeastern Ontario, Canada. *Environmental Earth Sciences*, 77(12), 463. <https://doi.org/10.1007/s12665-018-7625-x>

SRK. (2002). *Supporting document 5: Giant Mine arsenic trioxide dust properties. Prepared by SRK, Canada Inc. Prepared for the Department of Indian Affairs and Northern Development (2002).* <http://registry.mvlwb.ca/Documents/MV2007L8-0031/MV2007L8-0031 - DIAND-GIANT - ATM - Supporting Document 05 - Arsenic Trioxide Dust Properties - Dec-02.pdf>

St. Pierre, K. A., Zolkos, S., Shakil, S., Tank, S. E., St. Louis, V. L., & Kokelj, S. V. (2018). Unprecedented Increases in Total and Methyl Mercury Concentrations Downstream of Retrogressive Thaw Slumps in the Western Canadian Arctic. *Environmental Science & Technology*, 52(24), 14099–14109. <https://doi.org/10.1021/acs.est.8b05348>

Steffen, A., Lehnerr, I., Cole, A., Ariya, P., Dastoor, A., Durnford, D., Kirk, J., & Pilote, M. (2015). Atmospheric mercury in the Canadian Arctic. Part I: A review of recent field measurements. *Science of The Total Environment*, 509–510(Supplement C), 3–15. <https://doi.org/10.1016/j.scitotenv.2014.10.109>

Stein, E. D., Brown, J. S., Hogue, T. S., Burke, M. P., & Kinoshita, A. (2012). Stormwater

- contaminant loading following southern California wildfires. *Environmental Toxicology and Chemistry*, 31(11), 2625–2638. <https://doi.org/10.1002/etc.1994>
- Steinnes, E., & Friedland, A. J. (2006). Metal contamination of natural surface soils from long-range atmospheric transport: Existing and missing knowledge. *Environmental Reviews*, 14(3), 169–186. <https://doi.org/10.1139/a06-002>
- Stern, G. A., Sanei, H., Roach, P., De La Ronde, J., & Outridge, P. M. (2009). Historical interrelated variations of mercury and aquatic organic matter in lake sediment cores from a subarctic lake in Yukon, Canada: Further evidence toward the algal-mercury scavenging hypothesis. *Environmental Science and Technology*, 43(20), 7684–7690. <https://doi.org/10.1021/es902186s>
- Stevens-Rumann, C. S., & Morgan, P. (2019). Tree regeneration following wildfires in the western US: a review. In *Fire Ecology* (Vol. 15, Issue 1, pp. 1–17). SpringerOpen. <https://doi.org/10.1186/s42408-019-0032-1>
- Streets, D. G., Horowitz, H. M., Jacob, D. J., Lu, Z., Levin, L., ter Schure, A. F. H., & Sunderland, E. M. (2017). Total Mercury Released to the Environment by Human Activities. *Environmental Science & Technology*, 51(11), 5969–5977. <https://doi.org/10.1021/acs.est.7b00451>
- Stretesky, P. B., & Lynch, M. J. (2001). The relationship between lead exposure and homicide. *Archives of Pediatrics and Adolescent Medicine*, 155(5), 579–582. <https://doi.org/10.1001/archpedi.155.5.579>
- Strode, S. A., Jaeglé, L., Jaffe, D. A., Swartzendruber, P. C., Selin, N. E., Holmes, C., & Yantosca, R. M. (2008). Trans-Pacific transport of mercury. *Journal of Geophysical Research: Atmospheres*, 113(D15), D15305. <https://doi.org/10.1029/2007JD009428>
- Sturges, W. T., & Barrie, L. A. (1987). Lead 206/207 isotope ratios in the atmosphere of North

- America as tracers of US and Canadian emissions. *Nature*, 329(6135), 144–146.
<https://doi.org/10.1038/329144a0>
- Sturges, W. T., & Barrie, L. A. (1989). Stable lead isotope ratios in arctic aerosols: evidence for the origin of arctic air pollution. *Atmospheric Environment (1967)*, 23(11), 2513–2519.
[https://doi.org/10.1016/0004-6981\(89\)90263-1](https://doi.org/10.1016/0004-6981(89)90263-1)
- Sturges, W. T., Hopper, J. F., Barrie, L. A., & Schnell, R. C. (1993). Stable lead isotope ratios in Alaskan arctic aerosols. *Atmospheric Environment. Part A. General Topics*, 27(17), 2865–2871.
[https://doi.org/10.1016/0960-1686\(93\)90317-R](https://doi.org/10.1016/0960-1686(93)90317-R)
- Swain, E. B., Engstrom, D. R., Brigham, M. E., Henning, T. A., & Brezonik, P. L. (1992). Increasing Rates of Atmospheric Mercury Deposition in Midcontinental North America. *Science*, 257(5071), 784–787. <https://doi.org/10.1126/science.257.5071.784>
- Taboada, T., Cortizas, A. M., García, C., & García-Rodeja, E. (2006). Particle-size fractionation of titanium and zirconium during weathering and pedogenesis of granitic rocks in NW Spain. *Geoderma*, 131(1–2), 218–236. <https://doi.org/10.1016/j.geoderma.2005.03.025>
- Talbot, J., Moore, T. R., Wang, M., Ouellet Dallaire, C., & Riley, J. L. (2017). Distribution of lead and mercury in Ontario peatlands. *Environmental Pollution*, 231, 890–898.
<https://doi.org/10.1016/j.envpol.2017.08.095>
- Tchounwou, P. B., Yedjou, C. G., Patlolla, A. K., & Sutton, D. J. (2012). Heavy metal toxicity and the environment. In *EXS* (Vol. 101, pp. 133–164). NIH Public Access.
https://doi.org/10.1007/978-3-7643-8340-4_6
- Teufel, B., & Sushama, L. (2019). Abrupt changes across the Arctic permafrost region endanger northern development. In *Nature Climate Change* (Vol. 9, Issue 11, pp. 858–862). Nature

Publishing Group. <https://doi.org/10.1038/s41558-019-0614-6>

Thienpont, J. R., Korosi, J. B., Hargan, K. E., Williams, T., Eickmeyer, D. C., Kimpe, L. E., Palmer, M. J., Smol, J. P., & Blais, J. M. (2016). Multi-trophic level response to extreme metal contamination from gold mining in a subarctic lake. *Proc. R. Soc. B*, *283*(1836), 20161125. <https://doi.org/10.1098/rspb.2016.1125>

Tinner, W., Hofstetter, S., Zeuglin, F., Conedera, M., Wohlgemuth, T., Zimmermann, L., & Zweifel, R. (2006). Long-distance transport of macroscopic charcoal by an intensive crown fire in the Swiss Alps - implications for fire history reconstruction. *The Holocene*, *16*(2), 287–292. <https://doi.org/10.1191/0959683606hl925rr>

Tomlin, A. D., Protz, R., Martin, R. R., McCabe, D. C., & Lagace, R. J. (1993). Relationships amongst organic matter content, heavy metal concentrations, earthworm activity, and soil microfabric on a sewage sludge disposal site. In *Soil Structure/Soil Biota Interrelationships* (pp. 89–103). Elsevier. <https://doi.org/10.1016/b978-0-444-81490-6.50058-3>

Turetsky, M. R., Harden, J. W., Friedli, H. R., Flannigan, M., Payne, N., Crock, J., & Radke, L. (2006). Wildfires threaten mercury stocks in northern soils. *Geophysical Research Letters*, *33*(16), L16403. <https://doi.org/10.1029/2005GL025595>

Turner, M. G., Braziunas, K. H., Hansen, W. D., & Harvey, B. J. (2019). Short-interval severe fire erodes the resilience of subalpine lodgepole pine forests. *Proceedings of the National Academy of Sciences of the United States of America*, *166*(23), 11319–11328. <https://doi.org/10.1073/pnas.1902841116>

Tylmann, W. (2005). Lithological and geochemical record of anthropogenic changes in recent sediments of a small and shallow lake (Lake Pusty Staw, northern Poland). *Journal of*

Paleolimnology, 33(3), 313–325. <https://doi.org/10.1007/s10933-004-5506-7>

Uglietti, C., Gabrielli, P., Cooke, C. A., Vallelonga, P., & Thompson, L. G. (2015). Widespread pollution of the South American atmosphere predates the industrial revolution by 240 y. *Proceedings of the National Academy of Sciences of the United States of America*, 112(8), 2349–2354. <https://doi.org/10.1073/pnas.1421119112>

Ukonmaanaho, L., Starr, M., Mannio, J., & Ruoho-Airola, T. (2001). Heavy metal budgets for two headwater forested catchments in background areas of Finland. *Environmental Pollution*, 114(1), 63–75. [https://doi.org/10.1016/S0269-7491\(00\)00207-4](https://doi.org/10.1016/S0269-7491(00)00207-4)

USEPA. (n.d.). *2014 National Emissions Inventory Report*. Retrieved August 28, 2020, from <https://gispub.epa.gov/neireport/2014/>

USEPA, U. S. E. P. A. (2020). *Lead Trends | National Air Quality: Status and Trends of Key Air Pollutants* | US EPA. <https://www.epa.gov/air-trends/lead-trends>

Utermann, J., Aydın, C. T., Bischoff, N., Böttcher, J., Eickenscheidt, N., Gehrmann, J., König, N., Scheler, B., Stange, F., & Wellbrock, N. (2019). *Heavy Metal Stocks and Concentrations in Forest Soils* (pp. 199–229). Springer, Cham. https://doi.org/10.1007/978-3-030-15734-0_7

V. Pouyat, R., Pataki, D., Belt, K., Groffman, P., Hom, J., & Band, L. (2007). Effects of Urban Land-Use Change on Biogeochemical Cycles. In *Terrestrial Ecosystems in a Changing World* (pp. 45–58). https://www.researchgate.net/profile/Kenneth_Belt/publication/225192299_Effects_of_Urban_Land-Use_Change_on_Biogeochemical_Cycles/links/0deec52a5da628f902000000/Effects-of-Urban-Land-Use-Change-on-Biogeochemical-Cycles.pdf

- Van Den Berghe, M. D., Jamieson, H. E., & Palmer, M. J. (2018). Arsenic mobility and characterization in lakes impacted by gold ore roasting, Yellowknife, NWT, Canada. *Environmental Pollution*, 234, 630–641. <https://doi.org/10.1016/j.envpol.2017.11.062>
- Veraverbeke, S., Rogers, B. M., Goulden, M. L., Jandt, R. R., Miller, C. E., Wiggins, E. B., & Randerson, J. T. (2017). Lightning as a major driver of recent large fire years in North American boreal forests. *Nature Climate Change*, 7(7), 529–534. <https://doi.org/10.1038/nclimate3329>
- Vieira, D. C. S., Malvar, M. C., Martins, M. A. S., Serpa, D., & Keizer, J. J. (2018). Key factors controlling the post-fire hydrological and erosive response at micro-plot scale in a recently burned Mediterranean forest. *Geomorphology*, 319, 161–173. <https://doi.org/https://doi.org/10.1016/j.geomorph.2018.07.014>
- Vincent, W. F., Laurion, I., Pienitz, R., & Anthony, K. M. W. (2013). 2 *Climate Impacts on Arctic Lake Ecosystems*. <https://doi.org/10.1002/9781118470596.ch2>
- Violante, A., Cozzolino, V., Perelomov, L., Caporale, A. G., & Pigna, M. (2010). Mobility and bioavailability of heavy metals and metalloids in soil environments. *Journal of Soil Science and Plant Nutrition*, 10(3), 268–292. <https://doi.org/10.4067/S0718-95162010000100005>
- Visser, A., Kroes, J., Van Vliet, M. T. H., Blenkinsop, S., Fowler, H. J., & Broers, H. P. (2012). Climate change impacts on the leaching of a heavy metal contamination in a small lowland catchment. *Journal of Contaminant Hydrology*, 127(1–4), 47–64. <https://doi.org/10.1016/j.jconhyd.2011.04.007>
- Vonk, J. E., Tank, S. E., Bowden, W. B., Laurion, I., Vincent, W. F., Alekseychik, P., Amyot, M., Billet, M. F., Canário, J., Cory, R. M., Deshpande, B. N., Helbig, M., Jammet, M., Karlsson, J.,

- Larouche, J., Macmillan, G., Rautio, M., Walter Anthony, K. M., & Wickland, K. P. (2015). Reviews and syntheses: Effects of permafrost thaw on Arctic aquatic ecosystems. In *Biogeosciences* (Vol. 12, Issue 23, pp. 7129–7167). Copernicus GmbH.
<https://doi.org/10.5194/bg-12-7129-2015>
- Wakeham, S. G., Schaffner, C., & Giger, W. (1980). Polycyclic aromatic hydrocarbons in Recent lake sediments—I. Compounds having anthropogenic origins. *Geochimica et Cosmochimica Acta*, *44*(3), 403–413. [https://doi.org/10.1016/0016-7037\(80\)90040-X](https://doi.org/10.1016/0016-7037(80)90040-X)
- Walker, T. N., Ward, S. E., Ostle, N. J., & Bardgett, R. D. (2015). Contrasting growth responses of dominant peatland plants to warming and vegetation composition. *Oecologia*, *178*(1), 141–151.
<https://doi.org/10.1007/s00442-015-3254-1>
- Wällstedt, T., Björkvald, L., Laudon, H., Borg, H., & Mörth, C. M. (2017). Landscape control on the hydrogeochemistry of As, Co and Pb in a boreal stream network. *Geochimica et Cosmochimica Acta*, *211*, 194–213. <https://doi.org/10.1016/j.gca.2016.08.030>
- Wang, W., Peng, C., Kneeshaw, D. D., Larocque, G. R., & Luo, Z. (2012). Drought-induced tree mortality: ecological consequences, causes, and modeling. *Environmental Reviews*, *20*(2), 109–121.
<https://doi.org/10.1139/a2012-004>
- Wang, X., Thompson, D. K., Marshall, G. A., Tymstra, C., Carr, R., & Flannigan, M. D. (2015). Increasing frequency of extreme fire weather in Canada with climate change. *Climatic Change*, *130*(4), 573–586. <https://doi.org/10.1007/s10584-015-1375-5>
- Waters, C. N., Zalasiewicz, J., Summerhayes, C., Barnosky, A. D., Poirier, C., Galuszka, A., Cearreta, A., Edgeworth, M., Ellis, E. C., Ellis, M., Jeandel, C., Leinfelder, R., McNeill, J. R., Richter, D. deB, Steffen, W., Syvitski, J., Vidas, D., Wagreich, M., Williams, M., ... Wolfe, A. P. (2016).

- The Anthropocene is functionally and stratigraphically distinct from the Holocene. *Science*, 351(6269), aad2622. <https://doi.org/10.1126/science.aad2622>
- Waters, M. N., Metz, A. P., Smoak, J. M., & Turner, H. (2019). Chronic prescribed burning alters nutrient deposition and sediment stoichiometry in a lake ecosystem. *Ambio*, 48(6), 672–682. <https://doi.org/10.1007/s13280-018-1094-z>
- Watmough, S. A., & Dillon, P. J. (2007). Lead biogeochemistry in a central Ontario Forested watershed. *Biogeochemistry*, 84(2), 143–159. <https://doi.org/10.1007/s10533-007-9110-6>
- Watras, C. J., Back, R. C., Halvorsen, S., Hudson, R. J. M., Morrison, K. A., & Wentz, S. P. (1998). Bioaccumulation of mercury in pelagic freshwater food webs. *Science of the Total Environment*, 219(2–3), 183–208. [https://doi.org/10.1016/S0048-9697\(98\)00228-9](https://doi.org/10.1016/S0048-9697(98)00228-9)
- Webster, J. P., Kane, T. J., Obrist, D., Ryan, J. N., & Aiken, G. R. (2016a). Estimating mercury emissions resulting from wildfire in forests of the Western United States. *Science of the Total Environment*, 568, 578–586. <https://doi.org/10.1016/j.scitotenv.2016.01.166>
- Webster, J. P., Kane, T. J., Obrist, D., Ryan, J. N., & Aiken, G. R. (2016b). Estimating mercury emissions resulting from wildfire in forests of the Western United States. *Science of the Total Environment*, 568, 578–586. <https://doi.org/10.1016/j.scitotenv.2016.01.166>
- Weiss, D., Shotyk, W., Cheburkin, A. K., Gloor, M., & Reese, S. (1997). Atmospheric lead deposition from 12,400 to ca. 2,000 Yrs BP in a peat bog profile, Jura Mountains, Switzerland. *Water, Air, and Soil Pollution*, 100(3–4), 311–324. <https://doi.org/10.1023/A:1018341029549>
- Weiss, Dominik, Shotyk, W., Rieley, J., Page, S., Gloor, M., Reese, S., & Martinez-Cortizas, A. (2002). The geochemistry of major and selected trace elements in a forested peat bog, Kalimantan, SE Asia, and its implications for past atmospheric dust deposition. *Geochimica et*

Cosmochimica Acta, 66(13), 2307–2323. [https://doi.org/10.1016/S0016-7037\(02\)00834-7](https://doi.org/10.1016/S0016-7037(02)00834-7)

Whitehead, P. G., Wilby, R. L., Battarbee, R. W., Kernan, M., & Wade, A. J. (2009). A review of the potential impacts of climate change on surface water quality. In *Hydrological Sciences Journal* (Vol. 54, Issue 1, pp. 101–123). IAHS Press. <https://doi.org/10.1623/hysj.54.1.101>

Whitlock, C., & Millspaugh, S. H. (1996). Testing the assumptions of fire-history studies: an examination of modern charcoal accumulation in Yellowstone National Park, USA. *The Holocene*, 6(1), 7–15. <https://doi.org/10.1177/095968369600600102>

Widerlund, A., Roos, P., Gunneriusson, L., Ingri, J., & Holmström, H. (2002). Early diagenesis and isotopic composition of lead in Lake Laisan, northern Sweden. *Chemical Geology*, 189(3–4), 183–197. [https://doi.org/10.1016/S0009-2541\(02\)00131-6](https://doi.org/10.1016/S0009-2541(02)00131-6)

Wijngaard, R. R., van der Perk, M., van der Grift, B., de Nijs, T. C. M., & Bierkens, M. F. P. (2017). The Impact of Climate Change on Metal Transport in a Lowland Catchment. *Water, Air, and Soil Pollution*, 228(3), 1–20. <https://doi.org/10.1007/s11270-017-3261-4>

Wiklund, J. A., Hall, R. I., Wolfe, B. B., Edwards, T. W. D., Farwell, A. J., & Dixon, D. G. (2014). Use of pre-industrial floodplain lake sediments to establish baseline river metal concentrations downstream of Alberta oil sands: a new approach for detecting pollution of rivers. *Environmental Research Letters*, 9(12), 124019. <https://doi.org/10.1088/1748-9326/9/12/124019>

Wiklund, J. A., Kirk, J. L., Muir, D. C. G., Evans, M., Yang, F., Keating, J., & Parsons, M. T. (2017). Anthropogenic mercury deposition in Flin Flon Manitoba and the Experimental Lakes Area Ontario (Canada): A multi-lake sediment core reconstruction. *Science of the Total Environment*, 586, 685–695. <https://doi.org/10.1016/j.scitotenv.2017.02.046>

Wildland Fire Management, G. of Y. (2014). Fire History. In *Geoportal*. Wildland Fire Management,

Government of Yukon.

<https://geoweb.gov.yk.ca/geoportal/catalog/search/resource/details.page?uuid=%7B26A4B563-B9DD-4C6C-BB17-FD805B7799AF%7D>

Witt, E. L., Kolka, R. K., Nater, E. A., & Wickman, T. R. (2009). Forest Fire Effects on Mercury Deposition in the Boreal Forest. *Environmental Science and Technology*, 43(6), 1776–1782.

<https://doi.org/10.1021/es802634y>

Wolfe, S. A., Kerr, D. E., & Morse, P. D. (2017). *Slave Geological Province: An Archetype of Glaciated Shield Terrain* (pp. 77–86). Springer, Cham. https://doi.org/10.1007/978-3-319-44595-3_4

Wolfe, S. A., Morse, P. D., Kokelj, S. V., & Gaanderse, A. J. (2017). *Great Slave Lowland: The Legacy of Glacial Lake McConnell* (pp. 87–96). Springer, Cham. https://doi.org/10.1007/978-3-319-44595-3_5

Wong, H. K. T., Gauthier, A., & Nriagu, J. O. (1999). Dispersion and toxicity of metals from abandoned gold mine tailings at Goldenville, Nova Scotia, Canada. *Science of The Total Environment*, 228(1), 35–47. [https://doi.org/10.1016/S0048-9697\(99\)00021-2](https://doi.org/10.1016/S0048-9697(99)00021-2)

Woodruff, L. G., & Cannon, W. F. (2010). Immediate and Long-Term Fire Effects on Total Mercury in Forests Soils of Northeastern Minnesota. *Environmental Science & Technology*, 44(14), 5371–5376. <https://doi.org/10.1021/es100544d>

Wotton, B. Mike. (2009). Interpreting and using outputs from the Canadian Forest Fire Danger Rating System in research applications. *Environmental and Ecological Statistics*, 16(2), 107–131. <https://doi.org/10.1007/s10651-007-0084-2>

Wotton, B M, Flannigan, M. D., & Marshall, G. A. (2017). Potential climate change impacts on fire intensity and key wildfire suppression thresholds in Canada. *Environmental Research Letters*, 12(9),

95003. <https://doi.org/10.1088/1748-9326/aa7e6e>

Wu, L., Taylor, M. P., & Handley, H. K. (2017). Remobilisation of industrial lead depositions in ash during Australian wildfires. *Science of The Total Environment*, 599–600, 1233–1240.

<https://doi.org/10.1016/j.scitotenv.2017.05.044>

Wu, Y., Liu, J., Zhai, J., Cong, L., Wang, Y., Ma, W., Zhang, Z., & Li, C. (2018). Comparison of dry and wet deposition of particulate matter in near-surface waters during summer. *PLOS ONE*,

13(6), e0199241. <https://doi.org/10.1371/journal.pone.0199241>

Wuana, R. A., & Okieimen, F. E. (2011). Heavy Metals in Contaminated Soils: A Review of Sources, Chemistry, Risks and Best Available Strategies for Remediation. *ISRN Ecology*, 2011, 1–20.

<https://doi.org/10.5402/2011/402647>

Yang, H. (2015). Lake Sediments May Not Faithfully Record Decline of Atmospheric Pollutant Deposition. *Environmental Science & Technology*, 49(21), 12607–12608.

<https://doi.org/10.1021/acs.est.5b04386>

Yang, H., Shilland, E., Appleby, P. G., Rose, N. L., & Battarbee, R. W. (2018). Legacy Lead Stored in Catchments Is the Dominant Source for Lakes in the U.K.: Evidence from Atmospherically Derived 210 Pb. *Environmental Science and Technology*, 52(24), 14070–14077.

<https://doi.org/10.1021/acs.est.8b04099>

Yang, Z., Fang, W., Lu, X., Sheng, G. P., Graham, D. E., Liang, L., Wullschleger, S. D., & Gu, B. (2016). Warming increases methylmercury production in an Arctic soil. *Environmental Pollution*,

214, 504–509. <https://doi.org/10.1016/j.envpol.2016.04.069>

Yao, Z., & Gao, P. (2007). Heavy metal research in lacustrine sediment: A review. In *Chinese Journal of Oceanology and Limnology* (Vol. 25, Issue 4, pp. 444–454). Springer.

<https://doi.org/10.1007/s00343-007-0444-7>

Young, D. R., & Jan, T.-K. (1977). Fire fallout of metals off California. *Marine Pollution Bulletin*, 8(5), 109–112. [https://doi.org/10.1016/0025-326X\(77\)90133-3](https://doi.org/10.1016/0025-326X(77)90133-3)

Young, S. D., Tye, A., Carstensen, A., Resende, L., & Crout, N. (2000). Methods for determining labile cadmium and zinc in soil. *European Journal of Soil Science*, 51(1), 129–136.

<https://doi.org/10.1046/j.1365-2389.2000.00286.x>

Young, Scott D. (2013). *Chemistry of Heavy Metals and Metalloids in Soils* (pp. 51–95).

https://doi.org/10.1007/978-94-007-4470-7_3

Yuan, D., Liu, Y., Guo, X., & Liu, J. (2018). Characteristic contaminants in snowpack and snowmelt surface runoff from different functional areas in Beijing, China. *Environmental Science and*

Pollution Research, 25(36), 36256–36266. <https://doi.org/10.1007/s11356-018-3501-1>

Yukon Geological Survey. (2020). *Yukon Litho geochemistry data set*. [accessed February, 2021].

<http://data.geology.gov.yk.ca/Compilation/35>

Yukon Government. (2012). *Little Fox Lake fuelwood timber harvest plan*. <https://emr->

ftp.gov.yk.ca/emrweb/COMM/thp/whitehorse/approved_little_fox_lake_fuelwood_thp_20120718.pdf

Zdanowicz, C. M., Banic, C. M., Paktunc, D. A., & Kliza-Petelle, D. A. (2006). Metal emissions from a Cu smelter, Rouyn-Noranda, Québec: characterization of particles sampled in air and snow.

Geochemistry: Exploration, Environment, Analysis, 6(2–3), 147–162. <https://doi.org/10.1144/1467-7873/05-089>

Zdanowicz, C., Zheng, J., Klimenko, E., & Outridge, P. M. (2017). Mercury and other trace metals in the seasonal snowpack across the subarctic taiga-tundra ecotone, Northwest Territories,

- Canada. *Applied Geochemistry*, 82, 63–78. <https://doi.org/10.1016/j.apgeochem.2017.04.011>
- Zhang, H., Holmes, C. D., & Wu, S. (2016). Impacts of changes in climate, land use and land cover on atmospheric mercury. *Atmospheric Environment*, 141(Supplement C), 230–244.
<https://doi.org/10.1016/j.atmosenv.2016.06.056>
- Zhang, W., Chen, J., Ungar, K., & Cooke, M. (2015). Estimation of the Arctic aerosols from local and long-range transport using relationships between ²¹⁰Pb and ²¹²Pb atmospheric activity concentrations. *Journal of Environmental Radioactivity*, 141, 123–129.
<https://doi.org/10.1016/j.jenvrad.2014.12.008>
- Zhang, Yanxu, Jacob, D. J., Horowitz, H. M., Chen, L., Amos, H. M., Krabbenhoft, D. P., Slemr, F., St. Louis, V. L., & Sunderland, E. M. (2016). Observed decrease in atmospheric mercury explained by global decline in anthropogenic emissions. *Proceedings of the National Academy of Sciences of the United States of America*, 113(3), 526–531.
<https://doi.org/10.1073/pnas.1516312113>
- Zhang, Yanxu, Jaeglé, L., Thompson, L., Streets, D. G., Jaeglé, L., Thompson, L., & Streets, D. G. (2014). Six centuries of changing oceanic mercury. *Global Biogeochemical Cycles*, 28(11), 2014GB004939. <https://doi.org/10.1002/2014GB004939>
- Zhang, Yu, Chen, W., & Riseborough, D. W. (2008). Disequilibrium response of permafrost thaw to climate warming in Canada over 1850–2100. *Geophysical Research Letters*, 35(2), L02502.
<https://doi.org/10.1029/2007GL032117>
- Zhou, J., Wang, Z., Sun, T., Zhang, H., & Zhang, X. (2016). Mercury in terrestrial forested systems with highly elevated mercury deposition in southwestern China: The risk to insects and potential release from wildfires. *Environmental Pollution*, 212, 188–196.

<https://doi.org/10.1016/j.envpol.2016.01.003>

9 APPENDIX A – OTHER PUBLICATIONS AND PRESENTATIONS RELATED TO THIS RESEARCH

- 1) Lead contamination from gold mining in Yellowknife Bay (Northwest Territories), reconstructed using stable lead isotopes. Nicolas Pelletier, plenary talk scheduled for 2nd International Conference on Contaminated Sediments, date postponed (TBA), University of Bern, Switzerland
- 2) Peat bog and lake sediment archives reveal a lagged response of Taiga Shield lakes to diminishing atmospheric Hg and Pb pollution, N. Pelletier, J. C. Vermaire, M. J. Palmer, J. Chételat, oral presentation at the Arctic Change 2020 conference, online
- 3) Does wildfire atmospheric deposition increase metal loading to subarctic lakes?, N. Pelletier, J. C. Vermaire, O. Blarquez, J. Chételat, oral presentation at International Quaternary Association, 2019 (Dublin, Ireland)
- 4) Ninety years of lead accumulation in Yellowknife Bay, Northwest Territories, Canada: long-term impacts of pollution on lead flux and trajectories of ecosystem recovery in a large subarctic lake, N. Pelletier, J. Chételat, J. C. Vermaire, S. Zhang, D. Stepner, D.C.G. Muir and B. Cousens, poster presented at CANQUA 2018, Ottawa, ON, Canada and at the Ontario-Quebec paleolimnology symposium (PALS) 2019, Waterloo, ON, Canada
- 5) Impact of wildfires on the atmospheric deposition of metal(loid)s and major ions in lakes from the Taïga Plains and Canadian Shield. (Yellowknife, NT), N. Pelletier, J. C. Vermaire, O. Blarquez and J. Chételat, oral presentation at the Ontario-Quebec paleolimnology symposium (PALS) 2019, Waterloo, ON, Canada
- 6) The Influence of Forest Fires on Metal Loading to Northern Lakes and Peatlands N. Pelletier, J. C. Vermaire, J. Chételat, M. Palmer, J. Pellisey, B. Tracz, J. Black, S. van der Wieden (2017), poster presented at the 2017 Canadian Committee on Freshwater Fisheries Research and Society of Canadian Limnologist joint meeting (CFFR-SCL 2017), Montreal, QC, Canada and at the International Conference on Mercury as a Global Pollutant (ICMGP 2017), Providence, RI, USA
- 7) Linking Wildfire Activity and Metal Fluxes to Northern Lakes at Decadal Timescales N. Pelletier, J. C. Vermaire, J. Chételat, M. Palmer, J. Pellisey, B. Tracz, J. Black, S. van der Wieden (2017), oral presentation at the 2017 Yellowknife Geoforum, Yellowknife, NT, Canada
- 8) Impact of Wildfires on Metal Fluxes to Northern Lakes N. Pelletier, J. C. Vermaire, J. Chételat, M. Palmer, J. Pellisey, B. Tracz, J. Black, S. van der Wieden, (2017), poster presented at the AGU Fall Meeting 2017, New Orleans, LA, USA